DOCTOR OF PHILOSOPHY

The role of epidermal solutes in the control of stomatal movement

Anisiobi, Anthony

Award date:
2018

Awarding institution:
Bangor University

The role of epidermal solutes in the control of stomatal movement

A thesis submitted to

The School of Biological Science
Bangor University

By

Anisiobi Anthony Nnaemeka

For the degree of Doctor of Philosophy

PRIFYSGOL
BANGOR
UNIVERSITY

July, 2018
.

Declaration and Consent

Details of the Work

I hereby agree to deposit the following item in the digital repository maintained by Bangor University and/or in any other repository authorized for use by Bangor University.

Author Name: Anisiobi Anthony Nnaemeka

Title: The role of epidermal solutes in the control of stomatal movement.

Supervisor/Department: Prof Deri A. Tomos (SBS) and Dr. Katherine A. Steele (SENRGy)

Qualification/Degree obtained: Ph.D.

This item is a product of my own research endeavours and is covered by the agreement below in which the item is referred to as “the Work”. It is identical in content to that deposited in the Library, subject to point 4 below.

Non-exclusive Rights

Rights granted to the digital repository through this agreement are entirely non-exclusive. I am free to publish the Work in its present version or future versions elsewhere.

I agree that Bangor University may electronically store, copy or translate the Work to any approved medium or format for the purpose of future preservation and accessibility. Bangor University is not under any obligation to reproduce or display the Work in the same formats or resolutions in which it was originally deposited.

Dedication

To the loving memory of my father Onyenweego, Hyacinth Ibedum Anisiobi and my mother Ayalugbe, Christiana Okananwa Anisiobi both of whom I lost while in pursuit of this project.

Acknowledgements

I am sincerely grateful to my supervisor Prof A. Deri Tomos for his extraordinary patience, support and clear guidance throughout this project period. I am equally grateful to my administrative supervisor Dr. Katherine A. Steele for her encouraging words. Prof Peter Golyshin and Dr. Robert Brook also provided me with critical guidance during my committee meetings, and I am thankful for that.

To my lovely wife, Mrs. Anisiobi Augustina Ngozi, I am most indebted for her patience, company, care and understanding throughout these trying times. To our lovely children, Chinaecherem Aguluonu Emmanuella and Chukwudi Anthony Anisiobi, who have provided the best fun and relaxation after times of academic stress, I remain eternally devoted. In addition, I must in anticipation at this point, also thank Ebubechukwu Anisiobi for the love that is expected.

I am also thankful to Drs. Virender K. Sahota and Richard Joseph Kutshik for putting me through with the confocal microscope, and to Drs. Leon Civale and Serena Wagg for their very useful pieces of advice at the earliest part of this project. To everyone who has made my stay and studies memorable in this great institution I am very thankful.

Lastly but most importantly, I am most grateful to God, who has made known to us His fatherly desire for enabling good quality life for all peoples.

Abstract

Solute concentration and osmotic pressure patterns were studied in epidermal cells of *Tradescantia virginiana* at open and closed stomata conditions, using single cell sampling and analysis techniques. The studies were carried out in intact plants that were responding to light conditions under normal physiological situation. Only charged solutes were found to participate in stomatal movement and each cell type of the epidermis showed distinct patterns of solute changes both quantitatively and qualitatively. Individual solutes showed characteristic patterns. Two major patterns were observed when the stomata opened. K^+, Cl^-, tartrate and succinate moved into the guard cells. Malate, NO_3^- and PO_4^{3-} migrated to lateral subsidiary cells. A third group of solutes, citrate and SO_4^{2-}, were redistributed in all cells, suggesting a charge-balancing function for these solutes during stomatal opening. These movements reversed on stomatal closure. Patterns of solute changes were similar on both (right and left) sides of the midrib. Each cell type of the epidermis also showed predictable patterns of osmotic pressure changes when stomata opened. Guard cell osmotic pressure increased (1.75 ± 0.06 to 2.26 ± 0.12 MPa) during stomatal opening. Osmotic pressure remained unchanged in lateral subsidiary cells but, in contrast, decreased in apical subsidiary and juxta apical cells. A physiologically-distinct subset of the pavement cells, juxta apical cells, is being proposed.

These qualitative and quantitative differences found in the distribution of solutes between cell types, suggest that each cell type of the epidermis contributes a definite part in the orchestration of stomatal responses. Working together, these cell types are linked by solute concentration gradients that drive the stomatal movements.

Contents

List of figures

List of tables

List of plates

List of equations

Abbreviations

BGE	Background electrolyte
CZE	Capillary zone electrophoresis
ΔE	Net charge balance
IPCC	Intergovernmental Panel on Climate Change
I.D	Inner diameter
L3	Leaf 3 (young leaf)
L4	Leaf 4
L5	Leaf 5
L6	Leaf 6
NADP(H)	(Reduced) nicotinamide adenine dinucleotide phosphate
nl	Nanolitre
nm	Nanometre
O.D	Outer diameter
pl	Picoliter
P1	Plant 1
P2	Plant 2
P3	Plant 3
P4	Plant 4
ΔP	Changes in cell turgor
SD	Standard deviation
SiCSA	Single Cell Sampling and Analysis
γ	Osmotic coefficient
π	Cell osmotic pressure
ψ	Cell water potential

Chapter 1 Introduction

1.1 Summary

Although stomatal movements have, for long, been known to result from net turgor changes originating from solute concentration-driven osmotic changes in the cells of the epidermis, information on those concentration and osmotic changes occurring in these individual cells is limited. The gradients, patterns and uniformity or otherwise of these solute changes in the individual cells, as they work together to effect stomatal movement, are not known.

The major reason for this paucity of knowledge has been the lack of a suitable technique for the study of solute relations at single cell resolution in plants. The multiplicity of external and internal factors capable of playing simultaneously on stomatal responses has not helped the situation.

This study investigated the gradients and changes in the patterns of such gradients in individual cells of the epidermis during stomatal movements with a view to exposing the chemical basis of such movements. The study used and extended the use of established methods of single cell sampling and analysis techniques to determining the chemical characteristics of the guard cell and other trough cells of the epidermis under physiological conditions in intact leaves.

1.2 Introduction

This thesis describes studies on solute concentration changes that occur in *Tradescantia virginiana* leaf epidermal trough cells during changes in stomatal aperture (stomatal movements). Stomatal movements are major determinants of water use efficiency in terrestrial higher plants (Zeiger and Hepler, 1977; Farquhar and Sharkey, 1982; Meidner, 1987; Willmer and Fricker, 1996; Antunes *et al.*, 2012). Stomatal functioning impacts directly on the CO_2- and water-relations of plants, as the stomata form the interface between the atmosphere and the internal environment of land plants.

Plants are essentially sedentary, but need to respond efficiently to challenges posed to their internal milieu by the environment. As with all terrestrial life forms, one of the major challenges is access to water. Access to, and effective management of, water is critical to survival of land plants. Plants account for about 65%, by volume, of global fresh water use (Postel *et al.*, 1996).

However, scarcity of fresh water has become an obvious and worsening global issue in this new century; resulting in severe ecological degradation, limits on agricultural production and consequent threat to human health (Postel, 1993; Postel *et al.*, 1996). Together with water scarcity and the ongoing climate changes (Watson *et al.*, 1990), present high atmospheric carbon dioxide (CO_2) level (400 parts per million by volume) (Dlugokencky and Tans, 2017; Scripps, 2017), with potential for higher levels, present a good case for a more integrated understanding of the mechanics for efficient water and CO_2 use in plants, in order to maximize crop production. The (physical) elastic properties of plant cells and tissues (Steudle and Zimmermann, 1977), typified by and employed in plant guard cells, are a robust adaptive tool for controlling not only water relations and water economy of plants but also the inflow of atmospheric gases (Winner and Mooney, 1980; Meidner, 1987) and dissolved solutes (Eichert *et al.*, 1998; Eichert and Burkhardt, 2001).

Early in evolution, land plants developed a waxy leaf covering (cuticle) (Kenrick and Crane, 1997), which limits water loss but also prevents plants' access to their major carbon source – atmospheric CO_2. Plants, however, maintain a balance between carbon gain and water-use over large environmental ranges of temperature and moisture availability by relying, ultimately, on guarded openings (stomata) created through the cuticle. These openings lead to air cavities extending from below the leaf epidermal layer to the mesophyll layers. The size of the openings is controlled by a pair of specialized epidermal cells surrounding each opening. The control process, however, involves not only these two guard cells but also the surrounding epidermal cells (Klein *et al.*, 1996; Franks *et al.*, 1998; Felle *et al.*, 2000) and, possibly, mesophyll cells. This is in spite of the fact that isolated guard cells and guard cell protoplasts are able to function efficiently, responding (expanding and contracting) appropriately to all stimuli that would be expected when *in situ* (MacRrobbie and Lettau, 1980a; MacRrobbie, 1981; Zeiger, 1983; Tian *et al.*, 2015).

An understanding of the stomata as an integrated whole on a leaf (or plant) offers positive consequences for management of efficient and water-saving cropping

systems under drought conditions and will help in combating the effects of future climatic changes. These stomatal movements involve turgor changes occasioned by solute fluxes and consequent osmotic shifts across cell and vacuolar membranes. Analysis of the solute concentrations and gradients responsible for establishing and maintaining turgor at single cell resolution has demonstrated considerable cell-to-cell variation in the solute content of leaf epidermis (Willmer, *et al.*, 1974; Malone *et al.*, 1991; Leigh and Storey, 1993; Fricke *et al.*, 1994a, 1994b; Karley *et al.*, 2000).

Though stomatal aperture depends directly on the size of the surrounding guard cell pair, and guard cell size is in turn affected and determined by the turgor pressure in the surrounding epidermal cells (Franks *et al.*, 1998), the extent and the mechanics of the involvement of these epidermal cells remains to be elucidated. In addition, mounting evidence, appreciated since the early works of Heath (1975), suggests that a complete understanding of leaf-level stomatal conductance cannot be achieved without considering the stomata on a leaf (or plant) as an integrated whole.

Single cell sampling and analysis (SiCSA) techniques (Tomos *et al.*, 1994; Tomos, 2016) allow the analysis of individual cell behaviour in a fully-functional physiological context. Using these techniques, cells of the stomatal complex as well as other epidermal cells have been analysed for their osmotically-active contents. The findings from this analysis would have implications for management of efficient and water-saving cropping systems under drought conditions. Previous (SiCSA) works have provided a glimpse of dynamic spatial and temporal patterns in the contents of these of cells (Sawhney and Zelitch, 1969; Shackel, 1987). This work is set to explore the source of this intercellular solute variation in the epidermis in order to understand how the plant exploits these variations in the guard cell control of stomata.

1.3 Plant species used

1.3.1 *Tradescantia virginiana* L.

Tradescantia virginiana (Family, Commelinaceae) is one of up to 70 species of *Tradescantia*, an herbaceous plant that is native to the Americas. They are

spiderworts but were named *Tradescantia* by Linnaeus after a 17th century English botanist, John Tradescant, who brought them from Virginia, USA, while he was the gardener to Charles I of England (Armitage, 2008).

Students of plant cell physiology, especially relating to cell turgor (e.g. Hüsken *et al.*, (1978), Zimmermann *et al.*, (1980), Tomos *et al.*, (1981), Tomos and Zimmermann (1983)), osmotic pressure (e.g. Malone *et al.*, (1989) and Meidner and Bannister (1979)) or leaf developmental pattern in monocots (e.g. Croxdale *et al.*, (1992), Croxdale (1998)) found *Tradescantia virginiana* suitable for reasons of its relatively large stomatal complex cells and simple leaf cell arrangements (guard cell length and width of 70 and 21 µm respectively) (Willmer and Fricker, 1996). This contrasts with cereals, such as barley or wheat, which possess stomatal guard cell that are relatively small in size (guard cell length and width of 38 and 11 µm respectively) (Willmer and Fricker, 1996). *Tradescantia* also contrasts with its family member *Commelina communis* which, in addition to relatively small-sized stomatal complexes, has a more intricate arrangement of this complex (compare Edwards and Bowling (1984) and Penny and Bowling (1974)). Techniques developed from using *Tradescantia* have been successfully applied in studies on other plants, e.g. wheat (Malone *et al*., 1991), barley (Fricke *et al*. 1996; Fricke *et al*. 1994b); see also review by Zimmermann (1989). *Tradescantia virginiana* was chosen for this research because of its relatively large leaf cells and predictable arrangement of these cells on the leaf epidermis.

1.4 Leaf development

In order to understand the basis of the cell functional heterogeneity that is the basis of this thesis, some attention needs to be given to the current state of knowledge of the basis of leaf cell patterning in general. Leaves, simple or compound, in both eudicots and monocots develop from a leaf primordium in a phytomer of the shoot apical meristem (SAM) (Galinat, 1959; Dengler, 1984; Poethig and Szymkowiak, 1995). The phytomer is formed from a fast dividing lateral zone (of the SAM) which surrounds a more slowly dividing central zone that permanently retains a stem-cell status (Veit, 2004; Braybrook and Kuhlemeier, 2010). The SAM produces repeated

segments of the shoot system. Each segment (the phytomer), in eudicots or monocots, consists of an axillary bud between an outer leaf primordium and an inner internode (Satina and Blakeslee, 1941; Steeves and Sussex, 1989). The leaf primordia in *Arabidopsis thaliana*, maize and tobacco are made up of 30, 350 and 160 cells respectively arranged in three (outer, mid and inner) layers (Satina *et al*., 1940; Poethig, 1984). The first layer forms the epidermis while the second and third layers respectively produce the palisade and spongy mesophyll. At the point of formation of these cells, auxin transporters orient auxin accumulation in the cells to create an accumulation pattern (Paciorek and Friml, 2006). This determines the positioning of leaves in monocots, or leaves and axillary buds in eudicots. Asymmetric periclinal and anticlinal cell divisions throughout the leaf primordium result in the differentiation of the primordium into tissues and cell types (Sylvester *et al*., 1996). Leaf expansion follows these divisions and is thought to be dependent on the orientation of the cellulose microfibrils and is driven by cell turgor pressure (Green and Stanton, 1967); and reviewed in Taiz (1984). The pattern and timing of these divisions vary between monocots and eudicots (Steeves and Sussex, 1989).

In monocots (to which *Tradescantia* belongs), commonly, the maturation hypothesis (Freeling, 1992) explains the timing and pattern of cellular differentiations. It proposes that leaf regions acquire new competencies as maturation proceeds. This acquisition of new competencies proceed in a proximal to distal direction. For example, the leaf primordium is only competent to produce the leaf base which, as it matures, acquires the competence to produce the leaf blade. Acquisition of cellular identity is variously determined by cell lineage, cell orientation and relative cell position in the developing leaf (Sylvester *et al*., 1996; Larkin *et al*., 1997; Glover, 2000).

The cell lineage system consists of an ordered system of asymmetric cell divisions into categories that correspond to different cell fates. Thus at the end of these divisions, the final fate of each primitive cell type is predictable. In contrast, for cell orientation effects, inhibitory signals and other interactions, such as may be necessary for fulfilling some photosynthetic requirements (for example sub-stomatal air space) from neighbouring cells, may prevent a primitive cell from adopting the same developmental fate as all or some of its neighbours. In addition, determination by cell positioning may occur when asymmetric divisions dispose daughter cells to divide out of harmony. Various repetitions of this pattern of division may bring cells

into or next to clonally unrelated tissues. Such cells acquire the identity of the new tissue (Sylvester *et al*., 1996; Bar and Ori, 2014; Kalve *et al*., 2014).

In the differentiation of the leaf primordium into (about 13) different cell types, all of these systems operate singly or in varying degrees of combinations. For example, using periclinal chimeras of two tomato varieties and *Solanum nigrum,* the frequency of occurrence of stomata on tomato leaf was found to depend on cues from the first layer of the leaf primordium (Szymkowiak, 1990). It is thought that the species-defined number of progenitor cells in the leaf primordium, the size of the mature cells and the duration of cell proliferation stage during leaf development determine the final size and shape of each species' leaf (Dale, 1982).

Thus, cellular identity gradually accumulates as the leaf grows. This accumulation of identity depends on gene expression patterns. Four genes belonging to a knotted-like homeobox (*knox*) gene family (namely *knotted 1, knotted 3, knotted 8 and rs1* genes) are constitutively expressed in the SAM (Hake *et al*., 1989). The *knox1* gene also known as *SHOOT MERISTEMLESS* (*STM*) as well as *BREVIPEDICELLUS* (*BP*), an often redundant gene in the same *knox* family, are the main participants in leaf differentiation (Byrne *et al*., 2002). Knox gene in the SAM regulates the activities of (plant hormones) gibberellin and cytokinins. Regulation of the former is by inhibition of gibberellin20 oxidase gene (*GA20-oxidase*), an indispensable enzyme in gibberellin production pathway (Sakamoto *et al*., 2001). Regulation of cytokinins activity is by stimulation of cytokinin biosynthesis (Jasinski *et al*., 2005; Yanai *et al*., 2005). Gibberellin normally causes cell elongation and differentiation while cytokinins bring about cell proliferation. Leaf patterning is determined by an *ASYMMMETRIC LEAF1* (*as*1) gene (Byrne *et al*., 2000). Within the SAM, *knox*1, inhibits expression of *as*1 gene. Conversely, in differentiating tissues, auxin (Scanlon, 2003) and *as*1 gene, which codes for the *myeloblastosis* (*MYB*) transcription factors (Byrne *et al*., 2000; Heisler *et al*., 2005), inhibit the *knox* gene. In maize, *ROUGH SHEATH* 2 (*rs2*) codes for the *myb* transcription factors and is thus also involved in *knox* gene repression in differentiating tissues (Schneeberger *et al*., 1998). In both monocots (maize) (Jackson *et al*., 1994) and eudicots *(A. thaliana)* (Lincoln *et al*., 1994) inhibition of the expression of knotted 1 (*kn*1) gene in the SAM initiates the formation of leaf primordium. This inhibition is maintained in the leaf primordium of plants with simple leaves but not in plants like tomato, with compound leaves (Hareven *et al*., 1996). The function of the *kn*1 gene is to maintain

the expressing cell(s) in a state of pluripotency (Smith *et al*., 1992; Hareven *et al*., 1996; Jackson, 1996). Thus for compound leaf formation, *kn*1 is inhibited in the SAM to initiate the leaf primordium and subsequently activated in the margins of the formed primordium. Some genes belonging to the *knox* gene family, such as LG3 (*liguleless 3*), are expressed only in the internal part of the leaf (Fowler and Freeling, 1996) which forms the mesophyll. The external part forms the epidermis. Leaf final development involves development of its shape which proceeds in a proximo-distal, medio-lateral and ab- to ad-axial directions. While the *knox*1 gene is involved in the proximo-distal axis development, in the other two directions, two genes *HD-ZIPIII, KANADI* and a small RNA pathway control developments (Kerstetter *et al*., 2001; Emery *et al*., 2003; Chitwood *et al*., 2009).

While these developmental and other morphological changes are beginning to be quantified, the distribution and development of many classes of functional genes – e.g. membrane solute transporters – are far less understood. It is hoped that work described in this thesis may encourage work in this area.

1.4.1 Cellular differentiation in the epidermis

The early undifferentiated epidermal precursor differentiates into morphologically-specialized epidermis. This includes the cells of the stomatal complex and the different forms and modifications of the pavement cells. Within the past decade a litany of answers to many of the questions regarding mechanisms and determinants of epidermal differentiation and patterning has appeared. A number of them will be described in detail here. Some will be mentioned briefly but some others will receive no mention, depending on their perceived relevance to the physiology of the stomata. Mutant analysis has been the major tool that has helped to define the different events and stages of events leading to the differentiation of the homogenous primitive cells of the leaf primordium into terminally-differentiated specialized and non-specialized cell types (Bar and Ori, 2014; Kalve *et al.*, 2014).

A particular gene or gene product may direct cell development into a number of shapes depending on the competence of the cell at the time of expression of the gene (Meijer and Murray, 2001). For example the MYB gene expression may induce differentiation into trichome or conical cells (in petal) and inhibition of the

differentiation of cells of the stomatal complex (Glover *et al.*, 1998). Leaf shape in *A. thaliana* is controlled by a combined expression of *as2, bop1* and *bop2* genes in the lamina. They act synergistically to inhibit the expression of the *knox1* gene in the leaf primordia (Ha *et al.*, 2003).

Two major characteristics of cell differentiation in the epidermis involve the asymmetric distribution of cell wall materials between the inner (in contact with the mesophyll) and the outer (in contact with the cuticle) walls as well as the inside/outside polarity. This is important because the outer, thicker, walls secrete waxy cuticle. Studies in maize suggest that all mature cells located between two veins originate, following a series of anticlinal divisions, from a single progenitor once this primordial cell has grown to a four-cell stage (Cerioli *et al.*, 1994). It has been shown in maize that the final shape of the dividing epidermal cells is entirely determined by cues from the underlying (second) layer of the leaf primordium. Hake and Freeling (1986) as well as Harberd and Freeling (1989) showed that a *kn-O* mutation in the mesophyll leads to abnormal epidermal cells and that wild-type mesophylls in *dwarf8* mutant maize produced normal epidermal cells (Hake and Freeling, 1986; Harberd and Freeling, 1989; Sinha and Hake, 1990).

1.4.2 Differentiation of cells of the stomatal complex and formation of stomata

In both eudicots and monocots, stomata originate from protodermal cells in layer 1 of the leaf primordium (Liu *et al.*, 2009). The differentiation of all the other cell types of the epidermis is predicated on that of the cells of the stomatal guard cell (see fig. 1.1) (Larkin *et al.*, 1997; Tsukaya, 2013; Bar and Ori, 2014).

Four genes, *FAMA, MUTE, TMM* and *SPCH* (Ohashi-Ito and Bergmann, 2006; MacAlister *et al.*, 2007; Pillitteri *et al.*, 2007) (with conserved sequences in eudicots and monocots) have been found to be responsible for the differentiation of stomata. Though with slight variation in the functions of some of the genes (Liu *et al.*, 2009; Qu *et al.*, 2017). These genes are closely related to the basic HELIX-LOOP-HELIX (*bHLH*) transcription factor (Pillitteri and Bogenschutz, 2008). *SPEECHLESS1* (*SPCH 1)* is expressed in primitive epidermal cells and controls the first division that leads to stomatal lineage commitment (Pillitteri and Dong, 2013). *Glutamate mutase component E* (*mute*) gene is expressed in the (committed)

meristemoid, leading to the formation of the guard mother cell and also functions to terminate the stem cell identity of the meristemoid. *Fama*, on the other hand, is expressed in the guard mother cells and regulates its symmetric division into two guard cells (Ohashi-Ito and Bergmann, 2006). In *Arabidopsis thaliana*, two genes have been proposed. The first is *STOMATAL DENSITY AND DISTRIBUTION* 1 (*SDD1*) gene (Berger and Altmann, 2000), a protease that mediates signals which control cell development of cell lineages that lead to formation of guard cells. The second is the *TOO MANY MOUTHS* (*TMM*) gene (Berger and Altmann, 2000; Geisler *et al.*, 2000), which is part of a receptor complex that senses positional cues for position-dependent patterning during epidermal cell development.

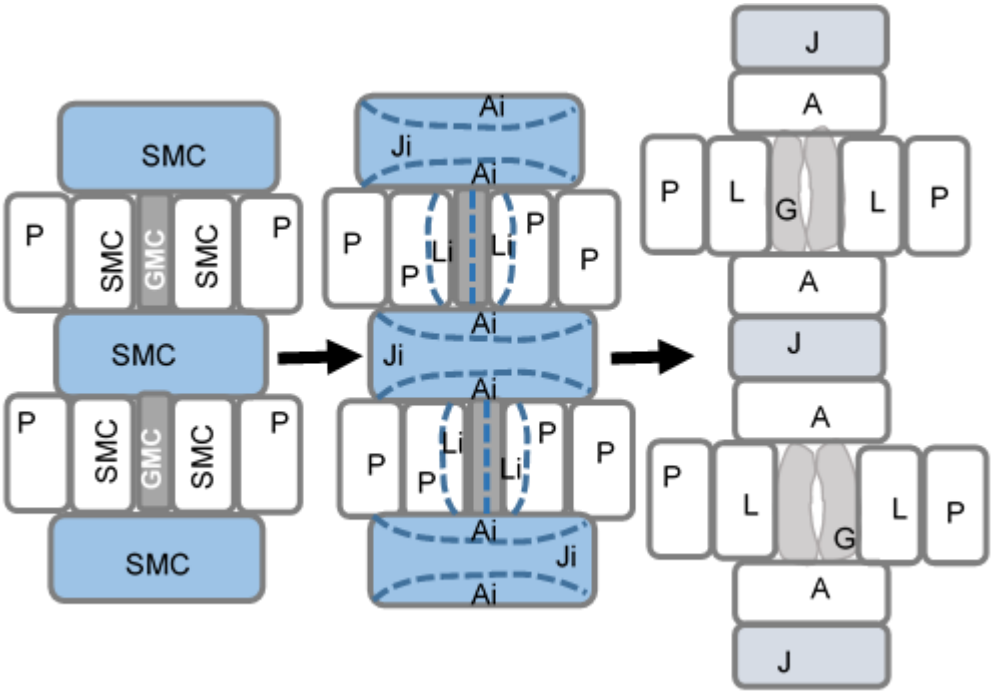

Figure 1.1 The formation of cells of the stomatal complex
The GMC and the SMC give rise to all epidermal cells depending on their orientations. The apically-placed subsidiary mother cell (SMC) gives the apical subsidiaries initials (Ai) which mature into apical subsidiaries (A) while the remainder (Ji) matures into the juxta apical cell (J). The laterally-placed SMC gives the outer pavement cells (P) and an inner lateral subsidiary initials (Li) which mature into the lateral subsidiary cells (L). The guard cells (G) form from the guard mother cell (GMC) (Stebbins and Jain, 1960).

In monocots, stomatal development follows a basipetal order. The initial stages occur at the base while the maturing (later) stages take place towards the tip of the developing leaf. The protodermal cell induced by *spch1* undergoes asymmetric division to produce a smaller meristemoid and a larger sister cell. These sister cells

form the pavement cells. The meristemoid retains stem cell activity and undergoes a few more divisions before differentiating into a guard mother cell (GMC) (figure 1.1). The number of divisions depends on the number of GMCs adjacent to the meristemoid (Stebbins and Jain, 1960). Its first division produces the cell lines for the GMC. Its second division gives the cell lines for the subsidiary mother cells (SMC). The number and spatial arrangement of these subsidiary cells, however, vary between species (Willmer and Fricker, 1996). The GMC lacks the stem cell activity of the meristemoid and undergoes one symmetric division to give the two guard cells. The guard cells then undergo morphological changes resulting in elongation and formation of a pore between the two of them (Sack, 1994).

Studies in the monocots *Chlorophytum comosum, Galanthus nivalis, Schizostylis coccinea* and *Scilla lancifolia* show that stomatal and, indeed, cellular development in monocots occur progressively in zones (Charlton, 1990). In these zones inductive interactions play a significant role in the arrangement of cells in files as the cells are being displaced from leaf base towards the tip (Stebbins and Jain, 1960). These zones include the proliferative zone, found close to the leaf base and in which cells may undergo proliferative mitosis before moving into the next zone of formative mitosis. In this second zone new cell types, namely the GMCs and SMCs, are formed. This is followed by the guard cell zone in which the GMC differentiates into the guard cells and the SMC into the subsidiary cells. Beyond this zone, no mitotic activity occurs and only cell expansion continues. Cells unable to start or complete the proliferative or formative mitosis when pushed into the respective zones do not form part of the guard cell line. Thus, the fate of any primitive cell at the leaf base is dependent on its stage in mitosis at entry into the proliferative and then the formative mitosis zones (Charlton, 1990). Hence, cell lineage alone does not determine cell fate in monocots (Hernandez *et al.*, 1999). Lineages account for at least part of the distance between neighbouring stomata. Effects of interactions are also indicated by developmental observations, which show that interactions modify stomatal development rather than inhibit stomatal initiation. In *T. virginiana*, the fate of a guard cell mother cell (GMC) with respect to stomata formation is determined by an inhibitory mechanism determined by five nearest stomata to the GMC. Where guard cell formation is successfully inhibited, the GMC becomes a pavement cell. These pavement cells appear irregularly hexagonal on surface view (Campbell, 1881) but are approximated to be circular for ease of analysis (Boetsch *et al.*, 1995)

(see Plate 3.1). The SMCs abutting successful GMCs differentiate to give the subsidiary cells (Campbell, 1881; Croxdale *et al.*, 1992; Willmer and Fricker, 1996). The fate of SMCs abutting inhibited GMCs is unknown. Similarly, whether the inhibition of a GMC, which produces the identifiable anatomical cell type, carries a physiological implications or not is unknown. Such investigation was not included in this project.

1.5 The cuticle

Over the external side of all the epidermal cells (and extending to the anticlinal walls of the guard cells) is the cuticle. This is a water-impermeable waxy layer covering the epidermis. It accounts for less than five percent of gas exchange by the plant, depending on the degree of hydration of the underlying epidermal cells; having higher conductance when well-hydrated epidermal cells cause it to stretch than when unstretched, as in dehydrated leaves (Boyer *et al*., 1997).

The cuticle is secreted from the external, thicker wall of each cell type of the epidermis. In maize, expression of *glossy 1 (GL1),* so named because its mutants confer a glossy appearance on an otherwise glaucous juvenile leaf, leads to the synthesis of cuticular wax (Sturaro *et al*., 2005). It encodes for a desaturase／hydroxylase enzyme needed for the synthesis of wax and cutin. Knowledge is by no means complete regarding the timing or biosynthesis of the cuticle in maize. However, a group of 18 possible glossy gene mutations, which show defective expression of different members of the fatty acid elongase (FAE) enzyme-complex in *A. thaliana*, enzyme β-ketoacyl-CoA synthase (KCS) and, in maize, the β-keto acyl reductase (KCR) enzyme, has been identified. In one mutant, the *fiddlehead (FDH)* mutant, fusion of all leaves and floral organs was observed while epidermal cells remained normal. In *A. thaliana*, 21 genes expressing the KCS protein have been identified but knowledge is still sparse on its (*A. thaliana*) cutin and wax biosynthesis (Javelle *et al*., 2011). The presence of cuticle limits transpirational water loss from leaves such that transpiration is mainly through the controlled stomatal pores.

1.6 Guard cells

Higher plants, in their evolution, have developed stomata as a structure that modulates the carbon gain and water economy to the advantage of the plant, under any prevailing environmental condition. These stomata are openings on the epidermis, created by the expansion of two opposing specialized cells, the guard cells. They (guard cells) connect the plant's internal and external environments. Guard cells account for approximately 1% of the leaf volume in higher plants (Outlaw Jr, 1987). The immediate surrounding epidermal cells together with the guard cell pair form a functional unit known as the stomatal complex. Guard cells are a pair of specialized kidney- or dumbbell-shaped epidermal cells that form, surround and regulate stomatal apertures through integrated signalling pathways activated by endogenous hormonal and environmental stimuli. These signalling pathways may be mediated by kinases/phosphatases, secondary messengers, and/or ion channels.

The guard cells, unlike other epidermal cells, contain chloroplasts which participate in stomatal control. Controversies abound on the existence and function of guard cell chloroplasts with respect to stomatal function (Lawson, 2009). Some recent evidence from chlorophyll-*a* fluorescence analysis seems to support the presence of chloroplasts and their participation in stomatal control (Nejad *et al*., 2006). However, the weight of evidence seems to tilt toward the fact that guard cell stomatal control responses require photosynthetically active mesophyll cells (Roelfsema *et al*., 2006).

Also contentious is the nature of guard cell vacuole in the closed stomata condition. There is evidence that guard cells contain multiple small vacuoles in closed stomata. However, the vacuoles enlarge and coalesce to form fewer or a single large central vacuole during guard cell enlargement (Faraday, 1982). Three-dimensional electron microscopy in *Commelina* ((Weyers and Meidner, 1990; quoted in Willmer and Fricker, 1996) and in *Vicia faba* (Tanaka *et al*., 2007) show that guard cell vacuoles in closed stomata conditions constitute a single convoluted organelle. The tonoplast surface area was 25% greater than that of the plasma membrane. The vacuoles appear as multiple small vacuoles following rapid closure of stomata, but gradually coalesce with time to form a single vacuole under closed stomata condition. Tanaka *et al.* (2007) observed that the perceived discrete small vacuoles of rapidly-closed stomatal guard cells are interconnected, and the coalesced vacuole

constituted at least 57% of the guard cell volume. Such studies have not been done in *Tradescantia*, but it is likely to imitate the observations in *Commelina*. If this were the case, the sampled sap in this study would be considerably vacuolar. Another unique property of the guard cell is its thicker cell wall especially in the anterior, posterior and ventral walls (see section 1.11.2).

1.7 The stomatal complex and stomata

Plant stomata were discovered by Malpighi in 1675. Fossil records, though, show that stomata appeared on leafless stems from Silurian rocks, more than 410 million years ago; about 50–60 million years before land plants (Edwards *et al*., 1998). These may, however, be comparable to lenticels on roots or tubers, stems, flowers and fruits of land plants (Adams, 1975; Hew *et al*., 1980; Lefebvre, 1985; Blanke and Lenz, 1989).

Stomata are pores surrounded and regulated by a pair of (specialized) guard cells, within the epidermis of leaves of land plants and the aerial side of leaves of aquatic plants. Stomata are also found in roots (Christodoulakis *et al*., 2002), where they function to increase gaseous exchange and transfer of nutrient and water to the growing primary roots. They also appear in stems and petioles, where they serve as nectar secretory ducts (Horner *et al*., 2003). In hornworts, the stomata are permanently open, and have an undetermined function, which is unlikely to be gaseous exchange (Pressel *et al*., 2014).

Some plants are astomatous. These are mainly aquatic plants and the bryophytes e.g. *Isoetes andicola* (Gonzalez and Markham, 1994). Most astomatous land plants (the bryophytes and lichens) do not grow above 50 cm in height (Woodward, 1998). A few tall plants, for example *Stylites andicola*, a primitive CAM land plant, are devoid of stomata in the aerial parts. They absorb CO_2 mainly through the roots (Keeley *et al*., 1984). This plant is, however, mostly found near glaciers, about four kilometres above sea level. Stomata are also not found in chlorophyll-free plants (e.g. *Monotropa* and *Neottia*) (Willmer and Fricker, 1996) and fully submerged aquatic plants.

Each plant species possess one of two types of stomata, dumbbell or kidney shaped, with reference to the shape of the surrounding guard cells (Willmer and Fricker, 1996). Mostly one or more (for example in *Commelinacae*) specialized cells, may surround the guard cells on every side. These are known as the subsidiary cells. In both eudicots and monocots, contiguous stomata do not exist (Tanaka *et al*., 2013).

Grasses possess dumbbell-shaped guard cells assisted by subsidiary cells and stomata are present on both (abaxial and adaxial) sides of the leaf (Willmer and Fricker, 1996). In eudicots and some monocots, guard cells are kidney shaped and subsidiary cells are often absent (Campbell, 1881; Taiz *et al*., 2015). *T. virginiana* combines the kidney shaped guard cells with features of grasses in possessing subsidiary cells. In most tree species stomata appear only on the abaxial (usually, lower) side (Willmer and Fricker, 1996). Non-tree species (except aquatic plants) have stomata on both sides of their leaves. In all species that have stomata on both sides of the leaf, more (stomata) are found in the abaxial than in the adaxial surface.

Plant stomata may open or close in response to abiotic and biotic stimuli such as light, CO_2 concentration changes, fungal and bacteria toxins among others (see section 1.11). In crassulacean acid metabolism (CAM) plants, stomata open at night but remain closed during the day (Lüttge, 2002). A rapid stomatal closure mechanism is required in response to environmental stresses such as pathogens and pathogen-associated molecular patterns (PAMPs) attacks. These include bacteria, fungi and their products, such as the flagellin peptide, lipopolysaccharides and yeast elicitor (*YEL*) (Melotto *et al*., 2006). Rising CO_2 levels has engendered a fall in stomatal density in some plants (Woodward, 1987), but an increase in others (Beerling *et al*., 1992). Stomatal density is unchanged by variation in CO_2 concentration in some plants such as conifer needles, corn and soybean (Thomas and Harvey, 1983; Apple *et al*., 2000). Despite the effect of the environment on stomatal frequency of some plants (Woodward, 1987) stomatal morphology has remained the same in all plants over the millennia (Edwards *et al.*, 1998). The anatomical position of stomata aids plants in managing the scarce (water) resources. The inner surface of adaxial epidermis (Fig. 1.2) for example, shows that the architectural design of the stomatal complex allows all cells of the complex to hang freely over the substomatal chamber such that mesophyll cells are in contact with only pavement (and juxta apical) cells.

Thus, no functional plasmodesmatal connection can exist between these (stomatal complex) cells and the mesophyll cells and none has been found between these stomatal complex cells and the pavement cells (Erwee *et al*., 1985; Palevitz and Hepler, 1985.

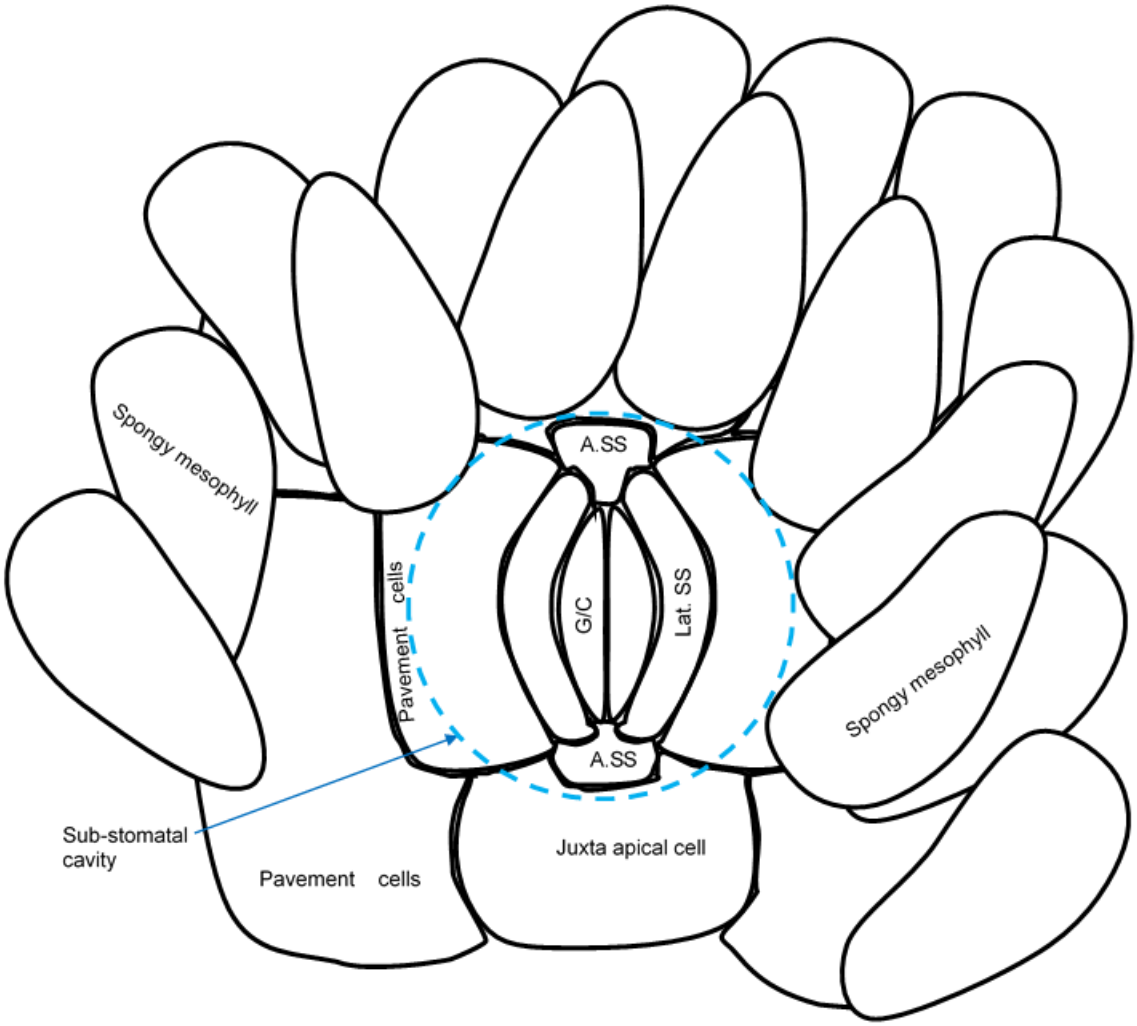

Figure 1.2 Inner surface of abaxial epidermis of typical monocot leaf (e.g. *Tradescantia)* at the sub-stomatal space.
Spongy mesophyll cells abut pavement cells but not stomatal complex cells (apical cell (A/SS), lateral subsidiary cells (lat. SS) as well as the adjoining guard cells (G/S). Spongy mesophyll cells at the front are to show the sub-stomatal space.

1.8 The stomatal complex of Commelinaceae

The stomatal complex is made up of the guard cell pair surrounded by a group of specialized cells known as the subsidiary cells (see chapter 3). In *Commelina communis*, which has two pairs of subsidiary cells on the sides and one pair at the apices, the outermost pair in the complex is the outer lateral subsidiary cells, which surround most of the circumference of the other cells in the complex (Penny *et al.*, 1976; Penny and Bowling, 1974). The terminal or apical subsidiary cells surround the two longitudinal extremes of the remaining cells of the complex. An inner subsidiary cell that covers the entire lateral aspect of guard cells is found between the other outer subsidiary and the guard cell. The frequency of occurrence of the complex per unit area on a leaf is known as the stomatal frequency or density, and is an adaptable characteristic of species (Willmer and Fricker, 1996).

In *T. virginiana,* the outer subsidiary is absent and only a single lateral and apical subsidiary cells are found (see plates 3.1 and 4.1). The guard cell complexes are surrounded by pavement cells which appear different (in surface shape) from the subsidiary cells. In addition, at least 70% of the apical subsidiary cells of adjacent stomatal complexes are separated by an, hitherto, unidentified cell type morphologically indistinguishable from other pavement cells (Croxdale *et al*., 1992). The physiological solute concentrations and patterns of changes of this cell type (understood from our present study) seems to set them functionally apart.

1.9 Mechanism for stomatal opening and theories of stomatal movement

Outstanding studies into the structure and function of the stomata have led to theories that inform the present knowledge on plant water relations and photosynthetic gains. During early stomatal research, von Mohl (1856) showed that stomatal opening and closing were as a result of increases and decreases, respectively, in guard cell intracellular osmotic pressure. Stålfelt (1929) subsequently demonstrated that stomata open in phases ((Stålfelt, 1929) quoted in Edwards *et al*. (1976)).

Two phases were identified, namely the *sphannungsphase* and the *motorphase*. During the *sphannungsphase*, guard cell intracellular osmotic pressure builds up, the cells change in shape and become more concave at the ventral wall. The walls also stretch and become more elastic, such that with any further increase in pressure (in the *motorphase)* the guard cells expand to open the stomata (Meidner and Edwards, 1975). The stomatal aperture continues to increase in the *motorphase* until maximum aperture. Concurrently, the pressure in the subsidiary cells reciprocally (albeit, not to the same degree) decrease (Meidner and Edwards, 1975; Laisk *et al*., 1980).

Two major theories for the mechanism of stomatal movement (opening and closing) were considered: namely the photosynthesis and the active transport theories.

1.9.1 Photosynthesis theory

Sayre (1926) proposed the photosynthesis theory which postulated that the presence of light led to CO_2 reduction due to photosynthesis. This reduction would lead to a rise in pH which favours the breakdown of starch to sucrose. The sucrose increases the cell osmotic pressure. The resultant decrease in water potential creates a negative water potential gradient between the cell and its surroundings, with consequent movement of water into the cell (osmosis). This was based on the observation that all major stomatal movements were accompanied by pH changes and a reversible transformation of the carbohydrate in the guard cell. This theory was contributed to and modified by many researchers and it was generally accepted that CO_2 accumulation in the dark caused stomatal closure by the reverse mechanism. The theory was based on the finding of the enzyme pyrophosphatase in plants (potato), which could reversibly convert starch to glucose-1-phosphate (Hanes, 1940).

Researchers, in the likes of O. V Heath, W.T Williams, G. W. Scarth and N. N. Kisselew found faults in the theory due to its inadequacies in explaining the rapidity of stomatal action. For example, Scarth (1932) showed that the carbohydrate changes and the stomatal aperture changes were not exactly correlated. Williams (1954) proposed that both the opening and closing movements involved movement of water by contractile vacuoles, as is common in unicellular algae and protozoa. He posed that the carbohydrate changes were only secondary effects, not linked to the primary

process. His theory claimed that the closing, not the opening, movement was the active, energy-requiring and important movement. It supposed that the opening was only a return to the resting state.

Other theories were also proposed. One such theory was the permeability theory, based on the fact that stomata in the vicinity of a wound on the epidermis, close, unaccompanied by changes in starch content of the guard cells, ((Kisselew, 1925) quoted in Williams (1954)). It supposed that solute escape from the cells was due to increased permeability, and accounted for the stomatal movements. Attempts by contemporaries to reproduce the results yielded inconclusive and often conflicting results. Following this, the amphoteric colloid hypothesis was then proposed by Scarth in 1929 ((Scarth, 1930) quoted in Scarth (1932)). It stated that guard cell pH increased in the presence of light and led to imbibition change in amphoteric colloidal materials in the cell sap and increase in guard cell size. The reverse was held to be occurring in the absence of light to lead to stomatal closure. This was also not supported by results from other laboratories at the time (Alvim, 1949). In addition, stomata of some plants such as *Allium spp.* that do not form starch (Shaw, 1954), were also shown to function efficiently and stomatal movements were noticed in plants before any starch to sugar conversions could occur ((Yamashita, 1952 quoted in Fujino (1967)).

In 1959, Fujino confirmed an observation by Imamura (1943) that a good correlation exists between K^+ content of guard cells and stomatal movements (Fujino, 1959 quoted in Fujino (1967)). This observation was corroborated by Fischer (1968) as well as Fischer and Hsiao (1968) and lead to rejection of the photosynthesis theory and emergence of an active transport theory (Fischer and Hsiao, 1968).

1.9.2 **Active transport theory**

A major reinforcement to this hypothesis was the observation that known inhibitors of active K^+ transport such as azide and dinitrophenol prevented guard cell movements (Fujino, 1967). However, both in single (detached) (MacRrobbie and Lettau, 1980a) and intact (MacRrobbie and Lettau, 1980b) guard cell preparations, changes in K^+ alone was inadequate to account for the changes in stomatal aperture; thus, suggesting the involvement of other factors. The work of Raschke and Humble (1973)

using *Vicia faba* showed that the proton pump is actively involved in stomatal movements.

A chemiosmotic hypothesis was then put forward by Zeiger (1983) and explained the generation of electrochemical gradient across cells by the activities of a proton pump (Zeiger, 1983). One of the major hypotheses that explained the chemiosmotic effect was the proton transport concept of photoactive stomatal opening (Levitt, 1974). This was based on the observation that illumination of green plants caused alkalinization of the chloroplast stroma and acidification of its thylakoid spaces thus confirming a light dependent proton transport across the thylakoid membrane (Heldt *et al.*, 1973).

These findings explained the passive diffusion of K^+ and its chemical coupling to proton pump in the form of active transport across membranes. Plasma and vacuolar membrane-bound NHX (Sodium/Hydrogen exchanger) proteins, which serve as H^+/K^+ or H^+/Na^+ antiporters, were subsequently identified (Blumwald and Poole, 1985). This chemiosmotic hypothesis, has been incorporated into the active transport theory, and is now established in the generally accepted models of stomatal movements (e.g. Xue *et al*., 2011).

1.10 Guard cell responses to stimuli

Since their appearance (Kenrick and Crane (1997), Willis and McElwain (2014)), plant guard cell has remained more or less unchanged (Franks and Beerling, 2009). Nevertheless, as the earth's atmospheric CO_2 concentration changed with time, their photosynthetic capacity has been increased through co-ordinated changes in their size and density of distribution (Franks and Beerling, 2009). These changes, coupled with acquisition of vascular tissues and cuticular cover as plants moved from aquatic to a terrestrial environment, improved their control of gas exchange and water use efficiency (Raven, 1977; Willmer and Fricker, 1996).

The role of the guard cells in optimizing the trade-off between gas exchange and water loss in plants under continuously changing endogenous, hormonal and environmental conditions requires the processing of multiple stimuli. All these stimuli are interpreted as signals and converted into turgor pressure responses. The guard

cell's turgor is regulated by numerous internal and external cues (Hetherington and Woodward, 2003). One of the factors enhancing this function in guard cells is their location on the leaf surface, being in contact above (outer lateral wall) with the atmosphere and below (inner lateral wall) with the intercellular air spaces (through the sub-stomatal air space) of the leaf (fig. 1.2). Ventrally (opposite stomatal opening), the guard cell contacts with the collapsible stomatal aperture. Its anatomical contact with other cells of the epidermis (subsidiary cells in *T. virginiana*) is essentially only through its dorsal wall. It senses and responds to internal and external cues, resulting in stomatal aperture changes.

Stomata open in response to external and internal stimuli, including light, temperature, humidity, CO_2, ABA, jasmonic acid, auxins, ethylene and salicylic acid (Zeiger, 1983). Guard cell plasma membrane and the tonoplast have been shown to possess two classes of K^+ channels each (Schroeder *et al*., 1987; Keller *et al*., 1989; Fairley-Grenot and Assmann, 1993). The plasma membrane channels are the rapid depolarizing (R-type) and the slow depolarizing (S-type) channels (Canny, 1990) while the channels at the tonoplast are the (fast) vacuolar K^+ (VK) channel and the slow vacuolar (SV) channel (Ward and Schroeder, 1994). These channels may be specifically responsive to membrane potential changes, ligand binding, light, phytohormone levels or modifications, such as phosphorylation. Guard cell membrane (plasmalemma or tonoplast) also contains several other channels, each activated by membrane potential, pH, reactive oxygen species (ROS), K^+, NO or Ca^{2+} concentration, among other effectors.

Changes in levels of these species activate the species-specific channel(s) to mediate a species or species-level-dependent signal transduction. ABA induces changes in these ion channels to cause efflux of both K^+ and anions at both (plasmalemma and tonoplast) membranes. Details of the signalling chain, including intermediates, by which these channels are linked to ABA are, however, still very sparse (Zhang *et al*., 2014; Wang *et al*., 2016). Nonetheless, it is thought that ABA, for instance, induces increase in cytosolic Ca^{2+} which causes membrane depolarizing and thus leads to the opening of these channels (Schroeder and Hagiwarat, 1990). Nitrous oxide- (NO) and CO_2-induced guard cell responses are similar to that of ABA in causing elevated free cytosolic Ca^{2+} (Schroeder and Hagiwarat, 1990). However, the mechanisms are not exactly the same; in that while NO acts through a cyclic guanosine monophosphate (cGMP)-dependent pathway,

ABA raises cytosolic pH and thus inactivates inward-rectifying K^+ channels while activating outward-rectifying K^+ and (anion) membrane channels (Karley *et al*., 2000).

The vacuolar K^+ pool is much larger than the cytosolic pool and generates the cell turgor (Linder and Raschke, 1992). The vacuole is thus the major control site of guard cell size. Bowling and Edwards (1984) showed that while vacuolar pH significantly changed with changes in stomatal aperture, cytoplasmic pH remained constant (Bowling and Edwards, 1984). Changes in cytosolic Ca^{2+} level appears to be the common step in control of stomatal movement (Kim *et al*., 2010).

1.10.1 **Guard cell response to light**

Guard cells perceive light through a dual mechanism involving the guard cell chloroplast and a blue light photosystem. They respond to light intensity (Mansfield and Meidner, 1966), and quality (Hsiao *et al*., 1973; Sharkey and Raschke, 1981). The light intensity stimulating this response may be different on the abaxial and adaxial sides (Sharkey and Ogawa, 1987) due to differences in pigment content (Lu *et al*., 1993). The action spectrum for stomatal movements is similar to that for photosynthesis, though stomata may respond to intensities below the photosynthetic compensation point. This is due to increased sensitivity of guard cells to blue over red light (Kuiper, 1964; Mansfield and Meidner, 1966).

Excitement of the blue light photosystem leads to H^+ extrusion by activating the H^+-ATPase pump. This creates the enabling electrochemical gradient for passive K^+ influx (Assmann *et al*., 1985; Shimazaki *et al*., 1986). The C-terminal of the H^+-ATPase contains a serine and threonine-rich domain as well as an auto-inhibitory domain that inhibits the serine and threonine domain. Phosphorylation of the serine and threonine domain activates the H^+-ATPase (Kinoshita and Shimazaki, 1999). An ubiquitous enzyme modulating protein, 14-3-3 protein, is a competitive inhibitor of the auto-inhibitory domain (Taiz *et al*., 2015). For example, the wilting action of the fungal toxin, fusicoccin, begins with increase in the affinity of 14-3-3 protein for the binding site on the auto-inhibitory domain (Gepstein *et al*., 1982). The bound 14-3-3 protein prevents the inhibition of the phosphorylation of the serine and threonine-rich domain and so keeps the H^+-ATPase irreversibly active (Johansson *et al*., 1993).

Blue light (with an action spectrum maximum between 430 and 460 nm) is about ten times more effective in activating H^+-ATPase pump than red light (with an action spectrum maximum between 630 and 680 nm) (Sharkey and Raschke, 1981). The blue light receptor in the guard cell is zeaxanthin, and the action of blue light on the stomata is directly proportional to the zeaxanthin content of the guard cells within the 24 hours cycle (Frechilla *et al*., 1999; Zeiger *et al*., 2002).

Zeaxanthin is also present in mesophyll chloroplasts but at concentrations that are three to four time less than guard cell levels (Zeiger *et al*., 2002). Guard cells respond quickly to blue light which has its maximum action spectrum at 450 nm. Zeaxanthin has an absorption spectrum that is similar to the action spectrum of blue light stimulated stomatal opening.

The blue light effect is reversed by green light. This was shown to occur because zeaxanthin exist in two interconvertible isomers, separately absorbing in blue and green light. The green light-absorbing isomer exists more commonly (Frechilla *et al*., 2000). Green light isomerizes zeaxanthin from the all-trans to a 13-cis-isomer. This isomerization changes the orientation of the zeaxanthin on the thylakoid membrane from the active vertical to an inactive horizontal position (Milanowska and Gruszecki, 2005). This green light action was exploited during the current work for sampling cells under closed stomata conditions such that visibility could be maintained while stomata remain closed.

Roelfsema *et al.* (2001) observed that blue, but not red, light caused both an increase in pump current in plasma membrane proton pump and a decrease in the inward rectifying K^+ channel conductance in *Vicia faba.* They, however, also observed that while blue light cause hyperpolarization temporarily, white light induced a steady hyperpolarization (Roelfsema *et al*., 2001). The reason for this difference is not known. This blue light effect on stomata may also occur in the absence of chlorophyll. This was shown by Assmann (1988) who demontrated that low CO_2 and low humidity enhanced blue light stomatal response in *Paphiopedilum harrisianum* plant which has no chlorophyll in the epidermis or guard cells (Nelson and Mayo, 1975; Assmann, 1988).

Red light also causes stomatal opening. Its stimulation of the guard cells is chloroplast-dependent. The chloroplast modulates the red light activation of the H^+ pump (Serrano and Zeiger, 1988). An *ht*1 protein kinase is involved in red, but not blue light responses in guard cell (Matrosova *et al*., 2015).

Thus, light affects the osmotics of the guard cells by stimulation of organic acid (malate) synthesis and activation of the proton pump and thus, solute uptake by the guard cells. Photoactive stomatal responses were used in this current research for normal growth and experimental stomatal manipulations. Due to the particular sensitivity of the system to light quality and quantity, white light of controlled intensity and diurnal variation was used for growth of the plants, and similar intensity of white light was applied for all open stomata experiments (sections 2.1 and 2.5).

1.10.2 Guard cell response to humidity

It has been known since 1898 that plants respond to changes in atmospheric humidity (Darwin, 1898). They respond to reduced humidity (drier air) by closing the stomata (Lange *et al*., 1971). This response helps plants to conserve water in dry environments. The immediate response on exposure to reduced relative humidity, however, is to initially open and then close the stomata (Darwin, 1898). This initial opening has been suggested to be as a result of initial reduction in the water potential of the epidermal cells (akin to Iwanoff effect – see chapter 5). All land plants (mosses and higher plants) are sensitive to this humidity stimulus (Chater *et al*., 2011), though some (e.g. C4 plants) are less so (Taiz *et al*., 2015). For example, cell size is affected by the relative humidity prevailing during the critical period of leaf development (Fanourakis *et al*., 2011). Stomata in plants grown under high relative humidity have bigger stomatal complex cells than those grown under mild to moderate relative humidity (Fanourakis *et al*., 2011), and smaller stomata respond faster to environmental cues (Drake *et al*., 2013).

Guard cell sensing of relative humidity is not yet fully understood. The major suggestions by researchers have been that humidity sensing by guard cells is entirely cuticular (peri-stomatal transpiration) (Lange *et al*., 1971; Schönherr, 1982) or that the inner surface of the guard cells is the site for humidity sensing (Meidner, 1975) or both (Sheriff, 1977).

Water vapour from the stomata has to diffuse through a boundary layer (layer of unstirred air) immediately above the stoma to reach the turbulent atmospheric air and *vice versa*. The effect of the boundary layer, especially in species with anatomical advantages that allow for a significant boundary layer such as those with

sunken stomata, is to shield the stomata from responding directly to changes in ambient air humidity (Bunce, 1985).

Response to humidity contributes in sensitizing the plant to respond to other environmental cues (Talbott *et al*., 2003). For example, in *Vicia faba*, short–term responses to CO_2 have been shown to be dependent on stomatal sensitivity to humidity changes (Talbott *et al*., 2003), and the effect of humidity on stomatal development in *Phaseolus vulgaris* has also been demonstrated (Pospíšilov, 1996). This work on *Phaseolus vulgaris* and also in *T. virginiana* (Nejad and van Meeteren, 2005; Nejad and van Meeteren, 2008), showed that the stomatal apparatus in the young plants or seedlings fail to develop under high humidity. This fact is key in the planning of stomatal-response experiments (Meidner and Mansfield, 1968), and care was taken in this research to grow all plants under similar moderate humidity conditions (see section 2.1).

Responses to other factors, on the other hand, also modulate plants' sensitivity to humidity (Waadt *et al*., 2014). Fluorescence resonance energy transfer (FRET)-based studies show that abscisic acid (ABA) concentration increases in response to decreased humidity (Waadt *et al*., 2014). Bunce, (1997) had suggested that ABA signals are involved in stomatal response to relative humidity (Bunce, 1997). Following this suggestion, Xie *et al.* (2006) showed that components of the ABA signalling network are involved in the signalling events in the response to humidity. They identified the *OST1* and *ABA2* genes, involved in ABA signalling, as genes encoding for stomatal response to humidity. Bauer *et al.* (2013a) subsequently demonstrated that guard cells have the capacity to synthesize their own ABA and that this autonomously synthesized ABA (initiated in guard cell chloroplasts) is involved in stomatal response to humidity changes. The findings corroborated an earlier work done on *Vicia faba* and *Pisium sativum*, which showed the formation of ABA in isolated protoplasts (Cornish and Zeevaart, 1986). This appears to explain the response of isolated guard cells and guard cells on epidermal strips to humidity. This finding does not, however, appear to have been reproduced by other workers. McAdam and Brodribb (2015), though accepting that the mechanism of response to humidity by angiosperms is driven by ABA, concluded that the ABA found in these species during the response did not originate from the epidermis (McAdam and Brodribb, 2015). This position held, against the background that ABA from the roots accumulate in the apoplast of the guard cells, due to the

evaporation which drives the transpiration stream, enabling higher concentration and thus increased sensitivity under situations of higher transpiration rate (Zhang and Outlaw, 2001). It appears, however, that the observation of Bauer *et al.* (2013a) was correct because in a work, co-authored by McAdam three years later (McAdam and Sussmilch, 2016), it was concluded from studies on the level of expression of 9-cis-epoxycarotenoid dioxygenase (NCED) synthesis gene, that the ABA involved in humidity responses in angiosperms was rapidly synthesized *de novo* in the guard cells. The activity of this enzyme (product of the NCED gene) is the rate-limiting step in ABA synthesis. An ABA efflux transporter has also been found, located in vascular tissues and guard cell plasma membrane (Zhang *et al*., 2014). Guard cell cytosolic ABA concentration has also been found to increase following reduced humidity (Waadt *et al*., 2014). Thus, response of guard cells to humidity is mediated by the (water) stress hormone ABA.

The possible manifestations of this stress hormone are undesirable in studies such as the one being described in this thesis. Thus, all possible causes of water stress were avoided as much as possible (see section 2.1).

1.10.3 Guard cell response to abscisic acid (ABA)

Abscisic acid has been particularly prominent as a phytohormone responsible for drought and water stress responses in plants, even though other phytohormones such as ethylene, brassinosteroids, jasmonic acid and cytokinins, as well as NO, have also been identified. The hormone abscisic acid (ABA) was first discovered as Inhibitor β, an inhibitor of coleoptile/stem elongation, seed germination and bud growth (Soding (1952) quoted in Dörffling, (2015)). It was also known to inhibit the action of auxin (indole acetic acid) (Went (1928) quoted in Dörffling (2015)). It is involved in management of water stress and developmental processes in plants. It was subsequently, found to be a stress hormone, following the demonstration, in 1969, by Wright, that ABA levels increased 40-fold in leaves wilted in the dark (Wright, 1969). This led Wright and Hiron, in 1969, to conclude after observing that the level of this hormone also increased in excised wheat leaf wilted in the absence of light, that ABA is involved in some of the physiological responses to water stress in plant (Wright and Hiron, 1969). Such responses include stomatal closure. This

conclusion guided Mittelheuser and Van Steveninck, in 1969, to suggest that ABA inhibits transpiration by inducing stomatal closure (Mittelheuser and Van Steveninck, 1969). Application of ABA was used to return a *wilty* tomato mutant to a normal water status and thus confirmed ABA as the hormone controlling plant water status (Tal and Imber, 1971). Pulvinar movements (in *Phaseoulus vulgaris*) have also been shown to be ABA mediated (Lino *et al*., 2001). Brodribb and McAdam (2011), however, showed with lycophytes and ferns that the function of early-diverging vascular plants is independent of epidermal cell turgor and hence of ABA (Brodribb and McAdam, 2011).

The source of the hormone was found initially to be the root tips, from where it is transported to the leaves (Zhang and Davies, 1987), but it has now been conclusively determined that leaf cytosolic ABA is from three sources. In guard cells the sources include *de novo* synthesis (McAdam and Sussmilch, 2016) from xanthoxin, release from inactive conjugated ABA form through cleavage (hydrolysis) of ABA-glucose ester by β-glucosidase (Cornish and Zeevaart, 1986; Schroeder and Nambara, 2006; Bauer *et al*., 2013b) (also see reviews by (Nambara and Marion-Poll, 2005; Finkelstein, 2013) and influx from extracellular sources (Kang *et al*., 2010; Zhang *et al*., 2014). Long standing ABA levels during plant development in *T. virginiana* may cause permanent physiological changes in the plant. For example, *T. virginiana* plants grown under low ABA concentration under high humidity and in a well-watered environment, fail to close stomata fully when challenged with droughting conditions under high humidity (Nejad and van Meeteren, 2007).

Abscisic acid-mediated responses exemplify the conclusions of Trewavas and Malhó (1998) and Jenkins (1998) that the final response of a plant cell to any stimulus is the result of complex interactions or cross-talks between different pathways (Jenkins, 1998; Trewavas and Malhó, 1998). In initiating stomatal closure and inhibiting opening, the mechanism of action of ABA involves both a Ca^{2+}-dependent and a Ca^{2+}- independent pathway. ABA activates the non-selective cation (Ca^{2+}) channels in the plasmalemma to create not only repetitive increases in cytosolic Ca^{2+} (Ca^{2+} transients) but also a decrease in cytosolic K^+ concentration (Schroeder and Hagiwarat, 1990). The Ca^{2+} transients then modulate the cellular responses that lead to stomatal closure. Presence of ABA also causes an increase in cytosolic Ca^{2+} concentrations and primes (enhances) Ca^{2+} ability to activate both the S-type as well as the R–type anion channels. It also inhibits the inward K^+

rectifying channels (Schroeder and Keller, 1992; Siegel *et al*., 2009). A *slow anion channel associated 1* (*SLAC* 1) gene encodes for this anion-conducting unit of the (S-type) anion channel (Negi *et al*., 2008; Vahisalu *et al*., 2008).

Two protein kinase genes, *open stomata* 1 (*OST1*) (Mustilli *et al*., 2002) and Serine-Threonine kinase (*SRK2E*) (Yoshida *et al*., 2002), are critically required for ABA actions. These two genes code for a *SNF 1 RELATED KINASE 2s* (*SnRK2s*) protein. The *OST1*/*SRK2E* contains two domains (I and II) at the C- terminal. Only domain II, but not domain I, is involved in ABA responses (Yoshida *et al*., 2005). ABA and osmotic stress activates the *ost1/srk2e* /*SnRK2s* by allowing auto-phosphorylation at the C-terminal domain II (Yoshida *et al*., 2005). Activation of *SnRK2s* then leads to a non-specific activation of the S-type anion channel by cytosolic Ca^{2+} and also the activation of the R-type anion channel. Increased cytosolic Ca^{2+} also inhibits the inward rectifying K^+ channel and increases the permeability of the anion channels (Schroeder and Hagiwara, 1989; Blatt, 1990). It also activates a *Two pore* K^+ *channel* 1 (*TPK*1) gene which in turn, activates the guard cell vacuolar K^+ channel for vacuolar release of K^+ (Ward and Schroeder, 1994; Gobert *et al*., 2007). These channels when activated, lead to plasma membrane depolarization and drive K^+ efflux through the voltage-dependent K^+ channels encoded by GORK. The *Guard cell outward rectifying potassium* (*GORK*) channel gene is a member of the *Shaker* superfamily of genes and encodes for a membrane bound voltage- and potassium concentration-dependent outward potassium channel (Ache *et al*., 2000; Hosy *et al*., 2003).

Three related genes, *PYRABACTIN RESISTANCE 1* (*PYR), PRY-LIKE* (*PRL*) and *REGULATORY COMPONENTS OF ABA RECEPTOR1* (*RCAR1*) genes which are members of the (*START)* family of genes have been demonstrated to encode the nuclear and cytosolic receptors of ABA known as the *pyra/prl and RCAR* proteins (Ma *et al*., 2009; Park *et al*., 2009). ABA in the cytosol binds to the *pyr/RCAR1* receptors. The binding allows ABA to bind to and inactivate *AB1 and AB2* proteins (Levchenko *et al*., 2005). *AB1 and AB2* proteins are part of the *protein phosphatase type 2c* (*PP2c*) family of proteins which normally dephosphorylate *SnRK2s* and *SLAC*1 in the absence of ABA to prevent the non-specific cytosolic Ca^{2+} concentration-dependent activation of the S-type anion channels (Brandt *et al*., 2015). This inactivation releases the inhibitory effects of the *PP2c* on *SnRK2s and SLAC*1 leading to non-specific cytosolic Ca^{2+} concentration-dependent activation of

the S-type anion channels, activation of the R-type anion channel, increase in the permeability of the anion channels, plasma membrane depolarization, inhibition of inward rectifying K^+ channel, K^+ efflux through the voltage-dependent K^+ channels (vacuolar and plasma membranes) and consequently, loss of turgor which produces stomatal closure and prevents opening. Reactive oxygen species (ROS) may also contribute in triggering this type of stomatal closure (Wang *et al*., 2016). Thylakoid formation 1 (*THF1*) gene forms a complex with High Chlorophyll Fluorescence 106 (*HCF106*) gene. The complex is basically involved in modulating chloroplast functions but also causes elevated reactive oxygen species (ROS) and increased stomatal closure to reduce water loss under water stress (Wang *et al*., 2016).

1.10.4 Guard cell response to temperature

Guard cell response to temperature changes is dependent both on the effect of temperature on saturated vapour pressure in the sub-stomatal space and on its direct effect on the chemiosmotic control of stomata. Increasing temperature increases the photosynthetic rate which leads to reduced CO_2 concentration and consequent stomatal opening. Every 10ºC rise in temp leads to 2 to 4 fold increase in rate of chemical reactions (Taiz *et al*., 2015). A temperature increase of about 10ºC in the bathing medium significantly decreased the activities of outward rectifying K^+ channels and also increased the activity of the inward rectifying K^+ channels in *Vicia faba* protoplasts (Rogers *et al*., 1979; Ilan *et al*., 1995). Thus increasing temperature favours the activities of the inward rectifying channels which lead to stomatal opening. At higher temperatures, the stomata become irresponsive to changes in CO_2 levels and remains widely open (Spence *et al*., 1984). On the other hand, lowered temperature increases apoplastic Ca^{2+} uptake which leads to stomatal closure in chill sensitive species (Wilkinson *et al*., 2001). For its part, saturated water vapour pressure increases exponentially with temperature increase. Thus leaf temperature affects stomatal transpiration rate by changing the saturated water vapour content of air in the substomatal space. This is sensed through the ABA signalling system involved in humidity control (see section 1.9.2). In the experiments described in this thesis, cold light sources were used during all

samplings and stomatal aperture manipulations, and leaf temperature was monitored as an extra measure (see section 2.3).

1.10.5 Stomatal response to CO_2

Elevated internal or external CO_2 leads to stomatal closure. Responses to internal CO_2 levels are more efficient than to external levels (Fitzsimons and Weyers, 1986; Mott, 1988). Guard cell sensitivity to CO_2 is mediated by the *slac*1 protein (Negi *et al*., 2008). The long term effect of high CO_2 level in most plants is a decrease in stomatal density (Royer, 2001). The decrease in stomatal density is effected through an *HIGH CARBON DIOXIDE (HIC)* gene (Gray *et al*., 2000). Raschke (1975) demonstrated in different plants, that CO_2 and ABA responses are linked (Rashke, 1975). Recent research has shown that these two are mediated by a common pathway involving the *pyr/rcar* receptors (Merilo *et al*., 2013) and the *pp2c* proteins (Webb and Hetherington, 1997; Leymarie *et al*., 1998). Stomatal response to CO_2, but not to light or ABA, is mediated by a protein kinase, HIGH TEMPERATURE 1 (*HT*1) protein (Hashimoto *et al*., 2006) and requires the generation of reactive oxygen species (ROS) (Chater *et al*., 2015). Recently, a *RESISTANT TO HIGH* CO_2 (*RHC1*) transporter protein which links increased CO_2 with the *HT*1 has been discovered (Tian *et al*., 2015). Activation of the *ht*1 leads to phosphorylation of *ost*1 and consequent inactivation of *slac*1 which then leads to stomatal closure (Matrosova *et al*., 2015; Tian *et al*., 2015) (refer to section 1.9.3).

Intracellular bicarbonate concentrations have also been linked to guard cell CO_2 responses with the demonstration of varying levels of beta carbonic anhydrase during stomatal response to CO_2 (Hu *et al*., 2010). Increase in the bicarbonate concentrations activates guard cell *ost*1 and *slac*1 proteins (Xue *et al*., 2011) (similar to the ABA pathway). It has thus, recently been concluded that the guard cell CO_2 response is ABA mediated (Chater *et al*., 2015). In *T. virginiana,* early researchers, for example Saito *et al*. (1993), unable to see this link, had thought that the plant's CO_2 response was a dual effect from dissolution and ion (K^+/Cl^-) fluxes. Some plants are, however, insensitive to changes in CO_2 concentration especially under optimum light intensity (Jarvis and Morison, 1981).

1.11 Circadian rhythms in stomata

All functional stomata (not stomata in roots and floral organs) go through rhythmic changes in aperture both in the presence of continuous light or continuous darkness (Heath, 1975; Willmer and Fricker, 1996). A shift in the phase of opening in the dark may occur if the plant is exposed to light at a time that is naturally dark but does not occur if exposure to light occurs at normal light-time of a day (Martin and Meidner, 1972). This appears to be an evolutionary adaptation to changes in day lengths. *T. virginiana* has an endogenous phase-shift in its circadian rhythm (Martin and Meidner, 1971). This may have implications in studies requiring photoactive stomatal opening at during naturally dark hours. Such sampling times were not needed and were generally avoided in all studies described in this thesis.

1.12 Important water-relations properties of the epidermis

An understanding of the water and solute relations of leaf epidermis is fundamental in discussing the osmotically-generated turgor pressure needed for stomatal movements. Water and other solutes arriving from the xylem are destined for cells that are at various distances from positions overlying the leaf vascular bundles. These dissolved solutes traverse cell walls (apoplast) and various membranes (the plasmalemma, possibly tonoplast(s) and membrane of other intracellular compartments) to arrive at these different destination cells. Transport across membranes is discussed in section 1.15. In this section attention shall be paid to transport across the cell wall and plasmodesmata. Transport of water and solutes across the cell wall (apoplast) is by both diffusion and bulk flow. The rate of these processes for individual solutes may be affected by properties of the cell wall.

1.12.1 Cell wall properties of leaf epidermal cells

Plant cell wall is a network of polymers of (90% of dry weight) carbohydrates, (2 – 10 %) protein and (< 2%) lipids interconnected in various ways to give mechanical support to the cell. The carbohydrates include mainly polysaccharides such as

cellulose and pectin. The lipid and protein components are predominantly phenolic esters and glycoproteins covalently bound to different minerals (1 – 5%). *In vivo*, water makes up about 70% of cell wall volume (Monro et al., 1976; O'Neill and York, 2003).

Leaf cells are surrounded by primary cell walls (fig. 1.3). Lignification (secondary cell wall formation) common in woody parts of the plant is absent in most leaves. The cell wall surrounds the outer part of each cell and is joined to (that of) the neighbouring cell by a middle lamella (part of the apoplast) which is composed of various forms of pectin.

Pectin also forms a principal component of the cell wall (Bidhendi and Geitmann, 2016) and its biochemical properties determine the mechanical strength of the primary cell wall (Palin and Geitmann, 2012). Three main types of pectin, rhamnogalacturonan I (RG-I) (7-36%), rhamnogalacturonan II (RG-II) (< 10%) and homogalacturonan (HG) (c.a 60%) exist in cell walls (Mohnen, 2008; Caffalla and Mohnen, 2009). Biochemical changes such as de-esterification, in any of these (types of pectin) lead to changes in cell wall properties. For example, HG maintains cell wall stiffness, but its de-esterification encourages its cross-linking with Ca^{2+} and consequent softening of the cell wall (Palin and Geitmann, 2012). This mechanism is employed in SAM (section 1.4) to enable cell elongation during leaf formation (Peaucelle et al., 2011). RG-I acts to covalently bind with both RG-II and HG (Vincken et al., 2003). It is thought that RG-I is a major constituent of the cell wall of guard cells, and its dominance reduces the proportion of HG. Decreased proportion of HG enable the guard cell wall to be less stiff and allow for expansion (Jones et al., 2003). This is thought to be due to the presence of highly flexible, space-filling arabinan which constitutes a substantial proportion of the RG-I component of cell wall of guard cells (Jones et al., 2003). Cell wall stiffness and tensile strength are also affected by biochemical changes in RG-II. Borate increases the cross-linking of RG-II; leading to decreased wall pore size and increased tensile strength (Fleischer et al., 1999; O'Neill et al., 2001). The lower the proportion of pectin (HG) in a cell wall the more rigid the wall becomes (Dick-Perez et al., 2012).This may be important for the outer, inner and the ventral walls of guard cells. Generally, pectins determine the stiffness, flexibility and thus, pore size of cell wall by controlling the mobility of the cell wall matrix.

The cell wall matrix is composed of the proteins, phenolic esters, hemicelluloses as well as the pectins. The proteins include structural proteins and enzymes. The most common structural protein in cell walls is extensin, a glycoprotein (Ceoper et al., 1987; Mcqueen-Mason et al., 1992). Strands (rods) of cellulose fibres run in several directions within the matrix. Cellulose is a polymer of glucose, and groups together to form micelles and microfibrils. The microfibrils form large groupings of the cellulose fibres that run in the hydrophilic matrix of the cell wall.

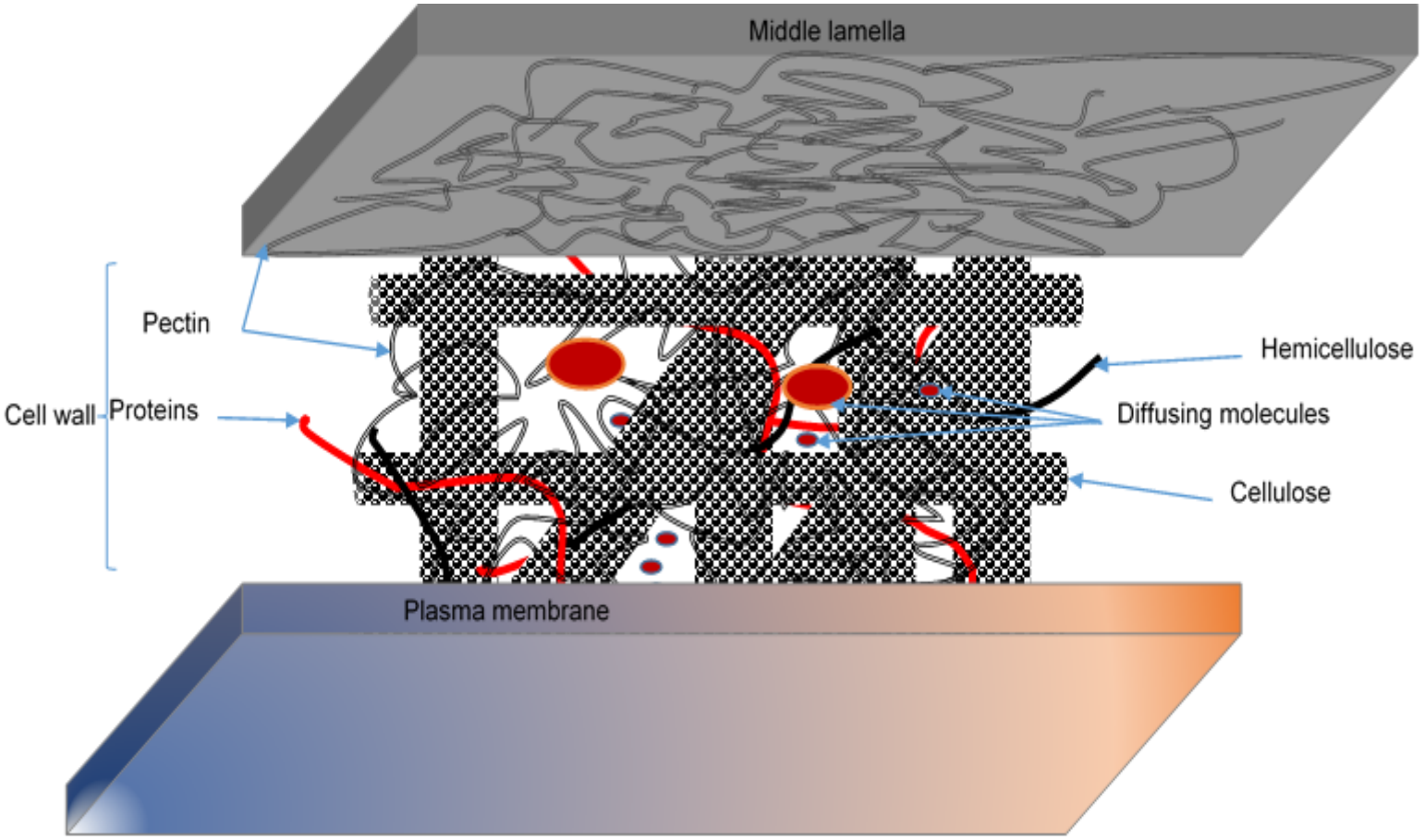

Figure 1.3 Cell wall of leaf epidermal cells
The cell wall is located between the middle lamella and the plasma membrane. It is composed of cellulose microfibrils arranged in several directions in a matrix of pectin, hemicellulose, proteins and little amount of lipids (not shown). Molecules are transported (by diffusion and bulk flow) through pores in the matrix. Small molecules and ions (K^+, Cl^-, etc.) may pass freely through the matrix in the cell wall and through the middle lamella which is made up of pectin.

Microfibrils contain defined hydrophilic and hydrophobic surfaces and are held together by the pectin (Zhao et al., 2014b). Another protein, expansin, reversibly loosens bonds at positions where two or more pectin chains are bonded together (non-covalent bonds) (McQueen-Mason and Cosgrove, 1995; Cosgrove, 2000). This action has been shown to be completed in time scale of minutes and occurs faster at acidic pH (Cosgrove, 2000). This is also important for guard cell wall expansion during turgor driven expansions occurring during stomatal opening (Wei et al., 2011).

The cell wall maintains direct contact with the plasma membrane through Hechtian strands (Lang-Pauluzzi, 2000). Some proteins known as wall associated kinases (WAKs) attach to the pectins, traverse the cell membrane and connect the cell wall to the cytoplasm (He et al., 1996; Wagner and Kohorn, 2001). These form a means of communications between the cell wall and the cytoplasm (Knox, 1997). The signals are sensed and transmitted by conformational changes at the cytosolic and cell wall terminal of these kinases (Knox, 1997). They do not, however, serve as transport routes for any molecule.

Transport of solutes and water across cell walls occur through pores in the wall matrix. In *Commelina* palisade cells, wall pore size is 4.5 – 5.2 nm (Carpita *et al.*, 1979), but generally pore sizes range between 5 and 30 nm (Yeo and Flowers, 2007). Thus, only solutes with sizes of less than 5 nm may move freely across the cell wall. The pore sizes may be varied by biochemical changes that affect the pectin or structural protein contents (commonly extensins) of the wall matrix. In this way the cell wall may restrict or allow the movement of molecules with sizes larger than the wall pore sizes.

The size rather than charge of a molecule is the major determinant of its transport properties within a cell wall. This is because the pore spaces are essentially neutral, since the (usually) fixed negative charges in the walls are counter-balanced by cell-wall-bound Ca^{2+}.

1.12.2 **Cell wall properties of guard cells**

Unlike in other leaf cells, the morphology of the cell wall of guard cells (and pulvini cells) is non-uniform around the cell. Guard cell walls must stretch and recoil within relatively short time frames of few minutes to few hours. For example, guard cells of

Alocasia macrorrhiza open to maximum size within 25 minutes of light (Kirschbaum et al., 1988). Walls of guard cells may thin out during stomatal opening (Sharpe and Wu, 1978; Raschke, 1979). The wall in kidney-shaped guard cells are designed such that the outer and inner walls (fig. 1.4) are thicker than the ventral wall which, in turn, is thicker than the dorsal wall (Meidner and Mansfield, 1968). This is important for guard cell expansion during stomatal opening. While the thicker outer and inner walls do not change during guard cell expansion the thin ventral, more than the dorsal, stretches considerably (Louguet et al., 1990; Willmer and Fricker, 1996). In dumb-bell shaped guard cells the walls at the bulbous ends are also thicker than those at the central parts (Willmer and Fricker, 1996).

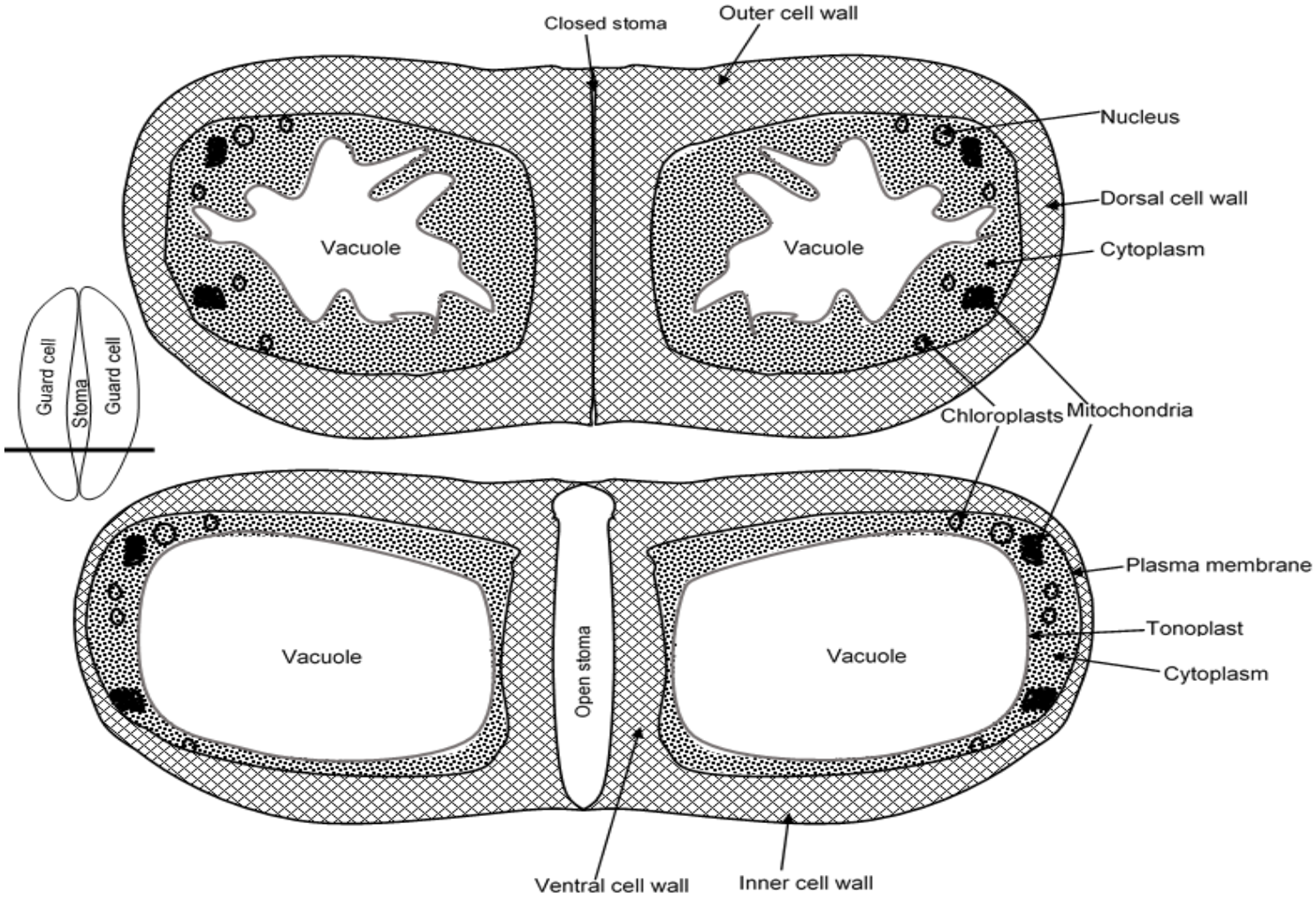

Figure 1.4 Cross-section of guard cells at closed and open conditions of the stoma.
Wall thickness differs on each side of a guard cell – Outer and inner > ventral > dorsal wall. The dorsal wall, becomes thinner during stomatal opening. In open stomata conditions guard cell vacuole enlarges, but reduces and becomes convoluted under closed stomata (for references - see text).

Cellulose forms the major component of all guard cell walls although they are also rich in pectins (Wille and Lucas, 1984; Sack, 1987). Cellulose microfibrils are arranged radially around the stomata in mature kidney-shaped guard cells but have both axial (within the central part) and radial (with the bulbous part) arrangements in dumb-bell stomata (Galatis, 1980). The action of expansins on pectin may also explain the greater extensibility of dorsal guard cell wall which contains greater proportion of pectin relative to other walls. Guard cell wall pH is reduced following H^+ extrusion that creates the membrane potential difference that causes K^+ influx. The reduced pH may enhance the action of expansins in loosening the cell wall for the subsequent pressure-driven expansion (Mcqueen-Mason et al., 1992; Wei et al., 2011). These cell wall properties make for the anisotropic properties of the guard cell (wall) and play very important roles in the water and solute relations of a plant.

1.12.3 Plant water relations

For an ideal solution, the relationship between the solute concentration and osmotic pressure is given by the van't Hoff equation (see section 1.12.5). The osmotic pressure of the solution in the cell determines the cell turgor (Tomos, 2000; Nobel, 2009). The water potential of a solution is the difference between free energy (chemical potential) of water molecules in the solution and that of pure water at the same temperature and pressure. A gradient of water potential exists between vascular bundle cells and epidermal cells (Glinka, 1971; Aylor *et al*., 1973), and water flows down gradients of water potential from vascular to adjacent epidermal tissues.

1.12.4 Cell water potential

Under standard conditions, the water potential of a solution is proportional to the solution's chemical potential of water (Nobel, 2009). Pure, free water at ambient temperature and pressure is commonly used as the reference point and has a concentration of 55.5 molal (Nobel, 2009). Addition of solutes to pure water lowers the concentration of water as well as the water potential of the solution, making it negative, relative to pure water. Thus, solute accumulation in a cell lowers the water the cell water potential. The lowered potential then creates a water potential gradient across

the cell membrane. Water moves down this gradient into the cell to increase its water potential until an equilibrium state (i.e. no net water flow) is attained. The reverse is true when solute is lost from a cell.

Response of epidermal cells to subsidiary and guard cell demand for water is very rapid (half-time of 1 to 100 seconds, though variously reported) (Zimmermann *et al*., 1980; Tomos *et al*., 1981; Malone *et al*., 1989). Movement of water within a plant is characterized by driving forces originating from differences in the potential of the different compartments – organelles, cells and apoplast (Nobel, 2009). Since the addition of solutes lower this potential, within a system with differing solute concentrations water potentials differ inversely according to the concentrations, and water moves down this water potential gradient. Similarly, between two compartments, apoplast and cytoplasm net water movement is into compartments with lower water potential. In both intra and inter-compartmental movements of water, net water movement continues until equilibrium is reached, at which point the net movement of water in the two directions becomes equal.

Solute accumulation (i.e. increase in osmotic pressure) in a cell leads to inflow of water. Increasing the inflow of water to a cell increases the cell's water potential supposing the membrane is selectively permeable to water. Thus, in the absence of any further change in the cell's water potential the increasing osmotic pressure leads to increase in cell turgor pressure – relative to properties of the retaining walls.

Water potential is given as

$$\Psi = P - \pi + \rho_w gh \qquad \text{(Equation 1.1) (Nobel, 2009)}$$

Where

Ψ	=	Water potential	(MPa)
P	=	Hydrostatic pressure	(MPa)
π	=	Osmotic pressure	(MPa)
$\rho_w g$	=	Gravitational component (0.0098 $MPa.m^{-1}$)	($MPa.m^{-1}$)
h	=	(reference) height (m)	

At a cellular level, gravitational component is negligible because the cell height (h) is in the order of few micrometres.

Equation 1.1 can be simplified as

$$\Psi = P - \pi \qquad \text{(Equation 1.2)}$$

If the plasma membrane is semipermeable, at equilibrium, water potential inside equals water potential outside the cell.

Meaning that

$$\Psi_{in} = \Psi_{out} \qquad \text{(Equation 1.3)}$$

Therefore,

$$(P - \pi)_{in} = (P - \pi)_{out} \qquad \text{(Equation 1.4)}$$

Rearranging equation 1.4, gives

$$P_{in} = \pi_{in} - \pi_{out} - P_{out} \qquad \text{(Equation 1.5)}$$

Since the cell wall effective hydrostatic pressure cannot be positive but may be negative due to transpiration tension, cell turgor is then a function of the osmotic pressure (inside and outside of the cell) and the transpiration tension. If the transpiration tension is less than the difference between the intracellular osmotic pressure and that of the apoplast, cell turgor pressure is positive. Under water stress, where the transpiration tension is greater, the cell loses turgor resulting in plasmolysis, which may manifest as wilting.

1.12.5 **Osmotic pressure and osmotic coefficient**

The number of solute particles in a solution is related to the osmotic pressure by van't Hoff equation (Nobel, 2009)

$$\pi = ciRT \qquad \text{(Equation 1.6)}$$

Where

π = Osmotic pressure

C = Concentration of the solution ($mol.kg^{-1}$)

i = A constant (accounts for ionization of the solute and other deviations from a perfect solution)

R = Gas constant (0.831 $l.MPa.mol^{-1}$)

T = Absolute temperature (Kelvin)

This is true for ideal solutions only. In non-ideal solutions, a constant known as osmotic coefficient is applied in order to correct for the interactions between solutes. The osmotic coefficient is the ratio of the measured osmotic pressure to the theoretical osmotic pressure that can be generated by the solute bounded by a membrane under ideal conditions. The ideal condition includes the membrane being completely impermeable to solutes but fully permeable to water. Thus the osmotic pressure of a solution such as cell sap, which contains different solutes, is the product of this

coefficient and the sum of the molal concentrations of all solutes in the solution. The osmotic coefficient can be determined experimentally using freezing point depression method (Robison and Stokes, 2002). This method has been applied previously in our laborlatory for epiermal cells of barley (Hinde, 1994; Fricke *et al*, 1994b) and wheat (Richardson, 1993).

1.13 Plasmodesmata

Plasmodesmata, are 20 to 50 nm diameter tubular extensions of the plasma membrane from one cell to another across their cell walls (Strasburger (1901) quated in Carr, (1976)). They play a key role in the functioning of heterogeneous tissue; the guard cell being a notable exception (Erwee *et al*., 1985; Palevitz and Hepler, 1985). Nevertheless, they account for a substantial proportion of solute movement between other cell types (Erwee *et al*., 1985). Stomatal opening and closing involve movement of solutes across several cells within a short time scale. Plasmodesmata provide the avenue for such solute movements by diffusion and bulk flow. They thus enable direct regulated transport of solutes between cells in a continuum of cell cytoplasm known as the symplast.

1.13.1 Anatomy

Transmission electron micrograph studies of plasmodesmata ultrastructure (Robinson-Beers and Evert, 1991) distinguish two types, simple and branched. Simple plasmodesmata consist of a straight tube while the branched have more than one tube that appear from a central or median cavity and traverse the cell wall in different directions (Ehlers and Kollmann, 2001). Figure 1.5 shows a diagrammatic representation of a simple plasmodesma.

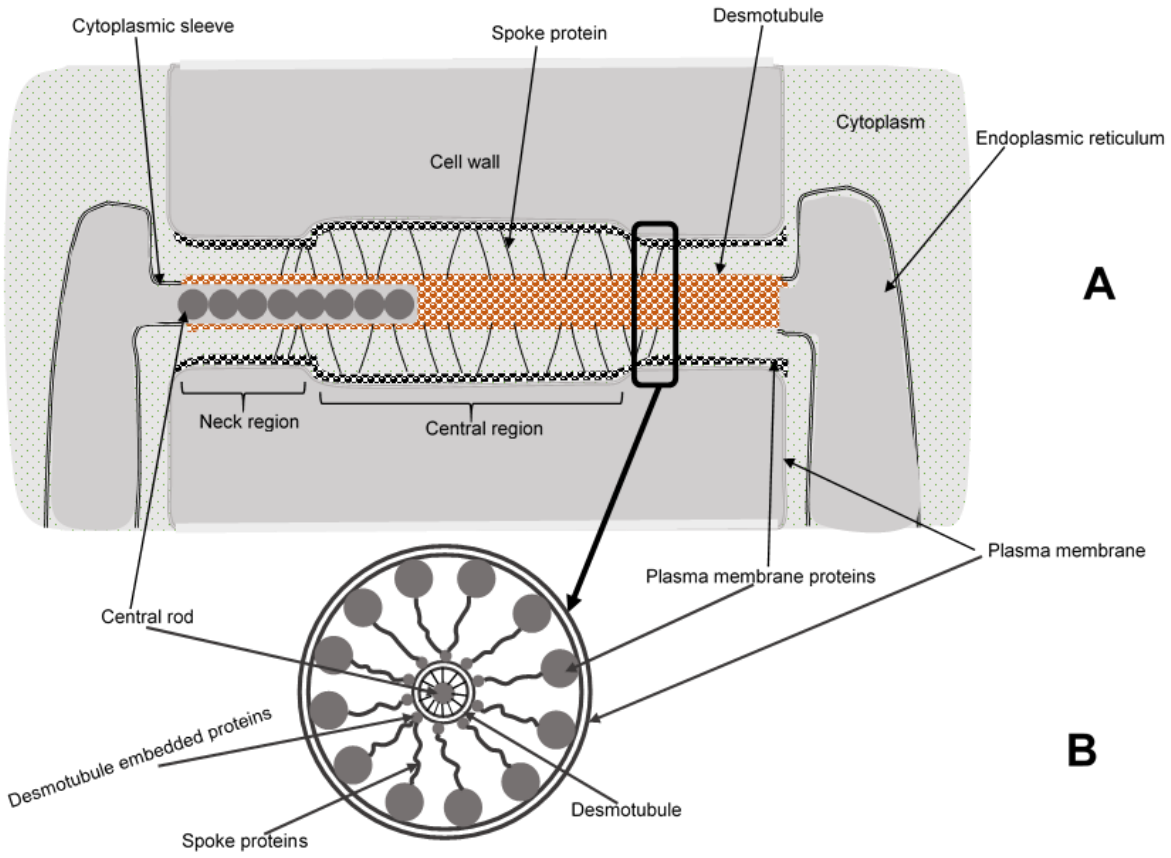

Figure 1.5 Plasmodesmata in longitudinal (A) and transverse (B) sections.
Diagram of electron macroscopic structure of a simple plasmodesma showing the neck regions and the central cavity. Insert shows the arrangement of membrane and spoke-like proteins around the central rod (Robinson-Beers and Evert, 1991).

It consists of a cylindrical sheath that runs across both the cell wall and the middle lamella. The tube is narrower at its orifices and for a short distance towards the centre, forming the neck of the tube at both its ends. The more central portion of the tube is wider, forming the central cavity. The outermost lining of the tube is formed by a continuation of plasma membrane. It is attached to the cell wall on the apoplastic surface and lined by membrane proteins on the cytoplasmic surface. The cytoplasm of neighbouring cells continues into the plasmodesmata as the cytoplasmic sleeve. Within this sleeve, the endoplasmic reticulum (ER) passes from one cell to the other, but is modified into a thicker protein-lined tubular structure known as the desmotubule. The centre of the desmotubule has an electron-dense structure known as the central rod. This is believed to be ER sleeves pressed close together (See Overall, 1999). Also within the cytoplasmic sleeve, cytoskeletal

proteins, actin and myosin, run between the plasma membrane- and desmotubule-embedded proteins (Overall and Blackman, 1996). Such structure is also seen within the desmotubule cavity, connecting the central rod to the desmotubule (Ding et al., 1992).

1.13.2 **Physiology**

The neck region of plasmodesmata contains a sphincter composed of closely-packed globular proteins on the cell membrane in close proximity to the desmotubule (Olesen, 1979). The neck region therefore, forms the size exclusion zone (SEL) which controls both the rate and the direction of solute movement through plasmodesmata (Olesen, 1979). Exchange of molecules between cells occurs through spiralling micro channels created by actin and myosin spoke-like extensions which run through the cytoplasmic sleeve and are attached to the plasmalemma and desmotubule proteins (Overall *et* al 1982; Wolf *et al* 1989; Lucas and Wolf, 1993). Non-selective transport of small solutes (< 1 KDa) occur through these channels (Goodwin, 1983). The SEL in epidermal cell plasmodesmata is, however, relatively smaller (c.a. 674 Da in *Egeria densa*) (Erwee and Goodwin, 1985). In this species, movement of injected dye between epidermal cells was several fold faster; being $1.1.10^{-4}$ cm. s^{-1} for smaller sized (376 Da) dye and $9.0.10^{-9}$ cm. s^{-1} for a larger (874 Da) sized dye (Goodwin and Erwee, 1990). Aside from this transport mechanism which is controlled in the SEL, another form of plasmodesmatal transport occurs following targeting of molecules to plasmodesmata, depending on conditions such as branching or otherwise (Oparka *et al*., 1999). This is the mechanism involved in the transport of proteins (up to 50 KDa) and transcription factors (Blackman and Overall, 2001) as well as transport of plasmodesmata-targeted proteins used for signal transduction and viral migration (Ehlers and Kollmann, 2001).

Such transports as these do not continue into guard cells as these lack plasmodesmata. The disappearance of all plasmodesmata in the mature guard cell may be important both for the control of the movement of signalling molecules and other solutes (Majore et al., 2002) as well as in aiding the rapid increase in turgor required for stomatal opening. This has been shown in cotton fibres where transient closure of plasmodesmata allow for the increase in turgor required for rapid

elongation (Pfluger and Zambryski, 2001; Ruan et al., 2001). Perhaps for this reason also no plasmodesmatal connections exists between the two mature sister guard cells of a stomatal complex (Erwee et al., 1985).

Plasmodesmata in other cells around the guard cell also have some peculiarities. They may be dilated to different degree that may allow passage of molecules as large as 27 KDa (such as green fluorescent protein) or double this size (Crawford and Zambryski, 2001). The proportion of the dilated plasmodesmata, dilated-low or dilated-high (Crawford and Zambryski, 2001) depends mainly on leaf age. The latter is more common in younger leaves since they require more protein movements (Crawford and Zambryski, 2001). The frequency of plasmodesmata between leaf epidermal cells has been estimated in *Populus deltoids* to be 0.05. μm^{-1} of cell wall interface in abaxial and 0.06. μm^{-1} of cell wall interface in adaxial epidermis (Russin and Evert, 1985). The frequencies in the different epidermal cell types has not been documented to date.

1.13.3 **Development of plasmodesmata**

Plasmodesmata may develop as primary plasmodesmata during cytokinesis or as secondary plasmodesmata post cell-division (Hepler, 1982; Staehelin and Hepler, 1996). Primary plasmodesmata are formed where the cytoplasmic strands that enclose some endoplasmic reticulum are trapped among fusing Golgi vesicles in an assemblage of materials (microtubules, microfilament, Golgi vesicles and endoplasmic reticulum) called the phragmoplast. The phragmoplast forms the cell wall plate during cell division (Staehelin and Hepler, 1996). This occurs in late anaphase, before the completion of the new cell wall. As the cell plate matures and grows, the trapped strands become increasingly constricted within the plasmalemma which is formed by the (trapping) Golgi vesicles. The enclosed endoplasmic reticulum forms the plasmodesmal desmotubule, but remains connected to the endoplasmic reticulum of the two sister cells (Staehelin and Hepler, 1996).
Most primary plasmodesmata (> 90%) are simple (unbranched), especially in immature cells (Oparka *et al*., 1999), but some may develop branching (Ehlers and Kollmann, 1996) which increases in proportion, in monocot leaves, as they move from sink to source of photosynthetic products (Roberts et al., 2001). The

significance of branching is not clear but most secondary plasmodesmata are branched.

Secondary plasmodesmata form, either from simple ones or *de novo* in an expanding cell, mainly due to inadequacy of the existing simple ones as the cell expands (Schnepf and Sych, 1983; Seagull, 1983). The molecular details of primary and secondary plasmodesmata formation is not yet elucidated in terms of the controlling genes.

The frequency of plasmodesmata in cells vary widely between species and cell types, generally ranging between 0.01 and 50 μm^{-1} (Robards, 1976). In leaf primordia, the plasmodesmata developed between the GMC and the SMC or pavement cell during the differentiation of the epidermis become sealed as the walls thicken just before the development of the stomatal pore (Wille and Lucas, 1984; Erwee *et al*., 1985; Palevitz and Hepler, 1985). The reason for this blockage is as yet unknown.

At this time, after the development of the primary, and before the development of secondary plasmodesmata, the development of the individual cell identities, the transport systems and other metabolic processes that will determine the functional intervention between adjacent cells are laid down. It is the activity of these processes that dictate the physiological behaviours that is the major subject of this research project.

1.14 The vacuole

The vacuole is a single-membrane-bound organelle found in most cells of plants. In mature plant cells, the vacuole occupies the greater portion of the cell volume especially in the epidermal cells. The mature plant vacuole may be single, as in the epidermal pavement cells, or multiple (some small and some large) as in flaccid guard cells, storage vacuoles in fruits and seeds, or in specialized cells such as the pulvini cells (Paris *et al*., 1996; Epimashko *et al*., 2004). For example, in pulvini motor cells of *Mimosa pudica,* Toriyama and Sato (1968) and later, Fleurat-Lessard *et al.* (1997), observed two functionally complementary vacuoles, tannin and colloidal vacuoles. While the colloidal vacuoles contained the osmotically-active solutes and

thus swell under appropriate hypotonic conditions, the tannin vacuole contracted reciprocally (Toriyama and Sato, 1968). Vacuoles thus play very important roles in plant physiology being central to turgor regulation involved in cell expansion, growth and stomatal aperture control (see review by Martinoia *et al.* (2006)).

The different vacuole forms are distinguished by a protein type found only in the tonoplast, the tonoplast intrinsic protein (TIP). Different combinations of α, δ and γ-TIP forms determine the vacuolar function. Vacuoles with tonoplasts containing only δ –TIP are storage, while ones with only γ-TIP are lytic vacuoles (Jauh *et al*., 1999). Tonoplasts of protein storage vacuoles of seeds may contain all three forms of TIP (α, δ and γ), while pigment and protein storage vacuoles in vegetative parts of plants contain δ and γ-TIPs in their tonoplast (Jauh *et al*., 1999). Plant vacuole thus, serve different functions dependent on their TIP constitution.

In this line, vacuoles may function as storage organelle for metabolites, organic and inorganic osmotica, colloids, or to save energy and nutrients in times of abundance. They also function to maintain optimum working conditions in cytosol and as sites of osmotic manipulations of the cell (Rogers, 1998; see also Wagner (1982)). The osmotic properties in the vacuole create the required turgor for the mechanical support of the plant tissue (contrast with wilting) and when needed, also create reversible cell/tissue or organ movements, such as pulvini and stomata (Irving *et al*., 1997).

The mature plant vacuole is more acidic and more aqueous (less protein content) than the cytosol. This, together with the availability of many membrane-bound transport systems, aid in its fast response to environmental conditions. The tonoplast transport systems are classified as ion channels, ion antiporters or proton pumps. The ion channels include the slow- and fast-activating channels, the Ca^{2+}- and malate-selective channels and the tonoplast intrinsic protein (TIP). These are complemented by the TIP-like aquaporin for water transport. Na^+/H^+ (Blumwald and Poole, 1985, 1987) and Ca^+/H^+ antiporters (Blumwald and Poole, 1986) (which can be respectively inhibited by amiloride and verapamil) have been determined as tonoplast ion antiporters also. Studies in *Mesembryanthemum crystallinum*, a model halophyte, demonstrated that increased cytosolic Na^+ ion induces production of Na^+/H^+ antiport proteins (Barkla *et al*., 1995). The proton pumps have been identified as an H^+- ATPase (V-ATPase) and H^+-pyrophosphatase (V-PPase). These function as proton translocating pumps (King *et al*., 2004).

The tonoplast membrane potential is 20 to 30 mV more positive than that of the cytosol. This maintains an electrical gradient which aids inorganic anion accumulation in the vacuoles (Taiz *et al*., 2015). The electrochemical potential gradient generated by the H^+-ATPase activity in the tonoplast drives the accumulation of cations and organic solutes (Taiz *et al*., 2015). In the guard cells, the SV channels sense intracellular (cytosolic) pH and Ca^{2+} concentration and respond by allowing the release of Ca^{2+}, K^+ and Cl^- (Schulz-Lessdorf and Hedrich, 1995). The sensing is mediated by calmodulin, the Ca^{2+} binding protein (Bethke and Jones, 1994). Humble and Raschke (1971) observed in *Vicia faba* that more than 90% of the K^+ (solutes) moved out of the guard cell during stomatal closing were vacuolar in origin (Humble and Raschke, 1971). The disproportionately larger size of the vacuole compared to the cytosol, permits a presumption that the sap samples analysed in the experiments described here are mainly vacuolar in origin.

1.14.1 **Heterogeneity in solute content of cell types**

Plants are permanently sedentary as a body but their body parts are variously capable of active movements, often within the range and time scale found in animals. Example of these forms of movement include the pulvinus movements in leaves (e. g. in *Phaseolus*), the opening and snapping movements of the carnivorous Venus flytrap plant, and very commonly, the opening and closing movement of stomata on plant leaves. These movements have been shown to occur due to differential pressure gradients created by differences in the distribution and redistribution of intracellular vacuolar solutes between cells or tissues. Differences in content and/or concentration of solutes may be found between leaf surfaces, along the longitudinal axis of a leaf – from base to tip (Nagai *et al*., 2013). The role of and the mechanisms behind cell-specific solute distribution in plants is poorly understood (Conn and Gilliham, 2010). The reason for these heterogeneous solute distribution is thought to be to enhance the function of tissue parts that have better anatomical positions enabling a more efficient osmotic adjustment or detoxification mechanism(s) for the plant (Gonzalez *et al*., 2002; Shapira *et al*., 2009). These differences may also arise in a bid to create a physiologically-conducive charge balance in the cell(s). These distribution patterns may be species-specific. Dietz *et*

al., (1992) suggested that the preferential accumulation of PO_4^{3-} found in the epidermis of *Lupinus* and *Vicia,* but not in *Sorghum* and barley epidermis, is due to species-specificity (Dietz *et al*., 1992). Family-specific compartmentation of solutes has also been noted in Fabaceae and Poaceae for chloride, calcium and phosphate (Dietz *et al*., 1992). Heterogeneity may also be due to differences in nutrient supply. Flavonol glysosides particularly kaempferol and quercintin aglyecones substituted for sulphates and glucueronates in guard cells of *A. cepa* (Weissenbock *et al*., 1987). Some workers, however, (see (Weissenbock *et al*., 1987) opine that the expression of these differences (quality and quantity) is driven by transpiration. Generally, ions/solutes that may combine to form insoluble products are not compartmentalized in the same location. For example Ca^{2+} and PO_4^{3-} are separated to prevent formation of insoluble $CaPO_4$ in the cell (see Conn and Gilliham, 2010).

The single cell 'omics' analysis - genomics (e.g. (Kalisky and Quake, 2011), transcriptomics (e.g. (Tang *et al*., 2011), proteomics (e.g. (Dai and Chen, 2012) and metabolomics (e.g. (Takashi *et al*., 2015), have collectively shown unequivocally, the vast differences in the content(s) and functions of individual cells in a tissue. These differences are found even between cells from same mother cell linage (Armbrecht and Dittrich, 2016). These functional differences in the content and concentrations of ionic solutes in individual cells of the epidermis have been studied in this project with a view to understanding qualitatively and quantitatively, the contributions of these individual cells and/or cell types to overall (hydraulic) control of stomatal movements. Knowledge of this differential compartmentalization and, to some extent, redistribution, has been employed in phytoremediation and phytoextraction studies in contaminated sites (Tandy *et al*., 2013). Stomatal aperture control is known to be effected ultimately by changes in intracellular solute concentrations in guard cells (Humble and Raschke, 1971; Zeiger, 1983) and the immediate surrounding cells (Heath, 1975). These surrounding cells differ between plant families. In monocots (*T. virginiana*, for example) the guard cells are surrounded at the lateral and medial, as well, as the distal and apical, aspects by cells known as subsidiary cells which, together with the guard cells form the stomatal complex. In *Commelina* and especially in *Tradescantia* these (complexes) are very uniform and predictable, as well as large, making them ideal subjects for the type of study described in this project.

1.15 Solute transport in the epidermis

Land plants are generally unable to change their physical locations and so, need to respond efficiently to environmental cues in order to thrive. The responses, as exemplified by stomatal responses, require changes in intracellular pH and solute concentrations. Changes in solute concentration within the apoplast may occur by bulk flow or, within short distances, by diffusion. Intracellular concentration changes require movement of solutes and/or H_2O across membranes. Solute transport processes across all plant membranes are similar, being either by diffusion – directly or through channels/pores, or by active – primary or secondary, transport. The rate of transport of these solutes, however, differs between cell types, depending on plasmodesmatal frequency (see section 1.13) and the number of transport proteins located on the cell membrane. For example, K^+ channels are few in mesophyll cells but abundant in guard cells (Ache *et al*., 2000).

Trans-membrane transport of ions require energy, which in plants, is generated from proton motive force created by both tonoplast and plasma membrane-bound H^+-ATPase (Zeiger, 1983; Sze, 1985). This creates electrochemical gradients across the membranes, and relative to the outside keeps the cytoplasm negatively charged and less acidic than the vacuole and the apoplast (Kurkdjian and Guern, 1989).

1.15.1 Cation transport

1.15.1.1 Potassium transport

For cations, the electrochemical gradient so generated drives K^+ down its electrochemical gradient into the cell through mainly voltage-gated K^+ channels (Schroeder *et al*., 1987; Fairley-Grenot and Assmann, 1993). Voltage-independent channels have also been identified in plasma membranes, but are not common in guard cells (Roelfsema and Prins, 1997). The voltage-dependent channels include outward-rectifying and inward-rectifying channels which respectively permit efflux and influx of K^+ depending on the voltage across the plasma membrane. While the outward K^+ channels are activated at depolarizing potentials (usually -50mV), and

depend on extracellular K^+ concentrations, the inward channels are activated at a more hyperpolarizing potential (usually more negative than -100mV), and are independent of K^+ concentrations (Roelfsema and Prins, 1997). Cytosolic K^+ concentration is, however, regulated closely (Leigh *et al*., 1996) by a tonoplast transmembrane H^+/Na^+ or K^+ antiporter protein, *nhx* (Blumwald and Poole, 1985). This protein enables sequestration of cytosolic K^+ into vacuoles against vacuolar membrane potential (Gaxiola *et al*., 1999). The cytosolic K^+ concentration is maintained approximately constant, while vacuolar concentrations may vary in order to maintain this cytosolic concentration required by K^+-dependent processes (Leigh and Wyn Jones, 1984; Leigh *et al*., 1996). The control of vacuolar K^+ and Na^+ concentration is pH dependent. The luminally-placed c-terminal of *nhx* protein binds to calmodulin at acidic pH leading to preferential H^+/K^+ antiporter activity (fig. 1.6). At alkaline pH, the calmodulin binding dissociates, and H^+/Na^+ exchange is favoured (Yamaguchi *et al*., 2005). Thus, both maintenance of the plants water status and stomatal opening benefit from the activities of the *nhx* protein (Barragán *et al*., 2012; Andrés *et al*., 2014).

Fast and slow vacuolar (FV and SV) K^+ channels exist in the tonoplast. These function to release K^+ from the vacuole into the cytoplasm at depolarizing tonoplast potential (more positive on cytoplasmic side). The SV is more abundant, and may also serve as a channel for K^+ transport into the vacuole at very high depolarization (Ivashikina and Hedrich, 2005). In guard cells, another type of vacuolar K^+ channel, simply known as vacuolar K^+ (VK) channel also exists (Ward and Schroeder, 1994). This channel allows K^+ movement into and out of the vacuoles to allow for K^+ homeostasis at sub-activation membrane potentials (Allen *et al*., 1998).

1.15.1.2 Sodium transport

Sodium entry from the apoplast is aided by cell membrane-bound HKT (high sensitivity K^+ transporter) 1 proteins (Rubio *et al*., 1995; Gassmann *et al*., 1996). Cytosolic Na^+ normally ranges between 1 and 10 mM in non-halophytes (Binzel *et al*., 1988). In the halophyte *Cakile maritima* Na^+ accumulates in guard cells and replaces K^+ as the major osmoticum for stomatal movements (Eschel *et al*, 1974 quoted in Willmer and Fricker (1996). This, though, has not been reported in any other halophyte. Excess cytosolic Na^+ inhibits protein synthesis (Hall and Flowers,

1973), photosynthesis (Tsunekawa *et al*., 2009) and several enzymatic reactions, such as enzymes in methionine biosynthesis pathway (Murguia *et al*., 1995). Thus, halophytes sequester excess Na^+ in vacuoles (Blumwald, 2000). This is achieved by using an NHX-type Na^+/H^+ antiporters in the tonoplast (Blumwald, 2000).

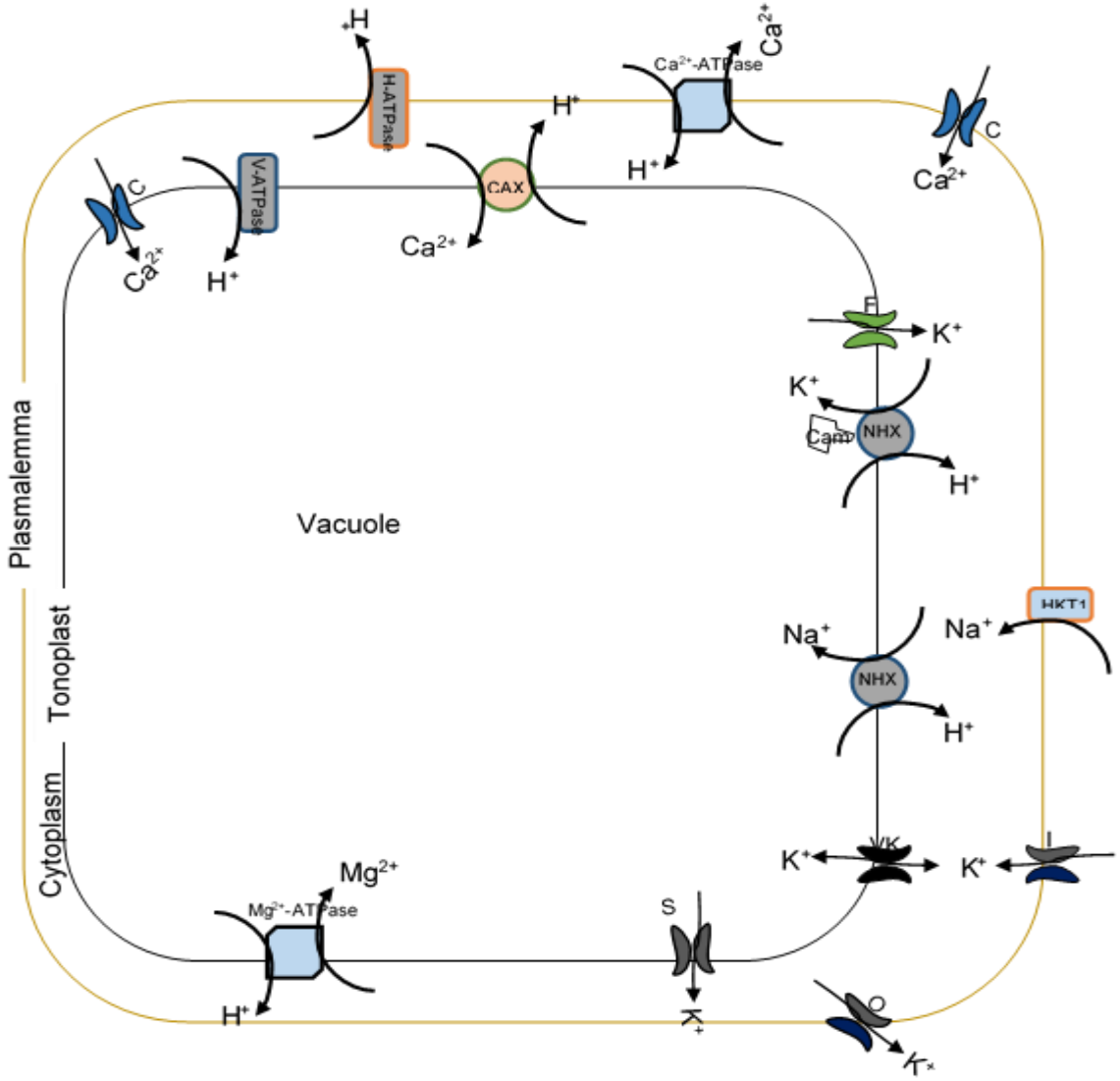

Figure 1.6 Cation carriers and channels in epidermal cells
This figure shows major cation channels and carriers in a typical plant epidermal cell. Calcium channel, C, and CAX protein in tonoplast sequester Ca^{2+} into vacuole. Ca^{2+}-ATPase causes Ca^{2+} efflux from cytoplasm to apoplast. Fast, F, and slow, S, K^+ vacuolar channels release vacuolar K^+. In the plasmalemma, the outward rectifying, O, and the inward rectifying, I, K^+ channels effect K^+ efflux and influx respectively. The *nhx* protein complexed with calmodulin preferentially sequesters K^+ into the vacuole. When free, it moves Na^+ instead. The H-ATPase in the plasmalemma and the V-ATPase at the tonoplast respectively pump H^+ from the cytoplasm into the apoplast and vacuoles and create the electrochemical gradients needed for ionic movements through the channels (for references see text above).

In glycophytes low cytosolic Na^+ is maintained by plasma membrane H^+-ATPase which extrudes excess Na^+ (Blumwald, 2000; Hasegawa, 2013).

1.15.1.3 Calcium transport

Transport of Ca^{2+} is of special importance to plants since Ca^{2+} also serves many signalling roles (see review by Dodd *et al.* (2010)) in addition to its roles in strengthening cell walls, stress protection (Liqun *et al*., 2009) and a counter-ion to vacuolar anions. Influx and efflux of Ca^{2+} across plasma membrane is through depolarization-activated, hyperpolarization-activated or voltage-independent Ca^{2+} channels (Miedema *et al*., 2001) as well as membrane-bound Ca^{2+}-ATPase, which extrudes Ca^{2+} from cytosol. Depolarization-activated channels are thought to be involved in Ca^{2+} transports during signalling, and hyperpolarization-activated channels mediate other functions including Ca^{2+} movements during stomatal opening (Hamilton *et al*., 2000). Calcium may also move across the plasmalemma or tonoplast through non-selective cation channels, which allow movement of both monovalent and divalent anions (see review by Demidchik *et al*. (2002)). While the Ca^{2+}-ATPase at the plasma membrane moves cytosolic Ca^{2+} extracellularly, a tonoplast protein family, Ca^{2+}/H^+ exchanger (CAX) proteins, also moves cytosolic Ca^{2+} into the vacuole (Hirschi *et al*., 1996). Thus cytosolic Ca^{2+} is kept very low (120-360nM) (Gilroy et al., 1989), except during transients (sudden increases) for signalling purposes. High cytosolic Ca^{2+} acts through the ABA signalling pathway to cause stomatal closure. Increase in extracellular Ca^{2+} may lead to high intracellular concentrations (Mcainsh *et al*., 1995). These changes are detected by Ca^{2+} sensors (CAS) in the plasmalemma (Han *et al*., 2003). Ca^{2+} sensors have been used for quantifying Ca^{2+} concentrations in endoplasmic reticulum (60 – 400 µM) (Miyawaki et al., 1997), guard cells (Siegel et al., 2009) and in relation to ABA changes during stomatal movements (Waadt et al., 2014; Brandt et al., 2015). By this means, extracellular Ca^{2+} concentrations are maintained low by increasing its sequestration in the vacuole (Hirschi *et al*., 1996).

1.15.1.4 Magnesium transport

Vacuolar sequestration of Mg^{2+} is also employed in regulating ion balance in cytosol and control of stomatal movements. Transport of Mg^{2+} across tonoplast and plasmalemma is through H^+/Mg^{2+} exchanger (Amalou *et al*., 1992, 1994; Pfeiffer and Hager, 1993; Shaul *et al*., 1999).

1.15.2 Anion transport

Anions are generally transported across guard cell and other epidermal cell membranes through tonoplast and plasma membrane-bound non-selective anion channels (Hedrich and Marten, 1993; Schmidt and Schroeder, 1994; Pei *et al*., 1996). In guard cells two types, rapid (R)-type (Keller *et al*., 1989) and slow (S)-type (Schroeder and Keller, 1992) anion channels have been characterized. Both channel types are depolarization-activated, but while the R-type channels can be activated by hyperpolarization, the S-type channels are insensitive to it (Linder and Raschke, 1992; Schroeder and Keller, 1992; Kolb *et al*., 1995).

These channels are permeable to all anions, which mostly move out from the cytosol (near neutral pH) into the more acidic vacuole and apoplast (see Kurkdjian and Guern (1989)). The pH differences between the compartments (vacuole, cytosol and apoplast) favour efflux of some anions, especially the carboxylic acids (citrate, malate, tartrate and succinate), since their protonation in the more acidic compartments establishes an electrochemical gradient. In addition, negative membrane potential, negative on cytosolic side (-100 mV), also helps drive anions out of the cytosol when the channels open. Anion sequestration in the vacuole is made possible by function of H^+/coupled co-transport proteins, such as H^+/NO_3^- (De Angeli *et al*., 2006) and H^+/malate (Emmerlich *et al*., 2003) co-transports.

As well as the non-selective anion channel some channels are selective to specific anions. These may play special roles, such as in salt tolerance and stomatal movements by Cl^--selective channels (Muelleri *et al*., 1994; Jossier *et al*., 2010), nitrogen balance and organic regulation by NO_3^-- selective channels (Guo *et al*., 2003) or pH regulation by organic acid (e.g. malate)-selective channels (Meyer and De Angeli, 2010; Geiger *et al*., 2011) (see fig. 1.7).

Most of these anion channels are voltage gated (Hedrich *et al*., 1990). Their activation depolarizes the membrane (Roelfsema *et al*., 2012) and thus in guard cells, leads to K^+ release since this brings the membrane potential to a level more positive than the Nernst's potential (E_m) for K^+. In this manner, activation of anion channels, such as occurs in response to ABA (see review by Kim *et al.* (2010)), evokes efflux of K^+ by activation of the voltage-gated outward rectifying K^+ channels and consequently closes the stomata (section 1.11.2).

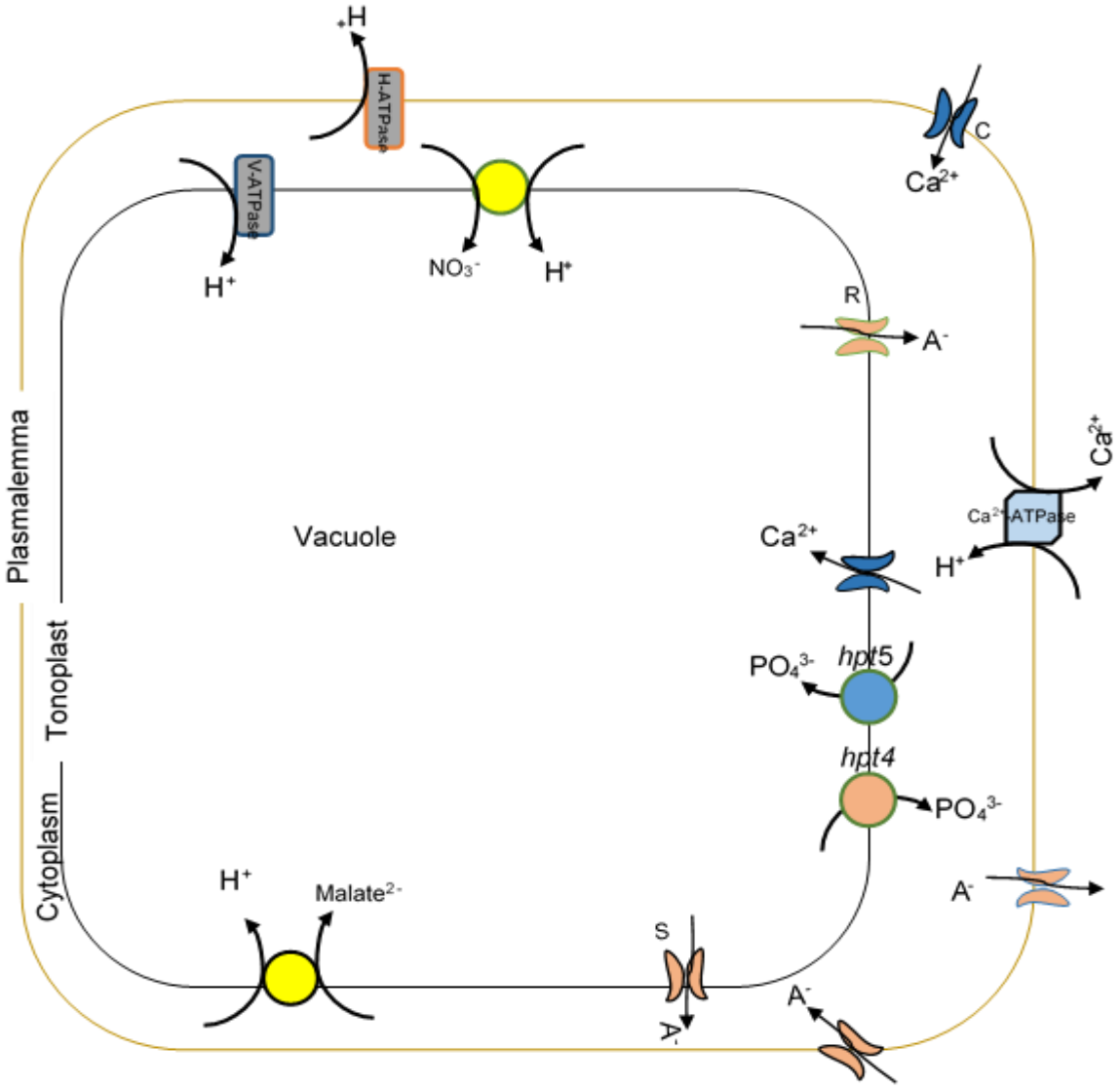

Figure 1.7 Anion carriers and channels in epidermal cells.
This figure shows channels and carriers involved in anion transport in plant epidermal cells. Rapid, R, and slow, S, anion channels are found in the tonoplast. Non-specific anion channels also abound in the plasma membrane. Malate and NO_3^- may be sequestered in the vacuole by symport with H^+. The *vpt*1 group of proteins (*hpt* 4 and 5) are involved in vacuolar PO_4^{3-} efflux and influx respectively. Ca^{2+} transporters have been shown to emphasize its importance in balancing of negative charges in the cell (for references see text above).

Phosphate transport in leaf cells does not, however, use the anion channels (Massonneau *et al*., 2000). Active transport is involved (Mimura *et al*., 1990), and VPT1 (vacuolar phosphate transporter 1) protein (also known as PHT5;1 (Phosphate transporter 1) functions at vacuolar membrane to sequester PO_4^{3-} into vacuoles (Wang *et al*., 2012; Liu *et al*., 2016). Vacuolar release of PO_4^{3-} is also through active transport by tonoplast-bound *pht*4;1 protein (Wang *et al*., 2015), a member of the same gene family SPX-MFS (major facilitator superfamily). In roots, *pht*1 proteins, also a member of the *mfs* family, are responsible for PO_4^{3-} uptake from soil into the cell cytosol (Misson *et al*., 2004; Shin *et al*., 2004). Similar proteins may also function in leaf cells for PO_4^{3-} transport across the plasmalemma, but research is on-going in this area (Rausch and Bucher, 2002; Luan *et al*., 2017). These work to maintain cytosolic PO_4^{3-} at 60 – 80 µM (Pratt *et al*., 2009). Most leaf PO_4^{3-} is, however, found in the mesophyll, while the epidermis has lower concentrations.

The *pht*1 protein is also involved in SO_4^{2-} transport across plasma membranes in roots (Preuss *et al*., 2010). Genes for these proteins are mainly expressed in roots, and the proteins serve as SO_4^{2-} - H^+ or $H_2PO_4^-$ - H^+ symporters (Smith, 2001). Sulphate transporter and/or transporters at leaf cell and vacuolar membranes have not been characterized to date.

1.16 Other considerations

The various movements of (these) charged, and possibly other uncharged solutes, form the basis of active stomatal movements. Transport of these solutes underpins the core studies discussed in this thesis, which describes, qualitatively and quantitatively, the solute concentration and consequent osmotic pressure changes involved in stomatal movements. Their transport across plasmalemma and tonoplast, in the main, is currently well understood (Santelia and Lawson, 2016). Equally, the changes in K^+ concentration and the patterns of these changes during stomatal movements have been well elucidated (MacRrobbie and Lettau, 1980; Zeiger, 1983; Schroeder, 1988; Blatt, 1992; Gao *et al*., 2017). Chloride and/or malate concentration changes involved in stomatal movements are much less understood (MacRrobbie and Lettau, 1980; Schnabl and Raschke, 1980; Azoulay-Shemer *et al*.,

2015; Azoulay-Shemer *et al*., 2016; Blatt, 2016; Daloso *et al*., 2016; Santelia and Lawson, 2016). In contrast, changes in NO_3^- concentration are relatively hardly described, while the participation of other ionisable and non-ionisable solutes are altogether almost unreported.

However, following the elucidation of K^+ concentration changes and their effect (Zeiger, 1983; Schroeder, 1988), knowledge of the full cohort of solutes involved in stomatal movement and their distribution in all the participating cells has remained limited despite decades of research on stomatal function (Taiz *et al*., 2015). Santelia and Lawson (2016) observed, among other things, that "challenges are evident in obtaining sufficient quantities of uncontaminated guard cell materials for biochemical assays at known time points or under specific environmental conditions". Heath (1975) had observed that "the tedious but beneficial task of conducting such biochemical assays at single cell resolution in a large number of cells was needed for a good understanding of stomatal function". Such observation was re-echoed by Shabala and Newman (1999) for a definitive determination of ion fluxes across plasma membranes in both epidermis and mesophyll.

Since the mid-1850s, it has been known that the subsidiary cells participate in stomatal control by tending to prevent opening and assisting in closure of stomata by pressing on the guard cells (Von Mohl (1856) quoted in Williams (1954)). Several researchers, such as Heath (1938), Meidner (1968), DeMichele and Sharpe (1973) and MacRrobbie (1980) have corroborated this finding. Bowling (2016) stated that in *Commelina communis*, all cells of the epidermis participate in stomatal movements with respect to solute redistributions. This suggests that similar solute concentration-driven osmotic changes may occur in all the other cells of the epidermis during stomatal movement. MacRrobbie (1980) showed that in order to maintain a certain stomatal aperture, guard cell turgor pressure may increase by 3.7 to 4.7 fold per unit increase in subsidiary cell turgor. The spatial and temporal distribution and/or redistribution of these solutes among all these participating cells, as well as the nature of the solutes is unknown to date.

This lag in knowledge has been attributed mainly to lack of robust techniques for the biochemical analysis of sap at cellular resolution especially under physiological conditions *in planta* (see Santelia and Lawson (2016)). Genetic manipulation of guard cells aimed at reducing stomatal conductance while increasing

stomatal frequency and improving water use efficiency (see Condon *et al*., 2004) in plants have yielded few, albeit encouraging, results.

It must be appreciated that solutes can only move between the mesophyll and guard cells through the pavement cells, since these are the only epidermal cells contacting the mesophylls (see fig. 1.2). This also implies that this mesophyll-to-epidermis contact decreases with increase in stomatal density.

Improvement in results from these aspects of plant physiological properties may benefit more from manipulations of the surrounding cells. In this sense, knowledge of the behaviour of these cells in terms of solutes accumulated or released during stomatal movement is invaluable for targeting membrane transporters of interest.

Thus, since cells surrounding the guard cells in the epidermis also participate in orchestrating stomatal movements through solute concentration change-driven turgor adjustments (Heath, 1938; Williams, 1954; Meidner and Mansfield, 1968; DeMichele and Sharpe, 1973; MacRrobbie, 1980), these changes must occur in a coordinated and predictable manner. It is, therefore, hypothesised in this research that solute concentration gradients exist within the cells of the epidermis, and these gradients drive stomatal movements in leaves under physiological conditions.

Studies on stomatal movement in epidermal strips (Levitt, 1974; Azoulay-Shemer *et al*., 2016) have confirmed that the control of stomatal aperture is entirely an epidermal affair. Hence, while stomata on strips placed in distilled water may open (Pallaghy, 1971; Willmer and Pallas, 1974), those of isolated guard cell-pairs (in the same medium) fail to do so.

The ionized solutes (cations and anions) appear to be the central players in stomatal physiology, and their redistribution patterns at open and closed stomata conditions is specifically described here.

1.17 Analytical techniques used to study the solute patterns in stomatal movements

Stomatal movements result from changes in guard cell turgor (MacRrobbie and Lettau 1980a; MacRrobbie 2006; Meidner and Mansfield 1968; Fischer 1973; Heath, 1938). Turgor (in plant cells) develops, following water movement into a cell as

directed by concentrations of osmotically-active solutes in the cell. Even in the different organelles and within the cytosol, turgor develops in a similar manner, and turgor is equal in all the intracellular compartments of a cell, though the nature of solutes may vary from one compartment to the next. It is the presence of these solutes that generate an osmotic pressure which draws water into the compartment.

Though the identification and quantification of these solutes, as well as the measurement of the resulting osmotic pressure at single cell resolution, is technically challenging, it is important that the process is investigated at cellular resolution. In studying solute concentration changes associated with stomatal movements it is essential to measure concentrations in each possibly participating cell. Bulk measurement of whole leaf or epidermal strip, apart from averaging the concentrations in all the cells types, gives only an overall average concentrations in protoplasts and apoplast (see Tomos (1988); Conn and Gilliham (2010)).

Bulk measurements, however, do give an *indication* of solutes expected from assay of individual cells. Such a cursory survey may address issues of solute heterogeneity at tissue type level. For example, solutes found in whole leaves but not in strips are likely of mesophyll origin while solutes with significantly higher concentrations in strips than in whole leaf samples are likely of epidermal origin.

1.17.1 **Extraction of whole leaf and strip samples**

Many studies on stomatal physiology have relied on use of leaf parts (including leaf discs) (Glinka, 1971; Hsiao *et al*., 1973; Ishikawa *et al*., 1983; Edwards and Bowling, 1984; Edwards and Bowling, 1984), epidermal strips (Sawhney and Zelitch, 1969; Raschke and Fellows, 1971), isolated guard cells (MacRrobbie, 1981; MacRrobbie, 2006) or guard cell protoplasts (Zeiger and Hepler, 1977; Shimazaki *et al*., 1986). These studies have led to important advances in the understanding of stomatal physiology although they are essentially *in vitro* studies and also lack molecular specificity (Svatoš, 2011). The extent to which *in vitro* studies on these materials represent the situation in an intact plant and *in vivo* is uncertain (Cram, 1988).

Tissue excision from any part of a plant affect the water relations of the plant part by truncating the hydraulic continuum – also disrupting transpiration - at the excised region (Tomos, 1988; Malone, 1992; Francesca and Malone, 1993). In

stomatal studies, the disruption of this continuum disconnects signals such as ABA or auxin signals that originate from the roots as well as all 'indirect' signalling. On the leaf cells, loss of turgor in the predominantly pavement cell populated epidermis leads to an initial transient stomatal opening (Iwanoff effect) (see Powles *et al.* (2006). In addition, wounding in plants causes intracellular Ca^{2+} influx (Zocchi and Hanson, 1982), which may lead to elevation of cytosolic Ca^{2+}. This leads to a closing of the plasmodesmata (Terena *et al*., 2000). This may be a physiological defence mechanism to prevent loss of solutes from other cells (see section 1.13) not directly affected by the injury. This, however, does not prevent apoplastic solute and water losses. Thus, between excision and analysis, the combined effects of solute and water loss, absent physiological signalling mechanisms and the possible effect of the triggered Ca^{2+} signalling mechanism may significantly distort the pre-existing solute status. In addition to this issue, such results present the tissue as uniform as may be found in a temporary union of unicellular organism. Thus, bulk analysis offers limited value. Nonetheless, lack of suitable techniques for solute extraction and analysis at single cell resolution has been hampering studies of single cell solutes (Bowling, 2016).

1.17.2 **Extraction of individual cell samples**

The use of SiCSA sampling method allows the extraction and isolation of sap from individual cells without significant time lag (Malone *et al*., 1989; Tomos and Sharrock, 2001). This avoids the dilution effect that may occur with time once a cell is impaled. Reduced turgor pressure in an impaled cell leads to movement of water into the cell and consequent reduction of solute concentrations and, therefore, osmotic pressure (Shackel and Brinckmann, 1985; Shackel, 1987; Malone *et al*., 1989).

Many single cell methods involving *in situ* imaging and analysis of solutes, usually by synchrotron-based X-ray (see Zhao *et al.*, (2014a)) or GFP (green fluorescence protein) (see Lin *et al.* (2011)) fluorescence, have recently been developed. Ion sensitive microelectrodes have also been used in single cell solute measurements.

1.17.3 Studying solute relations in intact tissue

Most techniques available for the study of solute redistributions during stomatal movements involve excision of the tissues (e.g. Willmer (1974)), cells (e.g. MacRrobbie (1980a)) or subcellular compartments (Eisenach and De Angeli, 2017). Few techniques are available for studying solute relations in intact tissues. These include use of microelectrodes – usually ion sensitive (Blatt, 1988), confocal microscopy (Oparka and Hawes, 1992) and the SiCSA technique (Tomos *et al*., 1994). These techniques are minimally invasive, and usually target only cells of interest, therefore, minimising chances of more generalized tissue responses. Patch measurements can be used (in epidermal strips) for a variety of ion species and is a non-invasive method; but cannot be applied in real time measurements (Miedema and Assmann, 1998).

1.17.3.1 Microelectrodes

Use of microelectrodes for measurement of ionisable solute concentrations and electrical properties in intact cells has been long established (see review by Felle (1993)). Microelectrodes are well suited for measurement of ion activities and thus where the potential differences across respective membranes are known, the driving force on the measured ions can easily be calculated (Bowling, 2016). This method offers high precision (Bowling, 2016) as well as good spatial and temporal resolution of its output (Miller and Wells, 2006; Conn and Gilliham, 2010) and has been used extensively for the study of K^+ and Cl^- concentration changes during stomatal movements (Penny and Bowling, 1974; Penny *et al*., 1976; Edwards and Bowling, 1984). Shabala and Newman (1999) used this method to assay ion (Ca^{2+}, K^+, Cl^- and H^+) fluxes in both epidermis and mesophyll.

However, only a single or few ions may be assayed at a time. For example K^+-sensitive electrodes have been used extensively in stomatal studies in different species (Penny and Bowling, 1974; MacRrobbie and Lettau, 1980). They are not suitable for studies that require assays of many/entire ionisable solutes at a snapshot.

1.17.3.2 Imaging techniques

Studies in which many or even unexpected solutes may be involved and need to be assayed in a snapshot benefit more from use of imaging techniques. Initially, this technique relied on the use of microinjection of specific stains or fluorescent-protein analogues such as 5(6)-carboxyfluorescein succinimidyl ester-labelled tubulin (NHS-FI) (Zhang *et al*., 1990) and monochlorobimane labelling of glutathione for quantification (Meyer *et al*., 2001). In gene expression studies, use of microinjection technique has now been replaced by use of green fluorescent proteins (*gfp*) (Chalfie *et al*., 1994; Haseloff *et al*., 1997). The *gfp* introduced in one plant is intrinsically replicated in all targeted cells or compartments in either transient or stable (permanent) manner spanning all generations of the plant (Haseloff and Siemering, 2006). This has been put to great use in studying stomatal patterning and development (e.g. Berger *et al.* (1998)). In addition to, and following the success of *gfp* use in plant research, many fluorescent protein (*fp*) probes such as yellow fluorescent proteins (*yfp*) (see review by Mathur (2007)) have been introduced.

Aside from proteins, methods for genetic encoding of ion sensors have been developed. Most ion sensors are, however, based on their fluorescence resonance energy transfer (FRET) to *gfp* following a targeted reaction. For example, calmodulin changes which follow its binding to Ca^{2+} increases the FRET available to *gfp* (Miyawaki *et al*., 1997). The *gfp* is then quantified as a proxy for the Ca^{2+}. Chloride sensors have similarly been developed and have been used for monitoring intercellular Cl^- fluxes *in vivo* (Lorenzen *et al*., 2004).

Nevertheless, sensors for a number of cations such as NH_4^+, and anions including $SO4_2^-$, PO_4^{3-} and malate, among others, await development. This formed a major hindrance to use of fluorescence microscopy method in the study reported in this thesis.

1.17.3.3 Single cell sampling and analysis (SiCSA) methods

Single cell sampling methods aim at dissecting the cellular heterogeneity in a tissue. In this sampling method cell sap from a single cell is obtained in a glass microcapillary back-filled with silicon oil and mounted on a micromanipulator (Tomos and Sharrock, 2001). This method relies on the positive (turgor) pressure in the cell

to push cell sap into the microcapillary on impalement of plasma membrane and/or tonoplast. The extracted sap is subsequently analysed using a battery of analytical methods which may include x-ray fluorescence, capillary zone electrophoresis, enzymic methods and picolitre osmometry. Concentrations of the individual solutes are then related to the total concentration of osmotically-active solutes (Tomos and Leigh, 1999). For example, turgor cannot exceed protoplast osmotic pressure and the total charge of anions and cations must balance. Additionally, the sum of solutes (adjusted for osmotic coefficients) must be related to the independently-measured osmotic pressure. Discrepancies in the solute balance sheet indicate either an artefact or that there are unidentified solutes (Tomos and Leigh, 1999).

SiCSA shows not only the intercellular distribution of solutes within and between cells but also the basis of osmolality and turgor regulation in cells. Sap extracted from epidermal cells is predominantly vacuolar (Fricke *et al*., 1994b). This is because up to 99% of the volume of epidermal cells is occupied by vacuole (Winter *et al*., 1993, 1994). Vacuoles of neighbouring cells may contain differing elements as plant cells serve different functions aimed at storage and detoxification (see section 1.14). The SiCSA method is accurate, specific, and covers all the elements in the sap at the time of sampling (Conn and Gilliham, 2010). Additionally, it can be used in intact plant tissues *in situ* as opposed to use of epidermal strip which cannot reflect the real physiological picture of the solute gradient involved in stomatal movements (Talbott and Zeiger, 1996). For example, Heide and Raschke (1978) observed in *Allium cepa* that epidermal malate content was positively correlated with stomatal opening when using whole plant but the correlation was negative when epidermal strips was used (Schnabl and Raschke, 1980). The main disadvantage of this method is that cells may be irreversibly damaged during impalement, either through shocks or vibration (Zimmermann *et al*., 1980).

1.18 Aim and objectives

The nature and concentration of only few solutes (K^+, Cl^- and malate) in four cell types (pavement, apical and lateral subsidiary as well as guard cells) of leaf epidermis during stomatal movement have been studied considerably previously. Of

these, only K^+ concentration changes have been clearly understood. This study aims to determine the epidermal solute gradients responsible for stomatal opening and closing by analysing epidermal cell (pavement, apical and lateral subsidiary as well as guard cells and juxta apical cell) sap of *T. virginiana* using the SiSCA technique.

In achieving this aim, the objectives were to determine the

- (charged) solute content and concentration in whole leaf of *T. virginiana*, a model plant for study of stomatal physiology and plant water relations parameters (Zimmermann *et al*., 1980; Tomos *et al*., 1981; Tomos and Zimmermann, 1983; Edwards and Bowling, 1984).
- charged solutes and their concentrations in abaxial epidermal strip of *T. virginiana*. This gave a general view of the charged solutes available in all the cell types (in troughs and ridges) of the epidermis (chapter 4).
- charged solutes and their concentrations in the five cell types (pavement, juxta apical, apical and lateral subsidiary as well as guard cells) of the epidermal trough of *T. virginiana* under open and closed stomata condition.
- osmotic pressure in each of the cell types of the stomata at closed and at open stomata conditions

A second set of objectives included to

- compare the solute concentrations in the individual cell types at open and closed conditions to show the solute concentration differences
- compare these differences between contiguous cells of epidermal troughs and
- deduce possible solute concentration gradients associated with stomatal movements in trough cells of the epidermis
- examine the balance of charges between the positively and the negatively charged species and
- compare the osmotic pressure directly measured (above) with that expected from the independently measured solute concentrations to assess the possible contribution of non-ionisable solutes (not assayed in this project) to cellular osmotics during stomatal movements.

Chapter 2 Materials and Methods

2.1 Plant material and growth conditions

Four week old *Tradescantia virginiana* L. plants were used for this study. The plants were clones from *T. virginiana* originally provided by Professor E. D. Schulze from Bayreuth University, Germany (Tomos, Steudle, Zimmermann, and Schulze, 1981). Supply of the plant was maintained by vegetative propagation of shoots obtained by splitting emerging root-buds from the parent plant before the start of first leaf expansion (see plate 2.1 A). Only buds with one to two roots were used. Each root-bud was potted in a 3.5 inch, round, lightweight, drained, plastic plant pot containing 1:1 mixture, by weight, of John Innes No.1 potting compost and Vermiculite and grown in a growth chamber. For the initial parts of this study a Sanyo Fitotron growth chamber, type SGC066.pfx.f (Sanyo Gallenkamp ltd. Monarch Way, Belton Park, Loughborough, Leicestershire. LE11 5XG, UK) was used for growing the plants. A Conviron (adaptis) CMP 6010 growth chamber (Controlled Environments Ltd, 590 Berry St, Winnipeg, MB R3H 0R9, Canada) was used for the rest of the experiments as noted in the relevant sections. In each of the growth chambers temperature and relative humidity were set at 24 ± 1ºC and 60% respectively, during all plant growths. Light intensity was set at 300 – 350 µmol.m^{-2}.s^{-1}, at plant height, on a 16h day/8h night schedule, with day set to start at 06:00hrs. Plants were watered daily, in the morning, with tap water that has been left, covered in the growth chamber for 24hrs, to prevent possible chilling effect and eliminate variations arising from changes in root temperature (Davidson, 1969; Atkin *et al*., 1973). On days 0, 1 – 10 and beyond day 10, each plant received 100ml, 40ml and 70ml of water respectively, per day. Overwatering or drying was avoided in order to prevent abnormal stomatal responses (Weyers and Meidner, 1990; Webb and Mansfield, 1992). Plants were fed on day 0 and fortnightly, with 100ml of Miracle-Gro general-purpose plant food (The Scotts Miracle-Gro Company, 14111 Scottslawn Rd, Marysville, OH 43040) mixed to a concentration of 50 ml (bed volume) per litre of water. The composition of the plant food (NPK, 24-8-16 blend) was as given in table 2.1.

Table 2.1 Composition of standard commercial plant food (nutrient) used for growing the *T. virginiana*
The powdery compound is mixed in appropriate volume of water. The pH of final solution was usually 5.9 to 6.4.

Chemical compound	Concentration in nutrient solution
Macronutrients	(%)
Nitrogen Total	24.0
Ammoniacal nitrogen	3.5
Ureic Nitrogen	20.5
P_2O_5 soluble in neutral ammonium citrate and in H_2O	8.0
K_2O	16
Others	27.68
Micronutrients	(%)
Boron	0.02
Copper	0.03
Iron (H_2O soluble)	0.19
Manganese (H_2O soluble)	0.05
Molybdenum	0.001
zinc	0.03

2.2 Selection of plants for measurement

Unless otherwise stated, all measurements were made on the fully expanded fifth leaf of plants, about two days after the 7^{th} leaf became visible (see plate 2.1C). Wherever applicable, all leaf longitudinal (axial) distances were measured from the leaf tip using a Perspex ruler. All plant samples were taken at approximately the same time of the days (10:30 am – 3:00 pm) to control for possible effect of endogenous rhythm (Martin and Meidner, 1971).

2.2.1 Selection of cells for measurement

In single cell sampling experiments, only cells of the leaf abaxial epidermis were used. Samples were taken at 6 cm from the leaf tip (see sampling in barley by Hinde (1994)). The leaf surfaces/parts used in other experiments are stated in the relevant sections. For convenience of nomenclature, the epidermis overlying veins (leaves were of parallel venation) were called ridges while the (epidermal) regions between

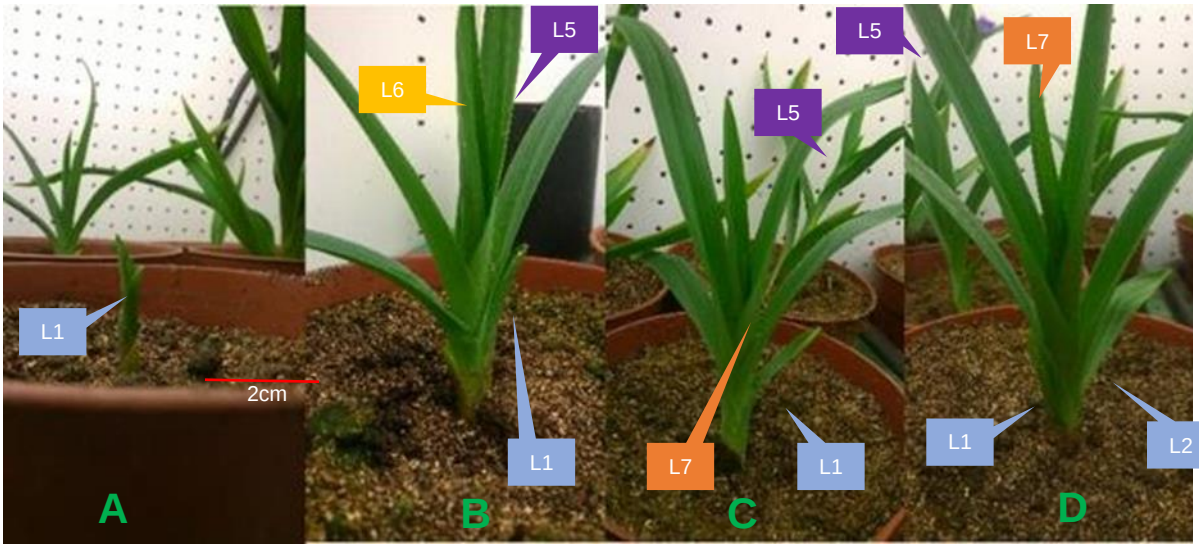

Plate 2.1 Stages for cloning and sampling of *T. virginiana* used for the experiments
Four potted *T.* virginiana plants labelled A – D are shown (in the foreground). A – Newly cloned plant; B – Six leaf stage (prior to sampling age); C – Early 7 leaf stage (**sampling age**); D – Late 7 leaf stage (past sampling age). L = Leaf. The leaves are numbered progressively according to their insertion position from the base of the plant. Leaf 1 (L1) is the leaf closest to the root at its insertion. The plants were pictured while in the growth chamber –hence other plants at the background.

the ridges/veins were termed troughs (Malone *et al.*, 1991). Samples were taken from only trough cells of the epidermis. Ridge cells were avoided. Troughs were numbered with respect to their proximity to the mid-rib; number one being closest to the mid-rib. Cells within each trough were also similarly numbered. Opposite sides were mirrored in numbering (see plate 2.2 A - C).

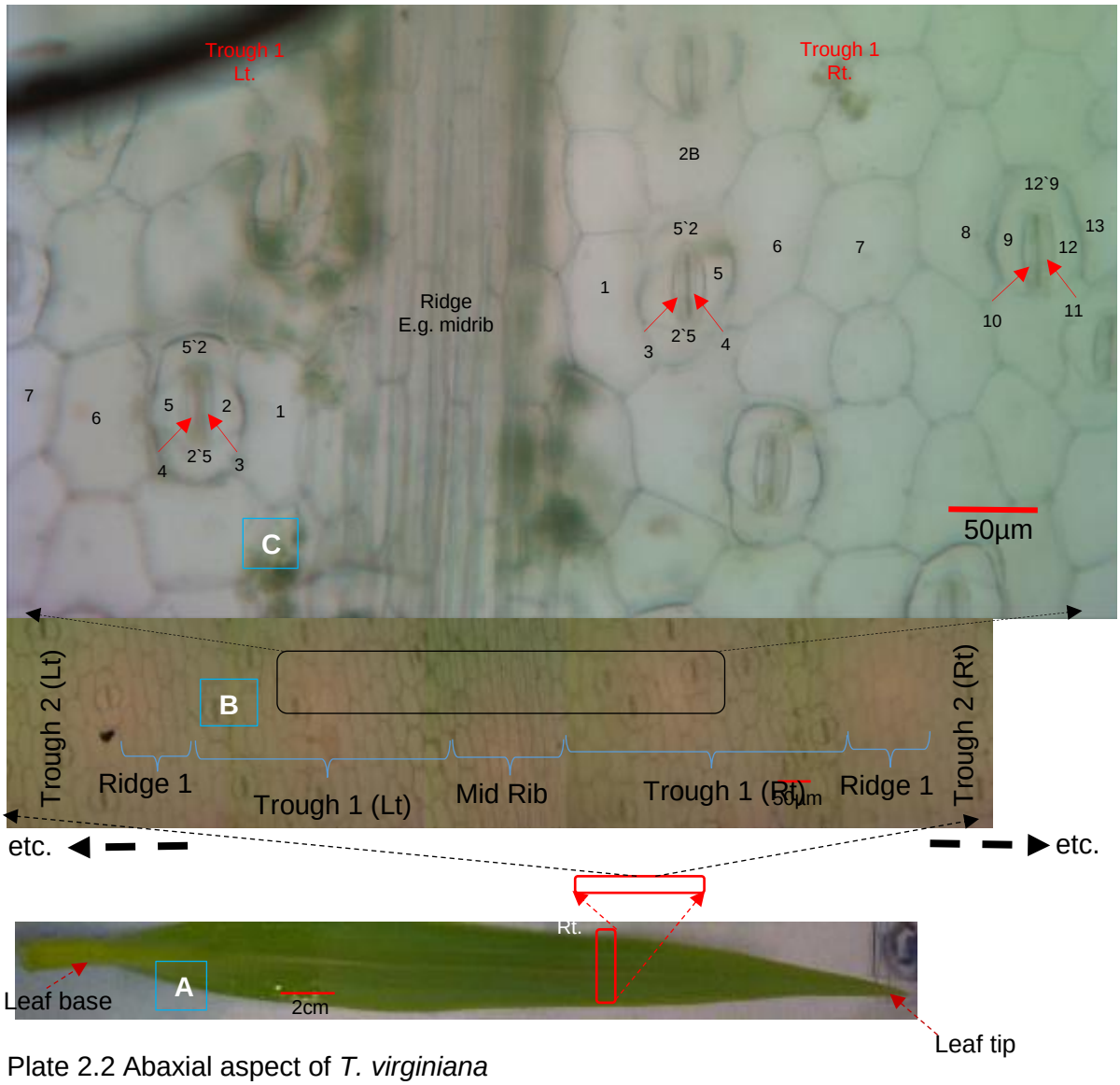

Plate 2.2 Abaxial aspect of *T. virginiana*

A – Abaxial aspect of *T. virginiana* leaf (number 5) cut from the leaf base. B – Microscope picture of a section of the leaf epidermal strip taken from the area in 'A' indicated. Ridges were numbered from the centre outwards on both (right (Rt) and left (Lt)) sides. The mid-rib (mid ridge) and veins/ridges (positions of vascular bundles) were not sampled. All samples taken from troughs (positions between vascular bundles). C – Enlargement of a section of image B, showing the numbering system used for identifying positions of individual cells. Cells 3, 4, 10 and 11 are guard cells. Apical subsidiary cells were labelled 2`5 (read as 2 prime 5) or vice versa, 5`2 and 12`9. Juxta apical cell was labelled 2B etc. Average leaf length (in all the experiments) in this research was 30.5 ± 1.3 cm.

2.2.2 Preparation of bulk leaf sap sample

A modification of the method by Fricke *et al.* (1994), was used for obtaining sap for analysis from bulk leaf samples. A pore, about 0.5 mm in diameter, was made at the tip of a 1.5 ml microfuge tube using a needle. Three leaf sections (4 cm in length), measured between 4 and 8 cm, 11 and 15 cm and 18 and 22 cm from the leaf tip, were obtained by cutting with a pair of scissors. The measurement avoided the leaf base. The mid-rib was dissected off using a sharp razor blade, and one side of each leaf tissue was closed in a prepared microfuge tube. The remaining half was used for preparation of epidermal strip (see section 2.2.3). Sides (right and left) were alternated between whole leaf and strip if replicates were studied. In some experiments (indicated in the relevant sections), however, both sides (right and left) were put in different tubes and used for whole leaf studies only.

The tubes were immediately frozen in liquid nitrogen. At the end of 2 minutes, tubes were removed and allowed to thaw at room temperature for one minute. A new 1.5 ml microfuge tube was attached under the perforated tube containing the thawed leaf section and was centrifuged (together) in a microfuge (Heraeus Sepatech, Biofuge 15) for 2 minutes at 13,000 g. Sap collected in the new microfuge tube was stored at -20ºC and was used for analysis within 24h to ensure minimal changes in solute concentration due to enzyme activity.

2.2.3 Preparation of epidermal strip sap sample

Epidermal strip samples were prepared, using the method of Weyers and Travis (1981), from the abaxial epidermis of the (complementary) leaf tissue obtained for the purpose of strip preparation referred to in section 2.2.2. As soon as the epidermis was stripped from the leaf tissue, the steps outlined in section 2.2.2 were again followed to obtain and store the sap.

2.3 Single cell sampling

Single-cell sap, from trough cells *in situ,* were obtained from the abaxial aspect of leaf in intact plants, by using silicone-oil-filled microcapillary as described by Malone *et al.* (1989 and 1991). All single cell samples were collected from trough 2, 3 or 4. Sampled cells were at least four cells apart, to minimize interference from punctured cells. Volume of extracted sap varied according to cell type, ranging from approximately 200 pl in pavement cells to about 10 pl in guard cells. In all studies involving guard cells, sap from 6 to 24 cells were pooled together, depending on the minimum volume requirement for the experiment. Extracted sap was immediately deposited in cold water-saturated paraffin oil (Tomos *et al*., 1994), and placed on ice, until analysis, to prevent evaporation and reduce metabolic rate within the sample. In experiments requiring open stomatal conditions for sampling, and for all subsampling, a Leica Wild M8 stereomicroscope (Leica UK Ltd, Wood Milton Keynes, MK14 6FG UK) was used. The microscope, in addition to its normal range of 16–100X when using 25X eyepiece, was equipped with a 1.6X extender. The extender was attached only when sampling. All other single cell sampling experiments and stomatal aperture manipulations were carried out using Zeiss LSM 510 Axioplan 2 imaging microscope (Carl Zeiss AG; Carl-Zeiss -Straße 22 73447 Oberkochen, Germany) at magnification of 250x. The higher resolution power and motorized stage of this system enabled better precision when sampling cells with small volume especially guard cells of closed stomata. Illumination for all sampling and subsampling procedures was provided by a 150W quartz-halogen Schott KL1500 cold light source (Schott Glaswerke, W – 6200 Wiesbaden 13). Leaf temperature (17.4 ± 0.8ºC) was measured in representative samplings before and after sampling sessions, using a fine copper/Constantan-wire thermocouple applied firmly to the leaf surface. Room temperature was 18.3 ± 1.3ºC.

2.3.1 Subsampling of extracted samples

Subsampling of extracted samples was done prior to quantitative analysis of solute content except where otherwise stated. All pipetting of microsamples (microdroplets) was performed under the water-saturated paraffin oil (see section 2.3) using a

constriction pipette. Equal volumes of the appropriate (internal) standard (i/s) (indicated in relevant sections) and the extracted sample were mixed in reverse-osmosis-purified 18 MΩ. cm^{-1} deionized water (dH_2O) (ELGA UHQ LabWater, Unit 10 Lane End Industrial Park, Lane End, High Wycombe HP14 3BY).

2.4 Production of microcapillary tips

Microcapillary tips were prepared from 1 mm O.D X 860 µm I.D borosilicate glass capillary tubing (Clark Electromedical Instruments, Pangbourne, Reading, England) using a commercial capillary-tip puller (Harvard Apparatus, Sheerness, Kent ME12 1RZ). The capillary tips were pulled to about 1 µm O.D. Heat and solenoid puller settings of 90 and 35 respectively were used, and gave tips with steeply tapering geometry. Tip I.D. of about 5 µm (used for all sampling and subsampling) was achieved by abrading the pulled tip against a cold heating element of a De Fonbrane microforge (Alcatel, 98 avenue de Brogny 74009, Annecy Cedex, France) until the required I.D (5 µm) was achieved. This microforge was also used for making the constriction pipettes.

To produce a constriction pipette, the heating element was used to heat a point on a prepared (as described above) sampling capillary tip placed in close proximity to it. The capillary then bends and constrict at this heated point. Typically constricted pipette volumes were approximately 10-15 pl volume (Fricke *et al*., 1994c). This is the volume from the prepared tip to the point of constriction.

2.5 Stomatal aperture manipulation

A time course for stomatal opening and closing was studied using white light (see light source in section 2.3) and green light respectively, for opening and closing the stomata. To obtain green light, a 12.5mm diameter KG-3 heat-absorbing green filter glass (supplied by Edmund Optics Ltd, 1, Opus Avenue Nether Oppleton, North Yorkshire YO26 6BL) was applied to the light source (in section 2.3). The light source was positioned to deliver 300 $\mu mol.m^{-2}.s^{-1}$ of white light on the leaf surface.

This corresponds to the light intensity at which the plants were grown (Björkman, 1981) (see section 2.1). Light intensity was measured using a SKP 2200 2-channel Ratio Display Meter attached to Pyranometer sensor (made by Skye Instruments Ltd, Unit 21, Dole Enterprise Park, Llandrindod Wells LD1 6DF). This light meter was also used for all light intensity measurements in this project except where otherwise stated.

Microscope pictures of three stomata were taken at intervals of 5 minutes for two hours, using a GX-CAM 9.0MP microscope camera (GT Vision Ltd, Aspen Grove Farm, Assington Green, Suffolk, CO10 8LY, UK), attached to a Windows laptop equipped with GT Camera Drivers and GX capture software version 7.3.1.7 (made by the same company) (Franks *et al*., 1995; Talbott *et al*., 1996). Stomatal aperture, taken as the diameter across the stomatal pore at the mid-point of the aperture of each stomatal complex (at maximum aperture width), was measured using the GX capture software (see plate 2.3) and plotted against time taken to achieve the aperture (see figure 2.1).

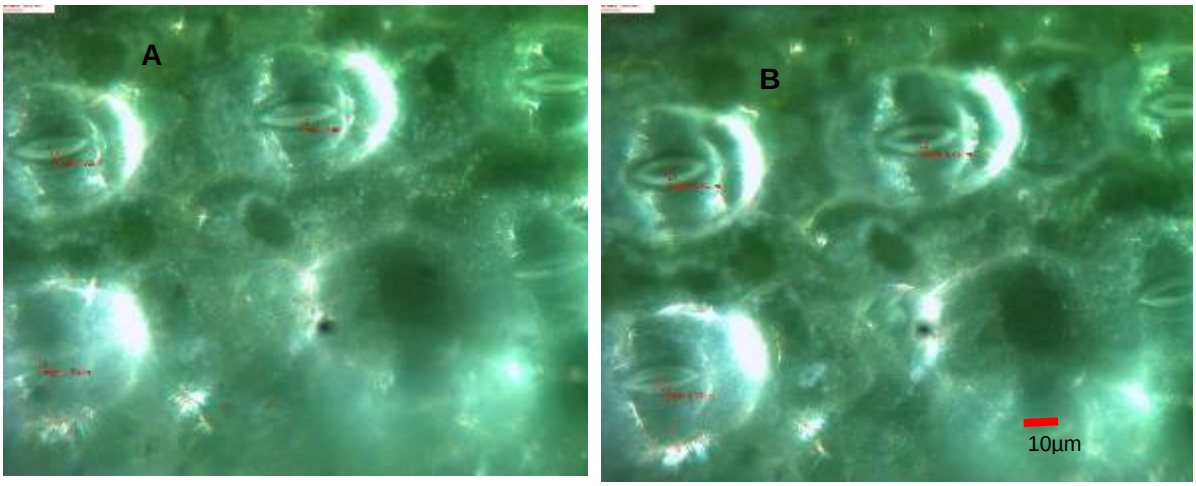

Plate 2.3 Stomatal aperture response to white light
Stomatal aperture after (A) 20 mins and (B) 110mins of exposure to white light at intensity of 300µmol.m^{-2}.s^{-1}.

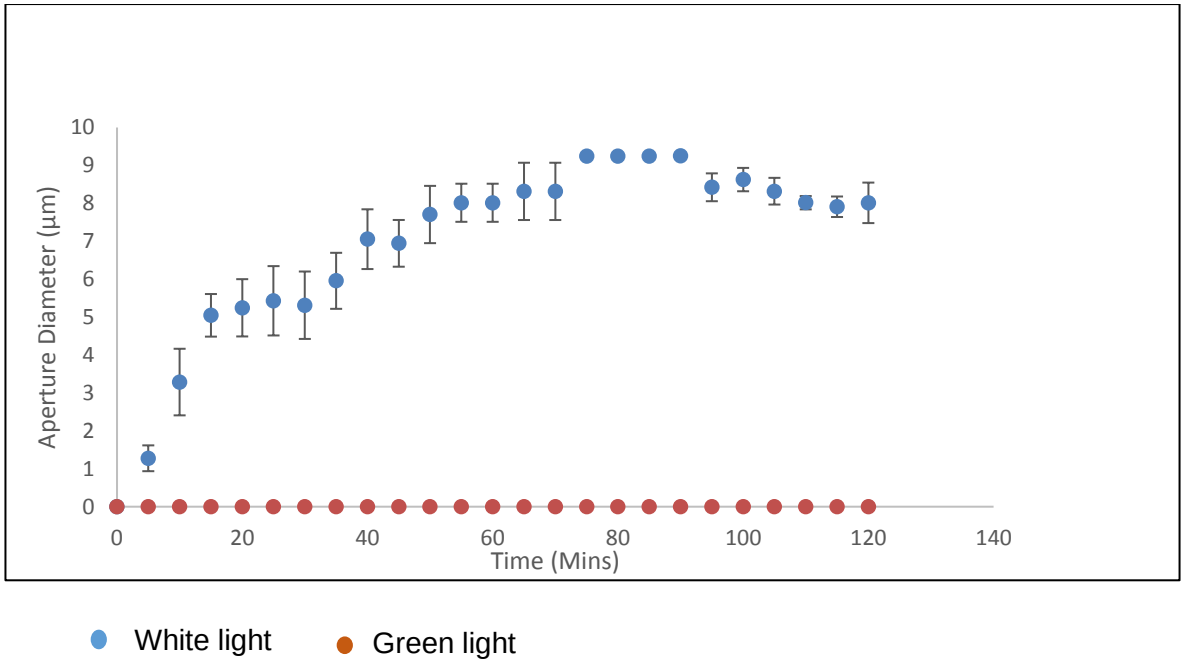

Figure 2.1 Time course for stomatal opening under white and green light
Stomatal aperture changes under 300 µmol.m-^{2}.s-^{1} of white light showed saturation to white light (blue colour) and decreasing aperture after 90 minutes. Green light (red colour) did not open stomata. (n = 3). Error bars represent ± sd

2.6 Determination of cation and anion content of samples

A modification of Bazzanella *et al*. (1998) method was used for the analysis of anion (inorganic and organic) and cation ($NH4^{+}$,Na^{+}, K^{+}, Ca^{2+} and Mg^{2+}) content of extracted sap (Tomos, 2016).

The experiments were carried out on a laboratory-built capillary zone electrophoresis (CZE) system, equipped with a Lambda 1000 UV detector (Bischoff, Leonberg, Germany) and a high voltage power supply type HCN 6 M-30000 from FUG (Rosenheim, Germany). Untreated fused-silica polyimide-coated capillaries (Chromatographie Service, Langerwehe, Germany) of 50 µm internal diameter (i.d.), 365 µm external diameter (O.D.) (Composite Metal Services Ltd, Shipley, W. Yorks, UK.) measuring 72 cm in length (57.5 cm effective length), were used. On the injection side, the outer diameter of the capillary tip was conically reduced to about 70 µm by manual grinding on a fast-rotating corundum disk (see plate 2.4 B) in order to facilitate sample injection into the capillary.

Sample injection was by manual suctioning with a syringe barrel (under paraffin oil). The suctioning (capillary) tip was then transferred into a buffer. All operations were observed with the stereomicroscope (see section 2.3).

Anions were analysed using a pyromellitic acid (PMA) buffer (pH 8.0), containing 3.5 mM pyromellitic acid (PMA) (Fluka), 21 mM Tris (hydroxymethyl) aminomethane and 1.4 mM DoTAOH (Dodecyltrimethyl ammonium hydroxide) (both, from Sigma-Aldrich). The DoTAOH was prepared from the bromide salt (DoTAB) using an anion exchange column. Imidazole buffer, pH of 4.5 (adjusted with H_2SO_4), containing 5 mM Imidazole (Fluka) and 2mM 18-crown-6 ether (1, 4, 7, 10, 13, 16-hexaoxacyclooctadecane) (Merck, Darmstadt, Germany) was used for cation analysis.

The CZE separation was achieved at 23 kV (320 $V.cm^{-1}$) using a current of 8 and 5 µA respectively, for running anions and cations. Detection was by the indirect UV method (PMA or imidazole displacement) at 246 nm for anions and 214 nm for cations. Bromide and caesium ions were used as internal standard (Dose and Guiochon, 1991) for anions and cations respectively (Tomos *et al*., 1994). The data was processed using Clarity Lite Chromatography version 5.0.3.185, (DataApex Ltd) commercial software. Plate 2.5 A and B) respectively show an example of lateral subsidiary cell sap separated in PMA (A) and imidazole (B) buffer.

Peaks were identified by spiking with standards of known concentrations to confirm each solute. To do this, a solute of four-fold greater concentration than prepared in the standard to be run is added to the mixture of the standards and analysed in the CZE. The peak for the spiked solute shows an increase corresponding to the increased concentration. The process is repeated three times for each solute to confirm its peak.

A standard calibration curve incorporating the internal standard at 50 mM was previously constructed using anion and cation concentrations ranging between 1 and 100 mM. This standard curve was used to determine the anion and cation concentrations in samples.

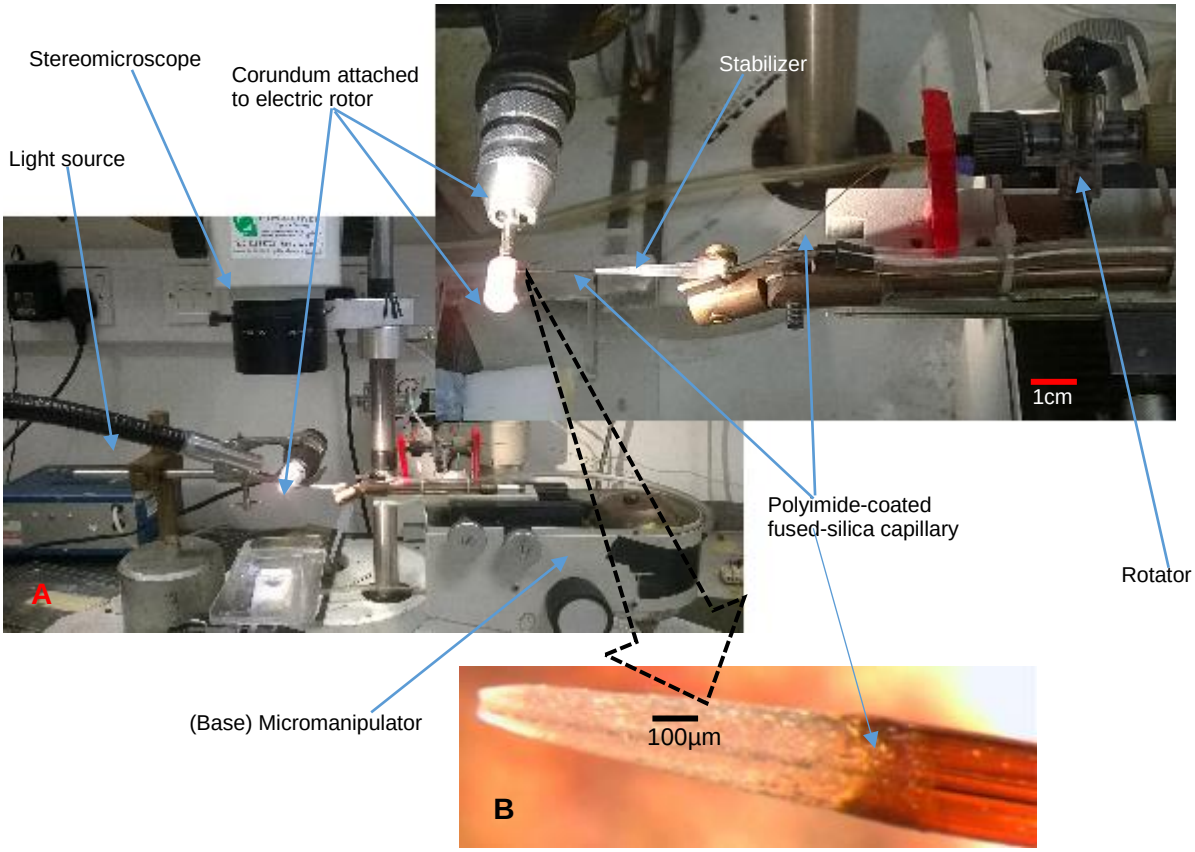

Plate 2.4 Equipment for conically grinding the fused-silica capillaries to reduce the outer diameter

The grinding process was observed through the microscope. Inset shows the capillary passed through a rotator and the stabilizer, to the corundum surface. A – The capillary was rotated and moved back and forth with the aid of the screw-attached rotator. The micromanipulator functioned both as the base and a lever for lifting the capillary off the corundum. Typically grinding duration was 4-7 minutes. B – Shows a typical tip post grinding.

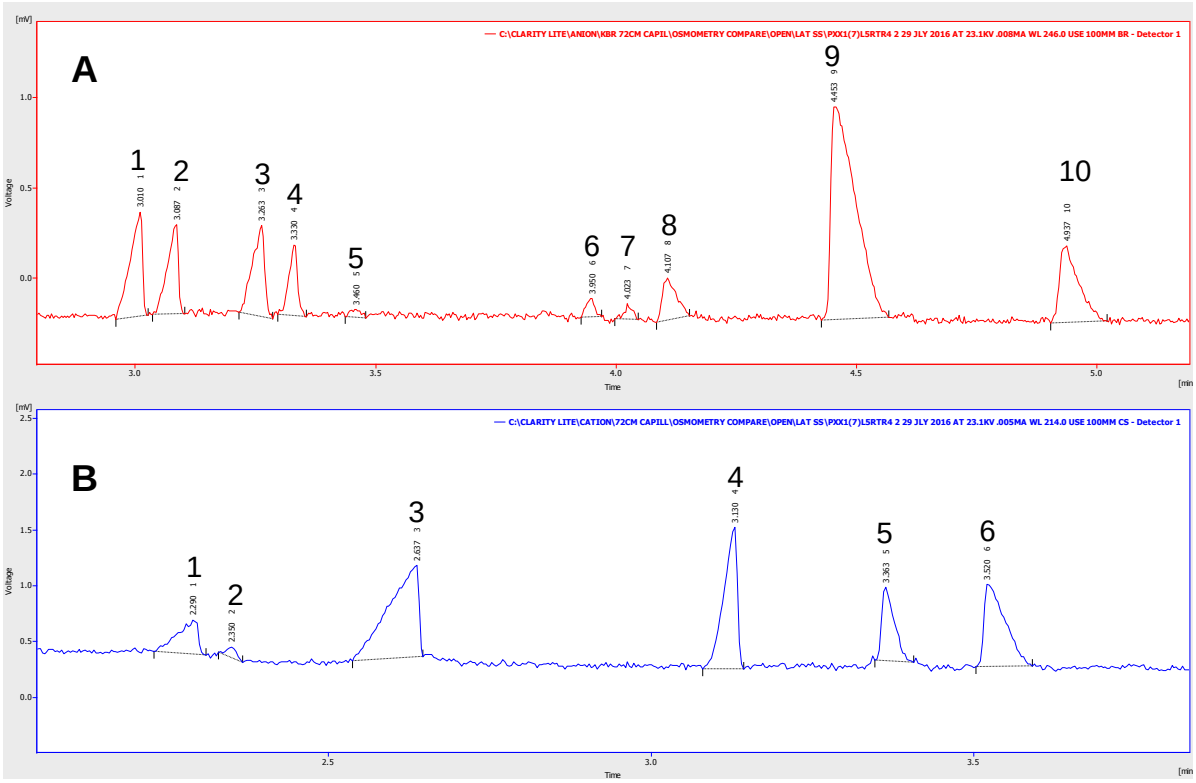

Plate 2.5 Separation of (A) anions (with PMA) and (B) cations (with Imidazole) in subsamples from the same lateral subsidiary cell vacuolar sap.
Two independent electrophoretograms are shown for anions (A) and cations (B). Capillaries: 72 cm (57.5 cm effective length) 50 µm I.D., 365 µm O.D.; 70 µm O.D. at injection tip. Vacuum injection at 206.86 torr (equivalent to 0.028 mPa) Indirect UV detection - reversed output polarity to achieve positive peaks. Electrolytes: (A) 3.5 mM pyromellitic acid, 24 mM Tris, 1.4 mM DoTAOH, pH 8.0; Indirect UV detection at 246 nm. (B) 5 mM imidazole sulphate, 2 mM 18-crown-6, pH 4.5.; Conditions: voltage 21.3 kV, (A) current 8 µA; (B) current 5 µA. Peaks: (A) 1- Bromide; 2 – Chloride; 3 – Sulphate; 4 – Nitrate; 5- Oxalate; 6 and 7 – unknowns; 8 – citrate; 9 – malate; 10 – phosphate
(B) 1 – Caesium; 2 – NH_4^+; 3 – K^+; 4 – Na^+; 5 – Ca^{2+}; 6 – Mg^{2+}.

2.7 Leaf geometry

Cell types were identified and parameters such as stomatal density, stomatal index (and the variations thereof), distribution and variation in cell sizes and relative proportion of the cell types per mm^2 of leaf epidermis were quantified. For parameters involving counting of cells, such as stomatal density and stomatal index, cells within 0.1 mm^2 squares (or rectangles) were counted (Gupta, 1961) instead of using a more conventional 1 mm^2. This is because the width of some troughs, especially near the tip, were often less than 1 mm. In addition, for these purposes

and wherever needed, all the components of the stomatal complex were counted and measured as if they constituted a single cell.

Leaves 5 and 6 of three randomly selected plants were cut at the leaf base and the leaf lengths were measured. Cuttings of 3 cm length were made (see section 2.2.2). Each (3 cm) cutting was split in two (right and left) at the mid vein and the abaxial epidermal strip of each side was prepared (as detailed in section 2.2.3). Using the GX-CAM microscope camera, images of the distal end of the strip were taken under the Zeiss LSM 510 Axioplan 2 imaging microscope (see section 2.3) at 250X. DAPI (4', 6-diamidino-2-phenylindole) LP 397 FSET01 filter which enabled cell wall auto fluorescence was applied for better demarcation of cell wall boundaries. The images were analysed with the GX capture software (see section 2.5). The number of veins (ridges) and regions between veins (troughs) were counted on each side. Stomatal index and density as well as the sizes of cell types and proportion of the epidermis occupied by the cell types were determined. Plate 2.6 shows one example of a sampled abaxial strip and the key measurements (ridge width, trough length and width and cell type sizes) made with the GX capture software. The number of different cell types within trough was manually counted. The GX capture software is intelligent only to the point of determining the distance between two points set by the user, labelling and organising such in tabular form. Therefore, all cell identifications were done manually.

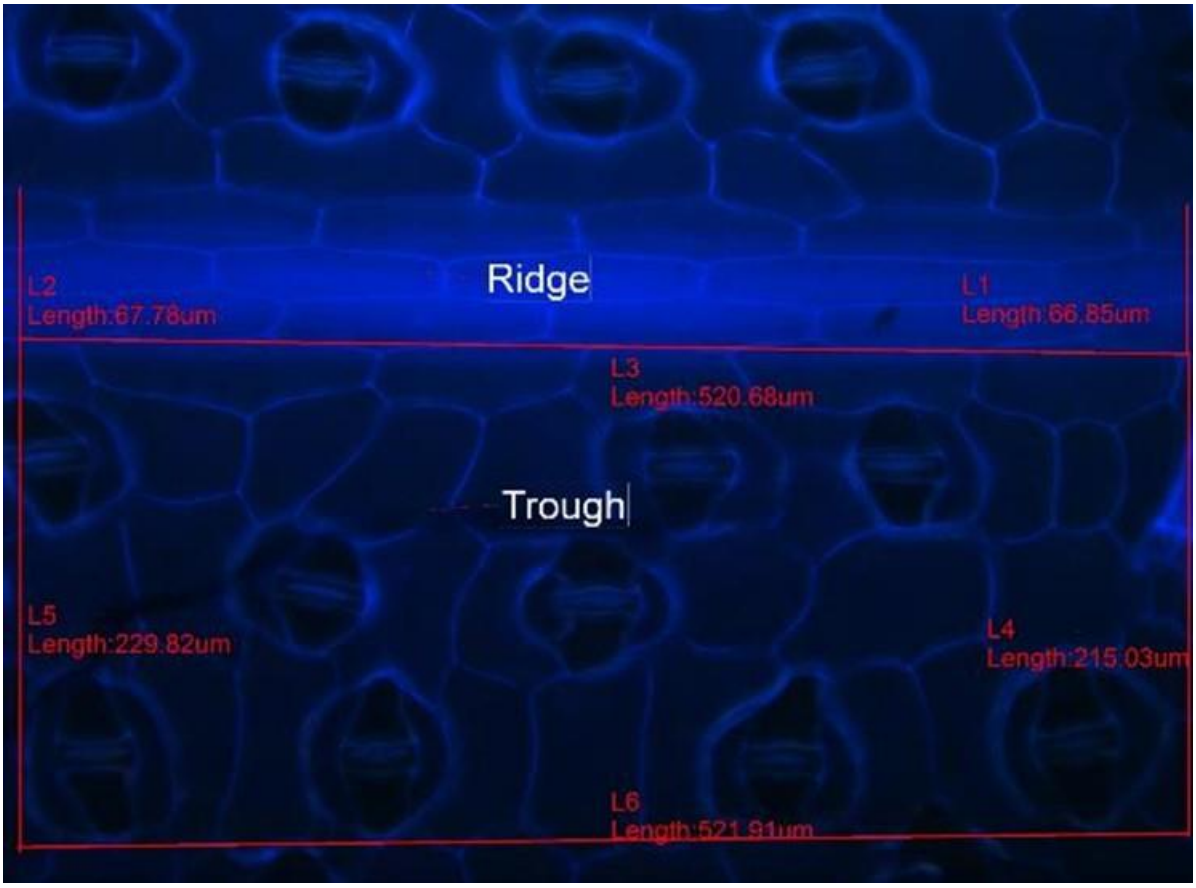

Plate 2.6 A typical abaxial epidermal strip.
This plate shows abaxial surface of *T. virginiana* epidermal strip auto-fluorescing under DAPI LP 397 FSET01 filtered light - the key measurements made with GX capture software. L = Measurement (followed by the nominal order in which measurement was done). L2 and 5 were nearer to the leaf base (proximal end) while L1 and 4 were nearer the leaf tip distal end). Difference between L2 and L1 showed the gradual decrease in vein width towards the leaf tip. Stomatal density and index were determined with and refer only to the trough cells.

2.8 Determination of bulk leaf sap solute concentration

Sap from the 5th leaf of three randomly selected plants were prepared for CZE analysis as described in sections 2.2.2, 2.2.3 and 2.6. The anion and cation contents of whole leaf and abaxial epidermis were determined as described in section 2.6.

2.9 Determination of leaf malate concentration using an enzymatic method

Whole leaf and strip sap samples obtained from leaf five (see sections 2.2.2 and 2.2.3) of four randomly selected plants, were analysed for malate content, using an enzymatic assay linked to the reduction of nicotinamide adenine dinucleotide (NAD^+) (from yeast) (Lowry, 2012). In the reaction, L-malic acid (L-malate) is oxidized by L-malate dehydrogenase (LMDH) (made from pig heart by Roche diagnostics, GMGH, Germany) to oxaloacetate in the presence of NAD^+. The amount of L-malate present in the sample is stoichiometric with the amount of reduced nicotinamide adenine dinucleotide (NADH) formed.

$$\text{L-malate} + NAD^+ \leftrightarrow \text{oxaloacetate} + NADH + H^+$$

The reaction is usually inhibited by the build-up of oxaloacetate as the reaction equilibrium tends to the left. A second enzyme, glutamate-oxaloacetate transaminase (GOT) (from porcine heart) is added to the reaction mixture to bring the reaction equilibrium to the right by converting oxaloacetate to L-aspartate in the presence of L-glutamate.

$$\text{Oxaloacetate} + \text{L-glutamate} \xleftrightarrow{\text{GOT}} \text{L-aspartate} + \text{2-oxoglutarate}.$$

The increase in NADH was measured with a spectrophotometer (Jenway, 6405 UV/Vis) using its absorbance at 340nm. Glass cuvettes were used. All the chemicals used, were of > 97% (HPLC assay grade) from Sigma-Aldrich, USA, unless otherwise stated.

2.10 Single cell solute content

Depending on the experiment being performed, vacuolar contents of single cells from the epidermis (Fricke *et al*., 1994) were sampled and analysed as detailed in sections 2.3 and 2.6. The sampled cells were described in the relevant subsections. The system used for numbering the cells is shown in plate 2.2 – C. All samples for

open stomata state were taken at between 1 and 2 hours of illumination (see section 2.3), unless otherwise stated.

2.10.1 Comparison of different troughs

Pavement, lateral and apical subsidiary cells at similar locations in troughs 2, 3 and 4 were sampled and analysed for anion and cation contents. Samples were obtained from 24 plants. Pavement cells at positions 1, 8, 18 and 28 (see plate 2.2 C), lateral subsidiary cells at positions 5, 12 and 22 as well as positions 2`5, 12`17 and 18`21 of apical subsidiary cells were sampled.

2.10.2 Comparison of troughs on different sides of the mid-rib

Pavement and apical subsidiary cells of troughs 2, 3 and 4 on both (right and left) sides of the mid-rib of four randomly selected plants were sampled and analysed. Similar positions as in section 2.11.1 above were used.

2.10.3 Comparison of open and closed stomata state

Samples were taken from each cell type of the epidermis (pavement, juxta apical, guard, lateral and apical subsidiary cells) of three randomly selected plants for study of each cell type when the stomata were either open or closed (Penny and Bowling, 1974) - using microelectrode). Pavement cells at positions 1, 18 and 28, juxta apical cells at positions 2B, 8B, 18B and guard cells at positions 3, 10 and 20 were sampled. Guard cell samples were pooled from 6 cells for each position. Apical and lateral subsidiary cells were sampled from similar positions used in section 2.11.1. Same plants were used, but sides (right and left) were alternated, for open and closed stomata studies. White and green light were applied as described in section 2.5, for opening and closing of the stomata.

2.11 Osmotic pressure measurements

The osmotic pressure of whole leaf, abaxial epidermal strips and each cell type of the epidermis (see section 2.2.1) of leaf five was measured with the picolitre osmometer, using the freezing-point depression method of Malone *et al*. (1989). A glass microscope slide with vertical and horizontal lines drawn on its blackened surface (using a felt pen) was mounted on the picolitre osmometer using a heat sink paste (RS components, Birchington, Corby, Northants, UK) placed on the blackened side. Approximately 120 pl of samples were dropped on the glass slide under 2 µl of dH_2O-saturated paraffin oil. A glass coverslip covered the sample chamber. The melting point of the last ice crystal in any sample droplet was recorded and used to determine its osmolality from a standard curve of know NaCl standards. A dry air stream and cooled water (conduit passed between ice packs) was used to respectively, prevent condensation to permit view from top and act as heat sink for the two Peltier coolers.

The osmotic pressure of an artificial sap solution of solutes made to the recipe of typical concentrations determined by CZE from whole leaf, abaxial epidermal strips and single cell samples (at opened and closed stomata conditions) was also measured. Wherever comparison of osmotic pressure was needed subsamples of the required sap were used. All the chemicals used for the artificial sap preparation were of Analytical laboratory grade (Analar) from Sigma-Aldrich.

2.12 Statistical analysis

Data was analysed using IBM SPSS version 22 for Windows. In single cell studies data, one-way ANOVA between cell-types was applied. Students' t-test was applied to all other data. Results included means and standard deviations assuming normal distribution of data and homogeneity of variance. Normality was tested using Kolmogorov-Smirnov test and showed data to be normally distributed ($p > 0.05$). Significance is expressed at 95% confidence limits. This analytical method was applied in all relevant experiments. Unless otherwise stated, in all reported *t*-tests,

the test statistics (*p* values) represent the probability at 95% confidence interval in an unpaired two tailed student's t-test assuming equal variance.

Chapter 3 Whole leaf and strip studies

3.1 Introduction

In preparation for the analytical work described in the ensuing chapters of this thesis, a survey was made of the overall geometry and charged-solute profile of mature *Tradescantia virginiana* leaf. Leaves are of central importance in the physiology of plants. In addition to being the main site of photosynthesis, they control the uptake of water and inorganic nutrients (Epstein, 1972), regulate water loss (Edwards *et al*., 1982) and CO_2 gain (water use efficiency) and regulate the plants' internal temperature (Nobel, 2009). The major site of this control is the leaf epidermis which is described as a multifunctional apparatus that, in the main, hydraulically manages the plant's interaction with biotic and abiotic environmental factors. These functions are performed by different specialized cell types acting in synchrony with some or all the other cell types. For this to be achieved, the cell types of the epidermis are distributed in an ordered (non-random) pattern throughout the leaf surface (Korn, 1972), and may vary in their solute composition depending on the prevailing supply of solutes from the environment (Epstein, 1966; Fricke *et al*., 1994b; Leigh, 1997).

The patterning of these epidermal cell types as well as the content and concentrations of charged solute in whole leaf and the epidermis (strip) are explored in the chapter. The epidermis comprises adaxial and abaxial epidermis, and heterogeneity in solute content and concentrations has been demonstrated, in previous works, between the adaxial and abaxial epidermis (see section 1.14.1). In addition, the abaxial epidermis of all non-aquatic plants have significantly higher stomatal frequencies than the adaxial epidermis (Willmer and Fricker, 1996). In all strip studies describe in this thesis attention is, therefore, focused on the abaxial epidermis.

3.2 Leaf epidermal geometry

3.2.1 Introduction

The determination and patterning of epidermal cell types depend on the cell lineage, cell orientation and relative cell position during the earliest parts of leaf development. Through cell expansion during maturation, the cells assume shapes, fit for the main purposes of providing the mechanical strength needed to support cells over the large air spaces in the underlying mesophyll layers as well as the control of CO_2 and water vapour gateway to the photosynthetic and water relations mechanisms.

Studies show that leaf epidermal anatomy and morphology affect the photosynthetic activity of the leaf (Chabot and Chabot, 1977; Jellings and Leech, 1984). Additionally, these morphologies change in response to environmental cues. For example, aside from stomatal adaptations (Berry and Bjorkman, 1980; Turner, 1986; Willmer and Fricker, 1996), the size of pavement cells decreases (with consequent increase in cell density) in order to better control water loss (Bosabalidis and Kofidis, 2002) under situations of drought. To this effect, the scope of and variations in these leaf epidermal parameters, such as stomatal frequency and size, in response to environmental cues, have been of great interest to biologists since the late 18th century (Hedwig, 1793, Humboldt, 1798; both quoted in Sack and Buckley (2016). These variations are observed in both eudicots (*Arabidopsis thaliana* as model) and monocots (*Tradescantia virginiana* as model) (Croxdale, 1998).

3.2.2 Stomatal parameters

3.2.2.1 Stomatal density

Stomatal density, also known as the stomatal frequency, is the number of stomata (defined in this research work and in literature, where applicable (Willmer and Fricker, 1996), as the stomatal complex) in a unit area of a leaf surface. Stomatal density varies in plants within phyla, classes and even species. For example within ferns and tracheophytes stomatal density ranges from as low as 16 mm^{-2} on the adaxial surface of *Larix decidua* (a gymnosperm) to as much as 2200 mm^{-2} in

Veronica cookiana, a dicot (Willmer and Fricker, 1996). Generally, in monocots (order to which *T. virginiana* belongs) stomatal density on the abaxial surface ranges between 23 mm^{-2} in *T. virginiana* and 175 mm^{-2} in *Allium cepa*. Within a plant, stomatal density is fairly constant from one mature leaf to another under constant growth conditions but varies between the adaxial and abaxial surfaces (Willmer and Fricker, 1996). On the same surface of a mature leaf, stomatal density may also vary from one region to another in a manner characteristic of the plant (Dunn *et al*., 1965), modulated by its growth conditions (Gindel, 1969; Gay and Hurd, 1975; Woodward, 1987; Woodward and Kelly, 1995). Plant ABA levels, which vary according to water availability, also affect the stomatal density (Nadeau and Sack, 2002; Lake and Woodward, 2008). On the whole, stomatal density increases with decreasing stomatal (complex) size (Drake *et al*., 2013). Invariably, since water movement in a plant is in a continuum, changes in the demand and supply are signalled continuously throughout the plant to modify stomatal aperture in mature leaves and stomatal density in developing leaves (Nadeau and Sack, 2000).

3.2.2.2 Stomatal index

The stomatal index, the percentage of the stomata out of all cells on the epidermis, on the other hand, is fairly constant in a plant (Salisbury, 1928; Meidner and Mansfield, 1968). It is expressed as

$$\text{Stomatal index} = \frac{\text{Number of stomatal complex X } 100}{\begin{array}{c}\text{number of juxta apical} + \\ \text{number of pavement cells} + \\ \text{number of stomatal complex}\end{array}}$$

Equation 3.1 Equation for stomatal index (Salisbury, 1928) modified.
In the original equation all cells that did not belong to the stomatal complex were classed as pavement cells).

This chapter gives a quantitative description of the epidermis of *T. virginiana* leaf with a view to observing the positional relationship between the cell types and ascertaining the optimum representative location(s) on the epidermis for sampling of individual cells throughout this research project. The data was generated using the GX-CAM microscope camera on the Zeiss LSM 510 Axioplan 2 imaging microscope and processed with the GX capture software (section 2.7).

It had been envisaged at the onset of the programme to generate a detailed map-matrix upon which to record the single-cell data. Such larger scale mapping was not achieved.

3.2.3 Results

3.2.3.1 Summary

The epidermal cells are arranged in files as troughs separated by ridges (plate 3.1). Cell sizes (measured as their surface area) were larger in troughs around the midrib and the central portion than at the leaf edges (see figure 3.4). The proportion of the trough area per mm^2 occupied by the pavement cells were higher (71%) in troughs near the midrib but lower (60.5%) in troughs near the leaf edge (see figure 3.5). Thus the stomatal density within the troughs showed an increase from 17.1 mm^{-2} to 40.1 mm^{-2} from the midrib troughs to the edge (see figure 3.10). The stomatal index was similar in all the troughs (see figure 3.7).

3.2.3.2 Cell types on *T. virginiana* epidermis

The surface of *T. virginiana* leaf (plate. 3.1) is composed of two alternating file types containing, altogether, six different cell forms. One file type (the ridge) is composed of a single, uniform, cell form. Ridges overly the vascular bundles; the leaf being of parallel venation. At the edges, the ridge is made up of single file of cells, but as many as ten cell files may be found at midrib. The other file type (the trough) is composed of 5 cell types; the pavement, 'juxta apical', apical and lateral subsidiary cells and the guard cell. All the cells in all the files are arranged such that their long axis lie along the long axis of the leaf, except the apical subsidiary cells which lies across this axis. The apical as well as the lateral subsidiary cells surround a pair of

guard cells and, together with it, constitute the stomatal complex. The lateral subsidiary cell is in contact with the whole extent of the dorsal wall of the guard cell leaving the small apex of the guard cell to contact with the apical subsidiary cell. In this way the two lateral subsidiary cells appear to isolate the guard cell anatomically from the rest of the epidermis. The complex is dispersed at intervals along files of pavement cells. Between adjacent apical subsidiary cells of adjacent complexes, lie the juxta apical cells. Thus, six cell types were identified namely: Two pavement cell forms, one form each, of juxta apical, guard, apical and lateral subsidiary cells. The two pavement cell types are found, one in the ridges and the other on the troughs. Pavement cells in the trough are on average circular (on surface view) while the pavement cells on the ridges are strictly rectangular. The cell types differ in sizes though cell size does not constitute a distinguishing characteristic of the cell type. All the cell files in ridges and troughs lie on the same plane except the midrib which is elevated. Plate 3.1 shows a confocal microscope picture of a typical *T. virginiana* abaxial leaf surface.

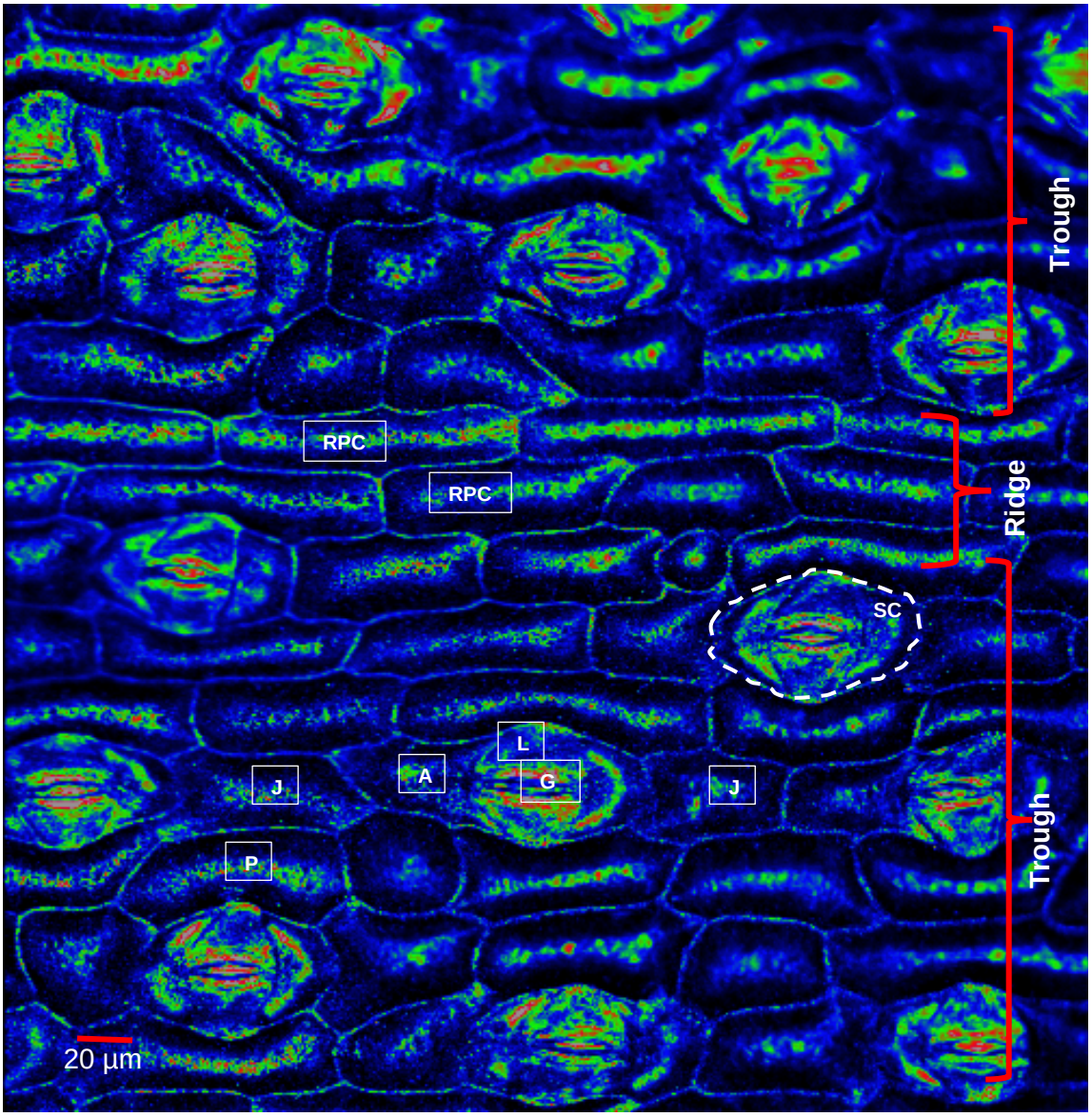

Plate 3.1 Auto fluorescence (excitation 351, emission 430 nm) image of a section of a typical abaxial epidermis of *T. virginiana* showing two troughs on both sides of a ridge. Auto-fluorescence was used for clearer demarcation of the cell boundaries.
RPC = Ridge pavement cells; P = Pavement cell; J = Juxta apical cell; A = Apical subsidiary cell; L = Lateral subsidiary cell; G = Guard cells; SC = Stomatal complex, shown within perimeters of the dashed line. The SC is made up of a pair each of guard cells, apical and lateral subsidiary cells.

3.2.3.3 Relative size (surface area) of each cell type of the epidermis

When calculating the surface area of the different cell types in troughs the cells were assumed to be circular in shape (Raschke, 1979). In practice, the average of the horizontal and longitudinal diameter was used in calculating the area and all the measurements were taken across the cell centre. Measurements were made

according to the schedule in chapter 2, using the microscope camera software. The diameters of three randomly selected cells in three randomly selected pictures at 6 cm intervals from the leaf tip were measured. The random selection of cells in any trough involved the selection of any set of three cell in the same longitudinal plane. The cells were the first and the last cells respectively next to the ridges, proximal and distal to the midrib (see plate 3.2 B) as well as the most central cell (of the type) for each cell type). This form of measurement was used in all the measurements done for this report, except where otherwise stated.

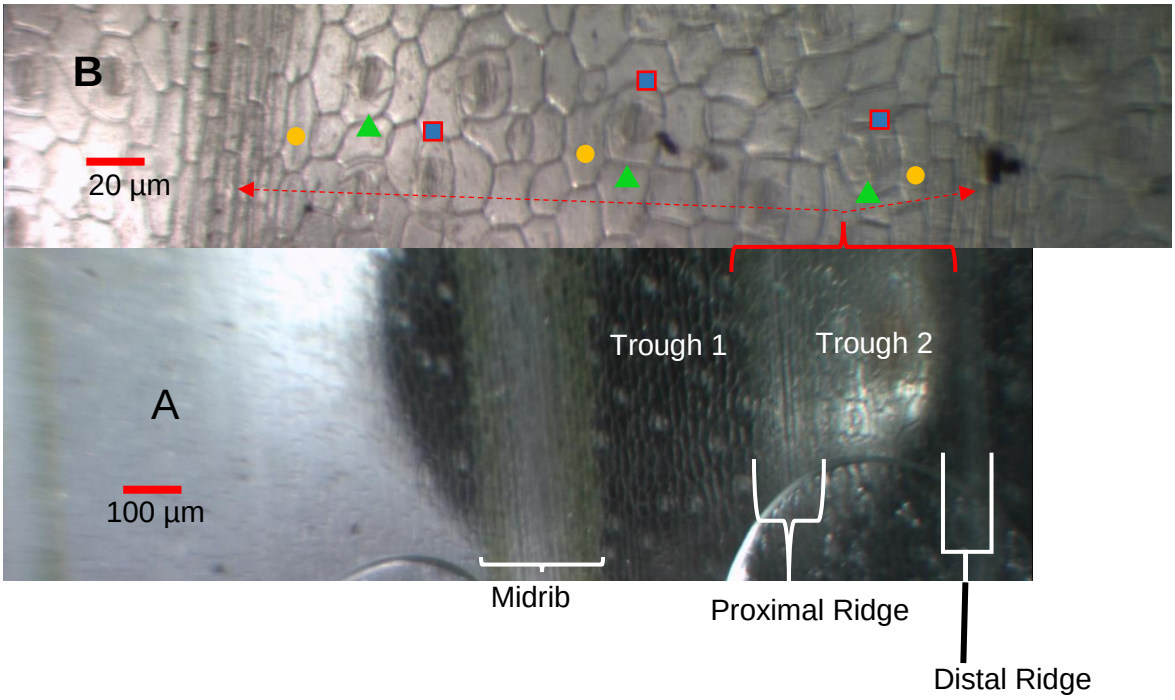

Plate 3.2 Sampling positions used for measurements involving cell types on the abaxial epidermis of *T. virginiana*.
'A' and 'B' are abaxial epidermal strips of *T. virginiana.* 'A' shows the midrib and two ridges on the right (and left – not emphasized) of the midrib subtending two troughs. 'B' shows an enlarged picture of trough 2. Pavement, Juxta apical and stomatal complex cells in the positions respectively marked with circle, square and triangle marks are measured in any selected trough.

Pavement cells Juxta apical cells Stomatal complex

Figure 3.1 shows the relative sizes (in terms of surface area) of individual cell types. Typically, the pavement cells were the largest component constituting 43% of the total area covered by the cell types. The juxta apical, apical subsidiary, lateral

subsidiary, and the guard cells made up 30, 13, 11 and 2.6% respectively of the total area of the cell types.

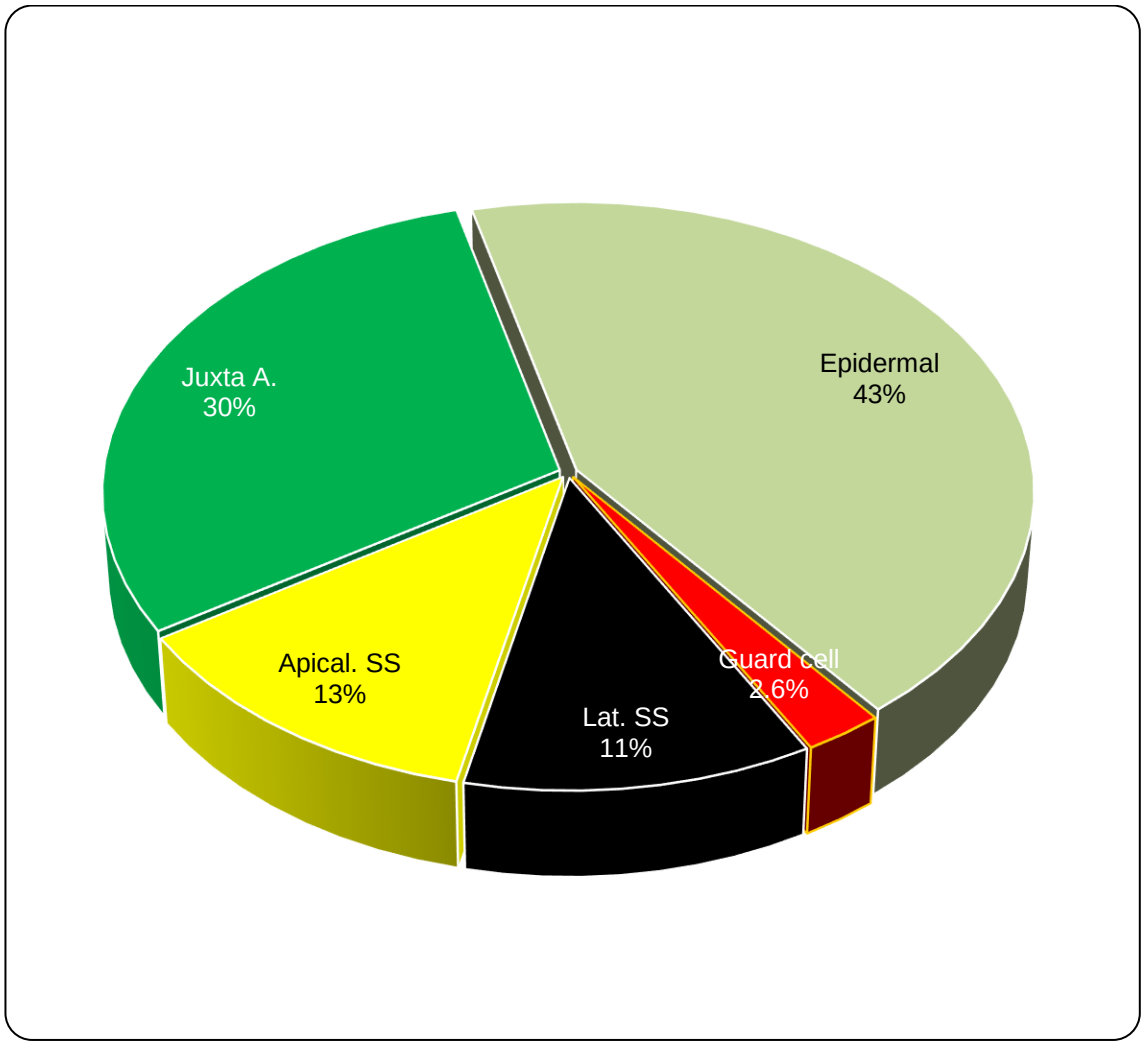

Figure 3.1 Surface area of the typical cell types in the abaxial epidermis of *T. virginiana* trough.

3.2.3.4 Variations in cell size along the longitudinal axis of a leaf

The sizes (surface area) of the stomatal complex (here treated at a single cell unit), the juxta apical and the pavement cells were measured in leaves 5 and 6 of three plants. Measurements were made as described in section 2.7. The stomatal complex was measured as if it constituted a single cell. All measurements were made in trough 3 on both (right and left) sides of the (leaf) midrib. Three cells were sampled at each spot starting at 1.9 cm from leaf tip and continuing at 3 cm intervals towards

the leaf base. Only three cells were used to avoid number bias against the stomatal complex in places where the number of stomata were limiting.

In all the leaves, cell sizes showed a steady increase from the leaf tip to 10.9 cm from the tip, plateaued through approximately 6 cm before steadily decreasing to below 0.02 mm^2 at 28.9 cm distance from the tip (appendix 12). As well, in all but one unusual leaf (leaf 5 of plant 3) sizes of the stomatal complexes, pavement and juxta apical cells were similar within the distal third (from the 22.9 cm from leaf tip) of the leaf.

In the proximal third of the same, unusual, leaf (appendix 12 E), the pavement cells were larger than the stomatal complex and the juxta apical cells, while the three cell types were of similar sizes in other plants. In contrast, in the middle third of all the leaves (10.9 to 16.9 cm from tip) the different cell type had significantly different sizes, which was similar to the results in the other leaves.

In all the other leaves, generally, pavement cells were significantly ($p < 0.05$) larger than the juxta apical cells throughout the length of the leaf. The stomatal complexes were the smallest. Within the mid third of the leaf, no significant change in size ($p > 0.40$) was observed for any of the cell types. Beyond this zone, in the distal third in all the leaves, the stomatal complex and the juxta apical cells show strong similarity in size. Juxta apical cells were, however, not found beyond 25.9 cm from the tip (i.e. in the leaf base) as little or no stomata ($< 0.02.mm^{-2}$) exist there. In one unusual leaf (leaf six of plant 3, (appendix 12 F)) only, stomatal complexes were not found beyond 25.9 cm from the tip.

Thus, the individual plants showed satisfactory uniformity to allow for a more generalized view of this variable cell size (figs. 3.3 and 3.4). The surface area of all the cell types varied according to their distance from the leaf tip and the position of the trough (relative to the midrib) in which they occur. Figure 3.2 shows the variation in the sizes of the stomatal complex as well as the pavement and juxta apical cells along the longitudinal axis of the leaf measured from the leaf tip. Cells were at least an order of magnitude smaller at the leaf base than around half way between the tip and the base (see plate 2.2(A)). Sizes of the stomatal complex ranged from 0.0004 to 0.086 mm^2, the juxta apical cells, from 0.0004 to 0.106 mm^2 and the pavement cells, from 0.0118 to 0.126 mm^2. Equally, cells at the tip were at least three times larger than those at the leaf base. Cell sizes (in all three cell types) increased dramatically from 0.015, 0.023 and 0.038 mm^2 for the stomatal complex, juxta apical

and pavement cells respectively, at 1.9 cm from the leaf tip to 0.077, 0.096 and 0.126 mm^2 at a distance of 10.9 cm from the tip. Between the 10.9 cm and 16.9 cm from the tip, no significant change in cell size existed ($p > 0.05$). From this point on, toward the leaf base, significant drop in cell sizes occurred, bringing cell sizes to 0.0004 mm^2 for the stomatal complex and juxta apical cells and 0.0118 mm^2 for the pavement cells, at 28.9cm from the tip (the leaf base). All the cell types varied in the same way from near the leaf tip up till 19.9cm from the tip. Beyond this point, the cell types behaved differently with respect to their sizes. While stomatal complex sizes remained unchanged between 19.9 and 25.9 cm, the juxta apical cell significantly decreased in size at 25.9cm having behaved in a similar manner to the stomatal complex before then. The pavement cells continuously decreased in size from the distance of 19.9 cm till 22.9 cm (0.087 to 0.052 mm^2) but then, reciprocal to the juxta apical cells, significantly increased to 0.073 mm^2 at 25.9 cm from the tip. From this point to the leaf base, all the cell types significantly decreased in size (see above). Throughout the leaf the pavement cells were larger than the other cell types. Also, in most parts of the leaf, the juxta apical cells were larger than the stomatal complex. At the two extremes of the leaf however, the stomatal complex was larger. Notably, juxta apical cells were absent near the leaf base, at the 28.9 cm distance from the leaf tip.

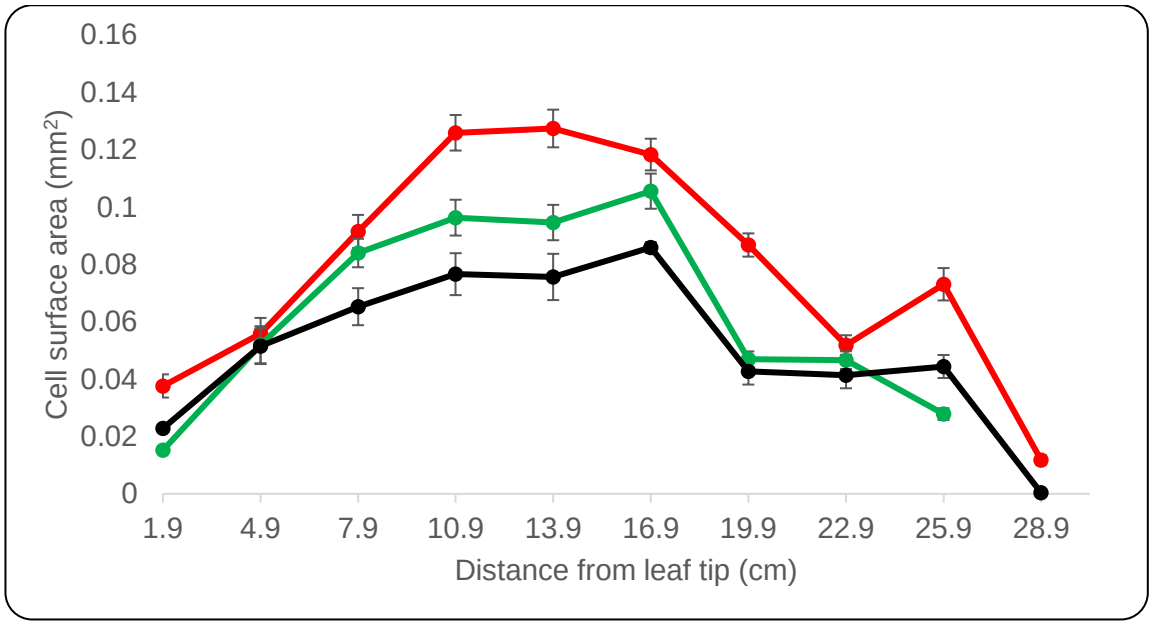

Figure 3.2 Variation in cell sizes (surface area) of the epidermis of *T. virginiana* leaf along the abaxial surface.

3.2.3.5 Size variations in the horizontal axis

Across the leaf, from midrib to the edge, sizes of all the cell types also varied. Figure 3.3 shows the mean surface area of each cell type (stomatal complex, pavement and juxta cells) in each trough (1 to 7). Trough one is immediately next to the midrib. Trough 7 is next to the leaf edge. Patterns of variation in the cell size were essentially similar in the pavement cells and the stomatal complex. The juxta apical cells behaved a bit differently especially at the extremes - near the midrib and near the edge.

In all the troughs, pavement cells were considerably ($p < 0.01$) larger than the other cell types. The juxta apical cells were larger ($p < 0.01$) in the more central troughs (troughs 2 to 5) but smaller in the more extreme troughs (1, 6 and 7) than the stomatal complexes. The stomatal complex maintained the same size (0.04 mm^2) in troughs 1, 2, 5 and 6 but became even smaller (0.03 mm^2) in trough 7. In centrally placed troughs, 3 and 4, the size became significantly ($p < 0.05$) larger (0.05 mm^2) than the cells in the other troughs. The pavement cells were of similar size (0.09 mm^2) between troughs 1 and 4 but became significantly ($p<0.05$) smaller (0.07 mm^2) decreasing to 0.06 mm^2 near the edge.

Near the midrib, the juxta apical cells had very small surface area (1.018 mm^2). A four-fold increase in the surface area (0.08 mm^2) was observed in the following trough (trough 2). Juxta apical cells in the most centrally-placed troughs (troughs 3 and 4) had similar surface areas (0.08 mm^2). Beyond trough 4, the cell size decreased progressively to 0.017 mm^2 in trough 7; near the leaf edge. In all, cell sizes of all the cell types were largest at the central troughs (troughs 2 to 4) and smallest at the troughs near the edge.

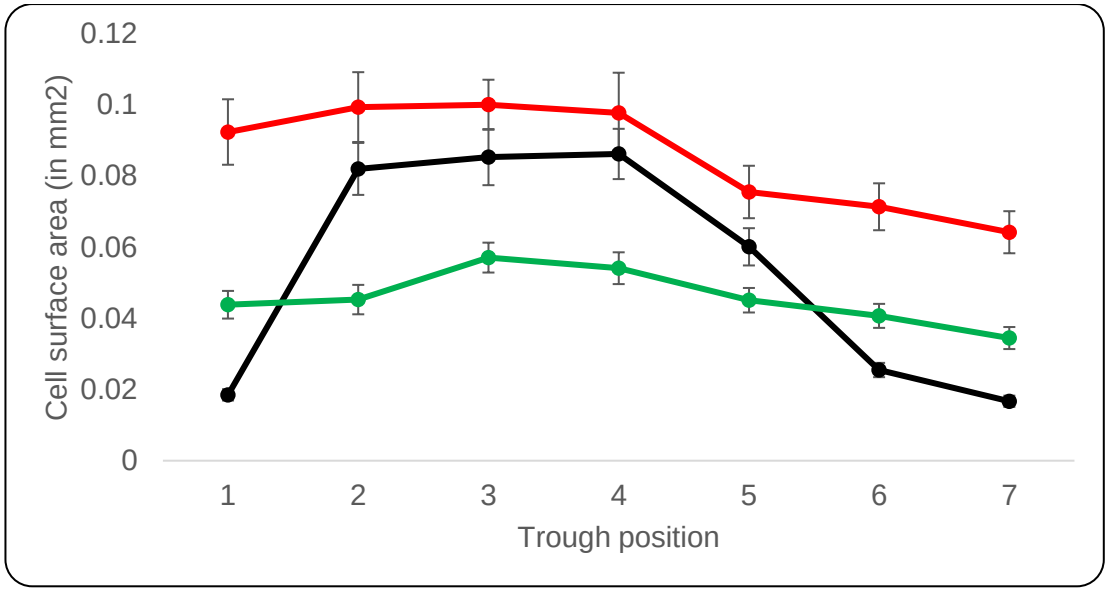

Figure 3.3 Variation in cell sizes (surface area) of the epidermis of *T. virginiana* from leaf edge to midrib on the abaxial surface
Error bars represent standard deviations. n = 6

Pavement cells Stomatal complex Juxta apical cells

3.2.3.6 Proportion of cell types in different troughs

From the above results, which suggest that cell types, especially the juxta apical cells, varied in their sizes according to their (horizontal) trough location, three zones were demonstrated. These include the zone where cell types were significantly small (trough 1), the zone where cell sizes remained unchanged (troughs 2 through 4) and the zone of gradual decrease in sizes (troughs 5 to 7). Sizes (surface areas) of all the five cell types were measured in the right and left sides of leaf five in three plants, at positions 10.9, 13.9 and 16.9 cm from the leaf tip. These measurements were done in three selected cells in each zone at the above distances from leaf tip, according to the schedule stated in section 2.7 above. The different cell types of the stomatal complex were measured and treated separately. Representation of the cell types in different parts of the leaf vary. The percentage share of cell types per mm^2 of trough surface area in three typical locations is shown in figure 3.4 (A, B and C). The locations were near the edge, the central portion and near the midrib, all at the midpoint of the leaf length (between 10.9 to 16.9 cm from leaf tip), where sizes of cell types appeared to be regular (see also figure 3.2). Area covered by stomatal complex (i.e. product of number of cells and cell size) increased towards troughs at the leaf edge from troughs near the midrib (from 7 to 10% for the subsidiary cells);

suggesting that as sizes of stomatal complexes remained fairly constant across the leaf, their number increased from near the midrib to the leaf edge. At the central portion, the pavement, juxta apical, apical subsidiary, lateral subsidiary and the guard cells covered 63, 18, 9, 8 and 2% respectively of the trough surface area. Near the midrib, the respective areas were 71, 14, 7, 7, and 1% while in troughs near the leaf edge, pavement cells constituted 60.5% of the trough area. The juxta apical, apical subsidiary, lateral subsidiary and the guard cells covered 17, 10, 10 and 2% of the trough area respectively. The juxta apical cell was associated with 88.45 ± 9.70% of stomatal complexes.

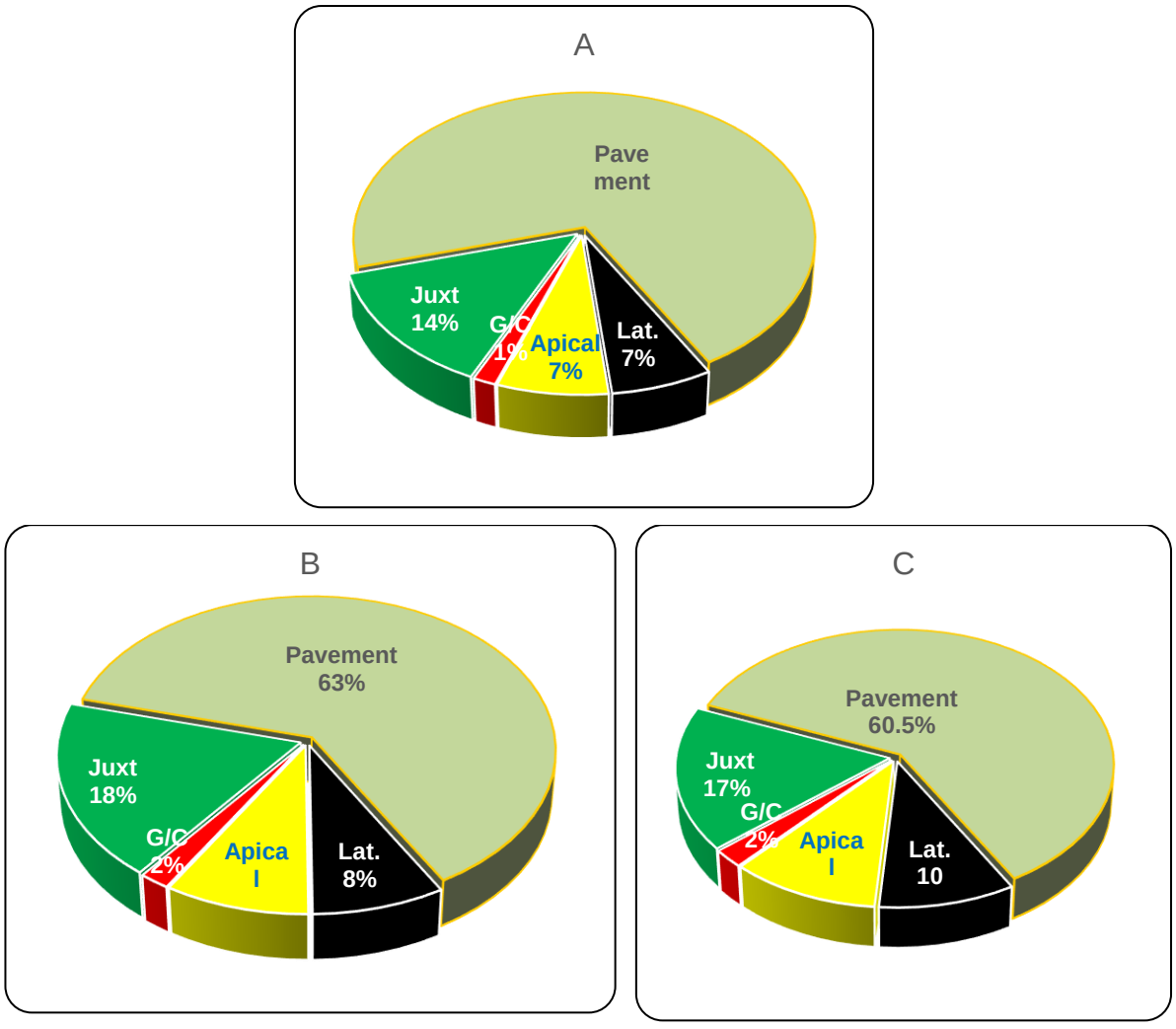

Figure 3.4 Percentage share of cell types per mm^2 of trough surface at:
(A) adjacent to the midrib,
(B) the central portion and
(C) leaf edge – all measured between 16.9 and 22.9 cm distance from leaf tip

3.2.3.7 Stomatal index

The stomatal index describes the proportion (expressed in percent) of cells, per unit area of the epidermis that is made up of the cells of the stomatal complex. Along the leaf length and across the width, the number of the pavement and juxta apical cells as well as the stomatal complex (as a unit) were counted. Starting from 1.9 cm and increasing by 3 cm towards the leaf base, from leaf tip, cells within 0.1 mm^2 at the centre of each trough were counted in leaves 5 and 6 of three plants. Average for all the troughs at each point (1.9, 4.9, etc.) was used for the index at that point in the long axis of the leaf. Across the leaf, an average from each point in a trough was taken for the index for each trough. In each case, the quotient of the number of stomatal complex over the sum of the number of the stomatal complex, pavement and juxta apical cells gave the stomatal index which was then expressed in percentage (see equation 3.1).

Figure 3.5 shows the stomatal index (bubbles) as well as the changes in the leaf width along the longitudinal axis of the leaves. Along the length of the leaf, stomatal index was higher (20.4 ± 0.9 to 30.6 ± 2.4 mm^{-2}) within the distal two third than in the proximal third (14.4 ± 1.1 to 7.0 ± 0.7 mm^{-2}). The stomatal index ranged between 7 ± 0.7 and 30.6 ± 2.4 %. It increased from the leaf tip (27.7 ± 2.0 %) to climax at a third of the leaf length (30.6 ± 2.4 %) and gradually decreased to 20.4 ± 0.9 % through the next third of the leaf. The remaining third of the leaf, mainly the leaf base, (towards the leaf attachment) showed a significant decrease to 14.4 ± 1.1% and subsequently decreased rapidly to 7.0 ± 0.7 % at the leaf base. At the leaf base, 30cm from the leaf tip, the stomatal index was five and half times less than the index at 8 cm from the tip. The leaf width at the corresponding positions had only 6.3% percent difference, being narrower at the leaf base. The mean index for the leaf (as a whole) was 21.5 ± 1.6 %. The index in the distal two third, the main photosynthetic (greenish) part of the leaf was, however, 26.3 ± 1.9%.

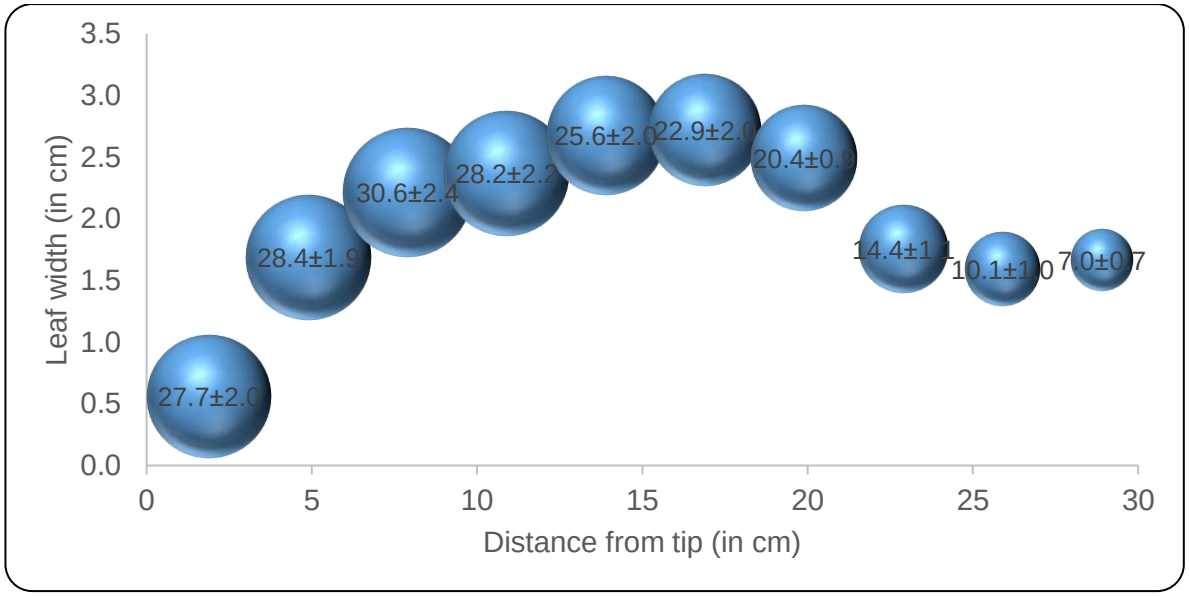

Figure 3.5 Variation in leaf width and stomatal index as distance increases from the leaf tip along the abaxial epidermis in mature *T. virginiana* leaf.
Bubble sizes represent the stomatal index (in % of total cell) and bubble positions show the leaf width. Bubble insert is mean ± sd.

On the other hand, no statistically significant variation ($p > 0.05$) was seen in stomatal index of different troughs (see figure 3.6). The stomatal index in troughs near the mid-rib and ones near the leaf edge were numerically similar. The central two troughs had slightly elevated index. The stomatal index ranged between 23 ± 2.0 % at the leaf edge and near the midrib to 30 ± 2.9 % within the more central troughs.

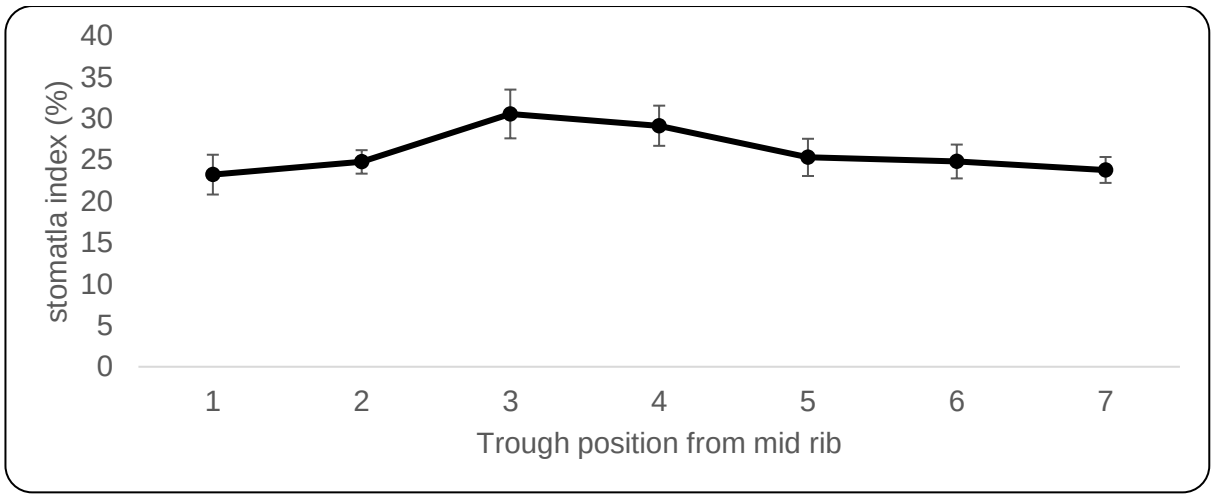

Figure 3.6 Stomatal index in troughs at different positions between the leaf edge and the midrib.
Mean stomatal index in troughs up to 28.9 cm from the leaf tip. Position 1 is closest to the midrib and position 7 is closest to the leaf edge.
Error bars represent standard deviation from 6 lengths from leaf tip taken at intervals of 3cm.

Figure 3.7 shows a three-dimensional plot of the stomatal index against the leaf length and width. Stomatal index was symmetrically distributed on both (right and left) sides of the leaf. The epidermis over the midrib and other vascular bundle positions did not contain stomata. Otherwise, the stomatal index appeared generally uniform across the leaf between 1.5 and 20 cm from the leaf tip. Distribution beyond 25 cm from leaf tip was very sparse (1 to 10%).

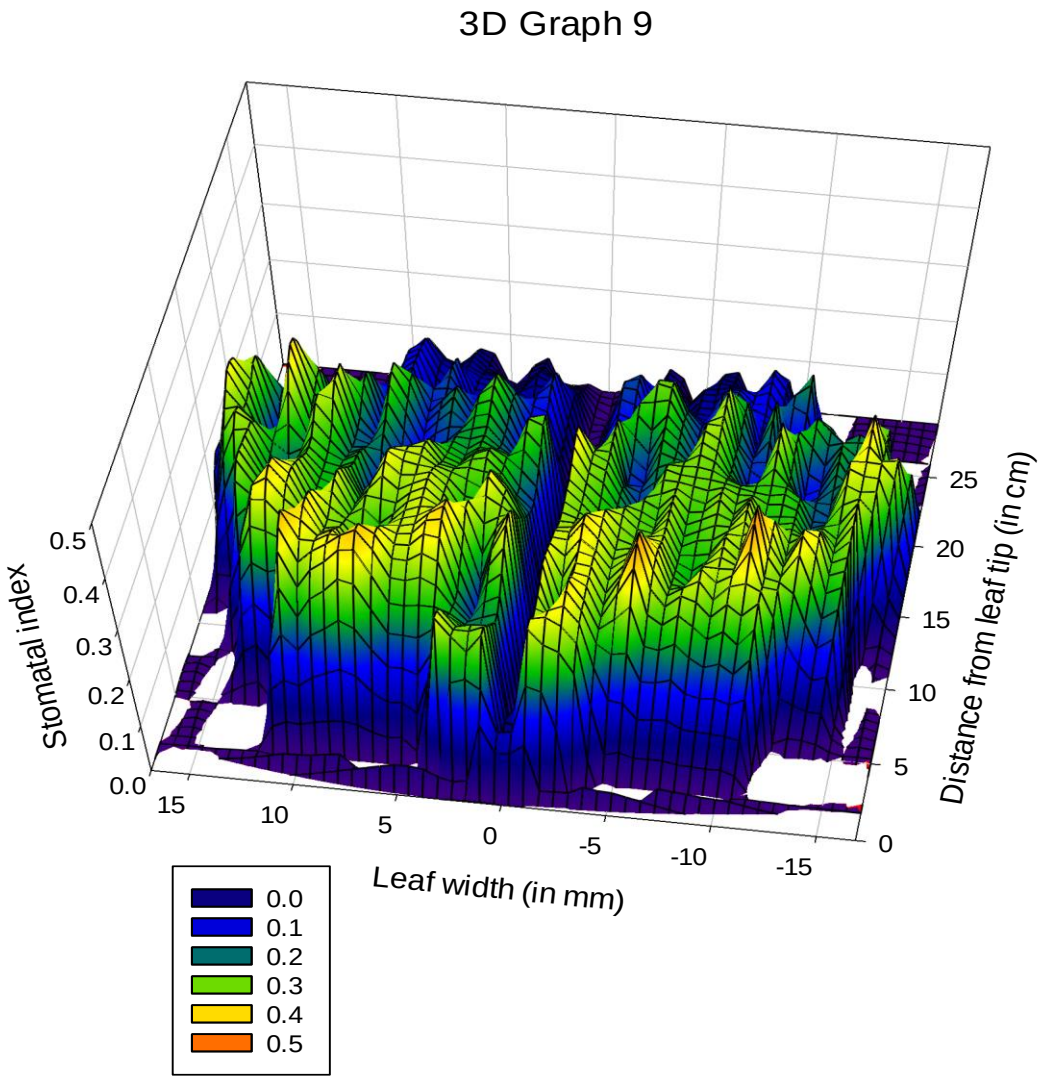

Figure 3.7 Pattern of the stomatal index on *T. virginiana* leaf.
Plot generated from Sigma plot software version 13.0.

0% 1 - 10% 11 - 20% 21 - 30% 31 - 40% 41 - 50%

3.2.3.8 Stomatal density

Stomatal density is the number of stomata in a unit area of a leaf surface. Distinct from, though of less descriptive importance, than the stomatal index, it indicates the number of stomata in a unit area, irrespective of the number of other cell types. Thus areas with smaller cell sizes (of all the cell types) tend to show higher density than area with lager cell sizes even when the stomatal index for both areas are similar. Stomatal frequency was studied along the longitudinal axis and across the width of six mature leaves (leaves 5 and 6) from three plants using the same method in section 3.2.3.7 above. The results show that stomatal density decreased along the longitudinal axis but increased across the width of the leaf (figure 3.8 and 3.9). Along the longitudinal axis, stomatal density decreased from 43.0 ± 3.0 cells per mm^2 at the distance of 1.9 cm from the leaf tip to 16.6 ± 1.5 cells per mm^2 near the leaf base (25.9 cm from the tip). Between the tip and the distance of 16.9 cm the stomatal density decreased steadily (43.0 ± 3.0 to 17.4 ± 1.2 cells per mm^2). From this point on, no significant variation occurred in the density until the leaf base (28.9 cm from the tip) where the density marginally increased to 22.4 ± 1.1 cells per mm^2. The average stomatal density was 25.06 ± 2.3 mm^{-2}.

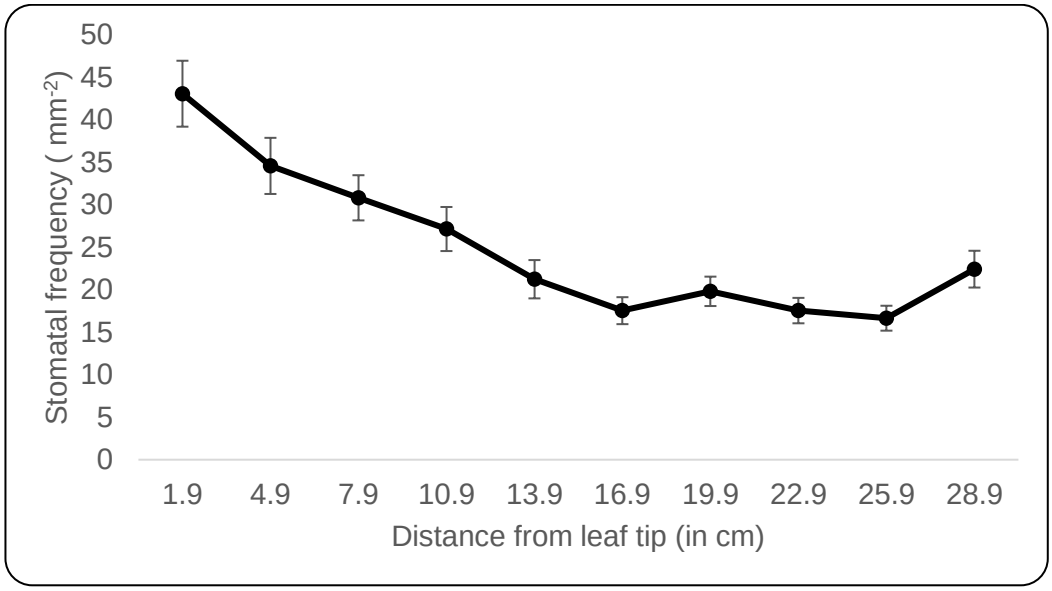

Figure 3.8 Variation in stomatal density as distance increases from the leaf tip along the abaxial epidermis of mature *T. virginiana* leaf

Error bars represent standard deviations. n = 6

Across the leaf width, stomatal density increased towards the edge from the trough closest to the midrib (see figure 3.9). No significant difference exited between the densities in the troughs near the midrib (troughs 1, 2 and 3). Density in the more central troughs (troughs 4 and 5) were different from each other, (32.7 ± 2.2 and 27.1 ± 1.9 cells per mm^2 respectively) and were significantly ($p < 0.05$) higher than those in troughs near the mid-rib. At the leaf edge, stomatal density was marginally higher ($p < 0.05$) than the density in the more central troughs.

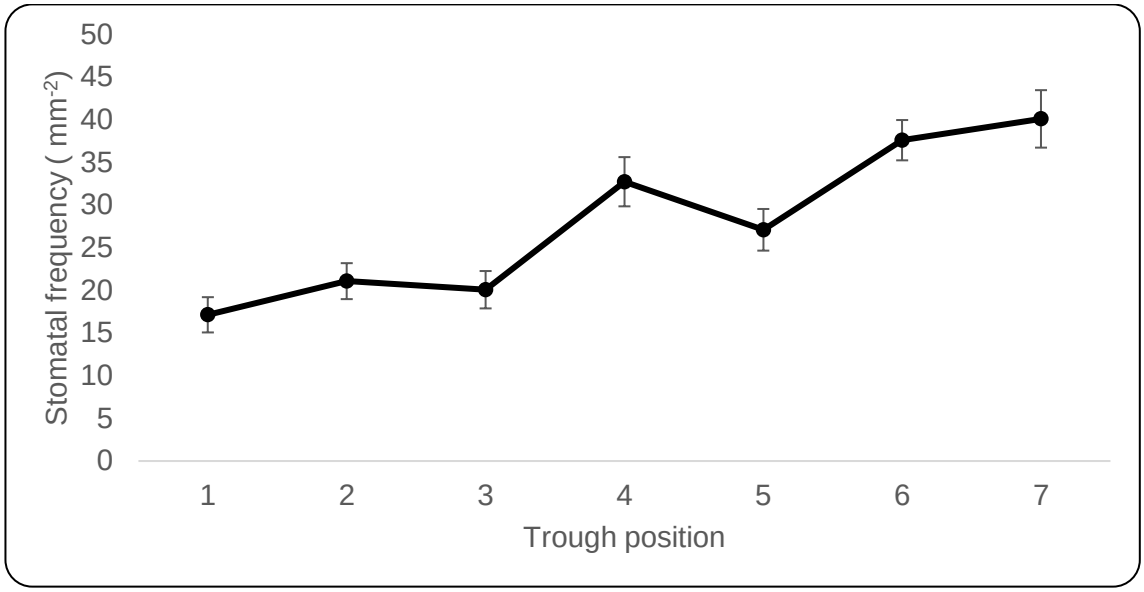

Figure 3.9 Stomatal density in troughs at different positions between the leaf edge and the midrib.
Position 1 is closest to the midrib and position 6 is closest to the leaf edge.
Error bars represent standard deviations. n = 6

3.3 Electrolyte content of bulk leaf

3.3.1 Introduction

This section describes scoping experiments designed to assess the global solute properties of the plant tissues used in the project. This provided a context within which the subsequent analysis of individual cells and tissue could be set.

The major osmotica in the epidermis of plant leaves are the inorganic solutes (Leigh and Tomos, 1993). Inorganic solutes in land plants are absorbed from the soil/growth medium through the roots; although foliar (trans-cuticular) absorption has also been observed following leaf spray (Mengel and Kirkby, 1978). Plant tissues may vary in their solute composition depending on the prevailing supply of solutes from the environment (Epstein, 1966; Fricke *et al*., 1994b; Leigh, 1997).

3.3.1.1 Effect of leaf age on solute composition

Previous works in our laboratory have shown that leaf solute composition changes with leaf age (Hinde 1994; Fricke *et al*., 1994b; Fricke *et al*., 1995). These works have shown that the assayed solutes (Cl^-, NO_3^-, Ca^{2+} and K^+) may vary in concentration as the leaf ages. In grapevine the concentration of the organic solutes as well as the inorganic solutes increase with leaf age (Patakas and Noitsakis, 2001). In addition, deficient solutes may be replaced by some more available ones. For example in Ca^{2+} deficiency, K^+ may replace Ca^{2+} (See Leigh and Wyn Jones (1984)). Differences in nitrogen have also been found (Ackerly, 1992).

Aside from the content and concentrations, patterns of solute distribution in a leaf also varies with leaf age. For example, Ca^{2+} and K^+ distribution in *Hordeum vulgare* epidermis change with increasing leaf age (Fricke *et al*., 1994). In the young leaves, neither Ca^{2+} nor K^+ show any differences in concentration on the two sides of the leaf. As the leaf ages Ca^{2+} becomes preferentially accumulated on the lower and K^+, on the upper epidermis. This demonstrates an uneven distribution of these solutes between the adaxial and abaxial epidermis with increasing leaf age. The reason for the redistribution of solutes appear to be due both to increased permeability of plasma membrane in aging leaves and a sustained rapid influx of solutes into younger tissues as against the lower influx capability in older tissues (Jacoby and Dagan, 1969). Associated with the differences in influx capabilities is the finding that the solute exchange rate is several orders of magnitude faster in the cytoplasm than in the vacuoles at 25ºC; and more at higher temperatures (Pitman, 1963). The decreasing influx to the vacuoles in older tissues, therefore, produces an increasing cytoplasmic (relative to vacuolar) concentration (Jacoby and Dagan, 1969). Perhaps the most dramatic change with leaf age, especially with regards to organic solute, is at the point when a leaf converts from a sink to a source of

photosynthetic products during development (see review by Turgeon (1989)). At this age, solutes for maturing organelles, such as Mg^{2+} for the chlorophylls, as well as solutes derived from photosynthetic products, such as malate, increase.

The variation with respect to individual *Tradescantia* plants and leaves within any individual plant is the focus of this section. The study of these osmotica in whole leaf was aimed at identifying these ions and the gross diversities and/or similarities between the plants used in this programme. A general picture of the solute content of the whole leaf was necessary to appreciate the dominant solutes involved in control of osmotic activities in the plant. To achieve this, standard curves were prepared for use in the quantification of solute concentrations obtained using CZE (section 2.6). Plants were found to be sufficiently uniform so as not to complicate subsequent work. Leaf age, however, was shown to be an important but predictable variable.

3.3.2 Results

3.3.2.1 Standard curves

3.3.2.1.1 Anion standard

Standard anion solutions containing 50 mM bromide as internal standard were prepared as described in section 2.6 and analysed by CZE. This, relatively recent, technique allows fast and efficient quantification of microscopic quantities, and involves little or no pre-analysis preparation of samples. Its basic requirement for quantification of solutes is a standard curve of identified solutes. Therefore, some analysis of the details of the standard curve is included here e.g. the relationship of the signal to the intensity of different ion species.

Plate 3.3 illustrates four examples of CZE runs for 25, 50, 75 and 100 mM anion mixes and the use of the Clarity software (section 2.6). Six anions (Cl^-, SO_4^{2-}, NO_3^-, Citrate, malate and phosphate) are shown together with the internal standard (Br^-) which was 50 mM in each run.

Plate 3.4 illustrates the equivalent for succinate and tartrate and plate 3.5 shows a similar plot for oxalate (without the 25 mM preparation). Plate 3.3 – 3.5 show contaminant peaks (labelled). These appear to be coming from the deionized

H_2O used for preparing the internal standard (Checks on the H_2O (blank) showed a similar peak). Similarly, dH_2O obtained from other locations (laboratories or machines) showed similar peaks. It was thus, concluded to be a contaminant in the H_2O supply to the laboratory system. It is noteworthy that other analysis run before this present one did not have such a contaminant (cf plate 2.5 A).

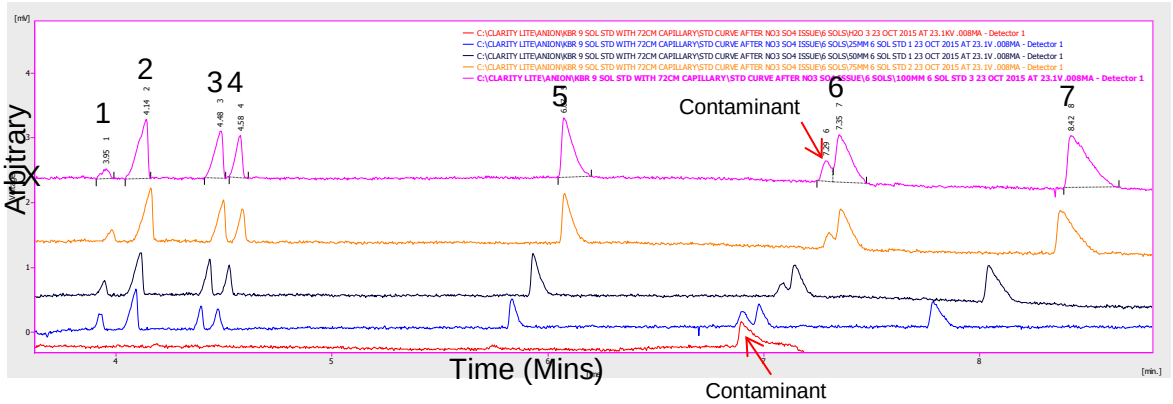

Plate 3.3 Constructing standard curves for six major anions (Cl^-, SO_4^{2-}, NO_3^-, PO_4^{3-}, citrate and malate)
Five independent electrophoretograms are shown each, containing an individual concentration (ranging from 0 to 100 mM) of solution. A constant concentration of 50 mM of Br^- was used as an internal standard in each run. The electrophoretograms are superimposed arbitrarily in the vertical axis (to avoid overlap). The Clarity software output is illustrated. Absolute mobility varied for a range of reasons and have not been normalized here. A contaminant can be seen in the H_2O blank and in all traces at around 7 minutes. Electrolytes: (A) 3.5 mM pyromellitic acid, 24 mM Tris, 1.4 mM DoTAOH, pH 8.0. Capillaries: 72 cm (57.5 cm effective length) 50 µm I.D. 365 µm O.D., 70 µm O.D. at injection tip. Conditions: voltage 21.3 kV, Current 8 µA;
1- 50mM Bromide; 2 – Chloride; 3 – Sulphate; 4 – Nitrate; 5 - citrate; 6 – malate; 7 – phosphate.

H_2O blank 25 mM 50 mM 75 mM 100 mM

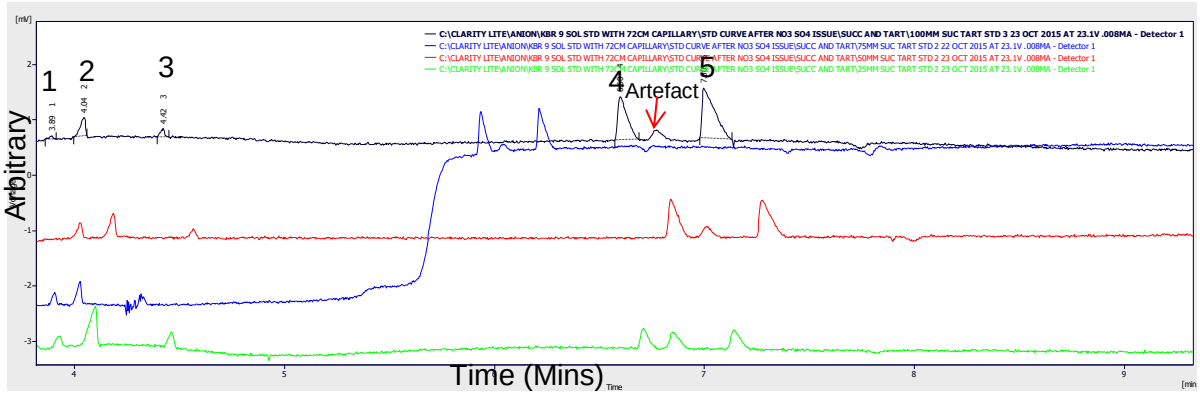

Plate 3.4 Constructing standard curves for succinate and tartrate
Four independent electrophoretograms are shown. Other details as with plate 3.3. Cl^- and NO_3^- were also included in the run. 1 – 50 mM bromide; 2 – Chloride; 3 – Nitrate; 4 – Tartrate; 5 – Succinate. 2 and 3 were used as position marker. The contaminant appeared just before the expected position for malate peak.

25 mM 50 mM 75 mM 100 mM

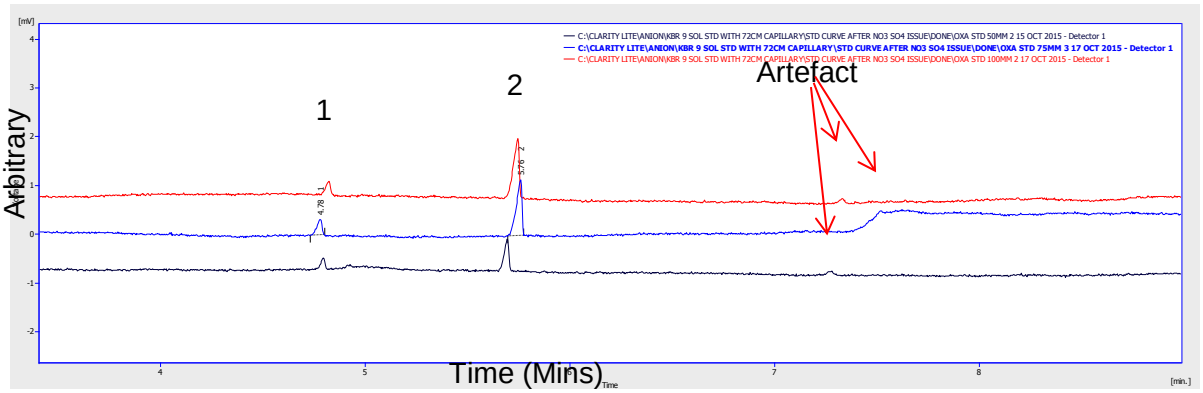

Plate 3.5 Constructing standard curves for oxalate
Three independent electrophoretograms are shown. Other details as with plate 3.3. 1 – 50 mM bromide; 2 – Oxalate. The last peak is a contaminant also seen in plate 3.3 and 3.4 above.

50 mM 75 mM 100 mM

The ratio of the solute to internal standard signal was directly proportional to the solute concentration in all the solutes. The gradient of that relationship was, however, different for each of the solutes although some were very similar (see appendix 1 and 3). Chloride had the lowest gradient of 0.0178 solute to internal standard signal ratio per unit change in concentration. Compared with Cl^-, all the other solutes had higher gradients, NO_3^- - 1.062, PO_4^{3-} - 2.000, succinate – 2.006, oxalate – 2.067, malate – 2.124, tartrate – 2.135, SO_4^{2-} - 2.135 and citrate – 3.011. Thus, Cl^- and NO_3^- had very similar gradients, and PO_4^{3-} succinate, oxalate, malate, tartrate and SO_4^{2-} also had similar gradients. The ionization of any solute

depends on the pH of the solution. In order to properly account for the movement of the species during electrophoresis and the charge balancing within the cell (charge must be essentially neutral), knowledge of the net charge expected for each species at any given (or expected) pH is needed.
Table 3.1 shows the calculated net charge for each of the anions – based on Henderson-Hasselbalch equation (Hasselbalch, 1916).

$pH = pKa + \log_{10} [A^-]/[HA^-]$ ……. Equation 3.2

(Where $[HA^-]$ is the molarity of the acid and $[A^-]$ is the molarity of the conjugate base of the acid). pKa values were obtained from Dawson *et al.*, (1986).
The gradient of the individual curves (appendix 3) followed their net charges at the pH of the running buffer (pH 8.0). For example, table 3.2 shows that both Cl^- and NO_3^-, which possess equal (one) negative charge, had equal gradient (0.018). Similarly, malate, oxalate, succinate and tartrate, with two carboxylic (-COOH) groups, as well as SO_4^{2-} each with two negative charges had approximately equal gradients (0.037). Their gradients were thus, twice that of Cl^- and NO_3^-. At pH 8 citrate possesses three carboxylic charged groups and therefore, had a gradient (0.056) approximately three times that of Cl^- and NO_3^- (appendix 3).

Table 3.1 Calculated net charge at pH 8 for the anions using Henderson-Hasselbalch's equation

		Cl^-		SO_4^{2-}		NO_3^-		PO_4^{3-}		Oxalate		Citrate		Tartrate		Malate		Succinate	
	Ion	pKa	Charge	pKa	Charge	pKa	Charge	pKa	Charge	pKa	Charge	pKa	Charge	pKa	Charge	pKa	Charge	pKa	Charge
	α	-7	1	-3	1	-1.3	1	2.15	1	1.27	1	3.13	1	3.04	1	3.4	1	4.21	1
	β			-2	1			6.82	0.938	4.21	1	4.76	0.999	4.37	1	5.05	0.999	5.64	0.996
	γ							12.38	0.000			6.4	0.975						
Obtained Gradient		0.018		0.038		0.019		0.036		0.037		0.053		0.037		0.037		0.036	
charge sum			1.000		2.000		1.000		1.938		2.000		2.975		2.000		1.999		1.995
Gradient normalized with Cl-		1.000		2.094		1.044		2.017		2.056		2.967		2.056		2.072		1.972	

Figure 3.10 shows that when normalized to Cl^-, a good correlation (R^2 >0.9) existed between the charge found on the species and the normalized gradients from the curves in (appendix 3).

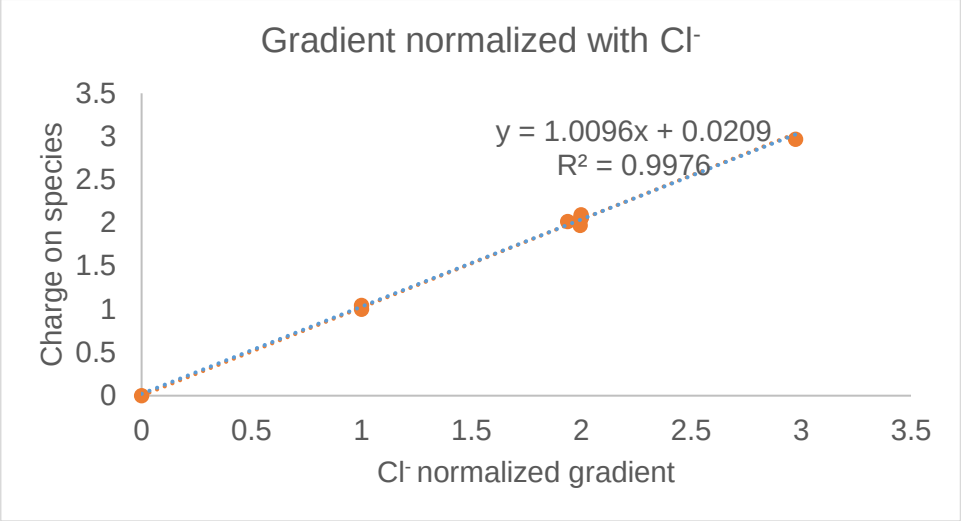

Figure 3.10 Charge to Cl^--normalized gradient for anions

3.3.2.1.2 Cation standards

Ionization of the cation species of relevance to this project is essentially unaffected by pH. Plate 3.6 illustrates four examples of CZE runs for 25, 50, 75 and 100 mM cation mixes. Five cations (NH_4^+, K^+, Na^+, Ca^{2+}, and Mg^{2+}) are shown together with the internal standard (Cs^+) which was 50 mM in each run. The progressive increase in the solute detection time with increasing concentration of standards is normal.

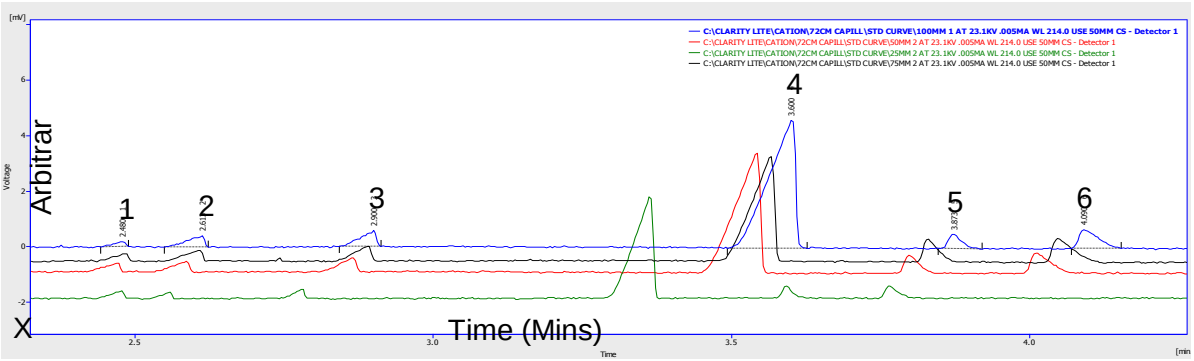

Plate 3.6 Four cation standards preparation separated with imidazole buffer

25 mM 50 mM 75 mM 100 mM

Four independent electrophoretograms are shown each, containing an individual concentration (ranging from 0 to 100 mM) of solution. A constant concentration of 50 mM of imidazole was used as an internal standard in each run. The electrophoretograms are superimposed arbitrarily in the vertical axis (to avoid overlap). The Clarity software output is illustrated. Absolute mobilities varied for a range of reasons and have not been normalized here. X is an arbitrary zero. Electrolytes: 5 mM imidazole sulphate, 2 mM 18-crown-6, pH 4.5. Capillaries: 72 cm (57.5 cm effective length) 50 µm I.D., 365 µm O.D.; 70 µm O.D. at injection tip; Conditions: Current 5 µA. Peaks: 1 – 50 mM Caesium; 2 – NH_4^+; 3 – K^+; 4 – Na^+; 5 – Ca^{2+}; 6 – Mg^{2+}.

Appendix 2 shows the individual analysis of all 3 repeats of each experiment, and the individual standard curves of all 5 cations involved are shown in appendix 4. The ratio of the solute to internal standard signal was directly proportional to the solute concentration in all the solutes. The gradients of that relationship were also different for each of the solutes, and followed their individual net charges. Table 3.2 shows the gradients of each curve as calculated from the plot (appendix 4) Ammonium had the least gradient of 0.0245 solute to internal standard signal ratio per unit change in concentration. Compared with NH_4^+, all the other solutes had higher gradients, K^+ - 1.065, Na^+ - 1.110, Ca^{2+} – 1.551 and Mg^{2+} – 1.927. As shown in table 3.2, Na^+, K^+ and NH_4^+ had approximatley same gradient (0.0264) while Mg^{2+} had approximately twice the gradient of NH_4^+. Ca^{2+} gradient was however, less than two times the NH_4^+ gradient. The gradients of the cations in the curve in appendix 4 are as shown in table 3.2.

Table 3.2 Gradients of the cation standard curves

Solute (mM)	NH_4^+	K^+	Na^+	Ca^{2+}	Mg^{2+}
Gradient	0.0243	0.0264	0.0274	0.0372	0.0473
Charge	1	1	1	2	2

The charges also showed a good correlation ($R^2 > 0.7$) with the NH_4^+-normalized gradients (fig. 3.11).

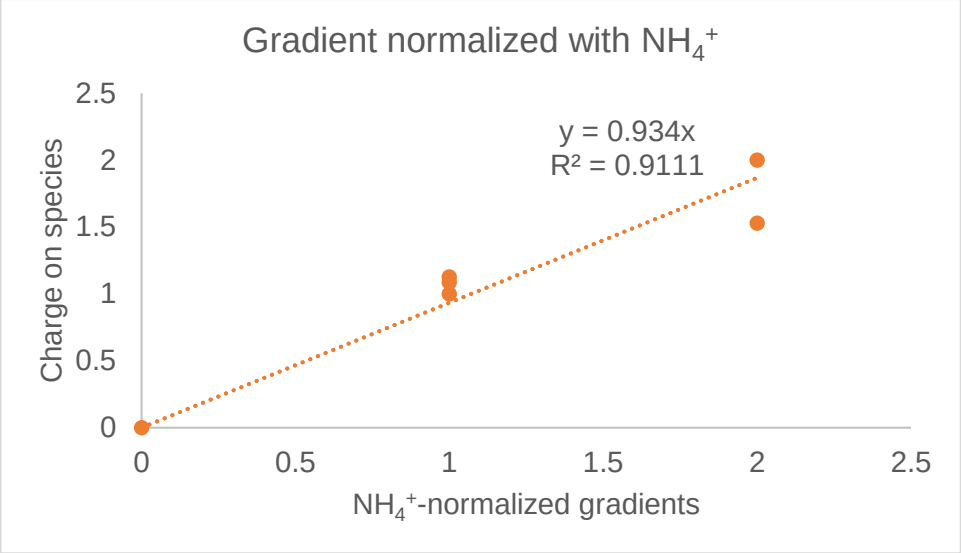

Figure 3.11 Charge to NH_4^+-normalized gradient for cations

3.3.2.2 Bulk measurement in leaf

3.3.2.2.1 Anions

To ascertain the possible solutes present in the plant (*T. virginiana*), their concentrations and possible variations in solute content between them, whole leaf sap was analysed. Four centimetre leaf lengths from (4 – 8 cm from tip of) leaf five of experimental plants at fully expanded 5th leaf stage (4 – 5 weeks old) were frozen immediately after cutting and centrifuged after thawing, to collect the sap content. Before freezing, each leaf cutting was split in two along its longitudinal axis, into right and left halves. The mid-rib was not included.

Nine anion species were recorded. Seven were identified and quantified (Table 3.3) from known standards. In addition, two further components were noted (Plate 3.7; also see plate 2.5A). A range of potential candidates (including formate and propionate) were eliminated on the basis of their CZE mobility.

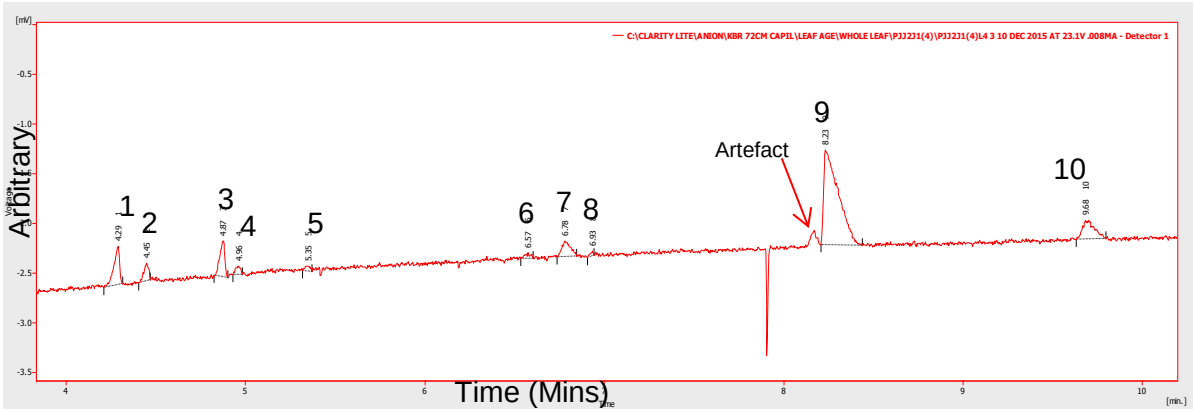

Plate 3.7 Example anion content of whole leaf - separated with PMA buffer
One electrophoretogram is shown. Other details as with plate 3.3 The peaks include 1 – 100 mM Bromide; 2 – Chloride; 3 – Sulphate; 4 – Nitrate; 5 – Oxalate; 7 – Citrate; 9 – Malate; 10 – Phosphate; 6 and 8 – Unknown 2 and 3. The artefact appeared as in H_2O blank (see plate. 3.3). Electrolytes: (A) 3.5 mM pyromellitic acid, 24 mM Tris, 1.4 mM DoTAOH, pH 8.0 Capillaries: 72 cm (57.5 cm effective length) 50 µm I.D. 365 µm O.D., 70 µm O.D. at injection tip; Conditions: voltage 21.3 kV, Current 8 µA;

Inorganic solutes, Cl^-, SO_4^{2-}, NO_3^- and PO_4^{3-}, in addition to organic solutes, oxalate, citrate and malate were found. Malate had the highest (approximately 160 mM) while oxalate had the lowest (approximately 1.3 mM) concentration. Malate concentration was more than twice that of Cl^- (mole for mole). No significant difference ($p > 0.05$) was found between plants. Among the inorganic solutes, Cl^- had the highest concentration (56.22 ± 8.38 mM) followed by SO_4^{2-} (46.24 ± 10.38 mM), NO_3^- (40.58 ± 16.57 mM) and PO_4^{3-} (29.57 ±3.14 mM). Average citrate concentration was 31.40 ± 2.53 mM.

Table 3.3 Mean whole leaf anion concentration in leaves 4, 5 and 6 of 3 plants
n = 9

PLANT 1							
LEAF	Chloride (mM)	Sulphate (mM)	Nitrate (mM)	Oxalate (mM)	Citrate (mM)	Malate (mM)	Phosphate (mM)
4	67.67 ± 19.05	53.02 ± 29.62	30.25 ± 0.67	1.27 ± 0.37	29.83 ± 5.28	168.39 ± 24.34	27.59 ± 3.53
5	63.42 ± 7.55	41.90 ± 11.47	30.15 ± 1.36	1.80 ± 0.42	30.91 ± 5.04	155.53 ± 9.22	26.97 ± 2.05
6	56.61 ± 9.42	24.64 ± 4.86	26.79 ± 2.13	1.19 ± 0.36	29.34 ± 1.80	150.26 ± 16.62	25.22 ± 2.30
PLANT 2							
LEAF	Chloride (mM)	Sulphate (mM)	Nitrate (mM)	Oxalate (mM)	Citrate (mM)	Malate (mM)	Phosphate (mM)
4	63.83 ± 29.06	59.51 ± 10.42	32.97 ± 1.34	1.57 ± 0.36	36.50 ± 1.82	162.73 ± 6.94	33.49 ± 4.39
5	61.67 ± 25.53	47.49 ± 19.26	31.36 ± 4.24	1.52 ± 0.74	31.46 ± 4.10	160.48 ± 10.93	31.90 ± 9.04
6	45.73 ± 6.84	37.72 ± 5.73	27.87 ± 4.62	1.19 ± 0.12	28.06 ± 5.22	149.06 ±1 6.03	26.35 ± 4.64
PLANT 3							
LEAF	Chloride (mM)	Sulphate (mM)	Nitrate (mM)	Oxalate (mM)	Citrate (mM)	Malate (mM)	Phosphate (mM)
4	52.06 ± 8.87	54.54 ± 15.90	53.57 ± 15.80	1.08 ± 0.38	33.45 ± 1.71	163.54 ± 5.32	33.05 ± 2.17
5	45.02 ± 12.39	48.72 ± 9.03	63.66 ± 31.39	1.00 ± 0.16	32.73 ± 4.25	162.04 ± 9.77	29.50 ± 4.28
6	49.98 ± 16.97	48.64 ± 4.20	68.60 ± 24.48	1.02 ± 0.50	30.33 ± 3.68	155.50 ± 8.91	32.05 ± 3.22
Solute Average	**56.22 ± 8.38**	**46.24 ± 10.57**	**40.58 ± 16.57**	**1.29 ±.028**	**31.40 ± 2.53**	**158.61 ± 6.44**	**29.57 ± 3.14**

3.3.2.2.2 Cations

Sap was subsampled from the samples used for anion analysis and analysed for cation contents. In all three leaves, NH_4^+ Na^+, K^+, Ca^{2+} and Mg^{2+} were found. K^+ had the highest (195.05 ± 9.43 mM) while NH_4^+ had the lowest (1.12 ± 0.07 mM) concentration (Table 3.4). K^+ concentration accounted for 50% of the total cation content of each of the leaves. Solute concentrations decreased with leaf age. Lowest concentrations were found in leaf 6 which were 10 to 20% below the leaf 4 levels for all the solutes except NH_4^+. NH_4^+ levels were approximately equal in all the leaves.

Table 3.4 Mean whole-leaf cation concentration in leaves 4, 5 and 6 of 3 plants
n = 9

	Plant 1				
LEAF	NH_4^+ (mM)	K^+ (mM)	Na^+ (mM)	Ca^{2+} (mM)	Mg^{2+} (mM)
4	1.03 ± 0.15	206.16 ± 9.20	4.43 ± 0.44	157.51 ± 4.96	28.27 ± 3.66
5	1.24 ± 0.17	201.19 ± 10.39	4.28 ± 0.37	156.29 ± 3.94	30.59 ± 2.56
6	1.12 ± 0.08	184.59 ± 11.11	4.25 ± 0.32	145.99 ± 4.25	22.06 ± 0.92
	Plant 2				
	NH_4^+ (mM)	K^+ (mM)	Na^+ (mM)	Ca^{2+} (mM)	Mg^{2+} (mM)
4	1.09 ± 0.38	200.13 ± 8.37	4.22 ± 0.45	177.15 ± 34.94	29.36 ± 0.57
5	1.04 ± 0.28	186.09 ± 10.27	4.05 ± 0.39	168.07 ± 14.37	28.74 ± 6.22
6	1.10 ± 0.12	182.39 ± 4.03	3.97 ± 0.21	153.62 ± 3.90	24.83 ± 2.29
	Plant 3				
	NH_4^+ (mM)	K^+ (mM)	Na^+ (mM)	Ca^{2+} (mM)	Mg^{2+} (mM)
4	1.11 ± 0.27	206.90 ± 17.72	4.31 ± 0.13	157.67 ± 7.22	34.52 ± 6.38
5	1.22 ± 0.32	198.04 ± 7.76	4.03 ± 0.20	154.92 ± 6.44	30.48 ± 3.71
6	1.13 ± 0.27	190.00 ± 5.31	4.01 ± 0.07	147.76 ± 8.27	28.39 ± 1.24
Solute average	1.12 ± 0.07	195.05 ± 9.43	4.17 ± 0.16	157.66 ± 9.67	28.58 ± 3.54

3.3.2.3 Balancing charges

Vacuoles make up as much as 95% of the volume of mature plant cells. Plant sap is thus predominantly vacuolar, though mesophyll cells possess more cytoplasmic content than epidermal cells. Vacuolar pH ranges between 5.5 and 6.3 (Bowling and Edwards, 1984; Tomos, Leigh and Koroleva, 2000) while cytoplasmic pH is tightly maintained at approximately 7.5 (Bowling and Edwards, 1984). Sap obtained by homogenization of whole leaf cells would be expected to have a pH of at least 6.4. This is higher than, but closer to vacuolar pH compared to cytoplasmic pH since vacuolar content forms the bulk of the sap.

Table 3.5 shows the calculated net charge of the anions in the leaf sap, using Henderson-Hasselbalch equation. The sap was obtained as detailed in section 2.2, and used for the studies described in section 3.3.2.2.1 and 3.3.2.2.2. The net charge of cations was assumed to be unaffected by pH changes and is used as shown in table 3.5 in all experimental analysis in this thesis. The calculated net charge in table 3.1 was used for the studies described in section 3.3.2.2.1.

Table 3.5 Calculated net charge for the leaf anions at pH 6.4 using Henderson-Hasselbalch equation

	Cl^-	SO_4^{2-}	NO_3^-	PO_4^{3-}	Oxalate	Citrate	Tartrate	Malate	Succinate
Ion	Charge	Charge	Charge	Charge	Charge	Charge	Charge	Charge	Charge
α	-1.000	-1.000	-1.000	-1.000	-1.000	-0.999	-1.000	-0.999	-0.994
β		-1.000	0.000	-0.275	-0.994	-0.978	-0.991	-0.957	-0.852
γ				0.000		-0.500			
Charge sum	-1.000	-2.000	-1.000	-1.275	-1.994	-2.477	-1.990	-1.956	-1.846

3.3.2.3.1 Charge balance for bulk measurement of leaf

Table 3.6 shows the charge balancing for the anions and cations in the bulk measurements in leaf. Charge sums ranged between and 695.92 and 546.25 $mEq.L^{-1}$ for anions, and between 618.46 and 547.44 $mEq.L^{-1}$ for cations. Net negative and positive charges balanced out in each of the leaves with a little excess of negative charge (anions). The charge imbalance in all the leaves was 9.82 ± 7.52 % of the positive charges.

Table 3.6 Charge balance for whole leaves 4, 5 and 6 of plants 1, 2 and 3

Plant	LEAF	(Mean)	Chloride	Sulphate	Nitrate	Oxalate	Citrate	Malate	Phosphate	**Total**	NH4+	K^+	Na^+	Ca^{2+}	Mg^{2+}	**Total**	Charge balance
1	4	Conc. (mM)	67.67	53.02	30.25	1.27473	29.83	168.39	27.59		1.03	206.16	4.43	157.51	28.27		
		$mEq.L^{-1}$	67.67	106.04	30.25	2.55	74.57	336.79	49.65	**667.53**	1.03	206.16	4.43	315.03	56.54	**583.19**	-84.34
	5	Conc. (mM)	63.42	41.90	30.15	1.79619	30.91	155.53	26.97		1.24	201.19	4.28	156.29	30.59		
		$mEq.L^{-1}$	63.42	83.80	30.15	3.59	77.27	311.06	48.55	**617.85**	1.24	201.19	4.28	312.58	61.17	**580.46**	-37.39
	6	Conc. (mM)	56.61	24.64	26.79	1.18654	29.34	150.26	25.22		1.12	184.59	4.25	145.99	22.06		
		$mEq.L^{-1}$	56.61	49.29	26.79	2.37	73.36	300.52	45.39	**554.33**	1.12	184.59	4.25	291.98	44.11	**526.05**	-28.28
2	4	Conc. (mM)	63.83	59.51	32.97	1.56551	36.50	162.73	33.49		1.09	200.13	4.22	177.15	29.36		
		$mEq.L^{-1}$	63.83	119.02	32.97	3.13	91.24	325.46	60.27	**695.92**	1.09	200.13	4.22	354.31	58.71	**618.46**	-77.46
	5	Conc. (mM)	45.73	37.72	27.87	1.18823	28.06	149.06	26.35		1.04	186.09	4.05	168.07	28.74		
		$mEq.L^{-1}$	45.73	75.43	27.87	2.38	70.15	298.12	47.43	**567.12**	1.04	186.09	4.05	336.14	57.48	**584.81**	17.69
	6	Conc. (mM)	32.40	28.05	21.21	1.18823	27.73	158.71	26.35		1.10	182.39	3.97	153.62	24.83		
		$mEq.L^{-1}$	32.40	56.10	21.21	2.38	69.32	317.41	47.43	**546.25**	1.10	182.39	3.97	307.24	49.67	**544.37**	-1.88
3	4	Conc. (mM)	52.06	54.54	53.57	1.07629	33.45	163.54	33.05		1.11	206.90	4.31	157.67	34.52		
		$mEq.L^{-1}$	52.06	109.07	53.57	2.15	83.64	327.08	59.48	**687.05**	1.11	206.90	4.31	315.34	69.03	**596.70**	-90.35
	5	Conc. (mM)	45.02	48.72	63.66	1.00066	32.73	162.04	29.50		1.22	198.04	4.03	154.92	30.48		
		$mEq.L^{-1}$	45.02	97.44	63.66	2.00	81.82	324.07	53.11	**667.12**	1.22	198.04	4.03	309.84	60.95	**574.08**	-93.04
	6	Conc. (mM)	49.9782	48.6372	68.6031	1.01561	30.3255	155.497	32.05		1.13	190.00	4.01	147.76	28.39		
		$mEq.L^{-1}$	49.98	97.27	68.60	2.03	75.81	310.99	57.69	**662.38**	1.13	190.00	4.01	295.51	56.78	**547.44**	-114.94

3.4 Bulk measurement of epidermal strips

3.4.1 Introduction

Results from section 3.3.2.2 showed the significant ionic solutes found in *T. virginiana* leaves. Malate (anion) and K^+ (cation) were the most abundant. The volume of whole leaf in perennials, such as *Tradescantia*, is made up of 57.7% mesophyll, 29.6% epidermis, 6.2% vascular tissue and 3.4% sclerenchyma (Garnier and Laurent, 1994). The epidermis comprises both the abaxial and adaxial epidermis, though heterogeneity has, as well, been demonstrated between the adaxial and abaxial epidermis (Fricke *et al*., 1994c). The aim of this section is to further describe and quantify the solute concentration in the abaxial epidermis with a view to exposing the context within which subsequent chapters describe the role of individual cells in the control of stomatal function, the primary charge of the epidermis in land plants.

Abaxial epidermal strips were prepared as described in chapter 2 (section 2.2.3). Sap extracted from the strips was analysed by CZE. Sap from each sample strip was divided into two subsamples – one for the solute concentration assay and the other for osmotic pressure measurements (chapter 5). The subsamples were separately used for anion and cation analysis.

All solutes found in whole leaf (see section 3.3.2.2) were present in the strip, though, with significant variations in their concentrations. The dominant solutes were malate (anion) and K^+ (cation). Two solutes, not detected in the whole leaf due to their very low concentration, were found in the strips. These corresponded to the standards for tartrate and succinate.

3.4.2 Results

3.4.2.1 Epidermal strip anion content

Each leaf strip sap was subsampled and run in the CZE (section 2.6) for the anion content. The quantified anion solutes are shown in table 3.7. In addition, the two unidentified components found in whole leaf extracts (section 3.3.2.2, plate. 3.7) were also present. The anion (Cl^-, SO_4^{2-}, NO_3^-, oxalate, citrate, tartrate, malate,

succinate and PO_4^{3-}) concentrations (without the unknowns as explained above) in abaxial epidermal strip of leaves 4, 5 and 6 of 3 plants are shown in the table. No significant differences existed between plants ($p > 0.05$).

Concentrations of almost all the solutes differed significantly ($p < 0.05$) between leaves, decreasing with (decreasing) leaf age in all the plants. Oxalate concentrations in leaves 4 and 5 were, however, similar. Leaf 6 consistently had concentrations that were 20 – 30% less than those of leaf 4. Concentrations in leaf five were mostly in-between those of leaves 4 and 6. Malate had the highest while tartrate had the lowest concentration in each leaf. In leaves 4, 5 and 6 malate concentrations were 142 ± 4.25, 130.58 ± 0.03 and 123.82 ± 0.82 mM respectively while tartrate concentrations were 0.41 ± 0.00, 0.37 ± 0.02 and 0.26 ± 0.05 mM in the same respective leaves. In each leaf (4, 5 or 6) NO_3^- and SO_4^{2-} had similar concentrations, which were generally four times lower than Cl^- and also half of PO_4^{3-} concentrations.

Table 3.7 Mean of anions in abaxial epidermal strips of leaves 4, 5 and 6 of three plants
This table shows the concentrations of anions in abaxial epidermal strip of *T. virginiana* measured by CZE. The 4th, 5th and 6th leaves of three plants were sampled. Each sampled leaf was mature and fully expanded. Results are given as mean ± sd (n = 9). The unidentified anions were not quantified (see appendix 5 for details).

Leaf	Cl^- (mM)	SO_4^{2-} (mM)	NO_3^- (mM)	Oxalate (mM)	Citrate (mM)	Tartrate (mM)	Malate (mM)	Succinate (mM)	PO_4^{3-} (mM)
L4	**62.52 ± 0.91**	**17.23 ± 0.79**	**16.28 ± 0.26**	**0.74 ± 0.08**	**18.62 ± 1.80**	**0.41 ± 0.00**	**142.60 ± 4.25**	**0.46 ± 0.02**	**29.55 ± 0.60**
L5	**53.46 ± 1.24**	**14.97 ± 0.32**	**13.18 ± 0.36**	**0.63 ± 0.02**	**14.46 ± 0.08**	**0.37 ± 0.02**	**130.58 ± 0.30**	**0.40 ± 0.00**	**28.08 ± 0.39**
L6	**48.13 ± 1.65**	**11.50 ± 0.55**	**10.88 ± 0.19**	**0.46 ± 0.06**	**12.37 ± 1.20**	**0.26 ± 0.05**	**123.73 ± 0.82**	**0.34 ± 0.02**	**48.13 ± 0.76**

3.4.2.2 Epidermal strip cation content

Sap samples were also analysed for cations. The results are shown in table 3.8. K^+, NH_4^+, Na^+, Ca^{2+} and Mg^{2+} were found. No significant differences existed between plants ($p > 0.05$). In each of the three leaves, K^+ had the highest concentration (289.64 ± 6.94, 272.14 ± 3.02 and 264.83 ± 3.49 mM in leaves 4, 5 and 6 respectively) while NH_4^+ had the lowest concentration (3.27 ± 0.02, 3.00 ± 0.05 and 2.44 ± 0.15 mM in leaves 4, 5 and 6 respectively). K^+ concentration accounted for approximately 70% of the total cation content of each strip.

Concentrations of almost all the solutes differed significantly ($p < 0.05$) between leaves. K^+ concentration in leaves 5 and 6 as well as Na^+ concentrations in

both leaves 5 and 6 and leave 5 and 4 were, however, statistically similar. Solute concentrations decreased with leaf age. Lowest concentrations were found in leaf 6 which were 10 to 20% below the leaf 4 levels for all the solutes. Concentrations in leaf 5 were in-between that of leaves 4 and 6. In each leaf, Ca^{2+} was generally twice more concentrated than Mg^{2+}, which was similar to Na^{+} in concentration.

Table 3.8 Mean of cations in abaxial epidermal strips of leaves 4, 5 and 6 of three plants
This table shows cation concentrations in the abaxial epidermal strip of *T. virginiana* measured by CZE. The 4th, 5th and 6th leaves of three plants were sampled. Each sampled leaf was mature and fully expanded. Results are given as mean ± sd (n = 9) (see appendix 6 for details).

Leaf	NH_4^+ (mM)	K^+(mM)	Na^+ (mM)	Ca^{2+} (mM)	Mg^{2+} (mM)
L4	**3.27 ± 0.02**	**289.64 ± 6.94**	**27.25 ± 0.44**	**58.17 ± 1.02**	**23.87 ± 0.78**
L5	**3.00 ± 0.05**	**272.14 ± 3.02**	**26.63 ± 0.35**	**54.73 ± 0.27**	**21.90 ± 0.59**
L6	**2.44 ± 0.15**	**264.83 ± 3.49**	**26.15 ± 0.14**	**51.97 ± 0.80**	**20.75 ± 0.25**

3.4.2.3 Solute concentrations in leaf five strip

Since leaf 5 has consistently shown significant differences from leaves 4 and 6 (see section 3.4.2.1 and 2), suggesting full maturity at the 5th leaf stage, leaf 5 was chosen for the single cell experiments which form the core of this thesis. A further analysis of the epidermal strip of leaf 5 was repeated in 4 plants to get a clearer picture of the epidermal solutes in that leaf stage and further study between plant differences. In addition, different plants for use in this study have been shown to have no significant difference in solute content and concentrations (sections 3.3.2.2.1, 3.3.2.2.2, 3.4.2.1 and 3.4.2.2). Confirmation of this with the main study subject (leaf 5) was considered appropriate.

3.4.2.3.1 Anions

Sap samples from abaxial epidermal strip from leaf 5 of four randomly selected plants were analysed for anion content using the CZE (sections 2.2.3 and 2.6). The results are shown in table 3.9. Cl^-, SO_4^{2-}, NO_3^-, oxalate, citrate, tartrate, malate, succinate and PO_4^{3-} were identified. No significant differences were found between the plants ($p > 0.05$). Malate had the highest (130.58 ± 3.36 mM) while Tartrate had the lowest (0.37 ± 0.02 mM) concentration in all the leaves. Solutes in plants 2, 3 and 4 showed similar patterns as seen in plant 1. Concentrations of SO_4^{2-} and NO_3^- were similar. Tartrate and succinate concentrations were also similar. Oxalate was

approximately twice more concentrated than tartrate, and similarly Cl^- had about twice the concentration of PO_4^{3-}.

Table 3.9 Mean of anion concentrations in abaxial epidermal strips of leaf 5 of four plants
This table shows anion concentrations in the abaxial epidermal strip of *T. virginiana* measured by CZE. Leaf 5 from four plants were sampled. Each sampled leaf was mature and fully expanded. Results are given as mean ± sd (n = 9).

Plant	Cl^- (mM)	SO_4^{2-} (mM)	NO_3^- (mM)	Oxalate (mM)	Citrate (mM)	Tartrate (mM)	Malate (mM)	Succinate (mM)	PO_4^{3-} (mM)
1	52.49 ± 0.19	14.83 ± 0.45	13.97 ± 1.46	0.65 ± 0.03	14.59 ± 0.40	0.38 ± 0.02	131.57 ± 8.20	0.38 ± 0.05	26.68 ± 1.00
2	51.58 ± 1.44	15.75 ± 0.35	12.73 ± 0.31	0.63 ± 0.03	15.45 ± 0.05	0.39 ± 0.02	128.19 ± 4.38	0.42 ± 0.01	27.80 ± 0.97
3	53.05 ± 0.72	14.16 ± 1.15	12.46 ± 0.73	0.63 ± 0.04	13.37 ± 1.15	0.36 ± 0.03	127.66 ± 2.09	0.37 ± 0.04	31.02 ± 1.36
4	53.07 ± 0.58	14.05 ± 0.33	13.58 ± 0.60	0.62 ± 0.01	14.44 ± 0.34	0.35 ± 0.02	134.91 ± 2.24	0.42 ± 0.03	27.69 ± 1.22
Average	**52.55 ± 0.70**	**14.70 ± 0.78**	**13.19 ± 0.71**	**0.63 ± 0.01**	**14.46 ± 0.85**	**0.37 ± 0.02**	**130.58 ± 3.36**	**0.40 ± 0.03**	**28.30 ± 1.88**

3.4.2.3.2 Cations

Samples were also analysed for cations. The results are shown in table 3.10. NH_4^+, K^+, Na^+, Ca^{2+} and Mg^{2+} were found. No significant differences existed between the plants. In all the leaves, K^+ had the highest (268.41 ± 4.67 mM) while NH_4^+ had the lowest (2.99 ± 0.13 mM) concentration. K^+ concentration accounted for approximately 70% of the total cation content of the strip in each plant. In plant 1 Na^+ and Mg^{2+} had similar concentrations (24.74 ± 3.82 and 22.56 ± 1.94 mM respectively), and Ca^{2+} concentrations (52.80 ± 2.61 mM) were two times that of Na^+ or Mg^{2+}. Similar patterns were repeated in all the other leaves.

Table 3.10 Mean of cation concentration in abaxial epidermal strips of leaf 5 of four plants
This table shows cation concentrations in the abaxial epidermal strip of *T. virginiana* measured by CZE. Leaf 5 from four plants were sampled. Each sampled leaf was mature and fully expanded. Results are given as mean ± sd (n = 9).

Plant	NH_4^+ (mM)	K^+ (mM)	Na^+ (mM)	Ca^{2+} (mM)	Mg^{2+} (mM)
1	3.13 ± 0.23	266.74 ± 16.79	24.74 ± 3.82	52.80 ± 2.61	22.56 ± 1.94
2	2.98 ± 0.31	266.50 ± 11.46	28.24 ± 2.95	56.15 ± 4.98	22.03 ± 1.16
3	2.82 ± 0.60	265.06 ± 8.18	27.06 ± 3.17	54.36 ± 1.15	20.61 ± 1.03
4	3.02. ± 0.36	275.33 ± 7.11	25.86 ± 0.86	55.00 ± 0.31	22.27 ± 2.14
Average	**2.99 ± 0.13**	**268.41 ± 4.67**	**26.48 ± 1.51**	**54.58 ± 1.40**	**21.87 ± 0.87**

3.4.2.4 Charge balance

As a cross-check for the quantification of solutes, balancing of the charges at the expected pH of the extracted sap was examined. Table 3.11 shows the calculated net charge of anions in the epidermal strip sap used for the studies described in sections 3.4.2.1 - 3.4.2.2 and obtained as detailed in section 2.2.3. Henderson-Hasselbalch equation (section 3.3.2.1.1) was used for the calculation. As vacuoles make up over 95% of epidermal cell volume, a pH of 6.3 (see section 3.3.2.1.1) was used for this calculation. Citrate (2.477) followed by SO_4^{2-} (2.000) carried the highest charge in solution at this pH. NO_3^- and Cl^- (1.000 each), as would be expected, had a single charge each. At this pH PO_4^{3-} (1.275) was poorly ionized. The dicarboxylic acids, oxalate (1.994), malate (1.956), tartrate (1.990) and succinate (1.846), to different degrees, were also not fully ionized at this pH. These degrees of ionization have implications on the balancing of charges within a cell, a situation on which many of the physiological processes discussed in this thesis depend.

Table 3.11 Calculated unit net charge for the leaf anions at pH 6.3 using the Henderson-Hasselbalch equation

Ionization	Cl^-	SO_4^{2-}	NO_3^-	PO_4^{3-}	Oxalate	Citrate	Tartrate	Malate	Succinate
Charge on α	-1.000	-1.000	-1.000	-1.000	-1.000	-0.999	-1.000	-0.999	-0.994
Charge on β		-1.000	-0.000	-0.275	-0.994	-0.978	-0.991	-0.957	-0.852
Charge on γ						-0.500			
Total charge	-1.000	-2.000	-1.000	-1.275	-1.994	-2.477	-1.990	-1.956	-1.846

3.4.2.4.1 Charge balance for bulk measurement of abaxial strips

Table 3.12 shows the charge balancing for the abaxial epidermal strip measurements in leaves 4, 5 and 6 studied in sections 3.4.2.1 and 3.4.2.2 (see tables 3.7 and 3.8). Net negative and positive charges approximately balanced out in each of the leaves with a little excess of cations. Charges ranged between 480.64 and 435.37 $mEq.L^{-1}$ for cations and 489.63 to 387.75 $mEq.L^{-1}$ for anions in the strips. In each leaf, malate charges (-275.96, -255.71 and -242.04 $mEq.L^{-1}$ in leaves 4, 5 and 6) balanced at least to 91% of K^+ charges (289.64, 272.14 and 264.83 $mEq.L^{-1}$ in leaves 4, 5 and 6 respectively).

Table 3.12 Charge balance for abaxial epidermal strip of leaves 4, 5 and 6 of the three plants.

Plant	LEAF	(Mean)	Cl^- (mM)	SO_4^{2-} (mM)	NO_3^- (mM)	Oxalate (mM)	Citrate (mM)	Tartrate (mM)	Malate (mM)	Succinate (mM)	PO_4^{3-} (mM)	**Total**	NH_4^+	K^+	Na^+	Ca^{2+}	Mg^{2+}	**Total**	Charge imbalance
1	4	Conc. (mM)	61.61	16.98	16.06	0.72	20.39	0.41	138.83	0.47	30.04		3.29	284.52	26.96	59.35	23.58		
		$mEq.L^{-1}$	61.61	33.96	16.06	1.44	50.51	0.82	271.59	0.87	38.31	**475.15**	3.29	284.52	26.96	118.71	47.16	**480.64**	5.49
	5	Conc. (mM)	52.38	15.33	13.81	0.61	14.60	0.37	131.06	0.40	28.30		3.03	269.54	26.31	55.05	21.49		
		$mEq.L^{-1}$	52.38	30.66	13.81	1.22	36.17	0.74	256.39	0.74	36.09	**428.19**	3.03	269.54	26.31	110.10	42.97	**451.94**	23.75
	6	Conc. (mM)	49.92	10.86	11.03	0.51	13.69	0.22	124.66	0.31	26.56		2.31	262.55	26.15	52.89	20.75		
		$mEq.L^{-1}$	49.92	21.72	11.03	1.02	33.91	0.44	243.87	0.57	33.87	**396.35**	2.31	262.55	26.15	105.77	41.50	**438.28**	41.93
2	4	Conc. (mM)	62.54	16.60	16.57	0.68	18.67	0.41	141.77	0.44	28.88		3.25	286.86	27.04	57.63	24.75		
		$mEq.L^{-1}$	62.54	33.20	16.57	1.36	46.25	0.82	277.34	0.81	36.83	**475.71**	3.25	286.86	27.04	115.26	49.51	**481.92**	6.21
	5	Conc. (mM)	54.81	14.70	13.18	0.63	14.46	0.37	130.50	0.40	27.63		2.95	271.42	26.57	54.56	21.64		
		$mEq.L^{-1}$	54.81	29.40	13.18	1.26	35.82	0.74	255.29	0.74	35.24	**426.47**	2.95	271.42	26.57	109.11	43.29	**453.34**	26.87
	6	Conc. (mM)	46.68	11.80	10.95	0.47	11.35	0.31	123.42	0.35	25.22		2.42	263.08	26.29	51.46	20.51		
		$mEq.L^{-1}$	46.68	23.60	10.95	0.94	28.11	0.62	241.44	0.65	32.17	**385.15**	2.42	263.08	26.29	102.92	41.02	**435.73**	50.58
3	4	Conc. (mM)	62.52	17.23	16.28	0.74	18.62	0.41	142.60	0.46	29.55		3.28	297.54	27.76	57.53	23.27		
		$mEq.L^{-1}$	62.52	34.46	16.28	1.48	46.12	0.82	278.96	0.85	37.69	**479.17**	3.28	297.54	27.76	115.06	46.54	**490.19**	11.02
	5	Conc. (mM)	53.19	14.88	13.78	0.65	14.45	0.34	130.58	0.40	28.30		3.03	275.46	27.00	54.59	22.58		
		$mEq.L^{-1}$	53.19	29.76	13.78	1.30	35.79	0.68	255.45	0.74	36.09	**426.77**	3.03	275.46	27.00	109.18	45.16	**459.83**	33.06
	6	Conc. (mM)	47.79	11.84	10.67	0.39	12.06	0.26	123.10	0.35	26.50		2.60	268.85	26.01	51.56	21.00		
		$mEq.L^{-1}$	47.79	23.68	10.67	0.78	29.87	0.52	240.81	0.65	33.80	**388.57**	2.60	268.85	26.01	103.12	42.00	**442.57**	54.00
Av. charge	4	$mEq.L^{-1}$	62.22 ± 0.53	33.87 ± 0.63	16.30 ± 0.26	1.42 ± 0.06	47.63 ± 2.50	0.82 ± 0.00	275.96 ± 3.88	0.84 ± 0.03	37.61 ± 0.74	476.68 ± 2.18	3.27 ± 0.022	289.64 ± 6.94	27.25 ± 0.44	116.34 ± 2.05	47.74 ± 0.91	484.25 ± 1.58	7.57 ± 3.01
Av. charge	5	$mEq.L^{-1}$	53.46 ± 1.24	29.94 ± 0.65	13.59 ± 0.36	1.26 ± 0.04	35.93 ± 0.21	0.72 ± 0.03	255.71 ± 0.59	0.74 ± 0.00	35.81 ± 0.49	427.14 ± 0.92	3.00 ± 0.05	272.14 ± 3.02	26.63 ± 0.35	109.46 ± 0.55	43.81 ± 1.24	455.04 ± 0.65	27.89 ± 4.74
Av. charge	6	$mEq.L^{-1}$	48.13 ± 1.65	23.00 ± 1.11	10.88 ± 0.19	0.91 ± 0.12	30.63 ± 2.97	0.52 ± 0.09	242.04 ± 1.61	0.62 ± 0.04	33.28 ± 0.97	390.02 ± 5.74	2.44 ± 0.15	264.83 ± 3.49	26.15 ±0.14	103.94 ± 1.59	48.13 ± 1.65	22.99 ± 1.11	48.84 ± 6.22

3.4.2.4.2 Charge balance for leaf five abaxial strip

The charge balance for the abaxial epidermal strip measurements in leaf 5 of four plants is shown in table 3.13. Net negative and positive charges approximately balanced out in each of the leaves with a little (25.54 ± 4.96 $mEq.L^{-1}$) excess of cations in each strip. Charges ranged between 432.46 and 418.90 $mEq.L^{-1}$ for anions, while cation charges ranged between 458.75 and 444.88 $mEq.L^{-1}$. Surplus positive charge (< 7% of total) in each leaf was present. This may be accounted for by the two unidentified anions (see section 3.4.2.1). Malate (-255.45 ± 6.58 $mEq.L^{-1}$) accounted for the largest negative charge, while K^+ (268.41 ± 4.67 $mEq.L^{-1}$) caused most positive charges.

Table 3.13 Charge balance for abaxial strips of leaf 5

Plant	(Mean)	Cl^-	SO_4^{2-}	NO_3^-	Oxalate	Citrate	Tartrate	Malate	Succinate	PO_4^{3-}	**Total**	NH_4^+	K^+	Na^+	Ca^{2+}	Mg^{2+}	**Total**	Charge imbalance
1	Conc. (mM)	52.49	14.83	13.97	0.65	14.59	0.38	131.57	0.38	26.68		3.13	266.74	24.74	52.80	22.56		
	$mEq.L^{-1}$	52.49	29.66	13.97	1.30	36.14	0.76	257.38	0.70	34.03	**426.4245**	3.13	266.74	24.74	105.61	45.13	**445.35**	18.93
2	Conc. (mM)	51.58	15.75	12.73	0.63	15.45	0.39	128.19	0.42	27.80		2.98	266.50	28.24	56.15	22.03		
	$mEq.L^{-1}$	51.58	31.50	12.73	1.26	38.27	0.78	250.77	0.78	35.46	**423.12**	2.98	266.50	28.24	112.30	44.06	**454.08**	30.96
3	Conc. (mM)	53.05	14.16	12.46	0.63	13.37	0.36	127.66	0.37	31.02		2.82	265.06	27.06	54.36	20.61		
	$mEq.L^{-1}$	53.05	28.32	12.46	1.26	33.12	0.72	249.73	0.68	39.56	**418.90**	2.82	265.06	27.06	108.72	41.23	**444.88**	25.98
4	Conc. (mM)	53.07	14.05	13.58	0.62	14.44	0.35	134.91	0.42	27.69		3.02	275.33	25.86	55.00	22.27		
	$mEq.L^{-1}$	53.07	28.10	13.58	1.24	35.77	0.70	263.92	0.78	35.32	**432.46**	3.02	275.33	25.86	110.00	44.53	**458.75**	26.29
Average	$mEq.L^{-1}$	52.55 ± 0.70	29.39 ± 1.56	13.18 ± 0.71	1.26 ± 0.03	35.82 ± 2.11	0.74 ± 0.04	255.45 ± 6.58	0.73 ± 0.05	36.09 ± 2.40	**425.22 ± 5.72**	2.99 ± 0.13	268.41 ± 4.67	26.48 ± 1.51	109.16 ± 2.79	43.74 ± 1.73	**450.77 ± 6.80**	25.54 ± 4.96

3.5 Effect of pH on charge balance

Section 3.4.2.4.1 and 3.4.2.4.2 described the net charge balance (ΔE) at pH 6.3 - the likely pH of the extract (which was not measured directly). As an exercise, however, analysis of how calculated ΔE varies with pH was done in order to determine the likely pH range of the extract (i.e. to exclude the range in which ΔE becomes significant).

Figure 3.12 computes the data for individual plants (1, 2 and 3) while figure 4.2 compares between the three studied leaves (4, 5 and 6) in the plants studied.

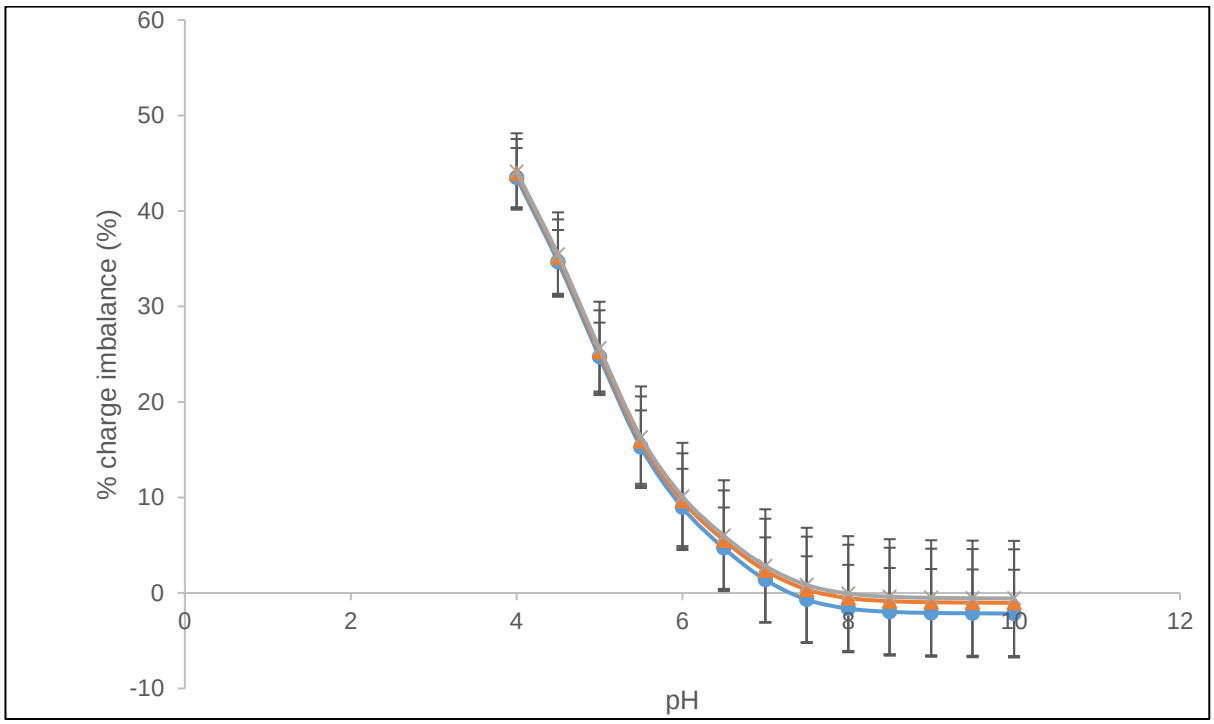

Figure 3.12 Mean % change in charge imbalance with changing pH using data from all three leaves, 4, 5 and 6 of each plant.
This figure shows the % change in apparent imbalance for every change in pH. The % change in imbalance reduces as the pH increases up to pH 8. Subsequently, increase in pH has little or no effect on % change in charge imbalance. Error bars = sd.

The data for leaves 4 – 6 (fig. 3.13) are consistent with pH values for the extract of 7.5 and above. This would appear to be considerably higher than that expected and likely from the literature (i.e. pH 6.3). The comparison between these individual plants (fig. 3.12) also points to a likely weakness in the approach.

However, the unidentified solutes and the possible variations in their concentrations in different leaves and plants may also be a contributing factor. Together with any

charged solute that may be below the detection limit of the CZE technique these may have made up the small proportion (mainly < 7%) of the charge required to balance the positive charges. Had these solutes been identified and included, the % charge imbalance could have reduced. Such reduction shifts the curve downward reducing the pH at which the calculated charges balance out.

Nevertheless, from the data, leaf 4 provided a unique value of pH 6.5 (L4 in fig. 3.13) for the sap. This is well in agreement with the expected pH 6.3. Mean data for leaf 5, however, indicated a range from pH 7.5 to above. While leaf 6 data was inconsistent with basic physics and the extreme standard deviation range, again, indicated the pH 7.5 and above result.

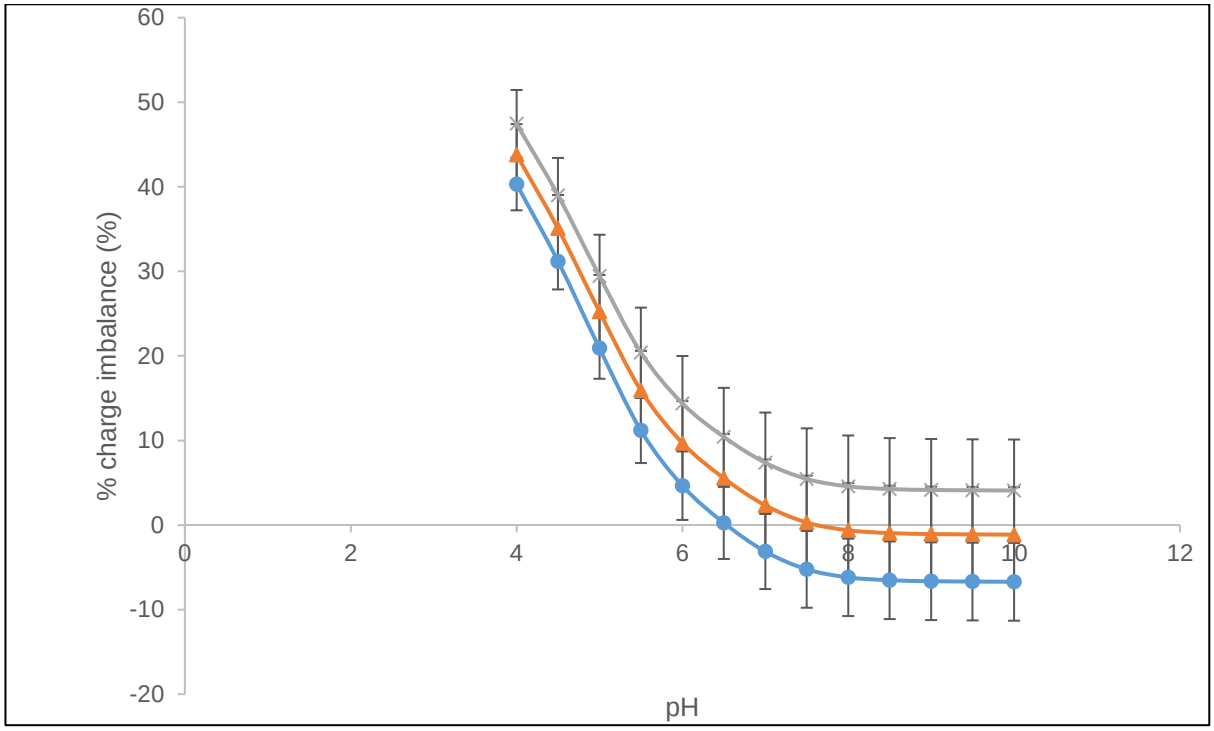

Figure 3.13 Mean % change in charge imbalance with changing pH using data from leaves of same age from plants 1, 2 and 3. Error bars = sd.

3.6 Malate concentrations in whole leaf and strip determined by enzymatic method

Malate has been identified as the major counter-ion to K^+ during stomatal movements in most species, with the commelinacae family being notable (Raschke and Fellows, 1971; see also review by Kollist *et al*. (2014)). Changes in its

concentration during stomatal opening and closing have mainly been studied in epidermal strips using an enzymatic analysis method (Allaway, 1973; Van Kirk and Raschke, 1978b; Van Kirk and Raschke, 1978a; Raschke and Schnabl, 1978; Schnabl and Kottmeier, 1984).

Analyses of malate content of leaves have also been carried out in our laboratory previously by use of an enzymatic method (see Tomos and Sharrock (2001)). As a means of standardizing the results in this project against what obtains in the literature as well as a comparison of the enzymatic method with the (newer) CZE method for solute content assay, malate concentrations in whole leaf and epidermal strip samples from leaf 5 of four plants were analysed by both methods. A standard curve (figure 3.14) for malate concentration-dependent NADH absorbance (at 339 nm) was used (see Tomos et al. (1994)) for obtaining the malate concentration from NADH absorbance.

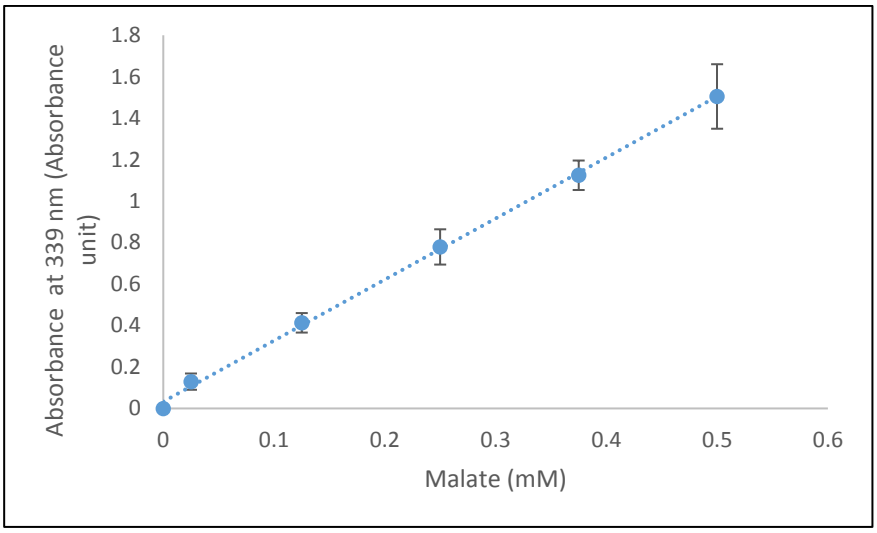

Figure 3.14 Standard curve of NADH absorbance at 339 nm
Error bars = standard deviation (n = 4)

The malate concentrations determined by CZE method were compared to those from the same sample, determined by the enzymatic method (table 3.14). The results from the two methods were 158.1 ± 12.3 and 166.7 ± 2.7 mM in spectrophotometer and CZE respectively for whole leaf and 131.4 ± 11.5 versus 134.3 ± 12.0 mM in spectrophotometer versus CZE respectively for epidermal strip. No statistically significant difference existed between results from the two methods ($p > 0.30$). Malate concentrations in whole leaf samples, by both enzymatic and CZE methods were about 20% higher than in epidermal strip samples.

Table 3.14 Malate concentration determined by CZE and enzymatic methods. Mean ± standard deviation. n = 12

Method	Whole leaf (mM)	Epidermis (mM)	*P* value
Spectrophotometer	158.1 ± 12.3	131.4 ± 11.5	*0.052*
CZE	166.7 ± 2.7	134.3 ± 12.0	*0.010*
P value	*0.302*	*0.778*	

3.7 Discussion

The aim of the studies described in this chapter was to identify and quantify the degree of variations in the epidermis. This identification and quantification of the degree of variations in the epidermis was for two purposes. The first, to determine how much care would need to be taken in selecting individual cells for detailed study during the entire project. The second drive, was to determine if any of the variations might be useful in testing hypothesis derived from the work at cell resolution. Pavement cells directly above the vascular bundle were not considered.

3.7.1 Cell types of *T. virginiana* epidermis

3.7.1.1 Stomata-associated cells (juxta apical cells)

The cell types and patterns found in this study were similar to ones found in other studies on *Tradescantia* (Sheriff and Meidner, 1974; Tomos *et al*., 1981; Bowling and Edwards, 1984; Edwards and Bowling, 1984; Croxdale *et al*., 1992; Franks *et al*., 1995). The stomata are arranged in linear files parallel to the veins as noted in other monocots (see (Esau, 1977)). In this current work, however, the “juxta apical” cells have been distinguished from the pavement cells both for reasons of their anatomical positions and their observed physiological role (discussed in chapters 4 and 5). No distinction between juxta apical and pavement cells has been made in previous literature; possibly because no physiological study relating to solute contribution from cell types has been conducted at the single cell level beyond the stomatal complex. No physiological role had been investigated nor found for this cell type. However, as we shall see in chapters 4 and 5, the cell measurements of solute behaviour provide evidence that these cells may have a different physiological role.

The ontogeny of these cells, as described in chapter 1 (fig. 1.1), stems from protodermal cells from which both ends (proximal and distal to stomata), along the long axis of the leaf, differentiate to form the apical subsidiary cells (Campbell, 1881; Croxdale *et al.*, 1992; Willmer and Fricker, 1996). The perigenous origin of *Tradescantia* stomatal complex (see fig. 1.1) supposes that cells which give rise to apical cells from both (its distal and proximal) ends are likely to have more link to these cells than other cells without such connection(s). It would be interesting to know if there is any plasmodesmata or plasmodesmogram peculiarities in these cells though time did not permit to extend the scope of this research to accommodate such investigations.

Juxta apical cells have for long been identified in literature without being named. Our results show that this cell type made up 13.3% of the epidermis (table 3.1) and is associated with as much as 88.45% of stomatal complexes (fig. 3.4). Croxdale *et al.* (1992) observed, without suggesting any peculiar function, that at least 70% of adjacent stomatal complexes in *T. virginiana* were separated by only one or two pavement cells. They concluded, after X^2 tests that the probability of this occurring by chance was less than 0.01%. Equally importantly, the study showed that these pavement cell types (juxta apical cells) were present in young and mature leaf (trough) regions with the same frequency. Such juxta apical cells (not distinguished from pavement cells by name) were also found in *Chlorophytum, Galanthus,* and *Schixostylis* species (Charlton, 1988). It is known that stomatal positioning is not random (Korn, 1972) and has been used for taxonomic classification of live and fossil plants (Stebbins and Shah, 1960; Upchurch Jr, 1984). It must be meant to play a role in the efficient functioning of leaves.

Mutant phenotype analysis is now revealing the mechanisms regulating the development of stomata. In monocot species such as *Dieifenbachia, Syngonium, Eichhornia,* and *Sagittar* which possess net, instead of parallel venation, as well as in eudicots, such cells have not been reported (Dunn *et al*., 1965). Anatomical identification of these cell types in eudicots may be very difficult since mature and immature cells (stomata) appear side by side in eudicots as against the basipetal sequence of maturity and linear files of stomata in monocots (Ziegenspeck, 1944; quoted in Dunn *et al*. (1965)). A SiCSA comparison of these cells would be interesting and may reveal functional differences between those mature cells around the stomata in eudicots.

3.7.2 **Stomatal index**

Unlike stomatal density, stomatal index is independent of cell size. In *Vigna sinensis*, in which stomatal index is influenced by incident irradiation received by the plant within the 6 day preceding the unfolding of the leaf, the intensity and fluence rate of the light received, determine the stomatal index of the leaf (Schoch, Zinsou and Sibi, 1980). The signal is received by phytochromes in older leaves and transmitted through the phytochromes in the developing leaf (Schoch *et al.*, 1984). Along the length of the leaf, stomatal index was higher (27.7 to 30.6 %) within the distal two third than in the proximal third (14.4 to 7.0 %) (fig. 3.5). Cell sizes, e.g. stomatal complex size (see section 3.2.3.4), were low (0.015 mm^2) near the leaf tip and leaf base (0.0004 mm^2) but higher (0.096 mm^2) within 6 to 20 cm from the leaf tips (fig. 3.2). The other cell types showed similar pattern. In all, ridges 2 through 5, at a distance of 4.9 to 19.9 cm from the leaf tip appear to be representative of the leaf and ideal for sampling.

The stomatal index obtained in this study was relatively uniform throughout the distal 20 cm (20 cm from the tip) and across the leaf width. The index was found to be significantly lower within the proximal 10 cm of the leaf which corresponds mainly to the leaf base and the environs. The average index within the 20 cm from the tip along the long axis of the leaf, 26.26 ± 3.5 %, was similar to the average index across the leaf width, 25.9 ± 2.8 %. This is consistent with the findings in literature which show that stomatal index is constant in all parts of a leaf (blade), not counting the leaf base (Schoch *et al.*, 1984; Salisbury, 1928; Weyers and Lawson, 1997). Along the length of the leaf, stomatal index was higher (20.4 ± 0.9 to 30.6 ± 2.4 %) within the distal two third than in the proximal third i.e. around the leaf base (14.4 ± 1.1 to 7.0 ± 0.7 %) (see fig. 3.5). Cell sizes e.g. stomatal complex size (see appendix 12), were low (0.015 mm^2) near the leaf tip and leaf base (0.0004 mm^2) but higher (0.096 mm^2) within 6 to 20cm from the leaf tips (fig. 3.5). The other cell types showed similar pattern.

3.7.3 **Cell size**

The epidermis of *T. virginiana* leaf is made up of cells within the troughs and cells overlying the ridges (vascular bundles). The former consists of 64.8% pavement

cells, 16.3% juxta apical, 8.7% apical subsidiary, 8.3% lateral subsidiary and 1.7% guard cells (Table 3.15). The juxta apical cells constitute 13.3% of the abaxial epidermis. Croxdale *et al*., 1992 referring to this cell type, although described as pavement cell located between apical subsidiary cells, concluded that it was associated with up to 70% of stomatal complexes. Our results show that this cell type makes up 13.3% of the epidermis (table 3.15) and is associated with as much as 88.45% of stomatal complexes (fig. 3.4).

Table 3.15 Percentage content of cell types in troughs and whole leaf abaxial epidermis of *T. virginiana*.

Cell types	Pavement	Juxta apical	Apical	Lateral	Guard
% of trough surface area of leaf (%)	64.8	16.3	8.7	8.3	1.7
% of the whole epidermis (%)	52.9	13.3	7.1	6.8	1.4

These troughs constitute 81.6 ± 4.6% of the leaf epidermis. The pavement and juxta apical cells show consistent patterns, increasing in size from the tip to the centre of the leaf and then declining towards the base. For a 30 cm leaf, this is relatively uniform in the region 6 – 17 cm from the tip. Cells 6 cm from the tip were also, for this reason, chosen for most of the experiments described in this thesis. Initially, it had been envisioned to apply SiCSA to contrasting regions of the leaf. This turned out to be impractical in the time available.

Across the leaf, pavement cell sizes were relatively uniform. Juxta apical cells, however, showed a consistent pattern of being much smaller close to the midrib (trough 1) and leaf margins (troughs 6 and 7). Therefore, pavement and juxta cells in troughs 2 and 4 were used in this work. Size of the stomatal complexes showed a similar distribution to the pavement cells along the long axis of the leaf and also across the leaf width – being relatively uniform across the leaf. This also gave further justification for the sampling 6 cm from the leaf tip.

Despite the significant variation in the sizes of pavement and juxta apical cells, the stomatal index was remarkably uniform along the level 17 cm from the tip. The extreme size and stomatal index values found near the base and at the leaf margin provided possible variation for hypothesis testing. In the event no time was available to take advantage of this. Hopefully this and other variations can be

exploited in the future. Nonetheless, previous works done in *Commelina* show the same pattern for stomatal distribution (Smith *et al*., 1989). It was, in addition, observed that apart from the smaller sizes of cells at the margins, tip and base, stomatal function in these areas were less efficient than in the central zones. For example, stomatal aperture in the margins, tip and base of the leaf was relatively closed when stomata at the more central parts of the leaf were fully open. It is thought that the decrease in function in these areas with small sizes of stomatal complex was due to the reduction in the average effective area (substomatal area) available for CO_2 assimilation (Raschke *et al*., 1990). The differences in size as well as stomatal density, increasing towards the margins and the leaf base, have also been reported in terms of photosynthetic activities (Reviewed by Terashima (1992) and by Weyers and Lawson (1997)). This also agrees with the results shown in fig. 3.9 which indicate that stomatal frequency increased towards the leaf edge. The increase of the subsidiary cells from 7 to 10% with only 1% increase in the proportion covered by the guard cells was not surprising as a significant increase in the number of guard cells is required for a unit percent increase in its share of space on the leaf surface. It appears that at least a 3% increase in the proportion covered by the subsidiary cells is required for a 1% increase in that of guard cells.

3.7.4 **Stomatal density**

Stomatal density (fig. 3.8) decreased along the leaf length from 43.0 mm^{-2} near the tip to 25.9 mm^{-2} near the leaf base. Generally, since stomatal, but not pavement cell, number is influenced by irradiance (Meidner and Mansfield, 1968; Gay and Hurd, 1975), the parts of the leaf that are more exposed to light at the stage of stomatal initiation have a higher, while parts less exposed, have a lower number of stomata per unit area. The result in this survey agrees with this. They show higher stomatal density in the more exposed parts of the leaf (towards the tip and middle sections) and lower index in the less exposed parts - towards the leaf base. The slight but significant elevation in density near the leaf base may be explained by the sharp change in the angle of the leaf which disposes it to far greater exposure (of the abaxial aspect) to light than the immediate vicinity at the base. Nonetheless, due to the up to thirty fold difference in size between pavement cells and stomatal complex

in this region (more than ten times of the highest difference in any other part of the leaf) the number of stomata present per unit area is expectedly increased. Contrary to this finding, however, Slavik (1963) found significantly higher density near the leaf base than toward the tip in tobacco leaves. This difference is likely due the anatomical differences between the two leaf types which allows more exposure to light near the leaf base in tobacco during stomatal initiation.

Results in this study also show that stomatal density in troughs increased steadily towards the leaf edge. This increase is expected since cell number is known to increase as cell size decreases (Zalenskii, 1904; Salisbury, 1928; Kutik, 1973). Most workers have reported that the highest stomatal densities are found at the leaf tip and edges while lowest stomatal densities were found near the leaf base and near the mid veins (Salisbury, 1928; Gupta, 1961; Smith, Weyers and Berry, 1989 and Timmerman, 1927 (quoted in Gupta, 1961)). In *Zea mays*, however, highest stomatal densities were found in the middle region of the leaf blade (Meidner and Mansfield, 1968). The average density in the abaxial epidermis of *T. virginiana* was found to be 23 mm^{-2} (Meidner and Mansfield, 1968). This is similar to the stomatal density of 25.06 ± 2.3 mm^{-2} found in this experiment. The finding is in agreement with other studies of the epidermis (Reed and Hirano, 1931). This is likely due to the presence of only one cell form of similar shape and relative size in all the positions. This fact does not, however, preclude the chances of investigating possible function of these cells in the orchestration of stomatal action in intact leaf. Knowledge from this study is important in deciding the leaf to be used in this research and also in deciding the optimum representative position(s) for sampling.

3.7.5 Whole leaf solutes

Results in this chapter show no difference in solute content or concentrations ($p > 0.05$) between plants. This may have been due to two factors. Firstly, the plants are clones from the same plant (see section 2.1). Secondly, the plants were grown under similar strict controlled growth chamber conditions. Thus, solute content and concentration was similar in all the plants.

Malate was the most concentrated anionic solute (table 3.3). This may have implications in the counter anion that may be required in the regulation of stomatal

movements. Irving (1996) also found that malate has the highest concentration in *T. virginiana* leaf at every age.

Chloride, which is a common ion implicated in stomatal movements was about half the concentration (56.22 ± 8.38 mM) of malate (158.61 ± 6.41 mM), but was of similar concentration to SO_4^{2-} (46.24 ± 10.38 mM). This agrees with the findings by Irving (1996) which showed that SO_4^{2-} (14 mM) was similar in concentration to Cl^- (6 – 10 mM) in mature leaves of *Tradescantia.* In barley Cl^- is about an order of magnitude higher in concentration than SO_4^{2-} (Dietz *et al*., 1992b). The SO_4^{2-} level in *Tradescantia* is surprising considering the low solubility of sulphate salts of divalent cations such as Ca^{2+}. The concentrations of Mg^{2+} in the whole leaf (28.58 ± 3.54 mM) is consistent with findings in other studies (Irvings, 1996; Dietz *et al*., 1992b). In contrast, the Ca^{2+} concentration (157.66 ± 9.67 mM) found in this study was high. Considering the very low solubility of $CaSO_4$ (solubility product of 4.93×10^{-5} at 25ºC) and the SO_4^{2-} level in these plants, this result appears unexpected. However, most of the Ca^{2+} may be bound in cell walls or as calcium oxalate found in trichomes in plants of commelinaceae family (Ruiz and Mansfield, 1994) to which *Tradescantia* belongs.

Mg^{2+} is mainly contributed by the chlorophyll-associated Mg^{2+} in the mesophyll. Our results show no significant variation ($p > 0.05$) in solute concentration with leaf age. This is not in agreement with previous findings in our laboratory and elsewhere in other species (see section 3.3.1.1). No solute concentration variation(s) with leaf age has been reported in *Tradescantia*, though. Perhaps, as observed in this study, significant differences do not exist between mature leaves until approaching senescence and or abscission (Ferguson and Simon, 1973). At the other extreme, differences may be significant between leaves at different stages of development, such as those used in the works of Fricke *et al.* (1994b). Our results in comparison with other results from our laboratory (such as Fricke *et al*. (1994b)) suggest that after full leaf expansion, significant differences in solute content only exist between leaves that have significant age differences.

The organic solutes detected in these leaves may by no means be exhaustive since the CZE system used in this work is capable of detecting only ionized species. Non-ionized solutes such as sucrose and glucose which have been demonstrated in *Tradescantia* are not detected. The significance of these in the generation of plant

cell turgor is well established, and their relevance in the present study on stomatal movement will be discussed in chapters 4 and 5.

3.7.6 Solute locations

The whole-leaf sap analysis had shown that malate was the dominant anion in *T. virginiana* leaf (section 3.3.2.2.1). Analysis of epidermal strip (in a subsequent experiment) also showed that malate was the dominant solute in the epidermis of *T. virginiana*. Cl^- and PO_4^{3-} followed at distant second and third positions in order of abundance at approximately half and one fourth of the malate value (see table 3.7). Chloride and PO_4^{3-} showed almost entirely similar concentrations ($p > 0.49$) in both whole leaf and epidermal samples, concentrations in the strip (52.55 ± 0.70 and 28.30 ± 1.88 mM respectively for Cl^- and PO_4^{3-}) being only slightly less than those of whole leaf (56.22 ± 8.38 and 29.57 ± 3.14 mM respectively for Cl^- and PO_4^{3-}).

Malate was expectedly lower ($p < 0.01$) in the epidermis than in whole leaf. This may be because, except for the guard cells which contain few chloroplasts, epidermal cells are devoid of chloroplasts. The guard cell makes up 1.4% of the abaxial epidermis (table 3.15). It is thus expected that the contribution of the epidermis to observed malate is negligible. This implies that the malate found in the epidermal strips may have been imported - mainly from mesophyll sources. The epidermis comprising both ad- and ab-axial aspects makes up only 26.6% of whole leaf volume (see Garnier and Laurent (1994)). Thus, solutes with concentrations lower in whole leaf but higher in the epidermis (abaxial epidermis in this study) would suggest epidermal preponderance (> 5 fold more). By extension, the closer the concentrations of a solute in both sap (whole leaf and epidermal) the higher the chances of its abundance in the epidermis since concentrations in the epidermis have little impact on whole leaf concentrations. It is noteworthy that high malate concentration found in the epidermis was not likely due to contamination of the samples by mesophyll tissues as care was taken to eliminate such contaminations during strip preparations. Extra caution could have been taken by washing the strips, but this was not done since it might have risked dilution, in H_2O or, in an osmoticum, increased osmotic pressure of the strip sap. Even if contamination occurred, the less than 16% difference ((130.58 ± 3.36 mM in strip and 158.61 ± 6.44 mM in whole leaf - see table 3.16) between whole leaf and strip malate concentrations suggest a

significant epidermal source or store. Fricke et al. (1994c) showed that in barley adaxial malate is at least twice higher in concentration than abaxial malate. Such data is not available for *Tradescantia*. However, comparable solute patterns appear to exist within our results (from *Tradescantia*) and those from barley.

Chloride as well as PO_4^{3-} maintained similar ($p > 0.4$) concentrations in both whole leaf and the epidermis suggesting epidermal preponderance. Cl^- is preferentially accumulated in the epidermis in barley and many other species (Fricke et al., 1994c; Karley et al., 2000b; Gilliham, et al., 2011). PO_4^{3-}, however, is mainly epidermal in some species such as *Lupinus* and *Vicia* (Dietz et al., 1992), but preferentially accumulated in the mesophyll of other species such as barley (Fricke et al., 1994c; Karley et al., 2000b). The difference in PO_4^{3-} preferences has been attributed to species specificity (Dietz et al., 1992). NO_3^- on the other hand, was lower ($p < 0.05$) in the epidermis. Abaxial epidermal NO_3^- has, however, been known to be up to an order of magnitude lower than that in adaxial epidermis (Fricke et al., 1994c). Therefore the low (abaxial) NO_3^- in this study appeared to be consistent with results of previous studies in barley. SO_4^{2-} was significantly ($p < 0.01$) less in the epidermis. Citrate also appeared to be more concentrated in whole leaf suggesting mainly mesophyll origin. Curiously, oxalate also appeared to be mostly found in the whole leaf (mesophyll). However, its low concentration (1.29 ±.0.28 mM) suggests that its source was small when compared with the whole leaf - possibly epidermal. The observed difference may be due to differential distribution of oxalate between abaxial epidermis (used in this strip experiment) and the adaxial epidermis. This is especially important since oxalate may be employed as calcium oxalate in adaxial epidermis as a first line of defence against herbivores, as found in some species (Finley, 1999). We shall note later the absence of oxalate in single epidermal cell samples suggesting its storage in, most probably, the trichomes.

Table 3.16 Average concentration of anions in mature whole leaf and leaf 5 epidermal strip of *T. virginiana* compared
Cl^- and PO_4^{3-} have similar concentrations in whole leaf and epidermal strip. Malate concentration is higher in whole leaf. Similarly, oxalate as well as citrate, NO_3^- and SO_4^{2-} are all more concentrated in whole leaf than in epidermal samples.

Solute	Cl^-	SO_4^{2-}	NO_3^-	Oxalate	Citrate	Malate	PO_4^{3-}
Whole leaf (mM)	56.22 ± 8.38	46.24 ± 10.57	40.58 ± 16.57	1.29 ±.028	31.40 ± 2.53	158.61 ± 6.44	29.57 ± 3.14
Epidermal Strip (mM)	52.55 ± 0.70	14.70 ± 0.78	13.19 ± 0.71	0.63 ± 0.01	14.46 ± 0.85	130.58 ± 3.36	28.30 ± 1.88
P value	*0.492*	*0.007*	*0.046*	*< 0.001*	*< 0.001*	*0.003*	*0.580*

Similarly, the cations showed some preferential distribution patterns (table 3.17). Ca^{2+} and Mg^{2+} were mainly ($p < 0.001$ and $p < 0.05$ respectively) in the mesophyll while K^+, NH_4^+ and Na^+ appeared mainly ($p < 0.001$) in the epidermis. The importance of NH_4^+ in the epidermis is not immediately obvious, but Na^+ which may become toxic intracellularly may be preferentially sequestered in the cuticle or the trichomes. In cereals there are differences in cation distribution between abaxial and adaxial epidermis as well as between epidermis and mesophyll. For example, Leigh and Tomos (1993) found that Ca^{2+} content of epidermis was about an order of magnitude greater than that of mesophyll in barley. *Commelina* species, a close relative of *Tradescantia*, are however, known to be sensitive to Ca^{2+} and have preference for K^+ in its epidermis, possibly to compensate for the K^+ flux involved in control of it stomata (Schwartz, 1985). It is likely that this role of K^+ in stomatal function is the reason behind its preferential accumulation in the epidermis.

Table 3.17 Average concentration of cations in mature whole leaf and leaf 5 epidermal strip of *T. virginiana* compared
Whole leaf concentration of the divalent cations are higher than that of abaxial epidermis. Conversely, monovalent cations are more concentrated in the epidermis than in whole leaf i.e. in the mesophyll.

	NH_4^+	K^+	Na^+	Ca^{2+}	Mg^{2+}
Whole leaf (mM)	1.12 ± 0.07	195.05 ± 9.43	4.17 ± 0.16	157.66 ± 9.67	28.58 ± 3.54
Epidermal Strip (mM)	2.99 ± 0.13	268.41 ± 4.67	26.48 ± 1.51	54.58 ± 1.40	21.87 ± 0.87
P value	< 0.001	< 0.001	< 0.001	< 0.001	0.033

3.7.7 Effect of leaf age on solute concentration in the epidermis

Concentrations of all anions in the epidermal strip of *T. virginiana*, increased with increasing leaf age. The significant differences, however, were only apparent between leaves with appreciable age difference. Increase in Cl^- was by 14.4 mM and malate increased by 18.9 mM. The changes in the solute species with low concentrations were masked by their minuscule concentrations. Their differences were better appreciated in terms of percentage change (see table 4.18). This is most important for solutes such as oxalate which is thought to be important in herbivore defence (see section 3.7.6 above). Oxalate and tartrate changed the most (62.8 and 55.7% respectively).

Table 3.18 Percentage increase in concentration between leaf 4 and 6 of *T. virginiana*.

Solute	Cl^-	SO_4^{2-}	NO_3^-	Oxalate	Citrate	Tartrate	Malate	Succinate	PO_4^{3-}
Leaf 4 (mM)	62.5 ±	17.2 ±	16.3 ±	0.7 ±	18.6 ±	0.4 ±	142.6 ±	0.5 ±	29.6 ±
Leaf 6 (mM)	48.1 ±1.6	11.5 ±0.6	10.9 ± 0.2	0.5 ±0.1	12.4 ±1.2	0.3 ±0.0	123.7 ± 0.8	0.3 ±0.0	26.1 ±0.8
Increase	14.4	5.7	5.4	0.3	6.3	0.1	18.9	0.1	3.5
% increase	29.9	49.9	49.6	62.8	50.6	55.7	15.3	37.6	13.3

A similar pattern was also observed in the cations. NH_4^+ and K^+ increased more than Ca^{2+} and Mg^{2+}. Na^+ was essentially unchanged.

Previous studies have found significant increase in solute concentration with leaf age in *Tradescantia*. For example Irving (1996) found that Ca^{2+} changed by 50 mM and Mg^{2+} by 75 mM between leaves with age difference of 8 weeks. Four week old plants were used for this present research and the difference in the age of the leaves studies was less than two weeks. The leaf age classification applied in this study was in terms of leaf insertion on the stem but not in terms of the absolute age of the leaf. This is because it was thought that this system will suffice to show any differences and effects of age on stomatal function. Dating the leaf in a plant like *Tradescantia* may also be very subjective since new leaves are usually unexposed until some degree of expansion has occurred. Thus, sampling was timed at similar time as that for all the stomatal studies (see chapter 2). Since significant differences were noted in some solutes between leaves 4 and 6 at this age difference, it is likely that with greater age gap such concentration differences as observed by Irvings (1996) might be seen.

In other species such as barley, Ca^{2+} (Hinde, 1994; Fricke *et al*., 1994a) as well as Cl^- and NO_3^- (Fricke *et al*., 1994a) solute concentrations also increase with leaf age. Changes in levels of other solutes have not been reported to date to the best of our knowledge.

3.7.8 **Malate assay**

Comparison of the CZE and enzymatic methods of determining malate concentration in whole leaf and epidermal strip sap showed no significant difference ($p > 0.05$) between the results of the two methods. The enzymatic method showed

comparatively wider margins of error, considering that equal numbers of samples were used for both methods. Despite the margin of error, the concentrations were numerically similar to that found in earlier measurements reported in sections 3.3.2.1.1 and section 3.4.2.1 in this chapter. Koroleva *et al.* (2000) found malate concentrations of 120 – 180 mM in barley epidermis.

3.8 Conclusion

The work in this chapter was designed as a scoping exercise to aid planning of the detailed cell mapping. Its introduction also set out current understanding of the molecular basis of the functional design of the mature leaf. It was only possible to exploit some of this information during this project. However, it became apparent from quantitative and qualitative differences in solute (see chapters 4 and 5) that the anatomical position of the juxta apical cells is associated with functional physiological differences. As a result, this cell type was given particular attention in this chapter. The observation that juxta apical cells were absent within the leaf base (appendix 12 and section 3.2.3.4) where there were non-functional stomata suggests that the juxta apical cells may be strongly associated with stomatal functioning. This is also possibly supported by a similar observation to the effect that both at the leaf tip and base, and only in those places, the stomatal complexes are larger than the juxta apical cells, when present. Likewise, in the more peripheral troughs, where less functional stomata are expected, the juxta apical cells were smaller in size than the stomatal complexes. In the more central troughs, on the other hand, the juxta apical cells were larger. The proportion of juxta apical cells was also higher in the more central troughs (see fig. 3.4), where stomatal activity is usually higher. These results also show that the juxta apical cells decreased in functional size in areas where stomatal function was lower, again suggesting that these cells (juxta apical cells) are important for stomatal function in *Tradescantia*.

Another cell which, by its anatomical position, appears to be of great importance is the lateral subsidiary cell. In isolating the guard cell from the other cells of the epidermis it appears to be the portal for solute trafficking to and from the guard cells.

A general picture of the solute content of the whole leaf was necessary to appreciate the dominant solutes involved in control of osmotic activities in the plant. The dominant solutes found in this study were malate for the anions and K^+ and to a lesser extent, Ca^{2+}, for the cations. While malate has been implicated as a major osmotically-active anion with respect to stomatal function in some species, in grasses, Cl^- has been demonstrated as the major anion (Willmer and Fricker, 1996). The high position occupied by malate in this regard might have been due to the overriding contribution of the mesophylls over the epidermis (volume per volume). An assay of the epidermal (strip) content was thus, needed

Bulk whole leaf (section 3.3.2.2) and epidermal solutes (section 3.4) showed similar solute concentration patterns. However, some solutes, tartrate and succinate, which were not found in whole leaf (possibly due to low concentrations) were observed in the strips. In both whole leaf and strips, significant difference in K^+ and malate concentrations were observed between leaves that were at least one week apart in age. Very importantly, K^+ and malate were found to be the major osmotica in both whole leaf and strips, though concentrations of malate in whole leaf were higher. In epidermal strips, malate (255.45 ± 6.58 mEq.L^{-1}) accounted for almost all the negative charge, required to balance K^+ (268.41 ± 4.67 mEq.L^{-1}). This has been the conclusion of most researchers on the counter-anion for K^+ during stomatal movements. This is one of the major flaws of conclusions drawn from bulk measurements on physiological phenomena at cellular level (see section 1.16.1). It shall later be seen in chapter 4 that the major counter-ion for K^+ is Cl^- instead of malate as may be suggested by its higher concentration compared to Cl^- in the strips. The high malate (and citrate) concentrations noted in these bulk (whole leaf and strip) sap may possibly be the contribution of bundle sheath and ridge cell. Their contribution to stomatal movements has not been investigated though.

The effect of pH on the ionization of anions was also analysed. The anion and cation concentration of the epidermal strips balanced. Imbalances in the anions and cation content of any sap may be studied and may predict the pH of the sap. Finally, the results from CZE analysis was confirmed using a different method which yielded similar results as the CZE.

At a more general level, a region was identified within each leaf/plant that provided a uniform and reproducible target for the detailed SiCSA work, namely: leaf 5 at a distance of 6 cm from the tip in troughs 2, 3 and 4. This region showed no

variations in cell sizes and stomatal density (figs. 3.3 and 3.6), and was used for the single cell samplings for the studies described in the ensuing chapters (4 and 5).

Chapter 4 Solute concentrations in single cells at closed and open stomata conditions

4.1 Introduction

While organic solutes are mostly formed within the plant, in higher plants inorganic solutes are absorbed through the roots. The solutes entering the root hairs may continue into the xylem either through a transmembrane, a symplastic and/or an apoplastic path (Clarkson, 1993). Transmembrane transport may involve ion channels and/or carrier proteins (section 1.15). The symplastic path is provided by the plasmodesmata (section 1.13). Apoplastic solute movement in the root is hindered at the endodermis (the inner layer of the cortex) by Casparian strips lining the cells of the endodermis. Most solutes reaching the Casparian strip continue toward the xylem by transmembrane and/or symplastic paths, following their entry into the endodermal cells by transmembrane transport. A fraction of the apoplastic flow may not be hindered by the Casparian strip in places where lateral root emergesand in young roots where the Casparian strip is not fully developed - bypass-flow (Ranathunge et al., 2005).

Water is similarly absorbed and transported via the three paths, and hindered also by the Casparian strip. However, transmembrane water movement is by osmotic flow to the lower water potential inside the cell. The transport of ions into the cells maintains this lower water potential within the cell. Water transport is mainly enhanced though aquaporins (Chrispeels et al., 2001).

For the absorbed solutes to get to the leaves, they are carried in the transpiration stream through the xylem to the leaves where most of the water evaporates through the stomata (transpiration), leaving the solutes behind. The transpiration stream is, according to the cohesion-tension theory, driven by this evaporation (due to temperature and air humidity gradients). This causes evaporation from the leaves through stomatal pores. This transpiration creates a tension within the leaf apoplast. The force is transmitted, in the xylem conduit, to the roots. Water is thus, drawn into the roots and to the xylem by this tension, and travels by bulk flow to the leaves where transpiration sustains the tension. The absorbed solutes are brought by bulk flow in the transpiration stream to the extracellular spaces (the apoplast) within the leaf (Taiz *et al*., 2015). Most of the

solutes accumulating in the apoplast ultimately get into the cells where they are used and/or stored in the vacuole(s), depending on the physiological status of the cell. Solute entry into the cell may occur passively down electrochemical gradients (for K^+) through channels or against electrochemical gradients, through energy-requiring membrane-bound pumps (primary active transport) and/or transporters (secondary active transport). Water is also drawn into the cell by diffusion due to osmosis, through the membrane. Once accumulated, aside from active transport processes, cell to cell solute redistribution may occur symplastically between contiguous cells, through the plasmodesmata, by diffusion or bulk flow.

Significant differences may exist in solute distributions between the same plant species, depending on growth condition(s) (Leigh *et al*., 1986), between abaxial and adaxial surfaces (Boursier and Läuchli, 1989; Leigh and Storey, 1993), between epidermal and mesophyll cells (Küpper *et al*., 1999) or between contiguous epidermal cells of a leaf. For example, Leigh and Tomos, (1993) showed that while the potassium (K^+), sodium (Na^+) and nitrate (NO_3^-) concentrations in the epidermis, mesophyll and bundle sheet cells of barley were similar, significantly more calcium (Ca^{2+}) and chloride (Cl^-) were found in the epidermis and more phosphorus (as phosphate (PO_4^{3-})) was found in the bundle sheaths and mesophyll (Leigh and Tomos, 1993). Tomos *et al*. (1992) had earlier, demonstrated, using wheat leaves, that the sugar produced from photosynthesis is used in different forms in the mesophyll and epidermal cells. They found the photosynthetic products as sucrose in the mesophylls but as glucose in the epidermis (Tomos *et al*., 1992). Thus, there exist in plants, a controlled distribution of acquired as well as synthesized solutes between and within different layers of the leaf.

This cellular heterogeneity in solute content and/or concentrations may be related to function of individual cells or groups of cells (Tester and Leigh, 2001; Karley *et al*., 2000b). This content and concentration differences were investigated in all cell types in troughs of *T. virginiana* abaxial epidermis (see chapter 3) and forms the subject of this chapter. These were studied with a view to understanding the existence or otherwise of gradients (in solute concentration) during stomatal movements.

It is unknown if this complex works as a unit in the control of stomatal aperture, though the contribution of the lateral subsidiary cells has for long been acknowledged (Heath, 1938, 1975). In comparison to the lateral subsidiary cells, little

is known about the contribution of the other cell types in the epidermis. In *T. virginiana*, four cell types have been recognised; namely: guard cells, lateral and apical subsidiary and pavement cells. A sub-type of the pavement cells that is found between two adjacent apical subsidiary cells has been noted in this study and is termed the 'juxta apical cell' (see section 3.2.3.2). The five cell types (four previously recognised, together with the juxta apical cells) were studied individually in this project. Their vacuolar solute concentrations were analysed at closed and fully open stomata steady state conditions.

Work with the monocot, *Commelina communis*, and the dicot, *Vicia faba*, has shown that there is no significant solute movement between the mesophyll and the epidermis during stomatal movements (Willmer *et al*., 1974). Ions moving from the xylem to the epidermis could, in principle, move via the mesophyll cells or the vein extensions (Leigh and Tomos, 1993). Stomatal movements persist even when epidermal strips are placed in distilled water (Pallaghy, 1971; Willmer and Pallas, 1974) but disappear when isolated guard cells are placed in similar medium. Protoplasts obtain the required solutes from the bathing medium (Zeiger, 1983; Schnabl and Kottmeier, 1984). This suggests that the epidermis contains a store of the osmotica needed for stomatal movements (Felle *et al*., 2000).

4.1.1 **Stomata**

The stomata constitute less than 2% of total leaf area, but account for more than 90% of both water loss and the gaseous exchange in plants (Willmer and Fricker, 1996). This stomatal control of water loss is in two stages; long and short term controls. The long term control is achieved by the anatomical positioning of the stomata on the leaf (discussed in chapter 3). The physiological processes of closing and opening the stomata, using changes in solute concentrations in the epidermal cells, form the short term control of water loss. These concentration changes were the subject of this chapter. These changes determine the active (compared to the anatomical (passive)) responses of the stomata to environmental cues. Numerous biotic and abiotic factors affect plant wellbeing. The response of the plant to almost all of these is controlled by the stomata. Among the commonly-known factors include the abiotic effects of temperature, humidity, ambient and intercellular CO_2

concentrations, water availability (to the roots) and light as well as circadian rhythms (Fan *et al*., 2004). The biotic factors include bacteria and fungi. For example, a fungal toxin, fusicoccin, is known to cause wilting of leaves. Stomata also close to wall-off invading bacteria on leaf surface from entering into the leaf (Melotto *et al.*, 2006).

4.1.2 Guard cells

It is now known that the role of the guard cell chloroplasts is the provision of energy, in the form of ATP, needed during the stomatal movements independent of the mesophyll (Azoulay-Shemer *et al*., 2015; Daloso *et al*., 2015). The role of subsidiary cells in stomatal movement is to remove, store and release potassium (K^+) from the apoplastic space (Wilson *et al*., 1978). The released K^+ is then available to the guard cells for influx when opening, and is absorbed when released from the guard cells during closure. The subsidiary cells therefore, through the ionic concentration they establish in the apoplast, control the guard cell turgor (Raschke and Humble, 1973). Abscisic acid (ABA) controls stomatal opening by increasing K^+ absorption rate in subsidiary cells; thus indirectly decreasing stomatal opening and aiding closure (Wilson *et al*., 1978). Stomatal conductance is therefore, inversely related to ABA concentration (Trejo *et al*., 1995). Some authors, however, believe that ABA has a direct effect on K^+ movement into or out of guard cells rather than on subsidiary cell K^+ uptake (Wilson *et al*., 1978).

4.1.3 Guard cell volume regulation

By using some osmotic bathing media to control stomatal aperture more than one and a half centuries ago, Von Mohl (1856) (see (Franks *et al*., 1998), demonstrated that osmotic and turgor pressure changes drive stomatal movement. Subsequently, the photoactive concept of Fujino, (1967) and Fischer, (1968), explained that the mechanism of guard cell stomatal control is the influx or efflux of K^+, anions, sucrose and the interconversion of starch to malate (MacRrobbie, 1998). The direct source of the K^+ is the surrounding (epidermal) cells (Fujino, 1967; Fischer and Hsiao, 1968). Direct plasmodesmata connections do not exist between guard cells and other

epidermal cells; therefore all solute movements in the guard cell must finally turn apoplastic (Allaway and Setterfield, 1972; Singh and Srivastava, 1973; Wille and Lucas, 1984).

Raschke and Humble (1973), suggested that K^+ is exchanged with hydrogen ions moving in opposite direction to the K^+ flux and that calcium Ca^{2+} is involved only as a signalling molecule (Outlaw Jr., 1983). The organic solutes, mostly malate, account for as much as 95% of the opposite charges required to balance the positive charges on the K^+ in *Vicia faba* (Allaway, 1973). In plants such as *Allium*, where starch is not present in the guard cells, chloride ions (Cl^-) form the major counter ion for K^+ (Schnabl and Raschke, 1980; Allaway and Milthorpe, 2012). K^+ may increase 2 to 4 fold, malate and citrate, 6 and 3 folds respectively during stomatal opening (Raschke and Humble, 1973). Aspartic and glutamic acids also increase, but are of lower concentration compared to malate and citrate. Glyceric acid is not increased. The behaviour of Isocitrate is not well defined (Raschke and Humble, 1973). No major ion fluxes occur between mesophyll and epidermal cells during stomatal movements (Allaway, 1973). Turgor relations of the epidermis also do not depend on that of the mesophyll (Edwards and Meidner, 1978).

Stomatal apertures determine the rate of transpiration, which drives the bulk flow in the vascular tissue and by extension the solute supply to all cells (Talbott and Zeiger, 1998). Stomatal aperture in turn is determined by guard cell volume which is a function of its turgor pressure. Guard cell volume alone is, however, unreliable in predicting its turgor pressure in that the surrounding cells affects its volume-pressure relationship (Deeken *et al*., 2002). Thus stomatal aperture depends on the net turgor pressure difference between the guard cells and the other epidermal cells.

4.1.4 Guard cell and other epidermal cells

There is usually a good direct hydraulic contact between different cells of the epidermis (MacRrobbie and Lettau, 1980; Franks *et al*., 1998) and pavement cells have been shown to have a mechanical advantage over guard cells (DeMichele and Sharpe, 1973; Steudle and Zimmermann, 1977). The turgor in the other epidermal cells (mainly the pavement and lateral subsidiary cells where they exist) is more effective in determining stomatal aperture than guard cell turgor (Philip, 1958; Franks *et al*., 1995).

Thus the stomata can be kept closed by equally increasing the pressure in both the other epidermal cells and the guard cells at the same time (Zimmermann *et al*., 1980). Similarly, after the maximum stomatal aperture has been reached when opening in intact guard cell (on the epidermis), raising the pressure in surrounding epidermal cells to maximum decreases the stomatal aperture to half its maximum (Sheriff and Meidner, 1974). Unit pressure change in subsidiary cells has also been found to be about 1.54 times (Edwards *et al*., 1976; Franks *et al*., 1998) more effective in influencing stomatal aperture than unit change within guard cells (DeMichele and Sharpe, 1973; Meidner and Bannister, 1979). Guard cell turgor pressure at near-maximum aperture may be up to 4.1 MPa (Franks *et al*., 1995) but turgor ranges of 0.2 to 0.8 MPa in pavement cells and 0.15 MPa to 0. 45 MPa in subsidiary cells have been reported (Nonami and Schulze, 1989). Therefore, guard cell wall elastic properties may not be affected by those of other epidermal cells (Glinka, 1971), but are together exploited as a mechanical cellular machine, to effect desired changes in the stomata.

4.1.5 Solute content of epidermal cells

Studies using various sampling and analysis methods have shown that solutes are differentially distributed in plant leaves and that leaf epidermal cells contain a variety of organic and inorganic solutes, which differ significantly from the solute content of mesophyll cells (Meidner and Bannister, 1979). In barley leaves for instance, while Ca^{2+}, K^{+} and Cl^{-} are found exclusively in the epidermis, phosphorus and organic solutes accumulate more in mesophyll cells (Meidner and Bannister, 1979).

Within a leaf epidermis, considerable cell-to-cell variation in solute content has been demonstrated in barley (MacRrobbie and Lettau, 1980; Leigh and Storey, 1993), wheat (Malone *et al*., 1991), *Commelina communis* and *Vicia faba* (Irving *et al*., 1997) and in *T. virginiana* (Malone *et al*., 1991; Tomos *et al*., 1992, 1994, 2000; Leigh and Storey, 1993; Williams *et al*., 1993; Fricke *et al*., 1996; Koroleva *et al*., 1998). For example, Fricke *et al* (1994c) found that the solute content of cells at equivalent positions and distances from an immediate lateral vein (see for example, cells 1 and 1 or cell 7 and 7 in plate 2.2C) on the upper and lower epidermis were significantly different. Thus, a link between cell location and solute composition has been

suggested (Leigh and Storey, 1993). Adaxial epidermis has also been found to contain higher K^+ concentrations than the abaxial surface. The Cl^- and nitrate ion (NO_3^-) concentrations as well as the total negative and positive solute concentration (charges) were also found to be reversed in the upper and lower epidermis (Leigh and Storey, 1993); thus showing that differences also exist between the abaxial and adaxial aspects of the same leaf. There is also a difference in the distribution of sodium (Na^+) and Ca^{2+} between epidermal cells (Malone *et al*., 1991; Leigh and Storey, 1993). See Conn and Gilliham (2010) for review.

Even under nutrient starvation, physiological responses are different on either sides of a leaf (Fricke *et al*., 1994c). Ionic composition of epidermal cells also changes with leaf age. Ca^{2+} is proven to increasingly replace K^+ as the main cation as the leaf ages (Leigh and Storey, 1993; Fricke *et al*., 1996). The amino-acid concentration nonetheless, remains approximately constant from cell to cell, even during the aging process (Leigh and Storey, 1993).

Maintenance of these differences in inorganic solutes must require either an actively maintained cell-type-specific or a gradient-driven mechanism. Literature is sparse on the mechanisms controlling the distribution of these intercellular solutes and there is relatively little understanding of the importance of the intercellular nutrient distributions for either nutrient-use efficiency or for the responses of plants to stresses. However, available works, mainly on monocot leaves, suggest that this distribution is occasioned by the interaction between selectivity at plasma membrane of bundle sheath and the epidermal cells, and that of the vacuolar membranes (Willmer *et al*., 1974).

These differences in solute distribution cause the build-up of considerable differences in osmolality between the various cell types (Karley *et al*., 2000b). Hence it is evident that there might exist, a turgor and/or water potential gradient within the epidermis. Such gradients may represent the driving force behind the contribution of these epidermal cells to stomatal control.

4.1.6 Guard cell metabolism

Guard cells exhibit considerable flexibility in their metabolic pathways (Taiz *et al*., 2015). They also show a sucrose-dependent osmoregulatory phase (Talbott and

Zeiger 1998). Sucrose can originate from starch hydrolysis (Tallman and Zeiger, 1988). On the other hand, guard cells from detached epidermis irradiated with red light under ambient CO_2 concentrations operate a third metabolic pathway, showing no detectable potassium uptake or starch hydrolysis (Tallman and Zeiger, 1988). In these conditions, guard cells slowly accumulate sucrose, and this sucrose accumulation can be blocked by DCMU (dichlorophenyldimethylurea), an inhibitor of photosynthetic electron transport (Poffenroth *et al.* 1992; Talbott and Zeiger 1993). A recent study of guard cell osmoregulation under red light illumination and CO_2-free air showed that under these conditions, in which photosynthesis is inhibited by the absence of CO_2, red light activates the potassium-dependent pathway (Olsen *et al.* 2002). These studies underscore the remarkable metabolic flexibility of guard cells.

Schnabl and Kottmeier (1984) reported that during stomatal opening, malate synthesis is stimulated. However, the role of photosynthesis in guard cell function is still a subject of debate. A key photosynthetic product, starch, is lacking in *Allium* species without any guard cell functional deficiencies. Azoulay-Shemer *et al.*, (2015), in working with a chlorophyll-free-guard cell *Arabidopsis* transgenic line, showed that photosynthesis in guard cells is required for turgor production but is not necessary for guard cell ABA and CO_2 responses (Azoulay-Shemer *et al*., 2015). Approximately 45% of the stomata were abnormal and remained permanently closed. It has subsequently, been suggested that guard cell derived starch affects stomatal function only indirectly, through an effect on the anion channels while mesophyll photosynthesis contributes nothing to CO_2-induced stomatal responses (Azoulay-Shemer *et al*., 2016). It has recently been determined that the role of sucrose in stomatal movements is the provision of energy, in form of ATP, for cellular respiration (Daloso *et al*., 2015).

4.1.7 **Cellular heterogeneity**

Solute gradients have been demonstrated on the same leaf surface in many angiosperm and graminaceous leaves (see reviews by Conn and Gilliham (2010) and Nagai *et al*. (2013)). Higher concentration of cadmium (Chardonnens *et al*., 1998) and differential abaxial and adaxial mRNA levels have been demonstrated in the leaf folding process of *Samanea saman* (*Albizia saman*) (Author *et al*., 2002). In

pulvini movements, initiation of differential solute concentrations between the adaxial (extensor) and abaxial (flexor) aspects of the pulvinus powers the perceived leaf movement in *Phaseolus vulgaris* (Irving *et al*., 1997; Koller *et al*., 2001), *Albizia saman*, *Mimosa pudica* (Allen, 1969).

Though similar types of solute transporters exist across (plasma and tonoplast) membranes of mesophyll and epidermal cells, differences in types and concentrations of solutes have been recorded between them (Karley *et al*., 2000b). Expectedly flavonoids are more (in some cases ten folds more) in the epidermal than in the mesophyll cells (see (Dietz *et al*., 1994)). Preferential accumulation of SO_4^{2-} (Bell *et al*., 1995), Na^+, K^+, Ca^{2+}, Cl^- and NO_3^- in the epidermis, and PO_4^{3-} (Karley *et al*., 2000b) in the mesophyll has been demonstrated in barley. Epidermal cells of *Thlaspi caerulescens* preferentially accumulates Zn^{2+} and this has been put to advantage in the phytoremediation of Zn^{2+} contaminated areas (Frey *et al*., 2000). In *A. thaliana,* Ca^{2+} and Mg^{2+} concentrations are preferentially higher in mesophyll while Cl^- and K^+ concentrations are more in the epidermis (Conn, *et al*., 2011; Conn, Gilliham *et al*., 2011). In barley (Koroleva *et al*., 1997) and in wheat (Malone *et al*., 1991) epidermal carbohydrate concentration is much lower than levels in mesophyll. While Na^+ and K^+ concentrations are similar in mesophyll and epidermis, PO_4^{3-} is lower, but Ca^{2+}, Cl^- and NO_3^- are higher in the epidermis (Fricke *et al*., 1994c; Karley *et al*., 2000b).

Differences have also been shown within the epidermal cells of the same leaf surface (Karley *et al*., 2000a). The pavement cell type overlying the vascular bundles in cereal leaves preferentially accumulate some solutes, for example Cl^- (Karley *et al*., 2000a). In *Sorghum bicolor,* Cl^- is preferentially stored in the sheath instead of the blade epidermal cells (Boursier and Läuchli, 1989). In banana, Na^+ preferentially accumulates in leaf margins (Shapira *et al*., 2009). Hinde (1994) observed heterogeneity in concentration of individual solutes in barley epidermal cells measured across the leaf, at the same distance from leaf tip at a specific stomatal aperture condition. During Zn^{2+} accumulation by *Thlaspi caerulescens* epidermis, cells of the stomatal complex were not involved in the Zn^{2+} accumulation (Frey *et al*., 2000).

4.1.8 Cellular heterogeneity during stomatal movements

Differences have been recorded between contiguous cells in terms of solute content and/or concentration, pH and transmembrane potential difference during stomatal movements in different species. However, to date, only few solutes; K^+, Cl^-, malate, (Willmer and Mansfield, 1969; Penny and Bowling, 1974; MacRrobbie and Lettau, 1980b) and rarely, Na^+ and Ca^{2+} have been measured in contiguous cells in leaf epidermis in relation to stomatal movement. In all these studies, predictable variations were found in the assayed cells upon stomatal opening and closing, demonstrating solute gradients in contiguous epidermal cells during stomatal movements. The existence of these gradients has been corroborated by studies on pH (Bowling and Edwards, 1984) and transmembrane potential difference (Edwards and Bowling, 1984). These studies have enabled the prediction and calculation of the driving force on the involved solutes (mostly on K^+) required to maintain the uphill gradients towards the guard cells in open and the downhill gradients away from the guard cells in closed stomata conditions (Penny and Bowling, 1974).

4.1.9 Study aims

This chapter was aimed at determining possible solute content and/or concentration changes in the different cell types in *T. virginiana* epidermal trough during stomatal movement and to discover any solute concentration gradient developed during this movement. Essentially, it was designed to answer the question of whether all epidermal trough cells participate in generating stomatal movement. The specific objectives were to determine

- Any solute distribution pattern across the epidermal trough
- Charged solute content and concentration in each of the five cell types of the trough at
    - (a) closed stomata condition and
    - (b) open stomata condition
- The concentration differences between contiguous cells and within each cell to deduce any concentration gradients that may exist during the stomatal movements.

4.2 Results

4.2.1 Solute concentrations differences between the troughs

It was unknown if cell types at similar positions in different troughs were similar in their solute content and concentration although variations had been shown to exist between such cells in abaxial compared to adaxial epidermis (see section 4.1.5). This experiment was undertaken in order to determine any differences in solute contents or concentration between cells at similar positions in different troughs on the abaxial surface of *T. virginiana*. This was to then to use in conducting and analysing the experiment(s) on single cells sample in which samples were obtained from cells in different troughs.

To study the solute distribution pattern of the (*T. virginiana*) leaf epidermis, three experiments were run with the aims of detecting any solute distribution gradient(s) between troughs, comparing the distribution pattern in troughs on either sides (right and left) of the midrib and determining the within-trough solute distribution pattern. The between-trough solute distribution gradient was investigated by analysing solutes from pavement cells at equivalent positions in three troughs in leaf five of three plants. Cells at positions 1, 6, 18 and 29 (see plate 2.2 C) were sampled.

Since the analysis of (epidermal) strip samples showed more variability in concentration within the anions (see tables 3.12 and 3.13 in chapter 3) and the anion species are more affected by cell to cell variation in pH than the cations, only the anions were used in investigating the solute differences in these epidermal cells.

No interpretable solute distribution gradient(s) between the troughs was found (figure 4.1). Troughs 2 and 4 had equal concentrations of chloride ($p > 0.05$) but the chloride was higher in trough 3 ($p < 0.01$). Conversely, malate concentration was statistically the same ($p > 0.05$) in troughs 3 and 4 but higher ($p < 0.01$) in trough 2. Phosphate concentrations in troughs 3 and 4 were similar ($p > 0.05$) but significantly lower ($p > 0.01$) in trough 2. Thus, no general gradient(s), to or from the mid-rib with respect to the leaf edge was observed. In contrast, individual solutes showed similar concentration pattern in all the troughs. For example, in all the troughs chloride had the highest while citrate had the lowest concentration. Concentrations of malate in all the troughs was lower than that of chloride but higher than that for phosphate which

in turn, was consistently higher than those of citrate in all the troughs. Thus in all the troughs, the pattern of chloride > malate > phosphate > citrate was observed.

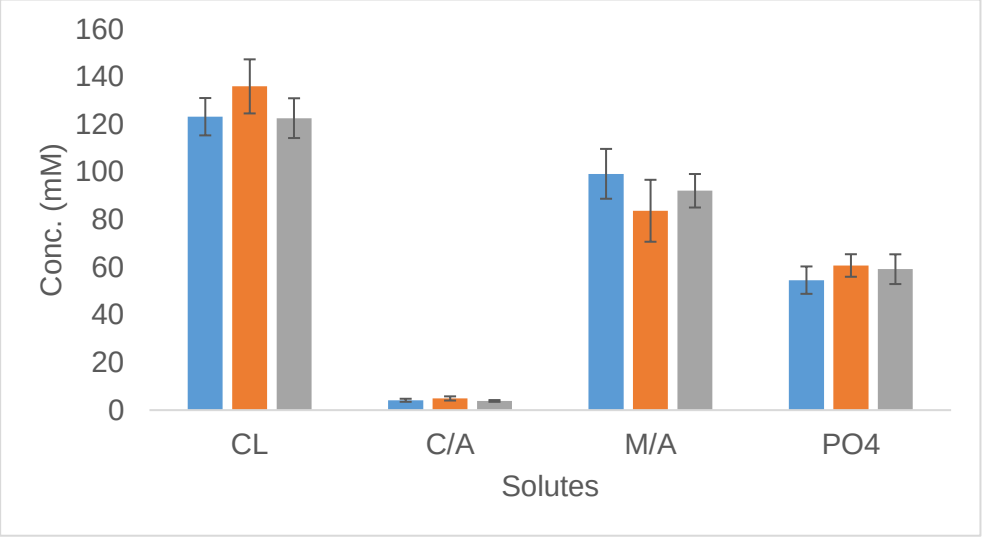

Figure 4.1 Solute concentrations in abaxial epidermal cells in troughs of leaf five Cl – Cl^-, C/A – Citrate, M/A – Malate, PO4 – PO_4^{3-}. Error bars – sd. See plate 2.2

4.2.2 Solute concentrations in the troughs on right and left sides of the midrib

Solute concentrations on the abaxial epidermis of leaf five in four plants were analysed for differences between troughs equidistant (in position) from the midrib. Three troughs on each side (right and left) of the mid-rib were compared. As in section 4.2.1, cells at positions 1, 6, 18 and 29 were sampled. Table 4.1 shows the mean concentrations of solutes in right and left troughs 2, 3 and 4. On both sides, in all the troughs, concentrations ranked from chloride, malate and phosphate to citrate in decreasing order. The two sides (right and left) show no statistically significant difference (at least $p > 0.10$) in solute concentrations of any of the individual solutes (Trough 2 (n=18), p = 0.86, Trough 3 (n = 8), p = 0.10, Trough 4 (n = 11), p = 0.87). Thus concentration of individual solutes on one side was (approximately) mirrored in the equivalent position on the other side. For example chloride in trough 3 on the right mirrored the chloride in trough 3 on the left.

Table 4.1 Solute concentrations in pavement cells at equivalent positions on the abaxial epidermis on opposite sides of the mid-rib. (mean ± sd. n = 6)

Trough	Side	Chloride (mM)	Citrate (mM)	Malate (mM)	Phosphate (mM)
2	LT	122.6 ± 10.2	4.1 ± 0.6	99.3 ± 10.8	55.6 ± 7.6
	RT	123.9 ± 4.3	4.2 ± 0.6	99.3 ± 10.4	53.5 ± 2.7
3	LT	136.7 ± 10.7	4.9 ± 0.9	83.7 ± 13.7	60.6 ± 5.0
	RT	134.7 ± 13.1	5.0 ± 0.8	83.8 ± 12.7	61.0 ± 4.5
4	LT	121.6 ± 10.9	3.6 ± 0.3	91.6 ± 6.6	61.7 ± 9.0
	RT	123.8 ± 5.9	4.0 ± 0.3	92.6 ± 7.6	57.4 ± 1.3

4.2.3 Solute concentrations within (epidermal) troughs

Following the observation that individual solute concentrations differed between troughs, the possibility of within-trough gradients was explored. Four pavement cells (at positions 1, 7, 13 and 30) as well as four lateral subsidiary cells (at positions 5, 11, 17 and 28) (see plate 2.2C) from troughs 2, 3 and 4 on leaf five of three plants were sampled and analysed for anion content. Chloride, citrate, malate and phosphate in pavement and lateral subsidiary cells as well as tartrate and succinate found only in the subsidiary cells were quantified. The concentrations in pavement cells at positions 1, 7, 13 and 30 in three troughs are shown in fig. 4.2. In all the troughs, no statistically significant difference existed between solutes in cells at different positions ($p > 0.05$, $f_{critical} = 2.01$, $f = 2.68$) except for chloride concentrations which showed significant differences ($p < 0.05$). Concentrations in C3 and C4 were not significantly different ($p > 0.05$). The hierarchy of solute concentration from chloride to citrate in descending order was maintained in all the cells.

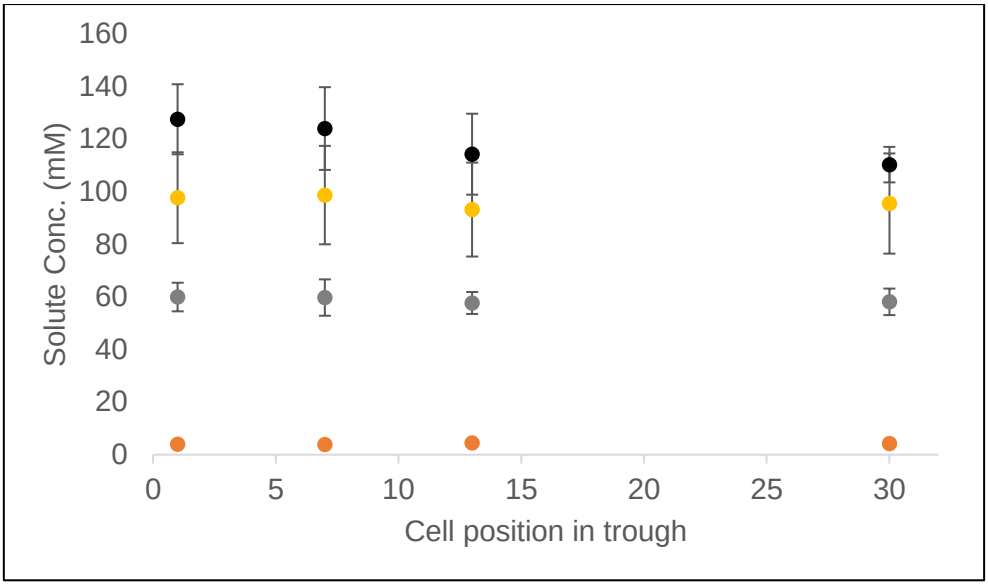

Figure 4.2 Solute distribution in pavement cells across a trough epidermis Concentrations of Cl^- (●), malate (●), citrate (●) and PO_4^{3-} (●) in pavement cells at different positions across the width of *T. virginiana* troughs is shown (see plate 2.2C). Citrate maintained the lowest concentration in all the positions followed by PO_4^{3-} and then malate, while Cl^- had the highest concentrations. Concentrations of each of the solutes was similar in the cells irrespective of their position in the trough. Error bars represent s/d. n = 12.

Figure 4.3 shows the solute concentrations in lateral subsidiary cells (at positions 5, 11, 17 and 28) across the trough. In all the cells, solute contentrations followed the same pattern (chloride, malate, citrate, succinate, phosphate and tartrate, in descending order). Individual solute concentrations differed remarkably between pavement cells and lateral subsidary cells. No difference in concentration ($p > 0.05$) existed between the cells at the sampled positions.

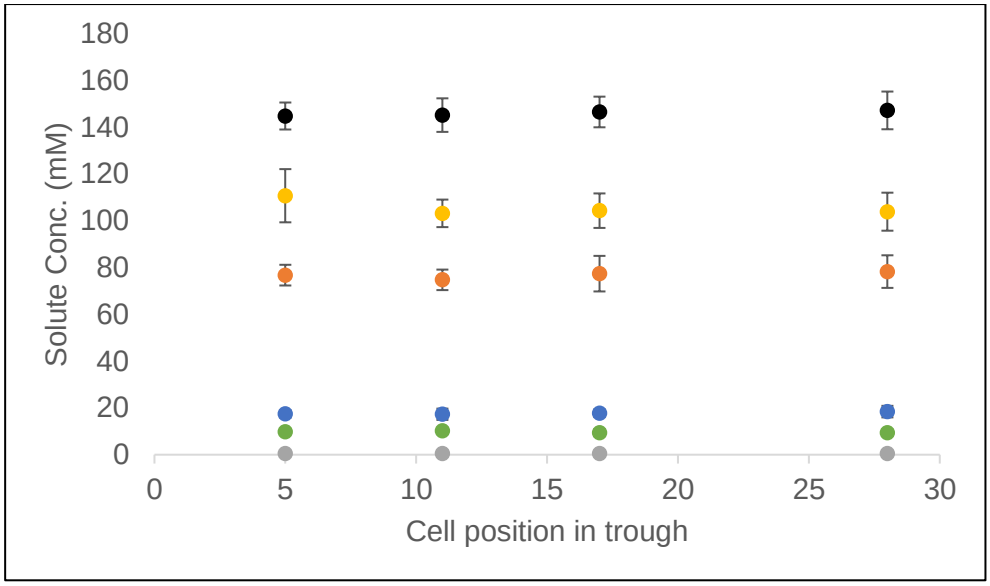

Figure 4.3 Solute distribution in lateral subsidiary cells across a trough epidermis Concentrations of Cl^- (●), malate (●), citrate (●), succinate (●), PO_4^{3-} (●) and tartrate (●) in lateral subsidiary cells at different positions across the width of *T. virginiana* troughs is shown (see plate 2.2C). Tartrate maintained the lowest concentration in all the positions followed by PO_4^{3-} and then succinate, citrate and malate, while Cl^- had the highest concentrations. Concentrations of each solute was similar in each cell irrespective of their position in the trough. Error bars represent s/d. n = 12.

4.2.4 Anion concentrations in cells of the epidermis at closed and open stomata conditions

All five epidermal trough cell types (pavement, juxta apical, guard cells, apical and lateral subsidiary cells) (see section 3.2.3.2) were sampled and the obtained sap was analysed using CZE tools. Samples were taken separately under closed and open stomata conditions (see section 2.3). Three replicates were sampled in each of three plants. Where possible (usually for pavement cells), sap obtained from one cell was subsampled into three replicates for anion and similarly for cation analysis. Otherwise, samples were taken from cells at equivalent positions in order to be adequate for combined cation and anion (subsampling for) analysis. The small volumes (about 10 pl) of guard cells did not permit replication using few guard cells. Thus repeats were obtained by pooling the samples from as much as ten or more guard cells.

Ten peaks comprising one internal standard (Br^-) and nine solute peaks were found. The peaks corresponded to the expected positions of bromide, chloride, SO_4^{2-}, NO_4^-, oxalate, unknown peaks 1 (U1), citrate, U2, malate, and PO_4^{3-} (see section

3.3.2.2.1, plate 3.7). Similar solutes were identified in both open and closed stomata conditions. The peaks, with the exception of the unknowns, were quantified using the solute to internal standard peak area ratios.

The results (fig. 4.4, also see appendix 7 - 10) show that Cl^- consistently had the highest ($p < 0.05$ or less) concentration in all the cells except in juxta apical cells under closed stomata condition and in apical and lateral subsidiary cells under open conditions. In those cells Cl^- and malate concentrations were similar ($p > 0.19$). Malate was next to chloride in concentration in all the cells except in the juxta apical under closed stomata where they were similar. Tartrate and succinate were not found in the pavement and juxta apical cells. All other solutes (see section 3.3.2.2.1) were present in all the cell types.

Each solute showed differences in concentration between closed and open stomata conditions, some in all the cell types but others in some cell types. Some solutes also showed differences in concentration in contiguous cells that form gradients - uphill or downhill. Note that the path of these gradients were chosen "expedientially" as representing possible solute movement rather than explicit paths – namely, Pavement > Juxta apical > Apical subsidiary > Lateral subsidiary > Guard cell). The patterns shown by each solute is now described.

4.2.4.1 Chloride

Under both closed and open stomata, Cl^- concentration was highest in guard cells (182.1 ± 1.7 and 204.44 ± 6.77 mM respectively) and lowest in the juxta apical cells (108.8 ± 8.0 and 102.96 ± 3.10 mM respectively). Concentrations in juxta apical, pavement and lateral subsidiary cells were similar ($p > 0.05$). When stomata were closed, concentration in these three cells were significantly lower ($p < 0.05$) than in the lateral subsidiary (147.4 ± 7.1 mM), and concentrations in the guard cells were also higher ($p < 0.01$) than those in lateral subsidiary cells. Similarly, in open stomata situation concentrations in the lateral subsidiary (146.62 ± 10.02 mM) were higher (($p < 0.05$) than in the three (juxta apical, pavement and apical subsidiary), but significantly lower ($p < 0.01$) than in the guard cells.

Cl^- concentrations were significantly higher ($p < 0.05$) in the pavement cells in closed stomata conditions compared with open conditions (the difference (Δ) was 27.3 ± 6.9 mM). In contrast, concentrations in guard cells were higher ($p < 0.01$) in

open stomata conditions (Δ 22.3 ± 5.1 mM). In all the other cells no difference (p > 0.05) in concentration existed between open and closed stomata conditions. Between contiguous cells, Cl^- concentration increased from the pavement, juxta apical and apical subsidiary cells though the lateral subsidiary cells to the guard cells under both open and closed situations, maintaining a steady uphill gradient towards the guard cells.

4.2.4.2 Malate

Malate concentrations were highest in lateral subsidiary cells (106.7 ± 9.6 and 135.68 ± 6.84 mM respectively), and lowest in the guard cells (60.3 ± 4.3 and 64.35 ± 2.64 mM respectively) under both closed and open stomata situations. Under closed stomata conditions concentrations were similar (p > 0.05) in all the cells except the guard cells in which it was lower (p < 0.01). In open stomata condition malate concentration in juxta apical cells decreased and became similar (p > 0.25) to the concentration in the guard cells (64.35 ± 2.64 mM). When stomata opened, its concentrations remained unchanged in pavement (p > 0.10), apical subsidiary (p > 0.07) and guard cells (p > 0.20), but increased (p < 0.05) in lateral subsidiary (Δ 29.0 ± 2.8 mM) and decrease (p < 0.001) in juxta apical cells (Δ -41.7 ± 0.0 mM). Comparing contiguous cells, malate concentrations increased progressively from the level in juxta apical cells through apical subsidiary cells to the lateral subsidiary cells when stomata opened. No malate concentration gradient was apparent under closed stomata condition.

4.2.4.3 Nitrate

NO_3^- concentrations changed (p < 0.05 or less) in all cell types as stomata opened except in the guard cells. Under closed stomata condition its concentrations in the pavement (63.5 ± 8.1 mM) and guard cells (77.3 ± 6.9 mM) were similar (p > 0.087), and in juxta apical, apical subsidiary and lateral subsidiary cells (45.0 ± 3.6 mM) concentrations were also similar (p > 0.25 or more).

Under open stomata condition, NO_3^- concentrations in pavement cells decreased (Δ -63.5 ± 8.1 mM; p < 0.01). Concentrations in juxta apical (Δ -13.1 ± 0.8 mM) and apical subsidiary cells (Δ -13.5 ± 1.4 mM) also reduced (p < 0.05) although marginally. In the lateral subsidiary cells NO_3^- concentration doubled (45.0 ± 3.6 to

87.0 ± 6.2 mM) on stomatal opening ($p < 0.001$). Considering contiguous cells, NO_3^- concentration remained the same in pavement, juxta apical and apical subsidiary cells and increased ($p < 0.001$) in the lateral subsidiary cells as stomata opened, but reduced in the lateral subsidiary cells to similar level with the other contiguous cells (apical subsidiary and juxta apical) and increased significantly ($p < 0.05$) in pavement cells as stomata closed.

4.2.4.4 Phosphate

The concentration of PO_4^{3-} changed significantly ($p < 0.01$ or less) in all cell types as stomata opened, mainly increasing in the guard cells (Δ 34.4 ± 3.0 mM; $p < 0.05$), lateral subsidiary (Δ 37.1 ± 5.3 mM; $p < 0.001$) and decreasing in pavement cells (Δ -31.6 ± 5.9 mM; $p < 0.001$). Under closed stomata condition its concentration decreased ($p < 0.05$ or less) from the pavement cells (56.5 ± 5.3 mM) through the juxta apical (38.9 ± 2.9 mM) and the apical (30.6 ± 2.0 mM) to the lateral subsidiary cells (9.3 ± 1.0 mM). Guard cell PO_4^{3-} concentration was also low (18.7 ± 1.9 mM), but twice as high as that in the lateral subsidiary cells. As stomata opened concentrations decreased in the pavement cells and increased in an uphill gradient from the juxta apical cells through the apical to the lateral subsidiary cells which had similar ($p > 0.21$) concentration with the guard cells (53.11 ± 4.86 mM).

4.2.4.5 Sulphate

SO_4^{2-} concentrations changed significantly ($p < 0.01$ or less) in all cells as stomata opened. Its concentrations increased in the pavement (28.5 ± 4.2 to 60.59 ± 5.18 mM; $p < 0.01$), apical subsidiary cells (40.6 ± 2.2 to 52.88 ± 3.11 mM; $p < 0.01$) and the guard cells (33.5 ± 2.5 to 54.3 ± 3.3 mM; $p < 0.001$), but decreased in juxta apical (53.2 ± 3.4 to 10.63 ± 1.02 mM; $p < 0.001$) and lateral subsidiary cells (51.4 ± 2.9 to 25.8 ± 2.9 mM; $p < 0.001$). Under closed stomata situation, the juxta apical and lateral subsidiary cells had similar ($p > 0.52$) concentrations. Concentrations in the pavement and guard cells were also similar ($p > 0.15$) and lower ($p < 0.01$) than those in juxta apical and lateral subsidiary cells, respectively.
Similarly, under closed stomata guard cell, apical subsidiary and pavement cells had similar concentrations (60.59 ± 5.18 mM; $p > 0.09$ or more). No definable concentration gradient existed in contiguous cells as stomata opened.

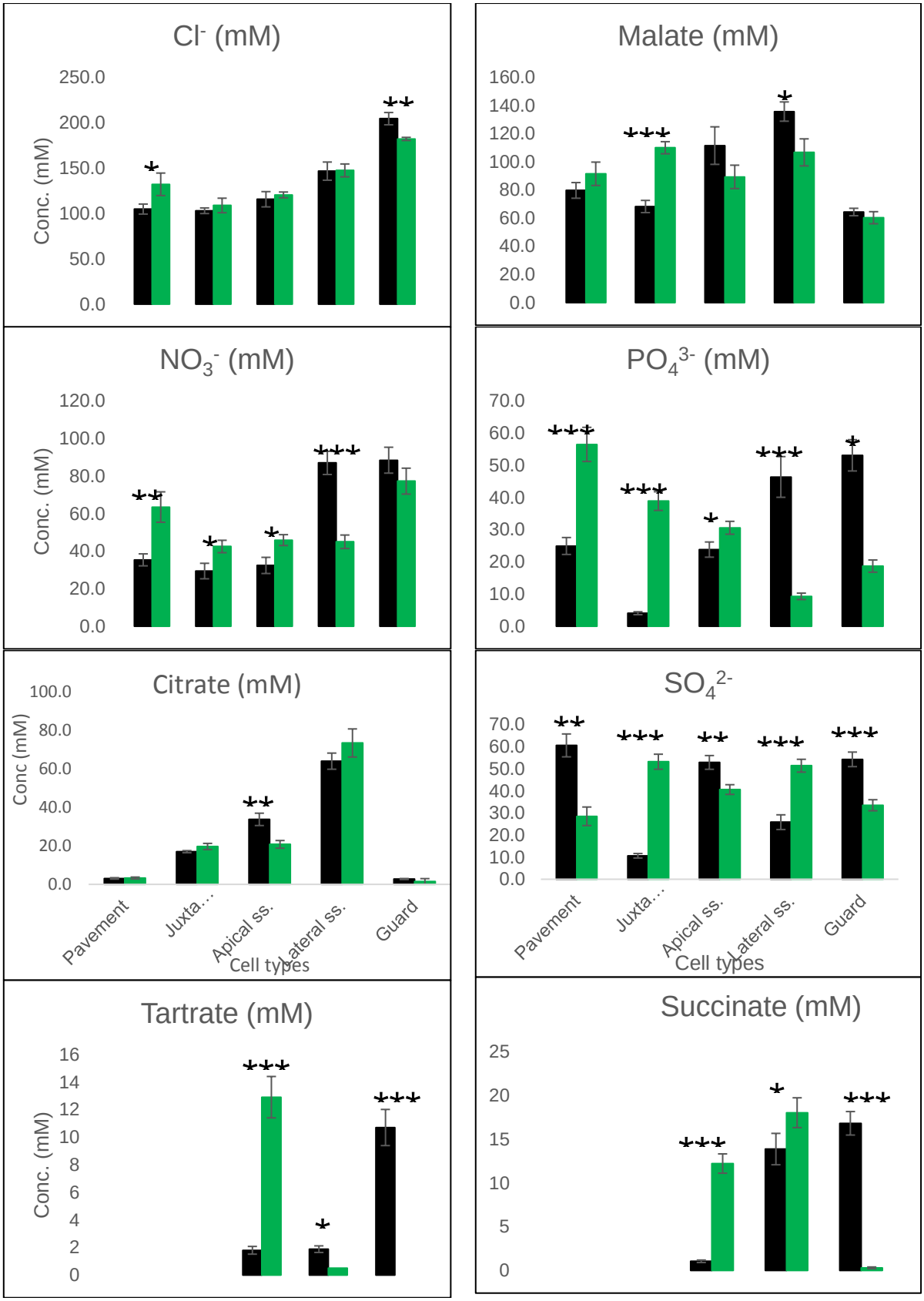

Figure 4.4 Anion concentration in cell types at closed (●) and open (■) stomata compared One, two or three asterisks (*) represent(s) *p* values < 0.05, 0.01 or 0.001 respectively at 95 % confidence interval. The test statistics (*p* values) represent the probability at 95% confidence interval in an unpaired two tailed student's t-test assuming equal variance.

4.2.4.6 Citrate

Citrate concentration was generally low in all cell types at both closed and open stomatal situations except in the lateral subsidiary cells where it maintained its highest and similar ($p > 0.05$) concentration (64.04 ± 4.2 mM) under both situations. Concentrations in all other cells except the apical subsidiary cells did not change ($p > 0.05$) under both open and closed conditions. In the apical subsidiary cells citrate concentration increase ($p < 0.01$) moderately under open stomata condition (20.8 ± 2.0 to 33.79 ± 3.21 mM). Contiguous cells showed increasing concentration gradient towards the lateral subsidiary cell.

4.2.4.7 Succinate

Succinate concentration gradients in contiguous cells were uphill toward the guard cells under open stomata conditions, and fairly downhill towards the apical subsidiary cells under closed stomata conditions. Under closed stomata situation guard cell succinate (0.3 ± 0.1 mM) was more than fifty times lower than its concentration in the lateral subsidiary cells (18.0 ± 1.7 mM). But on stomatal opening, succinate concentration in both cells were similar (13.85 ± 1.79 mM in lateral subsidiary and 16.79 ± 1.34 mM in guard cells; $p > 0.08$). On the other hand, its concentration in apical subsidiary cells decreased more than tenfold (12.2 ± 1.1 to 1.05 ± 0.14 mM; $p < 0.001$) when stomata opened.

4.2.4.8 Tartrate

Tartrate was not found in guard cells under closed stomata condition. Its concentration increased dramatically in the cells under open stomata condition (0.00 to 10.7 ± 1.31 mM; $p < 0.001$). Concentration in guard cells under this situation was similar ($p > 0.72$) to that in the apical subsidiary cells (12.9 ± 2.0 mM). Its concentration in the lateral subsidiary cells were altogether low under both open and closed stomata situations, but nevertheless, increased ($p < 0.05$) on stomatal opening. On stomatal opening, its concentrations in the apical and lateral subsidiary cells were similar ((1.8 ± 0.24 mM; $p > 0.91$), and sustained an uphill gradient with concentrations in the guard cell. A downhill concentration gradient of tartrate was also observed

under closed stomata condition starting from the apical subsidiary cells, through the lateral subsidiary to the guard cells.

4.2.4.9 Summary

In all, at open stomata most solutes developed uphill gradients towards the guard cell; some (citrate and malate) terminating at the lateral subsidiary and others reaching the guard cells. Sulphate, however, showed no long range gradient. The term “gradient” is used rather subjectively here. The objective was to describe an approximate functional path – pavement → juxta-apical → apical subsidiary → lateral subsidiary → guard cell (figure 4.6). The “gradient” is relative to this path (see plate 4.1). The results would suggest that no single path from pavement to guard cell actually exists, but that different solutes follow a network of functional exchanges. The role of the apoplast in this is discussed (chapter 6 section 6.3.2).

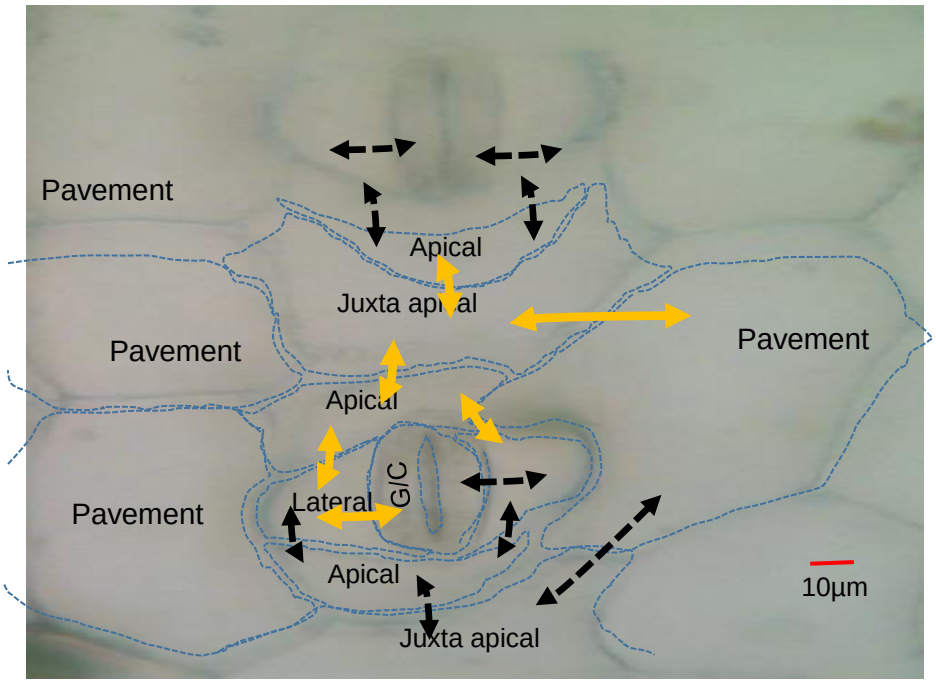

Plate 4.1 Possible inter-cell solute exchange trend in *T. virginiana* epidermis during stomatal movement
Five cell types (pavement, juxta apical, apical-, lateral-subsidiary and guard cell (G/Cell)) are shown. Inserted dashed lines show cell boundaries. The pavement cells are the largest cells. Their largest contact (with other cell types) is with the juxta apical cell which is sandwiched (above and below) between two apical subsidiary cells. The apical subsidiary cells also contact (mainly) with the lateral subsidiary cells which cover most of the perimeter of the guard cell outer dorsal (lateral) wall. The arrows show postulated functional solute exchange paths, and the dashed black arrows show the same paths in cells at other positions. The arrows are double headed to indicate the directions toward the guard cells during opening and away from the guard cells, towards the pavement cells, during closing of the stomata.

4.2.5 Cation concentrations in cells of the epidermis at closed and open stomata

All five epidermal trough cell types (pavement, juxta apical, guard cells, apical and lateral subsidiary cells) (see section 3.2.3.2) were sampled and also analysed for cation contents. Similar procedures as described in section 4.2.1 for anions were followed. Three replicates were sampled in each of three plants. Repeats for guard cells were made possible by pooling the samples from as much as ten or more guard cells.

Six peaks comprising one internal standard (Cs^+) and five solute peaks were found. The peaks corresponded to the expected positions of NH_4^+, Na^+, K^+, Ca^{2+} and Mg^{2+} (see section 3.3.2.1.2, plate 3.6). Similar solutes were identified in both open and closed stomata conditions. The peaks were quantified using the solute to internal standard peak area ratios.

The results (fig. 4.5; see also appendix 9 and 10) show that K^+ constituted more than 60% of the cation in all the cell types except in the lateral subsidiary cells, where potassium made up about 25% of the cations while calcium had the highest concentration. Ammonium had the lowest concentration in all the cells (< 5%). NH_4^+ and Na^+ together, made up less than 11% of the total cation content of each cell type.

Most of the solutes showed differences in concentration between closed and open stomata conditions, but only K^+ showed concentrations differences in all cell types. Only NH_4^+, in contrast, had no differences in concentration in all cells under these conditions. Each solute, including NH_4^+, showed some differences in concentration in contiguous cells which form gradients - uphill or downhill. The concentration patterns shown by each solute is now described.

4.2.5.1 Potassium

Under both closed and open stomata, highest ($p < 0.001$ or less) concentration of K^+ was found in the guard cells (305.7 ± 3.6 and 420.46 ± 12.73 mM respectively). Its lowest ($p < 0.001$ or less) concentration under closed conditions was found in the lateral subsidiary cells (94.8 ± 5.9 mM). But under open stomata condition no significant difference ($p > 0.05$) existed between its concentrations in the lateral

subsidiary (183.06 ± 0.84 mM) and juxta apical (182.65 ± 5.57 mM) cells. When stomata were closed, concentrations in pavement (268.0 ± 8.0 mM), juxta apical (263.1 ± 4.7 mM) and apical subsidiary cells (271.3 ± 3.8 mM) were similar (p > 0.07). Similarly, in open stomata situation concentrations in apical subsidiary (201.99 ± 2.50 mM) and pavement cells (207.77 ± 16.19 mM) cells were also similar (p > 0.57).

K^+ concentrations changed significantly (p < 0.05) in all cells as stomata opened, decreasing in pavement (Δ -60.2 ± 8.2 mM; p < 0.01), juxta apical (Δ -80.5 ± 0.9 mM; p < 0.001) and apical subsidiary cells (Δ -69.3 ± 1.3 mM; p < 0.001) but increasing in the lateral subsidiary (Δ 88.3 ± 5.1 mM; p < 0.001) and guard cells (Δ 114.8 ± 9.1 mM; p < 0.001). Between contiguous cells, K^+ concentration did not show any gradient, except between the lateral subsidiary and guard cells (p < 0.001) where it was uphill on stomatal opening and downhill on its closing.

4.2.5.2 Calcium

Under both closed and open stomata, Ca^{2+} had its highest concentration in lateral subsidiary cells (148.8 ± 7.4 and 152.86 ± 1.51 mM respectively), but its lowest was in the guard cells (36.9 ± 4.3 mM) under closed stomata condition and in the juxta apical cells (24.59 ± 3.06 mM) under open stomata condition. Its concentration differed significantly (p < 0.001 or less) from cell to cell in most cases except in the apical subsidiary and guard cells under closed condition in which concentrations in both cells were similar (p > 0.10).

Ca^{2+} concentrations did not change in pavement (p > 0.70), lateral subsidiary (p > 0.30) and guard cells (p > 0.30) when stomata opened, but significantly increased (Δ 46.9 ± 3.0 mM; p < 0.001) in apical and decreased in juxta apical cells (Δ -51.4 ± 2.3 mM; p < 0.001). Between contiguous cells, under closed stomata condition no concentration gradients were observed. When stomata opened, an uphill gradient was formed from the juxta apical, through the apical subsidiary to the lateral subsidiary cells.

4.2.5.3 Magnesium

Similar to Ca^{2+}, Mg^{2+} had its highest concentration in lateral subsidiary cells (105.9 ± 2.2 and 100.37 ± 1.60 mM respectively) under both closed and open stomata, but its lowest was in the guard cells (32.2 ± 2.6 mM) under closed stomata condition and in the juxta apical cells (27.03 ± 3.54 mM) under open stomata condition. When stomata were closed, its concentrations in apical subsidiary (56.4 ± 2.5) and juxta apical cells (54.8 ± 1.9 mM) were similar ($p > 0.40$), and significantly higher ($p < 0.01$) than in the pavement cells (40.1 ± 3.7 mM). In open stomata situation concentrations in the pavement (33.45 ± 3.39mM) and juxta apical (27.03 ± 3.54 mM) as wells as that in apical subsidiary (59.21 ± 3.24 mM) and guard cells (69.13 ± 7.33 mM) were similar ($p > 0.08$ and $p > 0.09$ respectively), but the concentration in the latter (group) was significantly higher (($p < 0.01$).

Mg^{2+} concentrations were significantly lower ($p < 0.01$) in the juxta apical (Δ -41.7 ± 0.0 mM; $p < 0.001$) and lateral subsidiary (Δ -5.5 ± 0.6 mM; $p < 0.05$), but higher in guard cells (Δ 36.9 ± 4.7 mM; $p < 0.01$) under open stomata situation. Concentrations in pavement and apical subsidiary cells did not change ($p > 0.05$) as stomata opened. Between contiguous cells, Mg^{2+} concentration increased from juxta apical through the apical subsidiary cells to the lateral subsidiary cells under open stomata situations, maintaining a steady uphill gradient towards the lateral subsidiary cells. Under both open and closed situations concentrations in the guard cells were lower than in the lateral subsidiary cells.

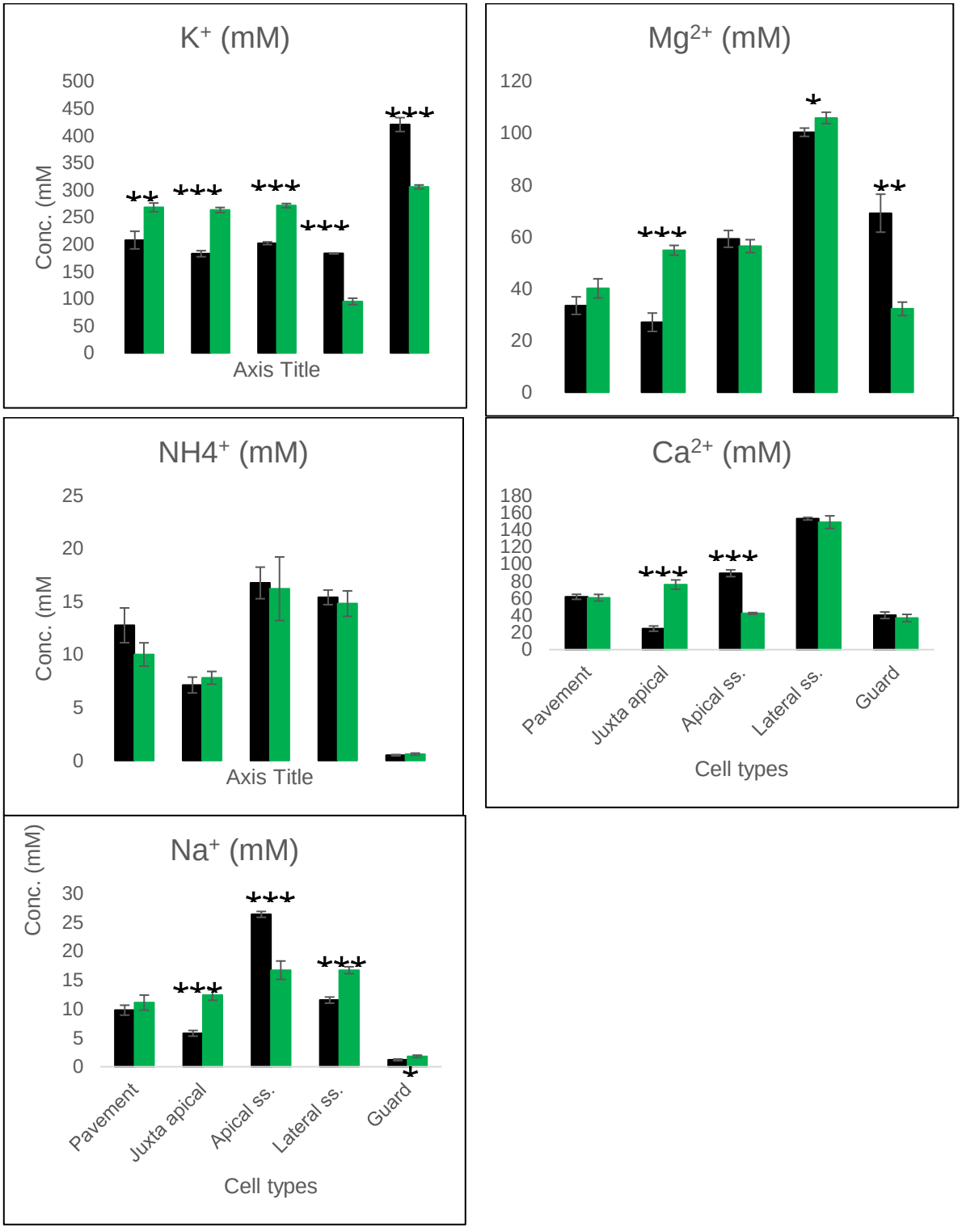

Figure 4.5 Cation concentration in cell types at open (■) and closed (●) stomata compared

One, two or three asterisk(s) (*) represent(s) *p* values < 0.05, 0.01 or 0.001 respectively at 95 % confidence interval.

4.2.6 Charge balance under closed and open stomata

As a control to the experiments, a balance of charge between the negative and positive charges measured were determined (as performed in chapter 3). Charged species that are capable of being involved in weak ionization reactions are affected by the pH of the medium. The charge balance in vacuolar solutes was thus determined at the estimated vacuolar pH. Bowling and Edwards, (1984) measured the vacuolar pH of *T. virginiana* cells using free-hydrogen ion-sensitive microelectrode technique and showed that pH varied between cell types and in each cell type, between open and closed stomatal situations (see appendix 11). Two cell types (apical subsidiary and juxta apical cells) though, were not mentioned but implied in the study. The apical subsidiary was implied in the measurement of subsidiary cells while the juxta apical cell was implied in the measurement of pavement cells, since juxta apical cells are a subtype of pavement cells (see section 3.2.3.2). Table 4.2 thus shows the expanded version of the results from Bowling and Edwards (1984).

Table 4.2 Vacuolar pH of the cells of the stomatal complex of *T. virginiana*
Mean ± standard error from six repeats.
Adapted from (Bowling and Edwards, 1984).

Stomatal aperture	Guard cell	Lateral subsidiary cell	Apical subsidiary cell	Juxta apical cell	Pavement cell
Open	6.0 ± 0.1	5.5 ± 0.1	5.5 ± 0.1	5.2 ± 0.1	5.2 ± 0.1
Closed	5.3 ± 0.1	5.3 ± 0.1	5.3 ± 0.1	5.8 ± 0.1	5.8 ± 0.1

The corresponding pH under the appropriate (open or closed) condition was applied in the Henderson-Hasselbalch equation (see equ. 3.2 in section 3.3.2.1.1) to calculate the charges of the observed species (Tables 4.3). Table 4.4 shows the charge balance in the cell types under closed stomata calculated from the charges on the ions at the respective vacuolar pH (Table 4.2). The charges on the cation and anion species balanced out in all the cell types up to at least 99.1%. In all cell types a slight (<1%) excess of positive charge was recorded (measured).

Table 4.3 Charges on ionized solutes in vacuolar sap of *T. virginiana* at open and closed stomata conditions.
All the charges are negative.

Cell type	stomatal condition	pH	**Cl^-**	**SO_4^{2-}**	**NO_3^-**	**Citrate**	**Tartrate**	**Malate**	**Succinate**	**PO_4^{3-}**
Guard cell	open	6.0	1.0	2.0	1.0	2.2	2.0	1.9	1.7	1.1
	Closed	5.3	1.0	2.0	1.0	1.8	1.9	1.6	1.2	1.0
Pavement	open	5.2	1.0	2.0	1.0	1.8	1.9	1.6	1.2	1.0
	Closed	5.8	1.0	2.0	1.0	2.1	2.0	1.8	1.6	1.1
Juxta apical	open	5.2	1.0	2.0	1.0	1.8	1.9	1.6	1.2	1.0
	Closed	5.8	1.0	2.0	1.0	2.1	2.0	1.8	1.6	1.1
Apical subsidiary	open	5.5	1.0	2.0	1.0	2.0	1.9	1.7	1.4	1.0
	Closed	5.3	1.0	2.0	1.0	1.8	1.9	1.6	1.2	1.0
Lateral subsidiary	open	5.5	1.0	2.0	1.0	2.0	1.9	1.7	1.4	1.0
	Closed	5.3	1.0	2.0	1.0	1.8	1.9	1.6	1.2	1.0

Table 4.4 Charge balance in cell types at closed stomata

Plant	(Mean)	Chloride	Sulphate	Nitrate	Citrate	Tartrate	Malate	Succinate	Phosphate	**Total**	NH_4^+	K^+	Na^+	Ca^{2+}	Mg^{2+}	**Total**	Charge imbalance
Pavement cells	Conc. (mM)	132.09	28.46	63.49	3.31	0	91.46	0	56.54		10.01	267.97	10.95	60.64	40.07		
	$mEq.L^{-1}$	132.09	56.93	63.49	6.96	0	164.62	0	62.20	**486.28**	10.01	267.97	10.95	121.29	80.14	**490.36**	4.08
Juxta Apical cells	Conc. (mM)	108.79	53.18	42.47	19.74	0	110.03	0	38.86		7.80	263.09	12.44	76.00	54.78		
	$mEq.L^{-1}$	108.79	106.36	42.47	41.44	0	198.05	0	42.75	**539.87**	7.80	263.09	12.44	152.01	109.55	**544.89**	5.02
Apical subsidiary cells	Conc. (mM)	120.41	40.69	45.87	20.82	12.92	89.26	12.23	30.64		16.22	271.32	16.66	42.26	56.37		
	$mEq.L^{-1}$	120.41	81.37	45.87	37.48	24.54	142.82	14.68	30.64	**497.82**	16.22	271.32	16.66	84.52	112.73	**501.46**	3.64
Lateral subsidiary cells	Conc. (mM)	147.40	51.40	45.01	73.45	0.51	106.66	17.99	9.31		14.75	94.81	16.69	148.75	105.90		
	$mEq.L^{-1}$	147.40	102.80	45.01	132.21	0.97	170.66	21.58	9.31	**629.94**	14.75	94.81	16.69	297.49	211.79	**635.53**	5.59
Guard cells	Conc. (mM)	182.04	33.54	77.27	1.47	0.02	60.26	0.34	18.67		0.60	305.70	1.78	36.90	32.20		
	$mEq.L^{-1}$	182.04	67.07	77.27	2.64	0.03	96.42	0.41	18.67	**444.55**	0.60	305.70	1.78	73.80	64.40	**446.27**	1.72

Table 4.5 Charge balance in cell types at open stomata

Plant	(Mean)	Chloride	Sulphate	Nitrate	Citrate	Tartrate	Malate	Succinate	Phosphate	**Total**	NH_4^+	K^+	Na^+	Ca^{2+}	Mg^{2+}	**Total**	Charge imbalance
Pavement cells	Conc. (mM)	104.81	60.59	35.38	3.10	0	79.70	0	24.94		12.75	207.77	9.79	61.68	33.45		
	$mEq.L^{-1}$	104.81	121.19	35.38	5.57	0	127.52	0	24.94	**419.41**	12.75	207.77	9.79	123.36	66.89	**420.57**	1.16
Juxta Apical cells	Conc. (mM)	102.96	10.63	29.41	16.99	0	68.26	0	4.06		7.12	182.65	5.79	24.59	27.03		
	$mEq.L^{-1}$	102.96	21.26	29.41	30.59	0	109.22	0	4.06	**297.50**	7.12	182.65	5.79	49.18	54.07	**298.81**	1.31
Apical subsidiary cells	Conc. (mM)	115.64	52.88	32.41	33.79	1.80	111.52	1.05	23.83		16.75	201.99	26.36	89.22	59.21		
	$mEq.L^{-1}$	115.64	105.77	32.41	67.58	3.42	189.59	1.47	23.83	**539.71**	16.75	201.99	26.36	178.44	118.43	**541.97**	2.26
Lateral subsidiary cells	Conc. (mM)	146.62	25.84	87.02	64.04	1.88	135.68	13.85	46.39		15.39	183.06	11.53	152.86	100.37		
	$mEq.L^{-1}$	146.62	51.69	87.02	128.08	3.56	230.65	19.39	46.39	**713.41**	15.39	183.06	11.53	305.72	200.74	**716.43**	3.02
Guard cells	Conc. (mM)	204.44	54.27	88.45	2.78	10.70	64.35	16.79	53.11		0.50	420.46	1.19	40.16	69.13		
	$mEq.L^{-1}$	204.44	108.53	88.45	6.11	21.41	122.27	28.55	58.42	**638.17**	0.50	420.46	1.19	80.32	138.25	**640.73**	2.56

Table 4.5 shows the charge balance in all the cell types under open stomata as calculated using table 4.3. The charges on the cation and anion species balanced out in all the cell types up to at least 99.5% (in contrast with the value for epidermal strip - chapter 3). In all cell types there was a slight (<0.5%) excess of positive charge. The highest total charge (sum charge (in $mEq.L^{-1}$) of all the positive or negative charged species) was found in the lateral subsidiary and the lowest in the juxta apical cells. In all cell types except the guard cell, malate had the highest negative charge. In the guard cells, chloride was highest. Similarly, in all the cell types, K^+ provided the highest positive charge except in the lateral subsidiary cells where Ca^{2+} gave the highest. NH_4^+ and Na^+ constitute less than 8% of total positive charge in all the cell types - less than 0.3% in the guard cells. Tartrate and succinate constitute 7.8% of the negative charge in the guard cells.

4.3 Discussion

Stomatal responses to internal and external cues are effected by the guard cells aided by the subsidiary cells in an intact epidermis. Solute transport to and fro the vacuoles of these cells enable the creation of the differential pressures required to effect the responses. The results presented in this chapter both aligns with the existing knowledge and also provides considerable additional information that extents the understanding of stomatal function in *T. virginiana.* All the cell types of the epidermis appear to play a part in the orchestration of stomatal responses to stimuli.

4.3.1 Guard cells

The guard cell pair is central to the functioning of the stomata. Stomatal opening is accompanied by increase in K^+ concentration ($p < 0.001$) as noted (for *T. virginiana)* by previous workers (Edwards and Bowling, 1984; Irving, 1996). Its concentration increases by 115 ± 9 mM. This is similar to 159 ± 26 mM found by Edwards and Bowling (Edwards and Bowling, 1984) in *Tradescantia* but contrasts with the 353 ± 35 mM (Penny and Bowling, 1974) and 290 ± 121 mM (MacRrobbie and Lettau, 1980) for *Commelina* as well as 300 ± 30 mM (Fischer, 1971) and 386 ± 73 mM (Outlaw and Lowry, 1977) for *Vicia faba*. It is, moreover, approximately one fourth of 449 ± 213 mM reported by Irving (1996) using the same clone of plants (*T. virginiana*) – but a different growth chamber and analytical technique (Energy

Dispersive X-ray Analysis). These two classes of data present a puzzle that was not solved during this present work. It is hoped that future work on growth conditions may find that they play a role in intracellular solute concentrations needed for stomatal opening. At present this can only be speculation.

A result not previously reported is a significant ($p < 0.01$) increase in Mg^{2+} (Δ 36.9 ± 4.7). High Mg^{2+} was, however, reported from epidermal strips of *Tradescantia* by Irving (1996) but not in guard cells and no previous reports have been documented. Such concentration (of Mg^{2+}) is unexpected since its divalent nature has and influence on the amount of anion that would be needed to provide the charge balance. Nevertheless, high Mg^{2+} concentration has been reported in plants and yeast. For example, in *Arabidopsis thaliana* leaf, a vacuolar Mg^{2+} concentration in excess of 30 mM has been reported in adaxial epidermal cells (Conn *et al*., 2011). In yeast vacuoles concentration in excess of 70 mM has been reported (Okorokov *et al*., 1980).

The changes found in anion concentrations during stomatal opening are more unexpected. As mentioned in the introduction, previous studies identified malate in *Vicia faba* (Allaway and Hsiao, 1973; Outlaw and Lowry, 1977) and Cl^- (Schnabl and Raschke, 1980) in *Allium* and plants that do not accumulate starch in their guard cells. In *T. virginiana* most studies have not identified the counter anion to K^+. Edwards and Bowling (1984) supported Martin *et al* (1983) in supposing that it is the organic acid malate. Irving (1996), on the contrary, showed that Cl^- is the major counter anion to K^+ in guard cells of *T. virginiana* during stomatal opening. Results from the present study show that neither of the two anions showed a sufficient change that may balance the increase in the cations (189 $mEq.L^{-1}$) (table 4.6). For statistical information see appendix 11.

Table 4.6 Balance of anion and cation activities in guard cells during stomatal opening in *T. virginiana*

Solute	Cl^-	SO_4^{2-}	PO_4^{3-}	Tart.	Succ.	M/A	**Total Anion**	K^+	Mg^{2+}	**Total Cation**	Cation Anion
Conc. (mM)	22.3	20.8	34.4	10.7	16.5	4.1		115.0	37.0		
Activity ($mEq.L^{-1}$)	22.3	41.5	39.8	21.4	28.1	25.9	**179.0**	1150	74.0	**189.0**	**10**

Chloride increased ($p < 0.01$) by 22.3 ± 5.1 mM but malate showed no significant change ($p > 0.2$) in concentration though it contributed to balance the cation charges. Increases in succinate ($p < 0.05$) (16.5 mM (28.1 $mEq.L^{-1}$)), tartrate ($p <$

0.001) (10.7 mM (21.4 mEq.L^{-1})), SO_4^{2-} ($p < 0.001$) (20.8 mM (41.5 mEq.L^{-1}) and PO_4^{3-} ($p < 0.05$) (34.4 mM (39.8 mEq.L^{-1}) sufficed in place of malate. These appear to be without precedence in *T. virginiana* literature, but succinate has been shown to increase in guard cells of *Vicia faba* during stomatal opening (Talbott and Zeiger, 1996). Additionally, the concentrations (and increase) of SO_4^{2-} and PO_4^{3-} are unexpected in the presence of the high concentrations of Mg^{2+} obtained (69 mM under open stomata), in which they would be expected to be mainly insoluble . For example, the solubility product of $Mg_3(PO_4)_2$ at 25ºC is 1 x 10^{-25} (http 1, 2006). Organic acids, malate, tartrate and succinate may, however, form soluble complexes with Mg^{2+} (Bradfield, 1976; Taiz *et al*., 2015).

The solubility problem notwithstanding, the net charge balance observed in both open and closed guard cells is evidence that all significant ions are accounted for. This is one of the advantages of the CZE technique which is its ability to detect all soluble ions regardless of their identity. The increases also correspond to the lower end of such (total) increases described in the literature (Edwards and Bowling, 1984; Irving, 1996). This aspect is dealt with further in the next chapter (chapter 5) that is concerned with measurement of (guard cell) osmotic pressure. It will be noted here, however, that there is a general correspondence of the sum of the ionic solutes presented in this experiment and the (independent) measure of osmotic pressure - which encompass all solutes. This is also, evidence, for the veracity of the data presented in this chapter.

In summary, it would appear that *T. virginiana* guard cells follow the common pattern of using K^+ as the main osmotic cation, but also utilise Mg^{2+}. They also use Cl^- and malate as medium of osmotic change, but only to a small degree. The other unexpected anions contribute equally.

4.3.2 **Epidermal pavement cells**

a) Comparison with bulk data

Most of the volume of the epidermis of *Tradescantia* is found in the vacuoles of the epidermal pavement cells. In the scoping experiment of chapter 3, the bulk analysis of abaxial epidermal strips (under conditions of open stomata) the results showed K^+ as the major cation (268.4 ± 4.6 mM), with substantial concentrations of Ca^{2+} (54.6 ± 1.4 mM) and Mg^{2+} (21.6 ± 0.9 mM). Malate was the predominant anion (130.6 ± 3.4 mM) and substantial concentrations of Cl^- (52.1 ± 0.7 mM), PO_4^{3-} (28.3 ± 1.9 mM), SO_4^{2-}

(14.7 ± 0.8 mM), NO_3^- (13.2 ± 0.7 mM) and citrate (14.4 ± 0.9 mM) were observed. Tartrate and succinate were also found as traces (< 0.5 mM) (see table 4.6).

Table 4.8 shows the similarities and differences between these bulk (strip) values and those determined from individual pavement cells. It is estimated (using surface area –see chapter 3) that the pavement cells occupy some 52.9% of the volume of the strips. The cations show broadly the same pattern, with the Mg^{2+} concentration, possibly being an exception. We shall see, below that this cannot be due to lower concentrations of Mg^{2+} in the cells of the stomatal complex. The reason remains unclear.

Table 4.7 Comparison of solute concentrations of individual pavement cells with those measured on bulk (abaxial) epidermal strips (under open stomatal conditions).

Solute	Conc. under open stomata condition	
	Bulk epidermal strip	Pavement cell
K^+	268.4	207.8
Ca^{2+}	54.6	61.7
Mg^{2+}	21.9	33.5
Cl^-	52.5	104.8
Malate	130.6	79.7
SO_4^{2-}	14.7	60.6
NO_3^-	13.2	35.4
Citrate	14.5	3.1
PO_4^{3-}	28.3	24.9
Oxalate	Trace	None
Tartrate	Trace	None
Succinate	Trace	None

There are striking differences in these ion concentrations. The differences may be due to i) large differences in the content of the cells of the stomatal complex as well as the juxta apical cells and/or ii) a cell type in the epidermis of different composition that was not measured. Unfortunately, the latter may be represented by the surface cells overlying the vascular bundles, which were omitted from the SiCSA analysis. We shall return to this difference in anion concentration between the two experiments after discussing the solute concentrations of the individual stomatal complex cells below.

Characterization of bulk or single cell epidermal solutes in *Tradescantia* has not been recorded in literature. In barley, bulk (Leigh *et al*., 1986; Fricke *et al*., 1994c)

and individual epidermal (pavement) cells solute concentrations (Fricke *et al*., 1994a, b) showed no differences. Similar results were obtained in wheat (Malone *et al*. 1991).

b) Changes due to illumination of plant

A main focus of this project, however, was on the role of the surrounding cells in supplying solutes to drive the opening and closing of the stomata. The pavement cells are potential source/sink for the tidal flow of solutes during stomatal movements. As with the guard cells, significant differences were noted in the pavement cell contents on illuminating the plants (stomatal opening, but also increasing transpiration). Major among these differences were decreases in K^+ (Δ -60.2 mM), and significant, unexpected changes in anions (decrease: Cl^- (Δ -27.3 mM), NO_3^- (Δ -28.1 mM), PO_4^{3-} (Δ -31.6 mM) and malate (Δ -11.8 mM); increase: SO_4^{2-} (Δ32.1 mM)). Qualitatively, the changes in K^+, Cl^- and PO_4^{3-} correspond to the opposite changes in the guard cells. In contrast, SO_4^{2-} appears to increase simultaneously in both, while malate loss from the epidermis is not accompanied by an increase in the guard cells.

Looking for equivalence between guard and pavement cells, however, is probably mistaken, as the other cells of the stomatal complex are likely to be playing differential roles (consideration must also be made of the different volumes of source and sink in each case). It is to this aspect that we shall turn now.

4.3.3 Solute concentrations in other cell types

a) Solute concentrations in lateral subsidiary cells

Potassium concentration increases significantly (Δ88.3 ± 5.1 mM ($p < 0.001$); appendix 9-10) in lateral subsidiary cells during stomatal opening. This corresponds with the findings (increase of Δ44 ± 13.4 mM) of Edwards and Bowling (1984) but contrasts with those of Irving (1996) (decrease of Δ -17 ± 36.2 mM) in *T. virginiana*. In outer lateral subsidiary cells of *Commelina*, however, Penny and Bowling (1974) found comparable (Δ101.0 ± 33.1 mM) concentration changes during stomatal opening. The reason for the inconsistencies in the reported values in *T. virginiana* is not known now, but may be due to differences in the solute contents of growth media and other environmental conditions. This has been demonstrated with *Vicia faba*

(Van Kirk and Raschke, 1978a). In spite of this, K^+ concentrations in lateral subsidiary cells at open stomata (183.1 ± 0.8 mM) compare well with the findings (166 ± 12 mM) of Penny and Bowling (1974).

The increase in K^+ was not mirrored by any of the other cations. The lateral subsidiary cells possess the highest concentrations of Ca^{2+} (152.9 ± 1.5 mM) and Mg^{2+} (100.4 ± 1.6 mM) compared to other cell types, including the guard cells. These Ca^{2+} and Mg^{2+} concentrations are maintained within a narrow range during stomatal movements (appendix 9-10).

The relatively high concentrations as well as the narrow range of change during stomatal movements may be the plants' adaptation to balancing the negative charge from malate, the dominant anion osmoticum in lateral subsidiary cells. Increases in malate (Δ29.0 ± 2.8 mM), equivalent to 60.8 $mEq.L^{-1}$, and in PO_4^{3-} (Δ 34.4 ± 3.0mM), equivalent to 37.1 $mEq.L^{-1}$ of the respective charged species, provide the negative charges that may balance the increase in positive K^+ charges adequately. Charge balance, however, depends not only on solute concentration changes but also, and mainly, on the actual concentration of the species at the different (open and closed) states. In considering the actual concentrations, the balance of charges on the lateral subsidiary cells is made possible by the increased concentration of another, less understood anion, NO_3^-.The observed increase in NO_3^- (Δ 42.0 ± 2.6 mM) may be important only in balancing out the positive charges in open stomata. Nevertheless, increase in NO_3^- concentration has been implicated in stomatal opening in barley (section 4.1.8). In barley, *Commelina* and *Tradescantia*, no counter anion has been identified previously as balancing the K^+ charges in the lateral subsidiary cells. The increases observed in malate and PO_4^{3-} in this studies suggest that malate may be the major counter-anion to K^+ in the lateral subsidiary cells.

b) Solute concentrations in apical subsidiary cells

As in all other cells discussed thus far, K^+ is the major solute changing ($p < 0.001$) in apical subsidiary cells during stomatal movement. Its concentration decreases (by Δ -69.3 ± 1.3 mM) on stomatal opening. Similar, but smaller (Δ -16.0 0 ± 19.7 mM), decrease has been reported previously in *Tradescantia* (Irving, 1996).

In contrast to the behaviour of the lateral subsidiary cells, significant ($p < 0.001$) increase in Ca^{2+} occurs in the apical subsidiary cells during stomatal opening.

Much as it contrasts with the K^+ change, this also contrasts qualitatively and quantitatively with the observations of Irving (1996), who found a decrease (of Δ -11.0 ± 17.1 mM) in *T. virginiana*. Citrate concentration increases significantly ($p < 0.01$), but significant ($p < 0.001$) decreases in tartrate and succinate concentrations occur in open stomata state. These suggest that the apical subsidiary cells may not play an active part in stomatal movement in *Tradescantia* except as a conduit for participating solutes to the lateral subsidiary and guard cells.

c) Solute concentrations in juxta apical cells

As has been prefaced in earlier chapters of this thesis, the juxta apical cells appear to be physiologically different. All the solutes (cations and anions) in this cell type decrease in concentration during stomatal opening, except Cl^- and NH_4^+, which make no change. Cl^- concentration in all cell types, except the pavement cells and the guard cells, showed no significant change. More than all the other cations, K^+ significantly ($p < 0.001$) decreased (Δ-80.5 ± 0.9 mM). Calcium, as well, decreased (Δ-51.4 ± 2.3 mM). This result describes, for the first time, a cell type in which the concentrations of nearly all ions decrease significantly during stomatal opening. The reverse occurs during stomatal closure. This has implications for the osmotic pressure in this cell type during stomatal opening (discussed in chapter 5) and suggests a storage role for this cell type.

A storage role by an epidermal cell type was suggested by Penny and Bowling (1974) and Raschke and Fellows (1971) for the ions involved in guard cell control of stomatal movements in *Commelina* and maize respectively. The cell in question may well be the juxta apical cell or its equivalent, as no distinction has been made between pavement and juxta apical cells before now. Both cell types, juxta apical and pavement cells, have always been assumed to be pavement cells (see chapter 3). No cell type has so far been identified as showing physiological attributes of a storage cell: such as reciprocating changes in ion concentrations compared with guard cells during stomatal movements (see table 4.8). Juxta apical cells releases most solutes but accumulate none during stomatal opening, and then accumulates most but releases none when stomata close. The accumulated solutes are released to the guard cell (PO_4^{3-} and Mg^{2+}), pavement cell (SO_4^{2-}) and apical subsidiary cell (Ca^{2+}). Chloride is stored in pavement cells. Potassium, on the other hand, has no

intracellular storage but may be stored in the apoplast of guard cells (Penny and Bowling, 1974; Edwards and Bowling, 1984) and of surrounding cells.

Table 4.8 Changes of solutes stored by juxta apical and pavement cells for stomatal opening in *T. virginiana*.

The table shows electrolyte accumulation mainly in juxta apical but also pavement cells during stomatal opening. The negative (-) sign stands for solute release while no sign (positive numbers) signifies its accumulation during stomatal opening. The juxta apical cell accumulates Ca^{2+}, Mg^{2+}, SO_4^{2-} and PO_4^{3-}, during stomatal opening. The solutes are redistributed to guard cell, lateral, apical subsidiaries and pavement cells when stomata are closing. Two tailed two samples student's t-test assuming equal variance was applied to compare the significance of the differences (samples from different cells of same plant). At 95% confidence interval, *P*-values compared (a) pavement and guard cells; (b) juxta apical to pavement and apical cells; (c) Juxta apical to guard cell; (d) pavement to lateral subsidiary cells; (e) juxta apical to apical subsidiary cells.

Anions			
Cell type	**Cl^- (mM)**	**SO_4^{2-} (mM)**	**PO_4^{3-} (mM)**
Juxta apical cells	Insignificant change (i/c)	-42.6 ± 2.4	-34.8 ± 2.4
Guard cells	22.3 ± 5.1	20.8 ± 0.8	34.4 ± 3.0
Apical	i/c	12.3 ± 0.9	-6.8 ± 0.4
Lateral	i/c	-25.6 ± 0.4	37.1 ± 5.3
Pavement cells	-27.3 ± 6.9	32.1 ± 1.0	-31.6 ± 5.9
p-value (a) Pavement vs guard cell	>0.3		
p-value (b) Juxta vs pavement and apical		> 0.3	
p-value (c) juxta vs guard cell			> 0.8
p-value (d) pavement vs lateral subsidiary			> 0.2
Cations			
	K^+ (mM)	**Ca^{2+} (mM)**	**Mg^{2+} (mM)**
Juxta apical cells	-80.5 ± 0.9	-51.4 ± 2.3	-27.8 ± 1.6
Guard cells	114.8 ± 9.1	i/c	36.9 ± 4.7
Apical	-69.3 ± 1.3	46.9 ± 3.0	i/c
Lateral	88.3 ± 5.1	i/c	i/c
Pavement cells	-60.2 ± 8.2	i/c	i/c
p-value (c) juxta vs guard cell	< 0.03		> 0.06
p-value (e) Juxta vs apical subsidiary		> 0.1	

4.3.4 **Malate in guard cell**

A consideration that suggests the exclusion of malate as a counter anion to K^+ in *T. virginiana* and which may determine which anion, malate or Cl^-, may be used in a

species, is the size of the change in guard cell vacuolar pH during stomatal opening. Guard cell cytosolic pH is essentially unchanged between closed and open stomatal conditions (Bowling and Edwards, 1984). The pH of a solution determines the ionization (i.e. charge) of a weak acid in solution. Multivalent acid-salts such as the dicarboxylic acid salts contain more than one ionisable proton. The pH of the solution as well as the pKa of the acid determine the number of protons that are ionized, and therefore, the charge on the salt in the solution (table 4.9). The overall charge on an ionized salt is the sum of the charges on the individual ionisable protons. This overall charge changes with every change in pH according to proximity of the pKa of the ionisable protons to neutral pH. The more the pKa of the ionisable protons approach pH range of the compartment involved the greater the variation in charges with any change in pH. Among the dicarboxylic acids malate and succinate possess second (β) ionisable protons whose pKa is considerably closer to the guard cell vacuolar pH in open stomata (pH 6.3) than that of the first (α) proton. Thus small changes in pH lead to significant changes in the charges on these salts (table 4.10).

Table 4.9 The effect of pKa of ionisable protons on the total charges on dicarboxylic acids found in *T. virginiana* guard cell.

	Citrate			Tartrate			Malate			Succinate		
		Charge at pH		pKa	Charge at pH		pKa	Charge at pH		pKa	Charge at pH	
	pKa	**5.3** (closed)	**6** (open)		**5.3** (closed)	**6** (open)		**5.3** (closed)	**6** (open)		**5.3** (closed)	**6** (open)
α	3.13	0.99	1.00	3.04	0.99	1.00	3.40	0.98	1.00	4.21	0.91	0.98
β	4.76	0.78	0.95	4.37	0.87	0.98	5.05	0.59	0.90	5.64	0.27	0.70
γ	6.4	0.07	0.28									
Total charge		**1.84**	**2.23**		**1.86**	**1.98**		**1.57**	**1.9**		**1.18**	**1.68**

The change occurring in the total charge on a dicarboxylic acid as a result of a change in its concentration can be calculated as follows:

$$\text{Change in total charge} = \text{Charge difference X (Final conc.)} + \text{Initial charge X } (\Delta \text{ conc.})$$

Equation 4.1 Change in total charge due to change in solute concentration

The change in total charge depends on the charge difference occurring as a result of the pH change. The change may therefore, be several times higher than expected for the concentration change if the change in pH is large (table 4.10). For example, if the change in malate concentration of 4 mM (60mM – 64mM) occurs during stomatal

opening in different cells that experience different degrees of pH changes, increasingly, greater change in malate charge than expected will be seen as the pH change increases. Thus as pH difference widens in a cell between closed and open stomatal states, the likelihood of surplus negative charge increases. This is because more positive charges are needed to balance the increasing negative charge caused by increased ionization.

Table 4.10 Changes in total charge on malate as intracellular pH varies

pH change	Final charge	Initial charge	charge diff.	Initial conc.	Final conc.	Conc. Change	Charge diff.	Expected change	Diff. between expected and actual charge	% of actual change
0.1	1.51	1.45	0.06	60	64	4	9.8	6.0	3.7	61.7
0.2	1.57	1.45	0.12	60	64	4	13.7	6.3	7.4	45.9
0.4	1.68	1.45	0.23	60	64	4	20.8	6.7	14.1	32.3
0.6	1.77	1.45	0.33	60	64	4	26.7	7.1	19.6	26.6
0.8	1.85	1.45	0.40	60	64	4	31.3	7.4	23.9	23.6
1	1.90	1.45	0.45	60	64	4	34.8	7.6	27.2	21.8

Plants with large pH changes in their guard cells (during stomatal movements) may therefore, avoid the use of malate as the major counter anion for K^+, while those with minimal pH change may use it. In such plants as the former, Cl^- becomes the major counter anion to K^+. Low concentrations of malate or other dicarboxylic acids may be used in such plants for balancing any excess positive charges unaccounted for by the Cl^- charges. On the other hand, if vacuolar pH is so low during stomatal opening, such that malate has a single charge (see Schnabl and Kottmeier (1984)), malate may serve the major counter-ion to K^+.

However, available literature has only recorded such pH changes in C*ommelina* and *Tradescantia*, and thus does not permit validation of this supposition. Nonetheless, in *Commelina* pH change of 0.4 (5.60 ± 0.13 to 5.20 ± 0.09) has been reported (Penny and Bowling, 1975). This places *Commelina* among species that may use the dicarboxylic acids as a major counter anion to K^+.

4.3.5 Possible functional organisation of *T. virginiana* epidermal trough cells

As the epidermal cells of *T. virginiana* (monocots) are arranged in files of trough cell separated by files of ridge cells, a clear morphological organisation of these cells is

obvious (see plate 3.1). Within the troughs, the morphological organisation of the individual cells or cell types do not appear in a clear file pattern (see figure 4.6). Thus, all the cell types, with the exception of the guard cells and juxta apical cells, appear to have anatomical contact with at least three other cell types when in the vicinity of the stomatal complex. In this area the pavement cells are anatomically in contact with the juxta apical, apical and lateral subsidiary cells. The lateral subsidiary contacts the guard cell, the pavement and the apical subsidiary cells which in turn, contact with both the guard cell and the lateral subsidiary as well as the juxta apical and pavement cells. The juxta apical cells contact the pavement and apical subsidiary cell. Outside this area the trough is populated only by pavement cells.

The size (in terms of cell perimeter) of these contacts vary. Each cell making contact with multiple cells has one particular cell with which it makes (disproportionately) the largest contact. The pavement cells make their largest contact with their likes, the pavement cells. The juxta apicals make their largest contacts with the pavement cells, the apical subsidiary with the juxta apical, the lateral subsidiary with the apical subsidiary and the guard cells with the lateral subsidiary cells.

The size of the contact surface may have import to transcellular solute transfers across these cells during stomatal movement. This is likely since, assuming even distribution of both plasmodesmata (except for guard cells) and solute transport proteins (channels and pumps) across plasma membrane, a disproportionately larger and, therefore, dominant solute transport might occur through and in the direction of these large contacts. Available literature suggests uniform plasmodesmatal frequency in all epidermal cells possessing plasmodesmata (see section 1.13.2). Edwards and Bowling (1984) using microelectrode traced a similar path for intercellular movement of K^+ in *T. virginiana* during stomatal movement.

Thus, an approximate functional path for intercellular solute movement during stomatal responses following this morphological network of dominant contact is likely. For this reason and for clarity in describing of the physiology of solute movements during stomatal responses a network of solute flow path– pavement → juxta-apical → apical subsidiary → lateral subsidiary → guard cell is being proposed. This supposes that solutes mainly move from the pavement cells, through the juxta apical, apical and then lateral subsidiary cells to the guard cells and vice versa during intercellular solute movements.

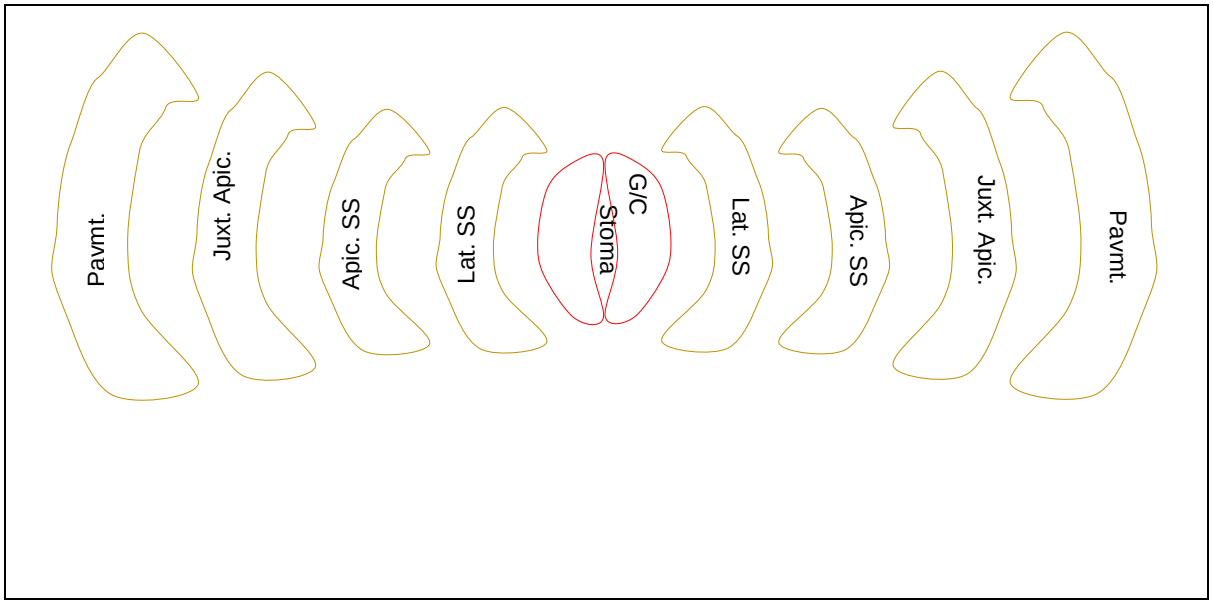

Figure 4.6 Proposed functional arrangement of cells of *T. virginiana* epidermal trough cells The pavement cell is in contact with the juxta apical cells but has no direct contact with the guard cell. The lateral subsidiary cell is in direct contact with the guard cell and the apical subsidiary cell, but has no contact with the juxta apical cells. The juxta apical contacts the apical subsidiary cell linking it to the pavement cell. Thus, the juxta apical cell is in contact with both the pavement and two apical subsidiary cells each of which belonging to different stomatal complexes.

4.3.6 Solute gradients during stomatal movements

The results from this study have shown that solute concentrations change in all cell types during stomatal movement. This finding generally agrees with that of previous workers (Penny and Bowling, 1974; Maier-Maercker, 1979; Edwards and Bowling, 1984; Irving, 1996). Consistent with the reports of these previous studies, solute concentration changes in contiguous cells are considered most relevant. Considering the anatomical position of each cell type relative to the guard cells (see figure 4.6), a hierarchy of contiguity starting from the pavements cells and ending at the guard cells was deduced. In between these two are the juxta apical cell, the apical subsidiary and the lateral subsidiary cells, in order of decreasing anatomic distance to the surfaces of the guard cells. This arrangement has also been used previously by Edwards and Bowling (1984) and Irving (1996) for *T. virginiana* and also by Penny and Bowling (1974) for *Commelina*. This arrangement describes the path of

solute flow from pavement cells to guard cells and *vice versa* during stomatal movements.

The flow of solutes that have significant mobility involves cells of significantly differing cell/vacuolar sizes (section 3.2.3.3). Despite the relative differences in volumes of these cells, observed changes in concentration are explained as due to transfer of solutes from one cell to the other. This was shown to be the case in *Commelina*, in which neutral red was shown to move from pavement cells, through the other intervening cells, to the guard cells (Willmer and Mansfield, 1969). On this basis, Penny and Bowling (1974) concluded that K^+ is transferred from pavement cells, through the lateral subsidiary cells, to the guard cells. Edwards and Bowling (1984) corroborated this conclusion by showing that K^+ is transferred from pavement cells to guard cells, and vice versa, as stomata open and close in *Tradescantia*, and calculated the driving force from measured potential differences across membranes of contiguous cells. The results presented here (figure 4.7) shows that there is no substantive difference between the curves of changes in concentration uncorrected for relative volume differences (A) and changes in concentration corrected for relative volume differences of cell types (B).

Literature also shows that solutes do not move into the mature guard cell from any other cell without crossing the guard cell membrane. This is because no plasmodesmata connections exist between mature guard cells and any other cell type(s). Instead, solutes accumulate in guard cell apoplast (Penny and Bowling, 1974; Bowling and Edwards, 1984; Edwards and Bowling, 1984) from where it moves down its electrochemical gradient into the guard cell. In intact leaves of *T. virginiana,* Edwards and Bowling (Edwards and Bowling, 1984) showed that K^+ is stored in guard cell apoplast, and its concentration changes by approximately three to ten fold in the apoplast during stomatal movements. In contrast, no K^+ concentration changes occur in the apoplast of the subsidiary cells. The potassium store in guard cell walls is fed by a gradient of potassium maintained from pavement cells through to the guard cell wall.

This supports our results which show a gradient of K^+ from the pavement cell, through the intervening cells, to the guard cells (see appendix 8 and10) during stomatal opening. Chloride as well as Mg^{2+} also maintains similar gradients. Gradients of some solutes such as malate, PO_4^{3-} and NO_3^- culminate in the lateral subsidiary cells, while the other solutes show no gradients (fig. 4.7). Notable among

the latter group are SO_4^{2-} and citrate which show increases, in the same pattern, in alternating cells. This suggests a possible charge balancing homeostatic role for these solutes during stomatal movements. Sulphate is the only multivalent anion that maintained a stable charge (-2) in all cells of *T. virginiana* epidermis at both open and closed stomatal states (table 4.3). Citrate, on the other hand, had the widest variation of charges as stomatal movements occurred. For instance, both solutes increased in apical subsidiary cells in which a 110% increase in Ca^{2+} concentration occurred, and in the guard cells which had up to 114% increase in Mg^{2+} on stomatal opening. On the other hand, their concentrations decreased in lateral subsidiary cells, which experienced little or no change in Ca^{2+} or Mg^{2+} concentrations, and in the juxta apical cells in which no cation increased in concentration during stomatal opening (see appendix 11). Tartrate and succinate, which were absent in pavement and juxta apical cells, maintained steep gradient from apical subsidiary cell through lateral subsidiary cell to the guard cell.

These different but patterned behaviours of groups of solutes: K^+, Cl^- and Mg^{2+}; PO_4^{3-}, NO_3^- and malate; tartrate and succinate as well as SO_4^{2-} and citrate, suggest firstly, that stomatal movement does not consist in only K^+ and a counter anion(s) fluxes and secondly, but that movements of a number of solutes into and out of the different cell types of the epidermis take place in a bid to achieve stomatal movement. Some of the solutes build gradients up to the guard cells, others build gradients to other supporting cells, while some others simply move to maintain charge balance. Thus all epidermal trough cells participate in bringing about the opening and closing of stomata in *T. virginiana*.

A: Cations

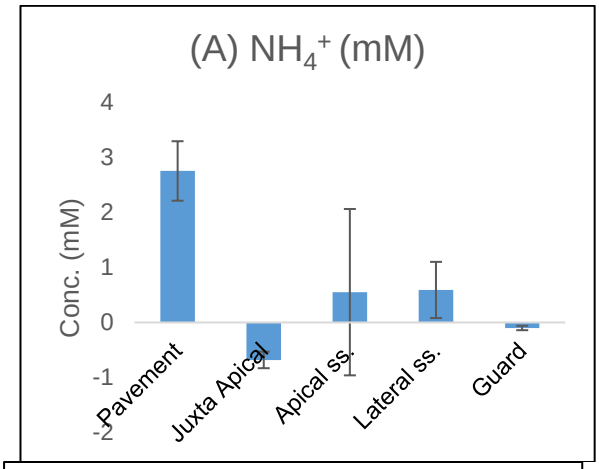
(A) NH_4^+ (mM)
Conc. (mM)
4
3
2
1
0
-1
-2
Pavement
Juxta Apical
Apical ss.
Lateral ss.
Guard

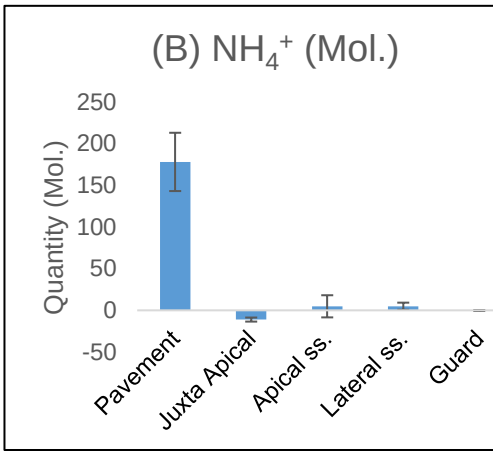
(B) NH_4^+ (Mol.)
Quantity (Mol.)
250
200
150
100
50
0
-50
Pavement
Juxta Apical
Apical ss.
Lateral ss.
Guard

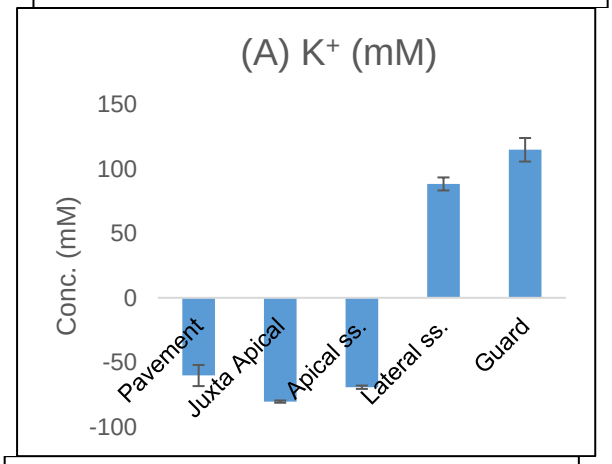
(A) K^+ (mM)
Conc. (mM)
150
100
50
0
-50
-100
Pavement
Juxta Apical
Apical ss.
Lateral ss.
Guard

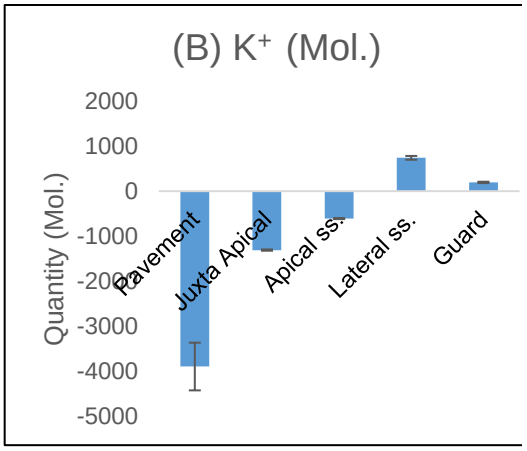
(B) K^+ (Mol.)
Quantity (Mol.)
2000
1000
0
-1000
-2000
-3000
-4000
-5000
Pavement
Juxta Apical
Apical ss.
Lateral ss.
Guard

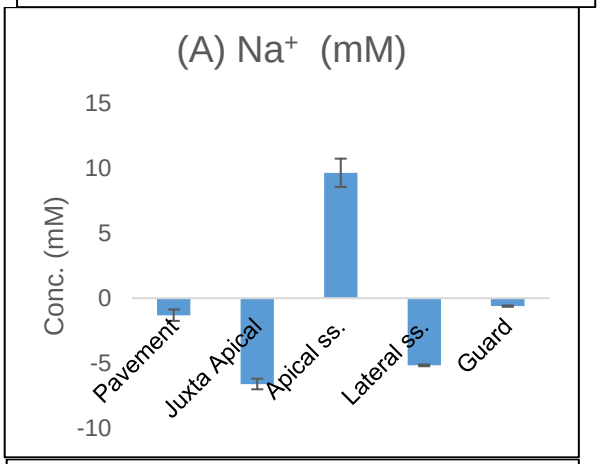
(A) Na^+ (mM)
Conc. (mM)
15
10
5
0
-5
-10
Pavement
Juxta Apical
Apical ss.
Lateral ss.
Guard

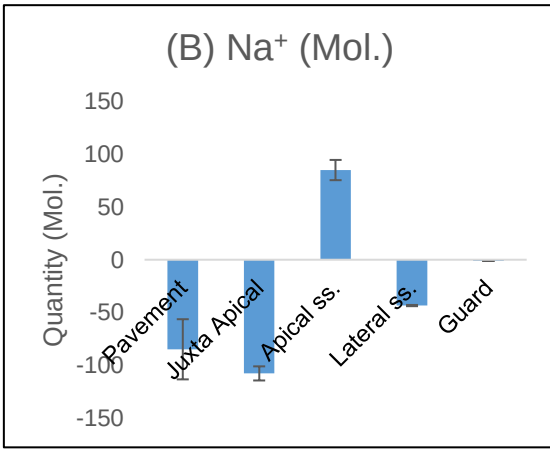
(B) Na^+ (Mol.)
Quantity (Mol.)
150
100
50
0
-50
-100
-150
Pavement
Juxta Apical
Apical ss.
Lateral ss.
Guard

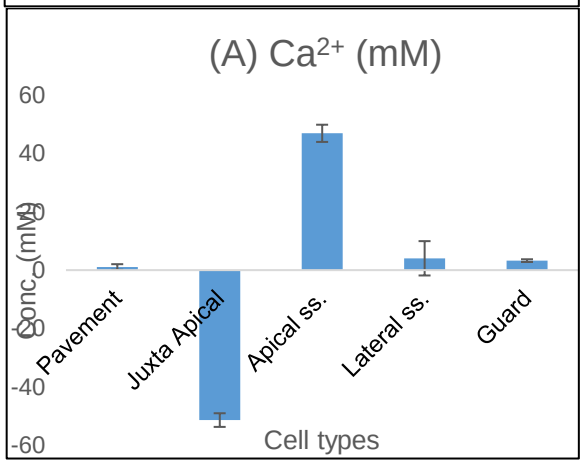
(A) Ca^{2+} (mM)
Conc. (mM)
60
40
20
0
-20
-40
-60
Pavement
Juxta Apical
Apical ss.
Lateral ss.
Guard
Cell types

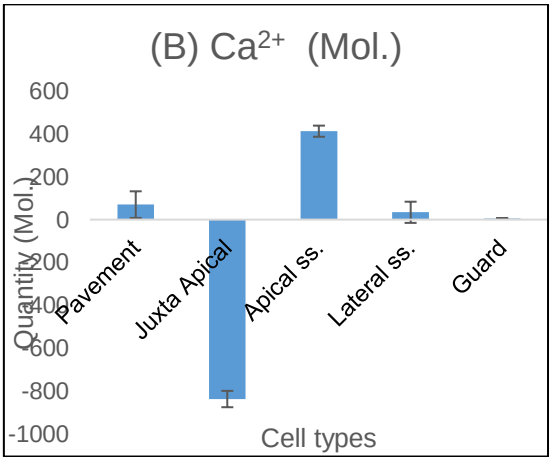
(B) Ca^{2+} (Mol.)
Quantity (Mol.)
600
400
200
0
-200
-400
-600
-800
-1000
Pavement
Juxta Apical
Apical ss.
Lateral ss.
Guard
Cell types

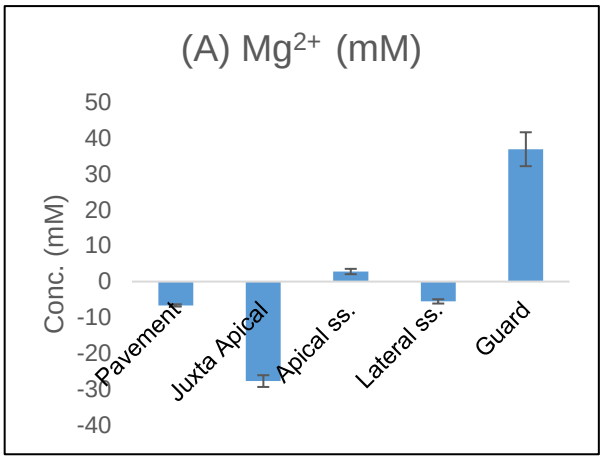
(A) Mg2+ (mM)
Conc. (mM)
50
40
30
20
10
0
-10
-20
-30
-40
Pavement
Juxta Apical
Apical ss.
Lateral ss.
Guard

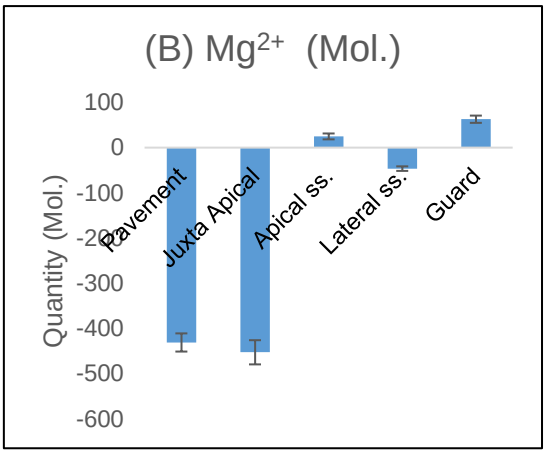
(B) Mg2+ (Mol.)
Quantity (Mol.)
100
0
-100
-200
-300
-400
-500
-600
Pavement
Juxta Apical
Apical ss.
Lateral ss.
Guard

B: Anions

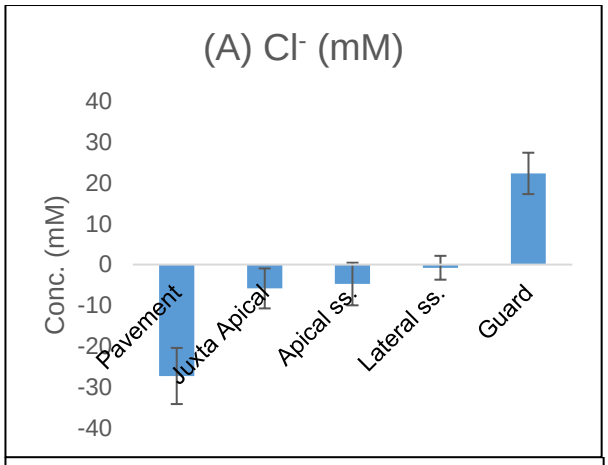
(A) Cl- (mM)
Conc. (mM)
40
30
20
10
0
-10
-20
-30
-40
Pavement
Juxta Apical
Apical ss.
Lateral ss.
Guard

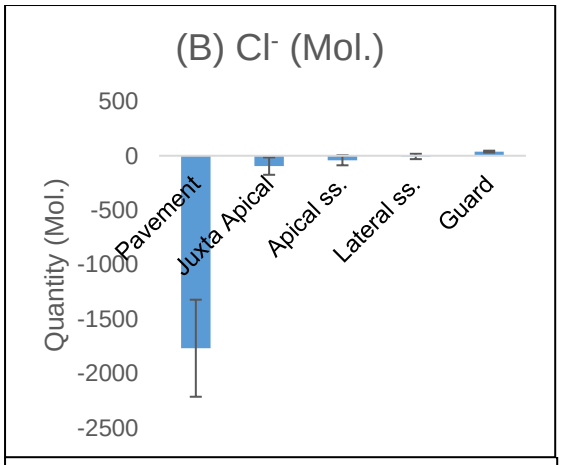
(B) Cl- (Mol.)
Quantity (Mol.)
500
0
-500
-1000
-1500
-2000
-2500
Pavement
Juxta Apical
Apical ss.
Lateral ss.
Guard

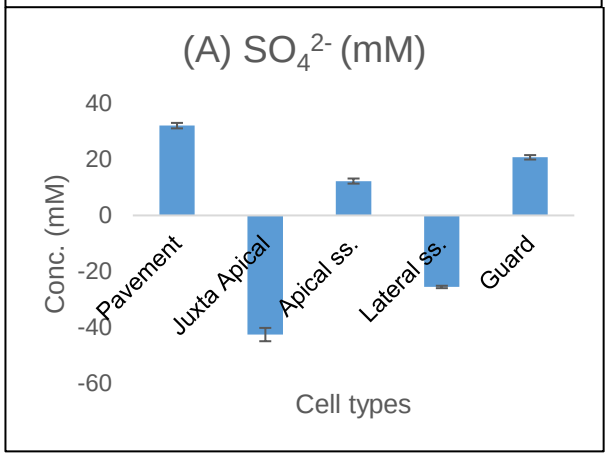
(A) SO4 2- (mM)
Conc. (mM)
40
20
0
-20
-40
-60
Pavement
Juxta Apical
Apical ss.
Lateral ss.
Guard
Cell types

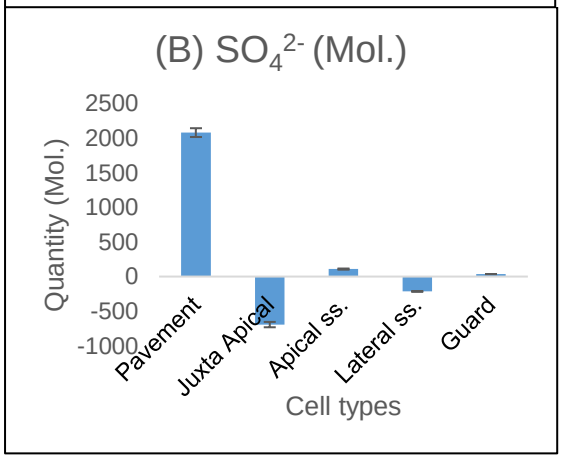
(B) SO4 2- (Mol.)
Quantity (Mol.)
2500
2000
1500
1000
500
0
-500
-1000
Pavement
Juxta Apical
Apical ss.
Lateral ss.
Guard
Cell types

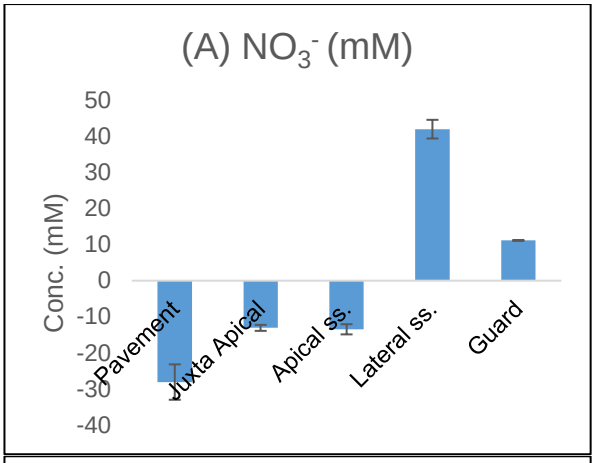
(A) NO3- (mM)
Conc. (mM)
50
40
30
20
10
0
-10
-20
-30
-40
Pavement
Juxta Apical
Apical ss.
Lateral ss.
Guard

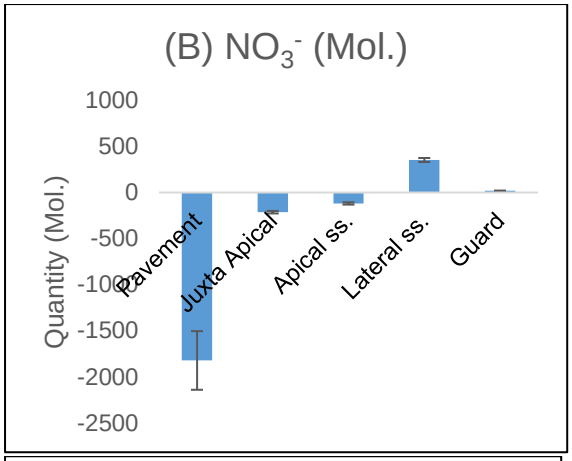
(B) NO3- (Mol.)
Quantity (Mol.)
1000
500
0
-500
-1000
-1500
-2000
-2500
Pavement
Juxta Apical
Apical ss.
Lateral ss.
Guard

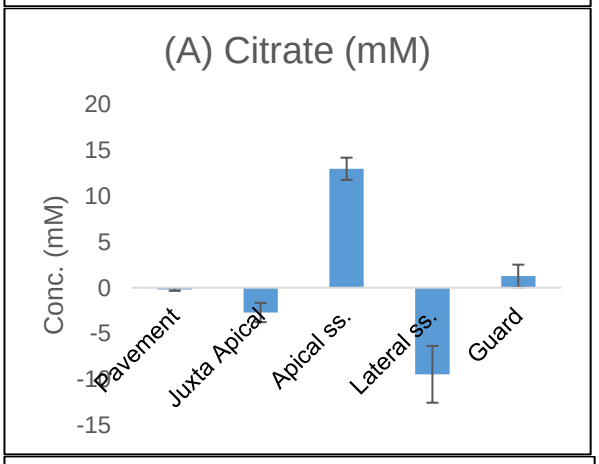
(A) Citrate (mM)
Conc. (mM)
20
15
10
5
0
-5
-10
-15
Pavement
Juxta Apical
Apical ss.
Lateral ss.
Guard

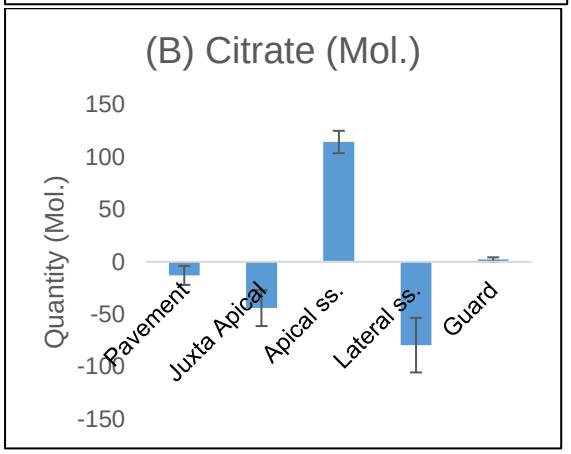
(B) Citrate (Mol.)
Quantity (Mol.)
150
100
50
0
-50
-100
-150
Pavement
Juxta Apical
Apical ss.
Lateral ss.
Guard

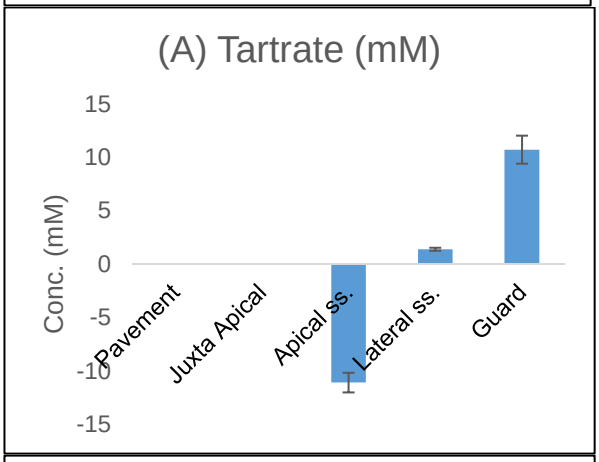
(A) Tartrate (mM)
Conc. (mM)
15
10
5
0
-5
-10
-15
Pavement
Juxta Apical
Apical ss.
Lateral ss.
Guard

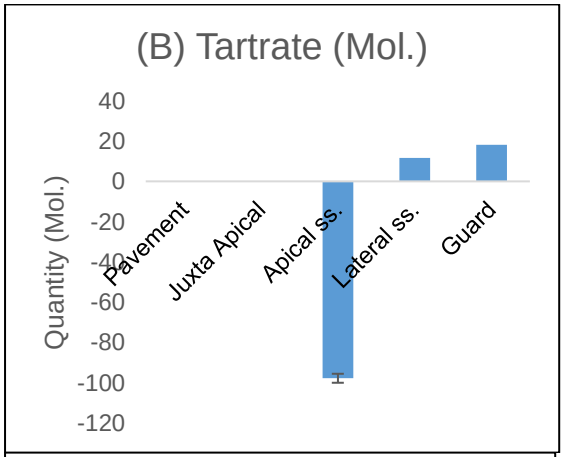
(B) Tartrate (Mol.)
Quantity (Mol.)
40
20
0
-20
-40
-60
-80
-100
-120
Pavement
Juxta Apical
Apical ss.
Lateral ss.
Guard

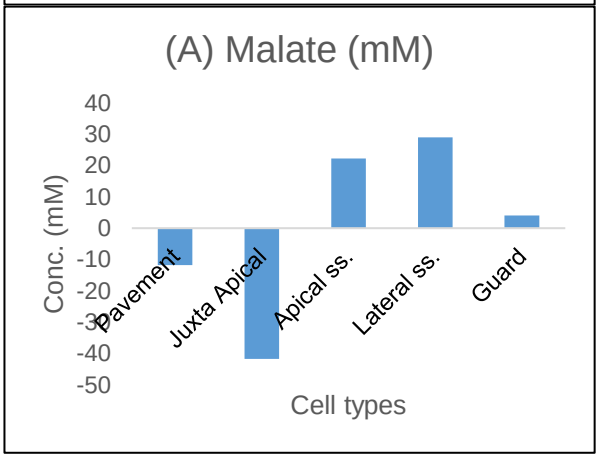
(A) Malate (mM)
Conc. (mM)
40
30
20
10
0
-10
-20
-30
-40
-50
Pavement
Juxta Apical
Apical ss.
Lateral ss.
Guard
Cell types

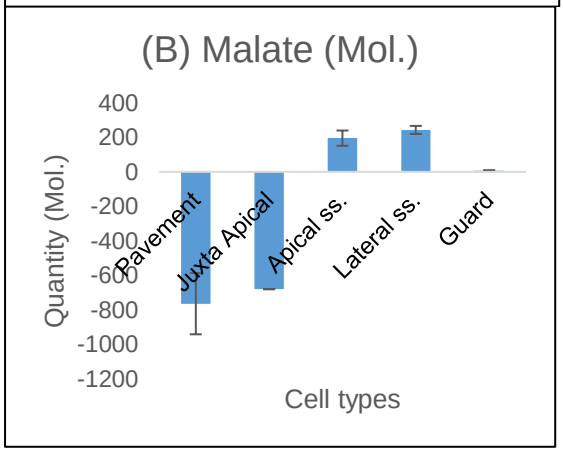
(B) Malate (Mol.)
Quantity (Mol.)
400
200
0
-200
-400
-600
-800
-1000
-1200
Pavement
Juxta Apical
Apical ss.
Lateral ss.
Guard
Cell types

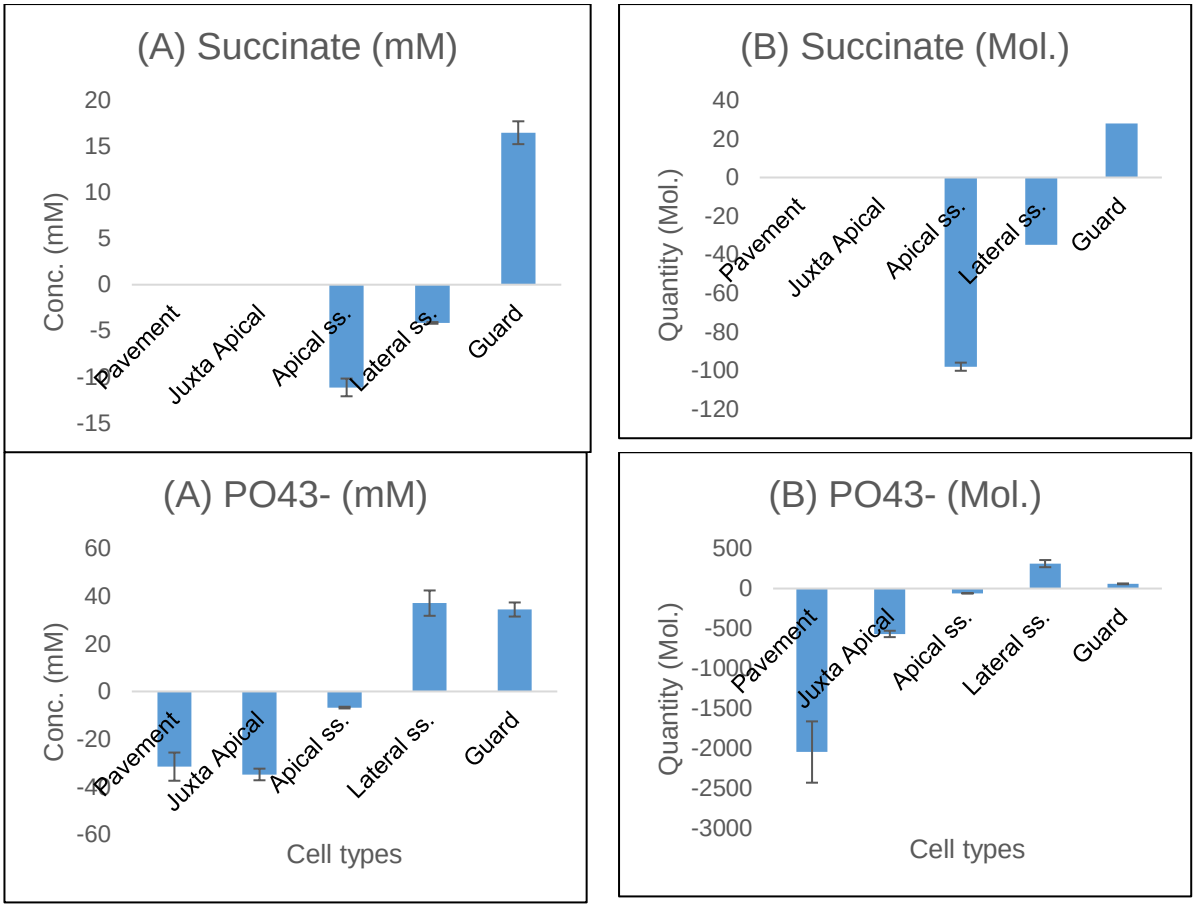

Figure 4.7 Solute concentration and quantity changes in abaxial epidermal cells of *T. virginiana* during stomatal movements.
The solute concentration changes occurring in epidermal trough cell types of *T. virginiana* during stomatal opening. (A) Indicates these changes without any consideration of the relative volumes of the cell types i.e. expressed as concentration. (B) Indicates the same changes corrected for relative differences in the volume of cell types i.e. expressed as total content of each electrolyte in each compartment. The negative figures stand for solute accumulation while the positive figures represent solute released from the cells. Both sets of curves appear qualitatively similar. Potassium, Cl^- and Mg^{2+} sustain an upwards gradient from pavement to guard cells. Tartrate and succinate also sustain such gradient but starting from apical subsidiary cells. Malate, PO_4^{3-} and NO_3^- sustain similar uphill gradients that start from pavement cells but terminate at lateral subsidiary cells. Citrated and SO_4^{2-} show no gradients.

4.3.6.1 Solutes moving up positive gradients into the guard cells

Potassium transport across guard cell plasmalemma and tonoplast, has been well established in the literature (Raschke and Humble, 1973; Levitt, 1974; Zeiger, 1983; Xue *et al*., 2011). Results in this study align with previous studies on stomatal movement that show that K^+ as the major ion involved in stomatal movements (Macallum, 1905; Sayre, 1926; Fujino, 1959; Fischer, 1968a; Fischer and Hsiao,

1968; Sawhney and Zelitch, 1969; Humble and Hsiao, 1969; Humble and Raschke, 1971; Penny and Bowling, 1974; Levitt, 1974; Edwards and Bowling, 1984; Hedrich *et al*., 1995; Szyroki *et al*., 2001; Kwak *et al*., 2001; Sottocornola *et al*., 2006). As guard cells have no plasmodesmatal connections with surrounding cells (see section 1.13), the immediate source of this K^+ must be the guard cell apoplast. Studies of transmembrane K^+ transport in *T. virginiana* (Edwards, 1984) and *Commelina* (Penny, 1974) showed that the K^+ accumulated by guard cells during stomatal movements originate from the apoplast. That guard cell K^+ increase has its origin solely in the apoplast cannot be sustained from the results of this study, since apoplastic K^+ concentration was not measured. If the extended apoplast (not just the immediate guard-cell wall) is considered, a higher apoplastic K^+ content may not alter apoplastic π by very much. Within it the apoplast is a continuum and water and solute diffusion and flow is unhindered. However, it is not forgotten that the apoplastic volume round a cell is small in comparison with the cell protoplast.

The observed decrease in the K^+ concentration in pavement (see also Edwards, 1984) as well as juxta apical and apical cells found in this study raises the question of where such K^+ goes. The results in this study suggest that such K^+ ends up in the lateral subsidiary cell (fig. 4.7). Potassium movement from these cells into the lateral subsidiary cell may be both symplastic and through transpiration-aided bulk flow in the apoplast (figure 6.1). However, it is possible that the purpose of the lateral subsidiary cells virtually isolating the guard cells (topographically) is that they can be in a position to control the solutes available to the guard cell apoplast. Considering the ratio of the volumes of pavement and lateral subsidiary cells (approximately 8:1), some of the moving K^+ from the lateral subsidiary cell may be fed to lateral subsidiary cell apoplast. Since the lateral subsidiary and guard cell apoplast are together, diffusion to guard cell apoplast would be fast (Fick's law). Solutes released from the lateral subsidiary cell enter the guard cell apoplast (shared with lateral subsidiary cell) and can become immediately available to the guard cell. It is reasonable to assume that the reverse is also true (see figure 6.1). Since the guard cell is at the lowest end of the water potential gradient of the epidermis, it is also likely that bulk flow in the apoplast may contribute substantially to the solute requirements of the guard cell during stomatal opening. This exulted position of the guard cells in epidermal water potential gradient may not, however, explain the re-accumulation of the K^+ into the apical, juxta apical and pavement cells when stomata

close, despite the removal of transpiration water loss at this time. Thus, although solutes may enter the apoplast from any and all of the cells, symplastic supply controlled by the lateral subsidiary cells appears the most likely mode of transfer. This may also imply that solute movement into the apoplast of other cells is possible in cases where volume ratio of the originating and destination cells are significantly different.

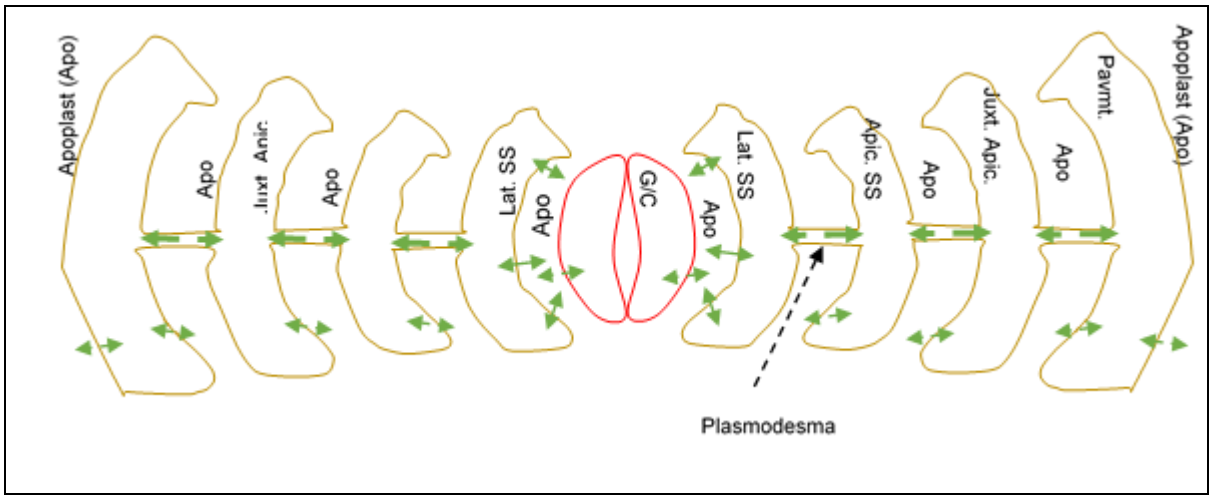

Figure 4.8 Possible solute distribution/redistribution paths in *T. virginiana* epidermal trough cells.
This figure shows the possible routes that solutes take to and from the stomata or other cells during stomatal movements in trough cells of *T. virginiana* epidermis. Except for the guard cells, solutes may move symplastically between all the other cells through plasmodesmata. The lateral subsidiary cells maintain no plasmodesmatal connection with the guard cells and so may transport solutes only into the guard cell apoplast. The apoplast of all other cells may also receive solute exports or leaks from all the other cells. Longer range apoplastic flow is omitted from this diagram in the interests of clarity.

Similarly, Cl^- originating from the pavement cells enters the guard cells. In contrast to K^+, however, during stomatal opening, Cl^- moves against an existing positive (concentration) gradient maintained in the epidermal tissue. Movement against positive gradient needs some form of active transport. This implies energy costs. To limit such expenditure, it is likely that the apoplastic route may play the major role in Cl^- transport to the guard cells during stomatal opening. This appears reasonable since no significant changes in concentration were found in any of the cells between the pavement and the guard cells (figure 4.7, see also figure 6.1). Return (of Cl^-) during stomatal closing may be symplastically through the cells down its concentration gradient to the pavement cells.

Nonetheless, since Cl^- is charged, the electrochemical, rather than the concentration gradient, is the determinant of the direction of movement. The electrochemical gradient may, sometimes, be in the opposite direction to the concentration gradient. If the potential difference across the membrane (or other path) is known, the force (electromotive force) driving the flow of Cl^- could be determined from Nernst's equation (see section 1.15.2). In this way the gradient could be determined. Essentially, Cl^- increases in guard cell during stomatal opening, coming from pavement cells by intercellular route down its electrochemical gradient or active transport, or by apoplastic transfer by bulk flow.

Tartrate and succinate, on the other hand, were below detection limit or absent in pavement and juxta apical cells, but present, albeit in relatively low concentration (see also Outlaw and Lowry, 1977), in stomatal complex cells. They are considered low in concentration relative to Cl^- because, despite being divalent, each had an activity that was less than 14% (tartrate, 10%; succinate, 13%) of Cl^- activity even at their highest concentrations. Unlike Cl^-, both of them maintain negative concentration gradients between the guard cells and the apical subsidiary cells under closed stomata situations. On stomatal opening, a reversal of this gradient occurred, being positive from the apical subsidiary toward the guard cell. Curiously, though the volume of the apical subsidiary cell is approximately 5 times that of the guard cell (table 3.1), the change in concentrations of both solutes was similar in both cells (apical tartrate, Δ11.1 mM; guard cell tartrate, Δ10.7 mM; apical succinate, Δ11.2 mM; guard cell succinate, Δ16.5 mM). For succinate, the lateral subsidiary cell even contributed to the pool during stomatal opening. Here a word of caution is needed. The data in this report is at low time-scale resolution. In the case of the minor organic acids, these interpretations are likely only if these samples were taken at the steady state, when there is a net export of these solutes from the guard cell such that, when the stomata closed, tartrate and succinate in the apical subsidiary cell sustained such high concentrations. It is likely that the solutes were redistributed in the apoplast of the stomatal complex during opening and then reabsorbed during closing. Equally, the small volume of the guard cell would expand about five times if the observed dilution of tartrate or succinate had been due to guard cell volume expansion alone. It appears then that tartrate and succinate are formed in the guard cell during photoactive stomatal opening, and may be used to power membrane transport processes while the unused/excess is stored away in the

apical subsidiary cells when stomata closes. Similarly, citrate appears to be generated through the same process, but is taken up into apical subsidiary cells. This is because its concentration does not change in any other cell type when stomata open. The citrate gained in the apical subsidiary cells when stomata open may be used for generating the ATP required for fulfilling its function as a transit route for most solutes stored in the juxta apical cell.

4.3.6.2 Solutes moving into the lateral subsidiary cells from other cells

Results in this study indicate that guard cell malate concentration is similar in open and closed stomata situations. Similarly, pavement cell malate does not change as stomata open. Malate increased only in the lateral subsidiary cells when stomata opened. The origin of this malate appears to be the juxta apical cells. As concentrations in the apical subsidiary cells do not also change, it is possible that malate is only transmitted symplastically from the juxta apical cells, through the apical, to the lateral subsidiary cells. The high buffering capacity of malate (Søndergaard *et al*., 2014) (pKa of 3.4 and 5.05) may be important in this cell due to the abundance of divalent cations in the cell. Together with PO_4^{3-}, these two ions may buffer over a wide range of pH (pH 2 to 13).

Nitrate behaves similarly to malate, but originates from the pavement cells. It is, however, not a physiological buffer. The importance of NO_3^- accumulation in lateral subsidiary cell during stomatal opening is not clear, but may be concerned with the high solubility of the NO_3^- salts of Ca^{2+} and Mg^{2+} (> 1200g/L). This may be needed by this cell since it has the highest divalent cation concentration among all epidermal trough cell types (table 4.10).

Phosphate (pKa of 2.15, 6.82 and 12.38) which maintained a negative gradient from pavement to lateral subsidiary cells in closed stomata situations showed reversal of this gradient in open stomata state. The source of this PO_4^{3-} was the pavement cells. It is likely that the abundance of PO_4^{3-} in the epidermis, for example in cereals (Dietz *et al.*, 1992) is connected to its buffering capacity. One pointer to this in this study is that PO_4^{3-} appeared to move from the pavement to the lateral subsidiary cells through plasmodesmata connections (see figure 6.1). Pavement and juxta apical cells showed decrease in concentration, more in the latter. No change in concentration was noticed in apical, but a marked (398%)

increase was seen in the lateral subsidiary (appendix 7 and 8). Thus, the two solutes, malate and PO_4^{3-}, had their destination as the lateral subsidiary cells, but their origin was varied; malate from juxta apical cells and PO_4^{3-} from pavement cells.

4.3.6.3 Other solutes redistributed to different cells to balance charges

Sulphate originated from two cell types, mainly, juxta apical, and also lateral subsidiary cells and was redistributed to mainly pavement, but also to apical and guard cells. Increase in guard cell SO_4^{2-} is unexpected, but may be important for charge balancing as its degree of ionization is little changed by the pH changes found in these cells during stomatal movement.

The increase in guard cell Mg^{2+} concentration observed in this study was unexpected. No divalent ion, except $Ca^{2+,}$ usually acts as a signalling molecule (Sanders *et al*., 1999, 2002). However, Mg^{2+} has been previously implicated in osmotic events that produce the turgor controlled stomatal opening (Thomas, 1970).

In all, it appears that most solutes used in stomatal movements are supplied by the pavement and juxta apical cells, but their availability to the guard cell is regulated by the lateral subsidiary cell. Such solutes as K^+, Cl^-, NO_3^- and PO_4^{3-} are supplied from the pavement cell while Ca^{2+}, Mg^{2+} malate and SO_4^{2-} come from juxta apical cell during stomatal opening. The apical subsidiary cell is the source for only tartrate and succinate, but also contributes to the supply of NO^{3-}, PO_4^{3-} and $K^{+\cdot}$(fig. 4.7).

4.3.7 Heterogeneity in the epidermis

Results in this study showed differences in solute content and concentration between cell-types within epidermal troughs (tables 4.11 and 4.12). Such differences have not been reported previously in *T. virginiana*. Significantly difference (at least, $p < 0.01$) existed between concentrations of citrate and PO_4^{3-}. Similarly, contents of some cell types, guard cells as well as apical and lateral subsidiary cells, differed from that of the other cells, pavement and juxta apical cells, in containing tartrate and succinate. These solutes have also not been reported previously in *Tradescantia*. However, succinate has been reported in subsidiary cells but not in pavement cells

of *Vicia faba* implying heterogeneity in the content of epidermal cells of the plant (Outlaw and Lowry, 1977; Talbott and Zeiger, 1996).

Since the ridge cells were all uniform and form boundaries between individual troughs (see plate 3.1) it is likely that they may only function as solute-supply route to the troughs. Sampling them may not give any useful information relating to stomatal movements. Perhaps for this reason, in stomatal studies, no clear record, of solute distribution in cell types overlying the vascular bundles (the ridges) is available to date (see Bowling (2016)). Nevertheless, it would have been interesting to assay the contents of these cells had time permitted.

Table 4.11. Solute concentration differences between pavement cells and lateral subsidiary cells in epidermal trough of *Tradescantia* abaxial leaf epidermis under closed stomata condition

Cell type	Citrate (mM)	PO_4^{3-} (mM)
Pavement	3.3 ± 0.5	56.5 ± 5.3
Lateral subsidiary	73.5 ± 7.3	9.3 ± 1.0
P value (at 95%)	< 0.001	< 0.001

Table 4.12 Solute concentration differences between apical and lateral subsidiary cells in epidermal trough of *Tradescantia* abaxial leaf epidermis under closed stomata condition

Cell type	Tartrate (mM)	Succinate (mM)
Lateral subsidiary	0.5 ± 0.1	18.0 ± 1.7
Apical subsidiary	12.9 ± 1.2	12.2 ± 1.1
P value (at 95%)	< 0.001	< 0.01

Chapter 5 Studies on osmotic pressure

5.1 Introduction

This chapter describes experiments carried out to determine qualitatively and quantitatively, at the level of individual cell types, the role of their osmotic pressure, π, in stomatal movement in *T. virginiana*. As in the rest of the programme, this included not only the guard cells themselves but also the other cell types in the epidermis.

Guard cell movement is a function of the osmotic pressure (π) differential rather than that of individual solute concentrations. Osmotic pressure can be calculated from the sum of the individual solutes (if they are all known – see chapter 4). However, it is possible to measure single cell π directly. This direct π measurement is described in this chapter. In addition to measuring this key parameter directly, this chapter also provides an indication of the sum total of solute concentrations – and thus a check on whether all the solutes involved in generating the π have been accounted for. Since only charged solutes were assayed in this work (see chapter 4) this check would reveal any contribution of uncharged solutes (such as sucrose) to π changes leading to stomatal movements.

Stomatal movements are brought about by changes in guard cell intracellular turgor (MacRrobbie and Lettau 1980a; MacRrobbie 2006; Meidner and Mansfield 1968; Fischer 1973; Heath, 1938) caused by π changes (MacRrobbie and Lettau, 1980a; MacRrobbie, 2006) and (von Mohl, 1856; quoted in Kollist *et al*. (2014)). It was initially thought to be due to starch to simple sugar interconversion but later (in early 1980s) found to be due to K^+, Cl^- and/or malate concentration changes (Zeiger, 1983). De Candolle (1827) was the first to suggest that stomata open and close due to osmotically induced changes in guard cell pressure (Ferrer *et al*., 2008; Beerling and Franks, 2009). Cell osmotic pressure depends on the concentrations of osmotica in the cell (Fischer, 1968a; MacRrobbie and Lettau, 1980). In the main, the electrolyte, potassium chloride, has been implicated (Humble and Raschke, 1971) as the dominant osmoticum. However, non-electrolytes such as glucose or sucrose (soluble sugars) have also been identified (MacRrobbie 1980; Ritte *et al*. 1999; Outlaw and

Manchester 1979). Aside from K^+ and Cl^- ions, other inorganic anions such as NO_3^- (Schmidt and Schroeder, 1994), SO_4^{2-}, PO_4^{3-} (Leigh, 1997; Conn and Gilliham, 2010) and cations such as Ca^{2+} (Schwartz, 1985; Irving *et al*., 1992), Mg^{2+} and Na^+ (Leigh, 1997; Conn and Gilliham, 2010) also form part of the guard cell osmotica. A number of organic anions, such as citrate and malate (Outlaw and Lowry, 1977) are also known contributors to the π in guard cells.

The measured π shows the sum of the partial pressure of the individual contributing solutes (section 1.15.2). The concentrations of individual electrolytes in sap obtained from whole leaf, epidermal strip and individual cell types were separately measured using the CZE method. This CZE-measured concentrations were used to calculate the π expected in individual cells with such solute concentration. These were compared with the directly measured osmotic pressure to deduce the contribution of uncharged solutes. The implications of the results are discussed.

5.1.1 **Mechanical advantage**

Stomatal aperture changes (inversely) with guard cell size. The size of an intact guard cell depends on the net pressure difference between the guard cell and the surrounding epidermis (Heath 1938). Kidney-shaped guard cells possess a thick ventral wall and a thin dorsal wall (Meidner and Mansfield, 1968). It has been reported that the dorsal wall of guard cells hinge to the ventral wall of the adjoining cell (subsidiary or pavement cell) and the ventral wall of such cells (abutting the dorsal wall of a guard cell) is thin (Schwendener (1881) quoted in (Willmer and Fricker, 1996)). This allows the guard cell to bulge into the adjoining cell during expansion (Martin *et al*., 1983).

In the elliptical (kidney-shaped) guard cells the cell wall cellulose microfibrils are arranged radially from the thick ventral to the thin dorsal wall (Mishkind and Palevitz 1981; Aylor *et al*., 1973). Expansion is, thus, directed towards the poles as well as into the adjoining subsidiary or pavement cell (Martin *et al*. 1983; Heath 1938). Very little expansion occurs in the thickened ventral wall. The unequal expansion of the ventral and dorsal walls results in the formation of a curvature at the ventral side observed as stomatal opening (Meidner and Mansfield, 1968).

Cooke and Baerdemaeker (1976) disagreed with this, though, but rather argued that the high turgor pressure in guard cell and the lower pressure in subsidiary cells are important for the functions of the feedback control loops which regulate guard cell responses.

In any case, cell expansion is due to forces acting on the cell wall. These forces are a function of the product of pressure and area. The area of the subsidiary or pavement cells abutting the guard cell is significantly larger than that of the guard cell. Thus, increase in pressure in these adjoining cells exerts more force against the guard cell such that for a unit increase in turgor pressure in both cells (guard cell and the adjoining subsidiary or pavement cell) net force is against the dorsal wall of the guard cell (Meidner and Mansfield, 1968; DeMichele and Sharpe, 1973). This difference in force/pressure is known as the mechanical advantage, and defines the ratio of the change in guard cell turgor pressure for every unit change in pavement or subsidiary cell pressure. The adjoining (pavement or subsidiary) cell therefore, are said to have a mechanical advantage over the guard cells (DeMichele and Sharpe, 1973). The ratio of the difference in the force between the guard cell and the subsidiary or pavement cells is known as the antagonism ratio (Cooke and Baerdemaeker, 1976). In *Commelina communis*, the antagonism ratio is 3.7 for equal changes in the water potential of both cells (MacRrobbie, 1980).

5.1.2 Analytical techniques for studying plant water and solute relations

5.1.2.1 Bulk methods

The osmotically-active solute content of cells has been studied at both cellular and subcellular resolutions using X-ray microprobe and energy dispersive X-ray analysis on thin sections or bwulk-frozen tissue (Raschke and Schnabl 1978; Leigh *et al.* 1986), ion-selective microelectrodes (MacRrobbie and Lettau, 1980; Miedema and Assmann, 1998), radioactive tracers (Outlaw, 1983) as well as enzyme cycling techniques (Outlaw Jr, 1987). These approaches have however, measured relative rather than absolute concentrations of elements involved (Malone *et al*., 1991). More importantly, these methods are applicable only to leaf developmental stages that permit isolation of tissue and can neither determine the *in-situ* concentrations of solutes (Fricke *et al*.,

1994a), the osmolality of cells (and thus, total π) nor distinguish between sub-populations of cells (Fricke *et al*., 1994b). Therefore, it becomes difficult to assess the relative importance of any solute to the overall cellular turgor.

Tomos *et al*, (1994) compared bulk extract with epidermal cell extracts of barley leaf and corroborated earlier findings that bulk extracts exhibited significantly lower concentrations of NO_3^-, Cl^- and Ca^{2+}, similar concentrations of K^+ and Na^+, but higher concentrations of phosphorus (Fricke *et al*., 1994b). Thus, bulk sampling results do not represent the physiological events at individual cells resolution.

Another technique, beyond the scope of this thesis is the pressure bomb technique. It is good for generating only estimates of osmotic and hydrostatic pressure. It usually works only over a large pressure interval (Cheung *et al*., 1975). Using the bomb technique for instance, it is impossible to determine the exact plasmolytic volume and the elastic modulus of cells (Tomos and Leigh, 1999).

Though some may be fast methods of identifying locations of desired solute content in cells (Williams *et al*., 1993), they are mostly slow and more invasive methods because they require excision of the required plant part. Thus their results do not present the quantitative picture of the physiological relationships between measured solutes. Ion-sensitive microelectrodes measure free ionized forms of solutes and thus do not give reproducible glimpse of the total solute content.

5.1.2.2 Pressure probe

The pressure probe technique is more accurate and possesses more internal control measures than the bomb technique. The possibility of generating false readings is excluded by several experimental controls. Cavitation and leaks, during insertion of microcapillary or during measurements are easily recognized (Miedema and Assmann 1998). Pressure probe technique offers an accuracy of up to 0.003 MPa for pressure and 10^{-5} µl for volume measurements (Malone et al. 1991).

This method has been modified for use in single cell sampling and analysis (SiCSA) technique (section 1.17.3.3). Sap is extracted and subsequently analysed using a battery of analytical methods including picolitre osmometer (section 2.11).

5.1.3 Study aims

This chapter was aimed at determining possible π gradients developed in the epidermis when stomata open, and also assess the level of the contribution of charged solutes to these π. The specific objectives were to

- Determine and compare the π in both whole leaf and epidermal strip.
- Directly determine the π in each of the cell types of *T. virginiana* epidermal trough at closed and at open stomata conditions.
- Compare these π in contiguous cells of the epidermal troughs to deduce possible π gradients in trough cells of the epidermis associated with stomatal movements and
- Compare the directly measured π (above) with that calculated from an independently measured solute concentrations to assess the possible contribution of non-ionisable solutes (not assayed in this project) to cellular osmotics during stomatal movements.

5.2 Results

5.2.1 Comparison of whole leaf and epidermal strip osmotic pressure

In order to determine the π range in *T. virginiana* epidermis, epidermal strip and whole leaf π were measured, and compared to gain insight into possible π differences at tissue level in leaves. The π of the sap from whole leaf and abaxial epidermal were determined, using the freezing-point depression picolitre osmometer (Malone *et al*., 1989; Irving, 1996). Three plants for whole leaf and four for epidermal strip were sampled in triplicates. Stomata were open at the time of obtaining the whole leaf and strip tissues for sample extraction (see chapter 2). The whole leaf and epidermal strip π (1.19 and 1.14 MPa respectively), showed no significant difference ($p > 0.05$) (Table 5.1).

Table 5.1 Osmotic pressure of sap from whole leaf (W.L) and abaxial epidermal strip of leaf 5 of *T. virginiana* under open stomata condition.

Mean	Whole leaf	Epidermal strip
Osmotic pressure (MPa)	1.19 ± 0.05	1.14 ± 0.05
n	9	12

The π and the sum of solute concentrations determined from the equivalent sap subsample were compared (table 5.2). The solute concentration in whole leaf and strip, each summed approximately to 630 $mEq.L^{-1}$ (634.5 for whole leaf and 629.5 $mEq.L^{-1}$ for the epidermal strip). The measured whole leaf and strip osmolality were 486.3 and 466.2 $mOsmol.kg^{-1}$ respectively. The osmotic coefficients of the two treatments were similar at 0.77 $mOsmol.kg^{-1}.\ mM^{-1}$ for whole leaf and 0.74 $mOsmol.kg^{-1}.\ mM^{-1}$ for strip.

Table 5.2 Osmotic coefficient of whole leaf and epidermal strip sap determined from sum of solute concentration and π of the equivalent sap samples.

	Whole leaf	Epidermal strip
Solute conc. ($mEq.L^{-1}$)	634.5 ± 51.4	629.5 ± 40.2
Osmolality ($mOsmol.kg^{-1}$)	486.3 ± 18.7	466.2 ± 20.0
Osmotic Pressure (MPa)	1.19	1.14
Osmotic Coefficient ($mOsmole.kg^{-1}.\ mM^{-1}$)	0.56 ± 0.03	0.53 ± 0.02

5.2.2 Contribution of uncharged solutes

The preceding chapter (chapter 4) has dealt with charged solutes (cations and anions) present in cells of the epidermis during stomatal movements. Uncharged solutes within these cells may also contribute significantly to turgor pressure changes necessary for stomatal movements. Turgor in a cell is dependent on the π. In the absence of uncharged solutes the sum of all the charged solutes (anions and cations) should add up to any measured π to the extent accounted for by the electrolytes.

In order to assess the contribution of any uncharged solutes that may be present in the sampled cells, the π of sap from all five identified cell types were measured directly and compared with the osmolality calculated from CZE-determined solute concentrations of subsamples of the same sap (see section 2.11). Samples from whole leaf and strip were also measured similarly.

Due to the small volume of sap in some cell types, for both open and closed conditions, pooled sap was used for the analysis. Depending on cell volume, different number of cells were pooled for each cell type (three for juxta apical, eight for lateral as well as apical subsidiary and 24 for guard cells). This allowed three replicate analysis to be made from each pooled sap. Pavement cell sap was not pooled as single cells provided enough sample volume for replicate analysis. From the solute content analysis, the mean cation and anion concentrations in each cell type was summed up to give the total solute concentration.

Under both closed and open stomata conditions the measured π was statistically equivalent ($p > 0.05$) to the calculated osmolality and both were well correlated with the sums of their solute concentrations (fig. 5.1). Concentrations in the pavement cells (756.3 mM) equalled that in the guard cells (756.8 mM) though their π values were significantly different ($p < 0.05$). Despite these differences, the π was well correlated with solute concentration ($R^2 = 0.65$) (figure 5.1). The osmotic coefficients also appeared remarkably similar (between 0.86 and 0.94 $mOsmol.kg^{-1}$ mM^{-1}) except in the lateral subsidiary cells (0.76 $mOsmol.kg^{-1}$ mM^{-1}) (appendix 13). The osmotic coefficients under open stomata were essentially similar to that in closed stomata state. Coefficients of between 0.9 and 0.93 $mOsmol.kg^{-1}$ mM^{-1} were found in all the cells except the two subsidiary cell types, apical and lateral, with coefficients of 0.68 and 0.69 $mOsmol.kg^{-1}$ mEq^{-1} respectively.

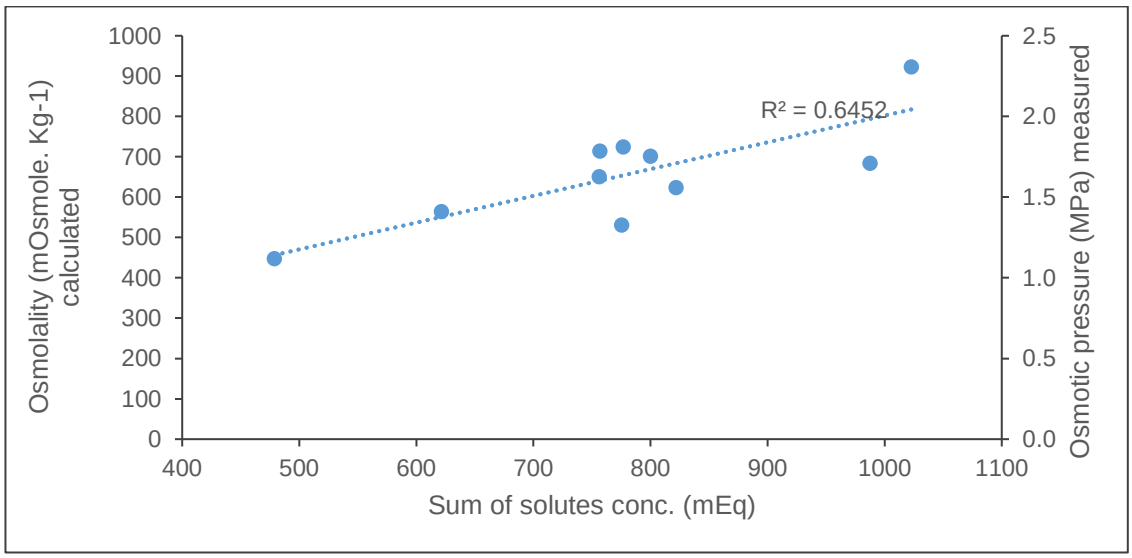

Figure 5.1 Osmotic pressure/osmolality with (concentration of) total ionisable solute in cells of *T. virginiana* epidermis under open and closed stomata conditions
A linear regression is fitted to the data with $R^2 = 0.65$.

Under open stomata condition, guard cells had both the highest sum of solute concentrations (1022.7 mM) and π (2.26 MPa). These parameters were approximately twice the level in the juxta apical cells (478.6 mEq.L^{-1} sum of concentration and π of 1.10 MPa). Within the stomatal complex, the apical subsidiary cell had the lowest sum of solute concentration (775.3 mEq.L^{-1}) and the lowest π (1.30 MPa).

In the pavement cells, both the solute concentration sum and the π decreased significantly ($p < 0.01$); from 650 mM and osmolality of 1.59 MPa at closed to 560 mM and osmolality of 1.38 MPa respectively at open stomata.

These results indicated that both the π and solute concentrations showed clear predictable patterns at both open and closed stomata conditions. The solute concentration sum correlated well with the measured π after considering a realistic osmotic coefficient (Robinson and Stokes, 2002). The π was found to increase from the pavement cells through the juxta apical, apical and lateral subsidiary to the guard cells when stomata opened, and decreased in the reverse order when stomata closed. The sum of the solutes (cations and anions) in the cells types showed similar trend. The osmotic coefficient, however, was less than unity (0.7 – 0.9). This was not expected.

5.2.3 Osmotic pressure in individual cell types

The osmotic pressure (π) in the pavement, juxta apical and the apical subsidiary cells were higher ($p < 0.05$, $p < 0.001$, $p < 0.001$ respectively) under closed than in open stomata conditions (Δ 0.21, Δ 0.62 and Δ 0.48 MPa respectively) (fig. 5.2). In the lateral subsidiary and guard cells, π was higher ($p < 0.05$, $p < 0.001$ respectively) under open than in closed stomata conditions (Δ 0.15, and Δ 0.51 MPa respectively).

Under closed conditions, the juxta apical, the apical subsidiary and the guard cells had similar ($p > 0.6$) π (1.75, 1.78 and 1.72 MPa respectively). The remaining two cell types, the pavement and lateral subsidiary cells, also had similar ($p > 0.2$) π (1.59 and 1.53 MPa respectively).

Comparison of π at open and closed stomata (Figure 5.2) showed that significant π changes occured in each of the cell types. Significant increases in guard cell (Δ 0.5

MPa; $p < 0.01$) and the lateral subsidiary cell (Δ 0.2 MPa; $p < 0.05$) occured during the stomatal opening. On the other hand significant decreases occured in pavement cells (Δ -0.2 MPa; $p < 0.05$), juxta apical cells (Δ -0.6 MPa; $p < 0.001$) and apical subsidiary cells (Δ -0.5 MPa; $p < 0.01$) at the same time. In summary, there appeared to be an increasing π gradient pavement, through the juxta apical, apical and lateral subsidiary cells to the guard cells as the stomata opened and a decrease from the guard cells, in reverse order, through to the pavement cells (see plate 5.1) as the stomata closed.

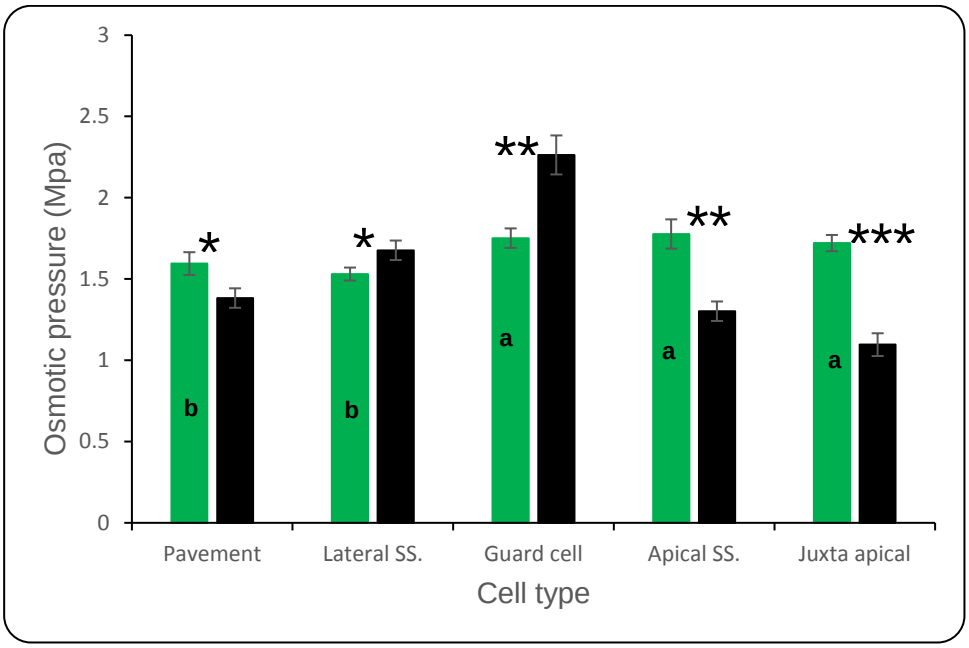

Figure 5.2 Osmotic pressure of cell types in the abaxial epidermis of *T. virginiana* at closed (●) and open (■) stomata states
This figure shows the measured π in cell types of *T. virginiana* abaxial epidermal trough under open and closed stomatal conditions. Π differences between cell types were minimal when stomata were closed, but marked differences appeared on stomatal opening (see text). Guard cell π was remarkably higher than that of others in open stomata situation. Only the guard cell and the lateral subsidiary cell had increase in π, while the other cells had a decrease in pressure on stomatal opening. Error bars represent standard deviations (n = 9). Guard cell samples were pooled into three lots, and three subsamples from each was measured. The average is presented here. One, two or three asterisks (*) represent(s) *p* values < 0.05, 0.01 or 0.001 respectively at 95 % confidence interval, and the letters a, b or c represents significant similarities between π of cell types. Absence of these letters stand for significant difference. The test statistics (*p* values) represent the probability at 95% confidence interval in an unpaired two tailed student's t-test assuming equal variance.

The spatial relationship between the different cell types is as shown in plate 5.1 (also see chapter 6). The lateral subsidiary and the apical subsidiary cells are in contact with the guard cell. However, lateral subsidiary cell covers almost all the ventral

aspect of the guard cell leaving a small portion in contact with the apical subsidiary cells. Between two apical subsidiary cells a juxta apical cells is sandwiched, but maintains extensive contact with pavement cells laterally.

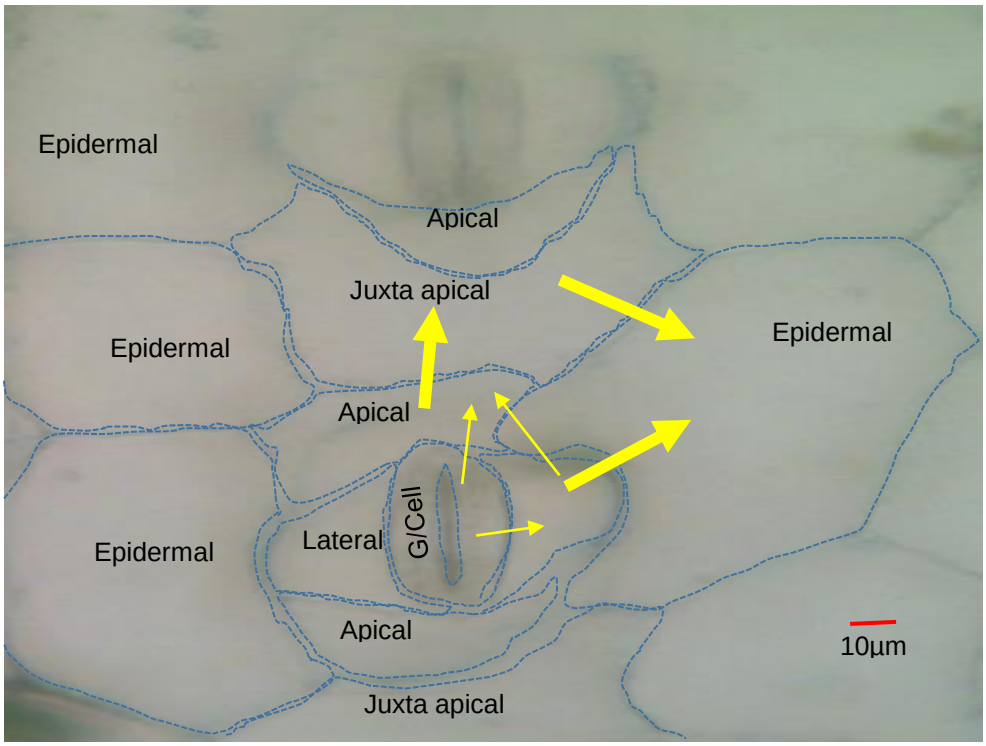

Plate 5.1 *T. virginiana* epidermis showing the five cell types (pavement, juxta apical, apical-, lateral-subsidiary and guard cell (G/Cell)).
Weighted arrows imply the observed differences and direction of changes in osmolality as stomata close (shown in figure 5.2).

Significant π differences also occured between contiguous cells during stomatal opening creating an uphill π gradient towards the guard cells (figure 5.3). In closed stomata no significant difference ($p > 0.07$) existed between the π in pavement, juxta apical and apical subsidiary cells. The π difference between pavement and juxta apical cells was 0.13 MPa ($p > 0.07$). The difference between juxta apical and apical was 0.06 MPa ($p > 0.3$). No significant difference also existed between the π in the guard cells and the juxta apical ($p > 0.3$) or apical subsidiary ($p > 0.6$) cells when stomata are closed. Under the same closed stomata situation, the lateral subsidiary cells, in contrast, had a significantly lower ($p < 0.05$) π than the cells contiguous with it. When stomata opened, π in juxta apical cells became 0.28 MPa lower ($p < 0.01$) than that in the pavement cells. At the same time the pressure in the apical cells became 0.2 MPa higher ($p < 0.05$) than that in the juxta apical cells, and pressure in

the lateral subsidiary cells were 0.38 MPa higher than those in the apical subsidiary cells. Guard cell π rose by 0.58 MPa above ($p < 0.01$) that of the lateral subsidiary cells at the same time. Under this situation of open stomata the guard cell as well as the lateral subsidiary cell π were significantly (at least $p < 0.001$ and $p < 0.01$ respectively) higher than that of any of the other epidermal cell types. Thus, under closed stomata condition, the π in the pavement, juxta apical and apical subsidiary cells were similar. Osmotic pressure in lateral subsidiary cells was lower than that in apical subsidiary cells. But the π in the guard cells was higher than that in the lateral subsidiary cells. In open stomata situation, the π in all the cell types changed. Juxta apical cell π became lower than that in the pavement cells, and an uphill gradient of π towards the guard cells developed in contiguous cells.

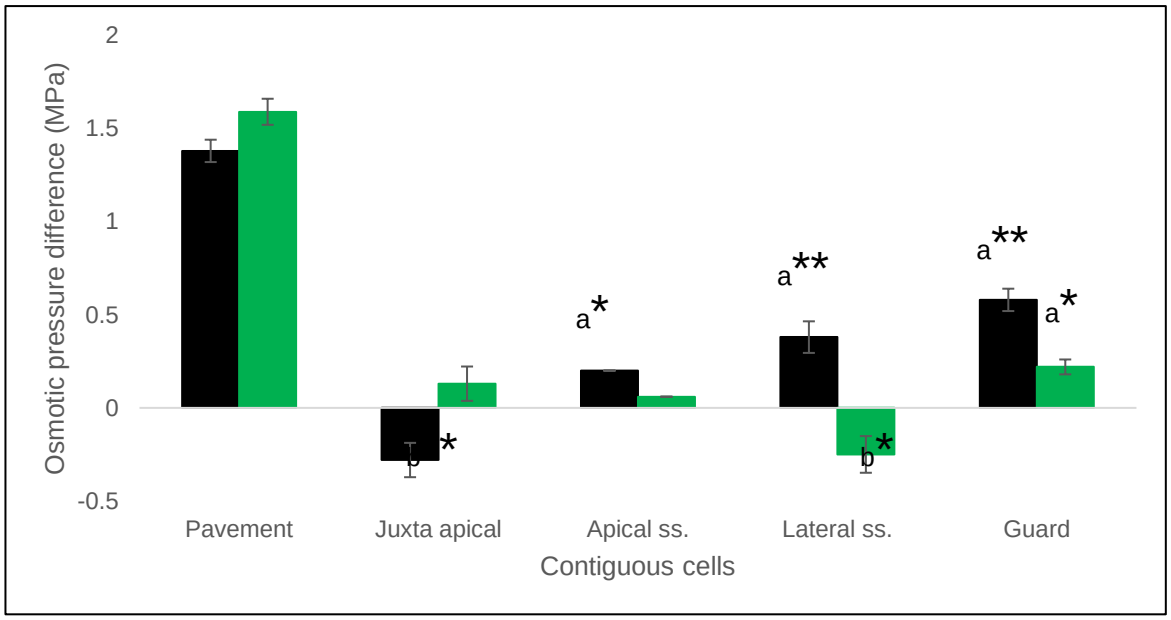

Figure 5.3 Osmotic pressure differences between contiguous epidermal cells (gradient) of *T. virginiana* under open (■) and closed (●) stomata situations.

The differences in π between contiguous cells starting with the pavement cells (as reference) when stomata were closed and when open. Osmotic pressure decreased across contiguous cell from the pavement to the lateral subsidiary, but the guard cell maintained higher π than in neighbouring lateral subsidiary cell under closed stomata condition. When stomata were open, increasing π gradient occurred through contiguous cells of epidermal troughs from the juxta-apicals and ending in the guard cells. Asterisk(s) (*) is used here as with figure 5.2 above but stand for statistical differences between contiguous cells. The letters 'a' and 'b' represent increase (a) and decrease (b) in π between contiguous cells. Error bars represent standard deviations.

For each cell type n = 9.

5.2.4 Osmotic pressure of artificial sap

In order to interpret the results from tissue and cell extracts which might contain unidentified components that influence π, a series of trials were performed in which the π of 'artificial sap' were measured. The artificial saps were made as mimics of the strip or whole leaf extracts by using as recipes the apparent composition as determined by CZE. They did not indicate any neutral compounds and minor electrolytes, including proteins, that might have disproportionate influence on the solute relations.

Osmotic pressure is generated by and depends on the concentration of the osmotica (MacRrobbie and Lettau, 1980a). The π of freshly prepared solutions of solute concentrations determined with the CZE in whole leaf and abaxial epidermal strips (artificial sap), was measured. The clear solutions (without precipitates) were prepared according to the mean CZE-determined solute concentrations in leaf five whole leaf (see tables 3.9) and abaxial epidermal strips (see tables 3.10). Clear solutions were necessary as precipitates would lead to falsely lower osmolality (and thus π) for the solution. The compounds used for the preparation, their concentration and the order of mixing (to avoid precipitation) are shown in table 5.3 (i) and (ii). These orders of mixing were determined by experiment. Three samples of each sap recipe were prepared and measured.

Table 5.3 Preparation of artificial sap: solute weight and mixing order used in preparing (i) Whole leaf artificial sap and (ii) Strip artificial sap.
The mixing order was the order in which compounds were added and mixed to fully dissolve before the addition of the next compound (in increasing order). Solutes A and B were mixed separately and then slowly added to the solution after the 8th compound (in (i)) or 13th compound (in (ii)) had been added and mixed. In (i), C and D were mixed separately and added to the solution after the 5th compound has been added and mixed. Final pH (i) = 6.5 (ii) = 5.8. Precipitates started to appear in these solutions after three days of standing in the fridge at 2ºC.

(i)

Mixing order	1	2	3	4	5	C	D	6	7	8	A	B
Solute	$CaCl_2$	Oxalic acid	$MgSO_4$	Calcium dihydrogen phosphate.(H2O)	Citric acid.(H_2O)	$Ca(OH)_2$	Calcium nitrate.($4H_2O$)	Sodium citrate.($2H_2O$)	NH_4NO_3	$CaSO_4$	Malic acid	KOH
Qty (mg) in 100ml)	226.96	12.67	363.32	444.79	716.99	607.09	300.04	42.66	8.37	400.23	2234.91	1183.13

(ii)

Mixing order	1	2	3	4	5	6	7	8	9	10	11	12	13	A	B
Solute	$Cacl_2$	Succinic acid	Calcium dihydrogen phosphate. (H2O)	$Mg(NO_3)_2 \cdot 6H_2O$	Tartaric acid	Mg powder	Oxalic acid	Calcium nitrate. ($4H_2O$)	Citric acid. (H_2O)	Sodium citrate. ($2H_2O$)	$MgCl_2$	$MgSO_4$	NH_4NO_3	Malic acid	KOH
Qty (mg) in 100ml)	284.34	4.69	148.12	134.02	5.48	10.72	5.54	120.40	165.06	194.85	6.22	176.91	21.84	1724.60	1138.90

The artificial sap π was measured using the freezing-point depression picolitre osmometer (Malone *et al*., 1989) (see chapter 2). Table 5.4 shows the osmolality of the whole leaf and epidermal strip artificial sap. The osmolality for the whole leaf artificial sap was 709.2 mOsmol.kg^{-1} while that for the strip was 561.4 mOsmol.kg^{-1}. The osmolality of the whole leaf artificial sap was 21% higher than that for the strip artificial sap

Table 5.4 Osmolality of artificial sap prepared according to solute concentrations found in whole leaf (W.L) and abaxial epidermal strip of leaf five. n = 9.

Sample	Whole leaf osmolality	Epidermal strip osmolality
Artificial (mOsmol.kg^{-1})	709.2 ± 14.5	561.4 ± 1 8.8
Solute sum (mOsmol.kg^{-1})	634.5	629.5
Osmotic coefficient (mOsmol.kg^{-1}. mM^{-1})	1.1 ± 0.07	0.9 ± 0.03

To ensure that this low osmotic coefficient obtained when measured and calculated π were compared (section 5.2.2) was not due to factors in addition to the measured solute (e.g. proteins), the π of freshly prepared solutions, at solute concentrations determined with the CZE (artificial sap) in whole leaf and abaxial epidermal strips was measured. An osmotic coefficient of unity (0.9 – 1.1) was obtained suggesting that all solutes involved in the osmotic control of stomatal movement were identified. Thus no significant contribution from non-electrolytes was predicted in the process of stomatal movement. This result also affirms the value of the CZE method as a tool in SiCSA kit.

The differences between the “expected” osmotic coefficient and the “mimic” osmotic coefficient is curious. It is as if “π” is released from the solutes as they are separated on CZE. This suggests that vacuoles have a mechanism, to reduce the π of their electrolytes (by complexing or forming of “micro-colloids” perhaps). This needs further work.

5.3 Discussion

5.3.1 Guard cell osmotic pressure

A gradient of increasing π towards the guard cells was demonstrated in contiguous cells when the stomata were open (figure 5.3). At closed stomata, a gradient increasing away from the guard cells was not observed. Instead, there appeared to be no gradient, all the cells being at similar π. This is consistent with previous findings in our laboratory using *T. virginiana* (Irving, 1996). It was noted in the study that the π of the pavement and apical subsidiary cells were higher in closed than in open stomata condition. Such works as this, involving π measurement in contiguous cells has rarely been performed in the past. Most measurements have been of turgor pressure, which is a good estimate for π if dilution effects are ignored (Meidner and Bannister, 1979). Additionally, at a cellular level, the π represents the cell turgor pressure, since the gravitation component of cell water potential tends to zero and apoplastic π may be negligible (see section 1.12.4) provided transpiration tension is not excessive. Negligible effect of transpiration tension on the π of the apoplast is expected in a well-watered plant especially under high to moderate humidity. Thus, indirect methods (mainly by plasmolysis) of measuring cell turgor pressure have been used in the past in contiguous cells (e.g. Edwards and Meidner (1979); Meidner and Bannister (1979)). The work of Meidner and Bannister (1979) showed an obvious gradient between the subsidiary and guard cells. In the study, pavement cells were, however, not present (destroyed) in the strips used and the cell sap was replaced either with water or paraffin oil. This situation does not present a natural environment and conclusions can only be made by deductions. Perhaps for this reason, a wide range of turgor pressure (0.72 to 7.2 MPa) was reported in the absence of subsidiary cells. In the presence of the subsidiary cells, though, turgor pressure ranged between 1.13 and 1.10 MPa at full aperture (15 to 16 µm) (Meidner and Bannister, 1979). This is equivalent to half the π found in our study. The findings of Franks and Farquhar (1978) using similar experimental methods as Meidner and Bannister (1979), but using the cell probe (direct turgor pressure measurement), showed that stomatal opening in *T. virginiana* does not begin until guard cell pressure reaches 1.25 MPa in the presence of subsidiary cells. At an aperture of 8 and 18 µm, respectively in the presence and absence of subsidiary cells, the turgor

pressure was 4.5 MPa. Edwards *et al.* (1976) also found guard cell turgor pressure of 8.6 MPa at fully open stomata of the same plant. Put together, these works suggest that the turgor pressure in intact *T. virginiana* guard cells under open stomata condition ranges between 1.25 and 4.5 MPa. Our finding of π of 922.5mOsmol.kg-1 (equivalent to turgor pressure of 2.26 MPa) at open stomata in intact whole leaf agrees with this. Also in agreement are the results of Irving (1996) which showed, by direct turgor pressure measurement, that the turgor pressure of intact guard cells in fully open stomata in *T. virginiana* is 2.7 MPa (equivalent to osmolality of 1100 $mOsmol.kg^{-1}$).

Two factors may have contributed to the very high extremes of both aperture and turgor pressures reported in the studies by Edwards *et al.* (1976), Franks and Farquhar (1978) or Meidner and Bannister (1979) above. Firstly, stomatal opening during the studies were achieved through application of pressure by instrumentation. Thus, pressures exceeding physiological range(s) may easily be applied. Guard cell walls have very high elastic modulus (Wu and Sharpe, 1979; Kondo and Maruta, 1987), thereby allowing both excess aperture(s) and natural recoil on release of the pressure. Secondly, the sap and the vacuole with associated tonoplast-bound channels and pumps were functionally replaced by fluid (water, paraffin or silicon oil) mechanically pressured. It would be expected that the pressure generated by physiological osmotica in guard cells, as applied in Irving (1996), cannot generate such (high) turgor pressures exceeding 4 MPa. This is because proton efflux into the apoplast causes the dissociation of Ca^{2+} from cell wall pectin due to decreasing pH (Jinno and Kuraishi, 1982). Increased dissociation of Ca^{2+} and pectin leads to a decrease in guard cell elastic modulus (Kondo and Maruta, 1987). Thus, the force generated in the cell wall must be lower than that possible in the absence of these physiological phenomena. For example, MacRrobbie and Lettau (1980) found maximum K^+ concentration of 400 mM in fully open intact stomata of *Commelina*, a close relative of *Tradescantia*. This is equivalent to approximately 720 $mOsmol.kg^{-1}$ of K^+ (approximately 1.74 MPa).

This is also similar to our results in *T. virginiana* (1100 $mOsmol.kg^{-1}$). Variations have, however, also been reported in the π in guard cells of other species. Meidner and Edwards (1975) found turgor pressure at fully open stomata in *Commelina* to be 2.8 MPa, contrasting with the above finding by MacRrobbie and Lettau (1980). In *Vicia faba* values as high as 4.5 (Raschke, 1975) and as low as 1.1

MPa (Meidner and Mansfield, 1968) have been reported. Different values between these two (values) have also been reported in the same species. For instance, Allaway and Hsiao (1973) reported 1.7 MPa while Raschke (1979) reported 3.7 MPa. These differences in results may be due to plant/species variations or errors inherent in the use of some methods. For example, using long incubation times during the plasmolysis method, leakages (e.g. (Glinka, 1971)) or entry of some osmotically-active solutes such as sucrose (e.g. (Edwards *et al*., 1976)) may occur in the (guard) cells. While the former may result in lower pressure the later may lead to overestimation of the pressure.

5.3.2 Relationship between guard cell turgor and osmotic pressure

Changes in epidermal cell turgor pressure cause changes in stomatal aperture (Itai *et al*., 1982; Mott and Franks, 2001). These turgor pressure changes are caused by changes in the π. The π in an intact (guard) cell may, however, be in excess of the turgor pressure (Edwards and Meidner, 1979). This is due to the counter effects of the π (due to solutes) in the apoplast as well as the effect of transpiration from the guard cells, especially when stomata are open. Turgor pressure is a function of the π difference across the plasmalemma and the transpiration tension (see section 1.12.4 and equation 1.5). Results from Edwards and Meidner (1979) as well as Meidner and Bannister (1979) show that guard cell turgor in *T. virginiana* may be up to 0.6 to 0.7 MPa lower than the measured π at a stomatal aperture of 7µm, for example. Edwards and Meidner (1977) studied the theory of mechanical advantage of subsidiary and pavement cells over the guard cells in *Tradescantia virginiana, Commelina communis, Vicia faba* and *Triticum vulgare*. In doing this they reported that differences existed between the osmotic and turgor pressure at different stomatal apertures in all the species, though most pronounced in *Tradescantia virginiana.*

Turgor pressure measurements were not carried out during this research. However, the hydrostatic forces involved in stomatal movement in *T. virginiana* have been previously characterized in our laboratory (see fig. 3.5 from Irving (1996)). In the study, the turgor pressure in abaxial epidermal cells of *T. virginiana* was 0.5 MPa in pavement cells and 0.49 MPa in apical subsidiary cells under both open and closed

stomata conditions. The lateral subsidiary cells had turgor pressure of 0.38 MPa in closed but 0.3 MPa in open stomata conditions. Turgor in guard cells were 0.4 MPa in closed and 0.7 MPa in open stomata conditions.

5.3.3 Wider osmotic pressure difference between the lateral subsidiary and the guard cell

With open stomata, the π in the lateral subsidiary cells increased marginally while the guard cell π significantly increased (fig. 5.2). This might be explained by the mechanical advantage of the subsidiary cells over the guard cells (section 5.1.1). Equating changes in π in each of the cells with changes in turgor, results from this study show an antagonism ratio of 3.4 (Table 5.5).

Table 5.5 Antagonism ratio between lateral subsidiary and guard cells of *T. virginiana*

	Osmotic pressure (MPa) in		Osmotic pressure change (MPa) during stomatal opening	Antagonism ratio
Cell type	Closed stomata	Open stomata		
Lateral subsidiary	1.53	1.68	0.15	3.4
Guard cell	1.75	2.26	0.51	

Osmotic pressure significantly decreased in cells at the apical aspect of the guard cells (the poles) as to permit the expansion of the guard cells in that direction. In reciprocation, the π in both the juxta apical and pavement cells decreased, the former significantly and the later marginally. This decrease in pavement and juxta apical cell π seem to align with the idea of antagonism ratio. This is because slight increases in π in these cells demand that guard cell π must be several fold higher in order to counter such pavement cell pressure.

Stomatal closing on the other hand, followed an increase in the π of the cells at the poles (apical aspect) of the guard cells as well as the pavement cells. A decrease in the π in the lateral subsidiary cells and the guard cells reciprocated the pressure increases in the other cells. At this point the guard cell π was similar to that of the apical subsidiary, but higher than that in the pavement cells. This has also been reported by Cooke and Baerdemaeker (1976). Their observation was,

however, limited to the pavement cells. These evidences together, suggests that all the cells of the epidermis actively participate in orchestrating stomatal movements. This fact had been suggested by Glinka (1976), but the parts played by individual cell types have not been elucidated since then.

5.3.4 Strip and whole leaf measurements

Both epidermal strip and pavement cells, measured separately, showed no significant difference ($p > 0.5$) in their sum of solute concentrations. This suggests that the apoplast may not have a significant electrolyte constitution (Clipson *et al*., 1985; James *et al*., 2006) since the pavement cells constitute the greatest proportion (48%) of the epidermis.

5.4 Conclusion

The sum of the solute concentrations measured in the cell types approximated their osmolality measured independently. This shows that all osmotically-active species have been accounted for, although the question of the osmotic coefficient makes a categorical conclusion difficult. Concentrations of some solutes (oxalic acid, and the unidentified ones in this experiment) were too low to be osmotically important unless preferentially accumulated in cytosol. However, a more accurate determination of the osmotic coefficients was needful and has been carried out in this studies using the artificial sap after the manner of Fricke *et al.* (1994). Osmolality of an artificial sap that resembles the extracted sap from whole leaf and epidermal strip (analysed with the CZE) were determined. The ratio of the osmolality to the total solute concentration was 0.9 ± 0.03. These results indicate that the epidermis uses mainly inorganic ions as its principal osmotica for stomatal control. The full picture of the solutes involved in stomatal movement in *T. virginiana* may then have been elucidated.

Chapter 6 General discussion

6.1 Introduction

Improvements in crop production following manipulations of stomatal density have started yielding encouraging results (Condon *et al*., 2002, 2004). This study has demonstrated the full cohort of intracellular solutes in the epidermis of *T. virginiana,* and has shown that all these solutes are reshuffled during stomatal movements. The study has also shown the different destinations of these solutes during stomatal opening and closing. These destinations were arrived at by following concentration gradients to or away from guard cells, lateral subsidiary cells or any cell developing charge imbalance during stomatal movements. The movement of these solutes from one location to the other is through channels, pores or proteins involved in active transport, as well as plasmodesmata.

The purpose of this study was to improve the understanding of the functioning of stomatal complexes in the context of the whole leaf. Before now this had been acknowledged as a salutary task left undone (Heath, 1975; Taiz *et al*., 2015). The task was left undone mainly due to lack of suitable analytical techniques. The single cell sampling and analysis technique, developed in our laboratory (Tomos and Sharrock, 2001) enabled the extraction of sap from individual cell as well as quantification of osmotically-significant solutes and the measurement of π from the extracted sap. This technique was employed to quantify the solutes and determine the π in both the stomatal complex and other epidermal cell types in open and closed stomata conditions.

This analysis of the solute concentrations and consequent π in all cells allowed, for the first time, a fully integrated description of the behaviour of the stomatal complex in the context of other epidermal cells. The study identified significant physiological differences between cell types hitherto classed as functionally the same.

6.2 Is stomatal movement associated with solute and osmotic gradients?

Stomatal movements are caused by intracellular turgor changes in cells of the epidermis (Heath, 1938; Meidner and Mansfield, 1968; MacRrobbie, 2006). The turgor pressure at which the stomatal aperture begins to change depends on the net turgor balance between the guard cells and the surrounding cells (Heath, 1975). These, in *T. virginiana*, include the pavement, juxta apical, apical and lateral subsidiary cells. The turgor develops as a result of osmotic changes within the membrane bound confines of the cell acting against the cell walls (Aylor *et al*., 1973; Fischer, 1973; Sharpe and Wu, 1978). The osmotic changes, in turn, arise due to changes in solute concentrations within the cells. The nature of the solutes vary in different species, and may include both organic and inorganic electrolytes as well as neutral compounds (Willmer and Fricker, 1996).

6.2.1 Solute concentrations

Results in this study indicate that solute concentrations change in all cells of the epidermis during stomatal movements (Appendix 7-10). Concentration of some of the solutes change in all the cell types while others change in only some of the cells. For example K^+, SO_4^{2-} and PO_4^{3-} concentrations change in all of the cells, while concentrations of Cl^-, malate, citrate, Ca^{2+} and Mg^{2+} change in some of the cells. Two solutes, tartrate and succinate, were found only in the stomatal-complex cells, and their concentrations changed in all of those cells during stomatal movement. No solute remained unchanged in concentration in every cell during stomatal movement.

Quantitatively, the changes that occurred in the different cells varied from cell to cell, both for the solutes that changed in concentration in each cell and those that did not. None of the solutes increased or decreased in concentration in every cell. On the contrary, concentrations of each of the solutes increased in some and decreased in other cells during the two tides of stomatal movements – opening and closing. Although not evidence by itself, this is consistent with previous findings that show that solutes used during stomatal movements are entirely epidermal in origin (Levitt, 1974; Azoulay-Shemer *et al*., 2016), and are redistributed between cell types in a coordinated manner (Penny and Bowling, 1974; Edwards and Bowling, 1984).

The studies identified only a few of the solutes namely; K^+, Cl^-, malate and citrate, but acknowledged the likely participation of more, as at then unidentified, solutes. A much fuller cohort of solutes involved in effecting stomatal movement (in *T. virginiana*) has been identified in the present project.

Three classes of solute movement were observed when stomata opened, namely; a) solutes moving into the guard cells (K^+, Cl^-, tartrate and succinate); b) solutes moving into the lateral subsidiary cells from other cells (malate, NO_3^- and PO_4^{3-}) and c) solutes (SO_4^{2-} and citrate) that are redistributed to different cells to balance charge differences created by solute movements caused by the above two groups.

These solute movements resulted in osmotic pressure (π) increase in the guard cells and the lateral subsidiary cells, and decrease in the π of all the other cells. This suggests that the solutes moving into the guard cells and lateral subsidiary cells originate from these cells experiencing decreased π. This pattern of π change aligns with the relationship between individual solute concentration and π i.e. increase in solute concentration leads to increase in π (equation 1.6).

6.2.2 Solute concentration differences lead to osmotic pressure changes

Our results show that K^+ concentration change alone, cannot generate the π that can translate into the turgor required for stomatal opening. For example, guard cell turgor pressure change for the initiation of stomatal opening in *T. virginiana* is at least 0.7 MPa (Meidner and Bannister, 1979; Franks *et al*., 1995). To generate this pressure at a temperature of 20ºC, for example, would require K^+ concentration increase of more than 280 mM (assuming osmotic coefficient of one). Our results, as well as that of Edwards and Bowling (1984), show that K^+ increase during stomatal opening is approximately half of this concentration (115 mM). Thus other solutes must also enter the guard cells to build up the π.

Results in the study indicate that the K^+ influx is counterbalanced by mainly Cl^- but also by organic anions, tartrate and succinate. The source of the Cl^- is from the relatively distant pavement cells, but the tartrate and succinate come from the neighbouring lateral subsidiary cells. It is possible that the initial event of K^+ influx is balanced by the organic anions before the arrival of Cl^-. This view has also been

express by Penny and Bowling (1974) from studies in *Commelina*. In *Vicia faba* influx of K^+ and the accompanying Cl^- has been variously reported to be at a ratio of 3:1 (Pallaghy and Fischer, 1974) or 2:1 (Raschke and Schnabl, 1978). The K^+:Cl^- ratio found in this study is 2:1. However, the K^+:Cl^- ratio for the respective concentration changes when stomata open is 5:1. This very low ratio of change in Cl^- to that of K^+ is not counter to the conclusion in this study, that Cl^- is the major counter-ion to K^+ in *Tradescantia*. Consideration of the total concentration of Cl^- in the guard shows that increase during stomatal opening contributes only little (12%) to the total Cl^- concentration (appendix 7 and fig. 4.7A). The sum of the concentrations of these solutes, K^+, Cl^-, tartrate and succinate adequately accounted for the π change required for opening of the stomata.

The solute content of epidermal cells is not only K^+, Ca^{2+}, Cl^-, PO_4^{3-} and malate. In many species cells also contain SO_4^{2-}, NO_3^-, and other metabolites from photosynthetically-accumulated starch, such as, citrate and succinate (Outlaw and Lowry, 1977; Fricke *et al*, 1994a, b). Results of this study have indicated that *Tradescantia* epidermis possesses similar epidermal solute contents (appendix 7). The patterns of distribution and redistribution of these solutes correspond to the patterns of changes observed in π during stomatal movements in cells of comparable volumes. The measured π found in both open and closed stomatal situations was equivalent to the osmolality calculated from the CZE-analysed solute concentration results. These also had a good correlation with the sum of solute concentrations (in chapter 4) (see fig. 5.1).

Pavement and juxta apical cells released most of the solutes used in stomatal opening, and their π correspondingly decreased during opening (fig.5.1). Due to its disproportionally larger volume, change in π in pavement cells is lower than that in the juxta apical cells. Osmotic pressure in the apical subsidiary cells also decreased during stomatal opening. The guard cell received most of the solutes, and had the highest increase in π. The lateral subsidiary cell had the smallest increase in π. Since it is on the expanding side of the guard cells, a decrease in π was expected. However, the π increase in the guard cell was approximately three times that of the lateral subsidiary. This may have the effect of controlling guard cell distention, hence stomatal aperture in intact guard cells is usually smaller than that in isolated guard cells per unit change pressure (Meidner and Mansfield, 1968; MacRrobbie and Lettau, 1980; Zeiger, 1983; MacRrobbie, 2006). As a mechanism of preventing over-

distention it may act as a wall, on one side preventing further extension of guard cells and on the other side preventing the pressure decrease in the pavement, juxta apical and apical cells from creating tension on guard cell walls.
Thus, the lateral subsidiary cell in *Tradescantia* may have important solute distribution function of controlling solute access to guard cells as well as a mechanical function of controlling the pressure to aperture size relationship. These two functions may be exploited in genetic engineering towards improving plant water use efficiency through manipulation of the stomatal aperture to pressure relationship.

6.3 Was *Tradescantia virginiana* a model plant?

Results in this project showed that *T. virginiana* epidermal trough is composed of clearly distinguishable cell types. This has enabled the identification of physiologically distinct subtype of the pavement cells, the juxta apical cells which are vital as major solute reservoir during stomatal movement (see chapter 4). Although it has not been named previously as a distinct cell type, its anatomical distinction was suggested (Croxdale *et al*., 1992) during studies on cell linage in monocots. Such identification was enhanced by the simple arrangement of the epidermal cells which makes for a clear distinction of the different cell types. *Tradescantia* also presents another interesting characteristic for the understanding of leaf water and solute relations. A clearly demarcated stomatal complex is in line with some of the advantages in using it for studies on the interactions of (other) epidermal cells with cell of the stomatal complex (Franks et al., 1998). This complements its relatively large and easily-accessible cells including its guard and subsidiary cells (Tomos and Zimmermann, 1983).

Flexibility in sampling and measurement options was also enhanced by the very low variation in its cell sizes in troughs across the leaf. Cell sizes (including stomatal complexes) were similar within up to three troughs across the leaf width (fig. 3.3) allowing for more sampling options and better reproducibility due to availability of predictable replicates for analysis. A number of the early developmental works on the cell pressure probe technique in the study of plant water relations parameters took advantage of this feature of *T. virginiana* (Hüsken *et al*.,

1978; Zimmermann *et al*., 1980; Tomos *et al*., 1981). The technique has subsequently been successfully applied to other plants with a wide range of pavement and guard cell sizes and arrangements (Reviewed by Zimmermann (1989)). *Tradescantia virginiana* thus offers a suitable system for the study of single cell physiology.

In addition to the stable cell sizes the stomatal density in contiguous troughs having similar cell sizes was also similar. This was invaluable in labelling cell positions for sampling and analysis. Perhaps for this reason *T. virginiana* has also been used in a number of early works on single cell sampling and analysis with modified pressure probe technique e.g. (Shackel, 1987; Nonami and Schulze, 1989). Nonami *et al.*, (1990) sampled cells as deep as the mesophyll. It is also considered a model plant in the study of leaf developmental patterns (Croxdale *et al*., 1992; Croxdale, 1998).

Importantly, *T. virginiana* combines the kidney-shaped guard cells of dicots with the subsidiary cells – a feature of grasses (Willmer and Fricker, 1996). Absence of subsidiary cells is common in dicots, which normally have kidney-shaped guard cells. In contrast, grasses have dumbbell-shaped guard cells surrounded by subsidiary cells (Willmer and Fricker, 1996). Most of the other monocots, however, lack subsidiary cells but do possess kidney-shaped guard cells (Willmer and Fricker, 1996). Other plants, such as *Commelina,* also show such characteristic (Willmer and Fricker, 1996). *Commelina* possess more subsidiary cells than *Tradescantia,* so *Tradescantia* stands in the gap between plants with no subsidiary and those with multiple subsidiary cells. This presented as an advantage in the interpretation and generalization of studies of its leaf solute and water potential parameters (see section 1.3).

T. virginiana was chosen for this study since it offers the best models in cell sizes, including stomatal complex cells, and simple geometric pattern of cells on the epidermis. These features have aided sampling precision, availed sizable volumes for analysis and simplified interpretation of results of solute gradients in contiguous cells in this project.

6.3.1 Sampling and measurement of osmotic pressure

The π of extracted sap was measured with the freezing point picolitre osmometer. This measurement of extracted sap represents the only minimally invasive (as long as it is finished well within 30 seconds (see Malone *et al*., 1989)) means of measuring π in individual cells of intact leaves without interference with apoplastic solutes (cf. Wenkert, (1980)). The method has been successfully used in previous studies in *Tradescantia* and *Commelina* (Malone *et al*., 1989; Irving, 1996), *Phaseolus vulgaris* (Irving *et al*., 1997) and in wheat, barley and *Suaeda maritima* (Malone *et al*., 1991; Fricke *et al*., 1995, 1996; Eltayef, 2014). Before these, π measurement in plant cells was by plasmolysis method (e.g. Meidner and Bannister (1979)). The general pattern of the π results in this study is similar to that of Irving (1996) though quantitatively higher. The higher π may be attributable to the degree of hydration of the plant since relative humidity was higher (75%) in the former study.

Sampling of individual cells, including the guard cells, was straightforward and the analysis revealed differences in behaviour of the individual cells during stomatal movement. These differences differentiated a subtype of the pavement cells, the juxta apical cells, for showing distinct osmotic behaviour during the movements. In previous studies in *Tradescantia* using this method (Irving, 1996; Tomos and Sharrock, 2001) such distinction between the pavement and juxta apical cells was neither emphasized nor identified.

Within the stomatal complex, the guard cells have been the main focus of previous studies (Meidner and Bannister, 1979). In this work, we have studied the guard cells in relation to other cells of the epidermis. In sampling the guard cells, though, the source of the sap was carefully considered. Sap from all the other cells was predominantly vacuolar both in open and closed stomata conditions (see section 4.2.4). Doubts remain as to whether guard cell samples were entirely vacuolar not only in closed and but also in open stomata.

6.3.2 Sap analysis using capillary zone electrophoresis (CZE)

Most of this study relied on the CZE for the qualitative and quantitative assessment of both organic and inorganic contents as described by Bazzanella *et al.*, (1998) and Tomos (2016) as described in section 2.6. Capillary zone electrophoresis is an established analytical method that has been applied in various fields for analysis of

plant, animal and soil extracts (Wildman *et al*., 1991; Shihabi *et al*., 1994; Wu *et al*., 1995; Soga and Ross, 1999). It has been used previously in our laboratory for analysis of plant (Eltayef, 2014) and soil (Tandy *et al*., 2013; Alnusaire, 2016). Quantification of solute concentrations was straightforward due to use of an internal standard.

Accurate pipetting of sample and internal standard is vital for reproducible and reliable quantification of the solute concentrations. To this end, samples were prepared such that it was possible to take several subsamples from the same sap sample. In cells such as the guard cell, with small volumes, this was achieved by pooling samples together from several cells. This introduces minimal error as all sampled cells are under the same experimental condition(s). Taking several aliquot samples from a sap sample permits the evaluation of any systemic errors in pipetting, distinguishable from cell to cell variations. Similarly, pipetting the same volumes of a sample and an internal standard to create a mixture ready for injection into the CZE capillary reduced injection error (Malone *et al*., 1991; Beckers and Boček, 2004).

6.3.3 Identification and quantification of solutes

Charged solutes in the plant sap were detected by an indirect UV absorbance method involving the use of an appropriate background electrolyte (BGE) as described in section 2.6. This assumes that the UV signal is directly proportional to the molar absorptivity of the BGE used. Observed electrophoretogram peaks are thus, inverted images of the displacement of the BGE in zones occupied by the UV transparent ionic solutes during the electrophoresis. This contrasts with direct detection mode in which all peaks represent the zone of the solute according to its individual UV absorbance (Yeung, 1989). The direct mode was not used in this study since indirect method is more sensitive than direct method and most solutes, including malate, expected in vacuolar sap are UV transparent.

The UV transparency of these solutes means that quantification of the solutes depends on the conversion factor of the BGE. The conversion factor may be determined experimentally, using standard curves of the expected solutes run in the BGE, or by calculation from the transfer ratios using the ionic mobilities and pKa values of the solutes (Beckers and Boček, 2004). In this study the use of standard

curves was preferred in order to allow for comparison with possible ionization status of these solutes at sampling time in the living cell. Peak identification by spiking with standards of known concentrations allowed for confirmation of each solute peak.

6.4 Has the whole picture of the solutes in stomatal movement emerged?

Stomatal response to stimuli involve changes in guard cell turgor as a consequence of changes in guard cell intracellular solute concentration modulated by similar changes in the surrounding cells. Results in this study indicate that all charged solutes of significant concentration in the sample vacuolar sap were identified and quantified. The charge balance between the cations and anions in all the cells affirm this. The balanced charge does not, however, preclude the participation of non-charged solutes such as sucrose and glucose as well as charged proteins in the osmotic activities of these cells. The test of the presence and activity of any proteins or sugars is in the measurement of the π of these extracted sap. The results presented here show that the measured solute concentration appeared to account for the measured π (appendix 13). The lowest osmotic coefficient was 0.5 $Osmol.Mol^{-1}$ in most cells. (Strictly, the units of the measured osmotic coefficient are $Osmol.Kg^{-1}.Mol.L^{-1}$) This suggests that proteins and sugars did not significantly contribute to the π responsible for the observed stomatal movements. This compares with the osmotic coefficient, 0.56 $Osmol.Mol^{-1}$ and 0.53 $Osmol.Mol^{-1}$, respectively found in whole leaf and strip. In the cytoplasm, balancing of pressure in the vacuole may be by use of soluble proteins, sugars and colloids, which may also have a non-colligative influence on the osmotic solutes. These were not assayed during this study.

The lateral subsidiary cell had an osmotic coefficient of 0.5 $Osmol.Mol^{-1}$, which did not change between open and closed stomatal conditions. Similarly, the pavement cells, but no other cell, maintained an osmotic coefficient of 0.67 $Osmol.Mol^{-1}$ in open and closed stomata situations. The import of this is not clear, but may be important for their stabilizing functions by the pavement or lateral subsidiary cells which are respectively major solute sources or guard cell solute access and expansion controllers. The curious discrepancy between this "*in vivo*"

and “*in vitro*” osmotic coefficients has been discussed above (section 5.5) and remains unresolved.

6.5 Are all cells identical in a tissue

Distinction of the functional differences between cell types is less obviously appreciated, but is the subject of this project. Single cell sampling techniques have demonstrated non-random heterogeneity in the distribution of solutes between the cell types in barley (Mimura *et al.*, 1990; Dietz *et al.*, 1992a). As may be similar in other species, in barley this pattern of distribution depends on the stage of development of the leaf (Dietz *et al.*, 1992b). Hence, in wheat, no heterogeneity was found between ridge and trough cells of the epidermis of young leaves (Malone *et al.*, 1991), but Fricke *et al.* (1994a and b and 1995) demonstrated heterogeneity in these cells in both abaxial and adaxial epidermis of more mature (second) leaves of the same plant.

To date, however, heterogeneity in solute contents of epidermal cell-types has not been described for *T. virginiana*. Reported differences in K^+ concentration were those associated with reversible (stomatal) movements (Humble and Raschke, 1971; MacRrobbie and Lettau, 1980b; Edwards and Bowling, 1984; Liu *et al.*, 2000). Differences in both content and concentrations were observed between cell types in this study. These differences suggest that major solutes needed for stomatal control are preferentially accumulated close to the site of the action. This emphasizes one of the advantages of multicellularity – low energy cost. By accumulating such solutes in cells near the guard cells fast stomatal response, especially during closing, is enhanced. It also enables the building of gradients necessary for such responses (fig. 4.7).

In addition to the differences in concentration between the pavement and lateral subsidiary cells, the finding of tartrate and succinate in cells of the stomatal complex exposes another level of heterogeneity. Although these two are being reported for the first time in *Tradescantia*, previous studies have demonstrated significant concentration of succinate in guard and subsidiary cells of *Vicia faba* (Outlaw and Lowry, 1977; Talbott and Zeiger, 1996). The importance of this single

observation may be in providing the answer to the question of how the guard cell counter-balances cationic charges in guard cells of open stomata while avoiding the excess negative charge that arises with use of malate (see section 6.6 and table 4.9).

6.6 Plants' guard cell dilemma, to use malate or chloride?

Malate and Cl^- are counter anions accompanying cations, usually K^+, into guard cells during stomatal opening in various plant species. Chloride is responsible for this role in *Allium* species (Shaw, 1954), and participates significantly (in varying degrees) in all species (Humble and Raschke, 1971; Penny *et al*., 1976; Van Kirk and Raschke, 1978a). In some plants, for example *Vicia faba*, either Cl^- or malate may function under different conditions (Talbott and Zeiger, 1996). Malate on the contrary does not participate at all in the stomatal movements of *Allium* species (Schnabl and Raschke, 1980).

Malate production through hydrolysis and oxidation of sucrose generates ATP needed for the proton pump in cells that accumulate starch. This oxidation is a cytoplasmic event. Malate concentration may therefore, correlate positively with stomatal aperture due to its continued production. There has been no prior documentation of malate concentration in *T. virginiana* guard cells, and malate concentrations reported in *Vicia faba* (Allaway, 1973) have all been of tissue, instead of specifically vacuolar origin. Whole cell (mixed vacuolar and cytoplasmic sap) concentrations, however, do not represent vacuolar concentration. This has been made clear in previous works using SiCSA techniques and can also be seen in the contrast between the epidermal strip malate and single cell vacuolar malate (130.6± 9.8 mM and 91.5 ± 8.3 mM respectively) found in this study (table 3.7 and appendix 7). Results from whole leaf samples (table 3.3) implicate malate as the likely major counter-anion osmoticum, a position which has been previously taken by some authors (see Martin *et al*., 1983; Irving, 1996). At the level of the whole leaf, Cl^- was very low. This relationship of low Cl^- and high malate concentration in the whole leaf was reversed in trough cells of the epidermis (cf. tables 3.3 and 3.7 with appendix 7 and 8) This suggests that the high whole-leaf malate was either due to

photosynthesis occurring mainly in the mesophyll or the ridge cells and/or the adaxial epidermal cells preferentially accumulating malate. Whole cell malate concentration is, therefore, not representative of the osmotic events in plant vacuoles. Epidermal strip malate concentrations are comparatively more representative of the vacuolar concentrations (see table 3.7 appendix 8).

For *T. virginiana*, no record of increasing malate concentration in guard cells during stomatal movement exists in literature. Increases in intracellular malate concentration during stomatal opening have been reported in other species by earlier (Pallas and Wright, 1973; Outlaw and Lowry, 1977) and recent (Azoulay-Shemer *et al*., 2015) studies, and phosphoenolpyruvate (PEP) carboxylase activity has been demonstrated in guard cell cytoplasm (Willmer *et al*., 1973).

Malate, tartrate and succinate are salts of dicarboxylic acids. As much as the current working theory of photoactive stomatal opening encompasses the involvement of a dicarboxylic acid groups (R $(COO^-)_2$) in guard cell vacuoles for increase in π during stomatal opening, increase in vacuolar malate had not been reported.

This study has identified two dicarboxylic acid salts, tartrate and succinate, which increase in concentration in the guard cell during stomatal opening. In contrast, malate, which commonly has been shown to increase during stomatal opening (usually in whole cell sap) showed no significant change in vacuolar concentration during stomatal opening. It may be that the cytoplasmic malate is used up in energizing the proton pump that maintains a K^+ electrochemical gradient or is transferred out of the guard cell or even both. The evidence to support the first supposition is beyond the scope of our study design, but our result suggest that the malate is transferred from juxta apical cells to lateral subsidiary cells. This is seen in the non-significant change (fig. 4.4) in guard cell malate concentration, and a concomitant increase in its concentrations in the lateral subsidiary cells and decrease in juxta apical cells (fig. 4.4). In addition, the malate concentration increase in the lateral subsidiary cells is not accompanied by any change in concentration in any of the other cells (pavement and apical subsidiary) contiguous to it. Thus the malate generated, through oxidation of products from sucrose, appears to be transported to the lateral subsidiary cells instead of the guard cell vacuole (fig. 4.7A), and does not participate in the vacuolar osmotica that build the turgor for stomatal opening.

6.7 Structure and function.

The mechanism for control of stomatal movement is entirely epidermal (Levitt, 1974; Van Kirk and Raschke, 1978b). Results in previous studies show that all cells of the epidermis participate in effecting stomatal movement in intact leaf tissues (e.g. Edwards and Bowling, 1984). The results in this study suggest that each participating cell type performs a unique task (section 4.2.4). For example oxalate was found only in whole leaf and strip samples but not in individual cell samples. Its concentrations were higher in epidermal strips than in whole leaf, suggesting that in *T. virginiana*, oxalate is only accumulated in the trichomes or in other places but not in abaxial epidermis. Similarly, tartrate and succinate were accumulated differentially in the stomatal complex cells only.

Guard cells possess striking functional plasticity especially with respect to the anatomical architecture of the stomatal complex. For example, in maize, as in some monocots and in grasses, which possess elaborate stomatal complex, the subsidiary cells function as reserve for solutes involved in stomatal movements, and stomata in epidermal strips are able to open in distilled water (Fischer, 1968b; Pallaghy, 1971). On the other hand, stomata in epidermal strips of *Vicia faba* that have no subsidiary cells are unable to open when placed in distilled water (Fischer, 1968b; Pallaghy, 1971). Results in this study suggest that in *T. virginiana*, this solute reservoir is mainly the juxta apical cells (section 4.2.4). This might be expected since it lies in close proximity with, and separates otherwise adjacent, apical subsidiary cells. Additionally, it is absent in leaf parts where functional stomata may be absent and its frequency reduces with that of the guard cells (see figures 3.2 and 3.4). Such a physiologically distinct pavement cell subtype has not been described in *Tradescantia* in the past nor has it been described in any plant to date. This makes comparative assessment of its function more difficult. It will be interesting to survey a fair sample of plant species with a view to identifying and characterizing this cell type. This search might best be started in monocots since their parallel venation and arrangement of cells in files may aid anatomic identification.

An overview of *Tradescantia* epidermis shows that cell sizes decreased from pavement cells towards the guard cells (figure 6.1 a diagrammatic representation of fig. 3.1).

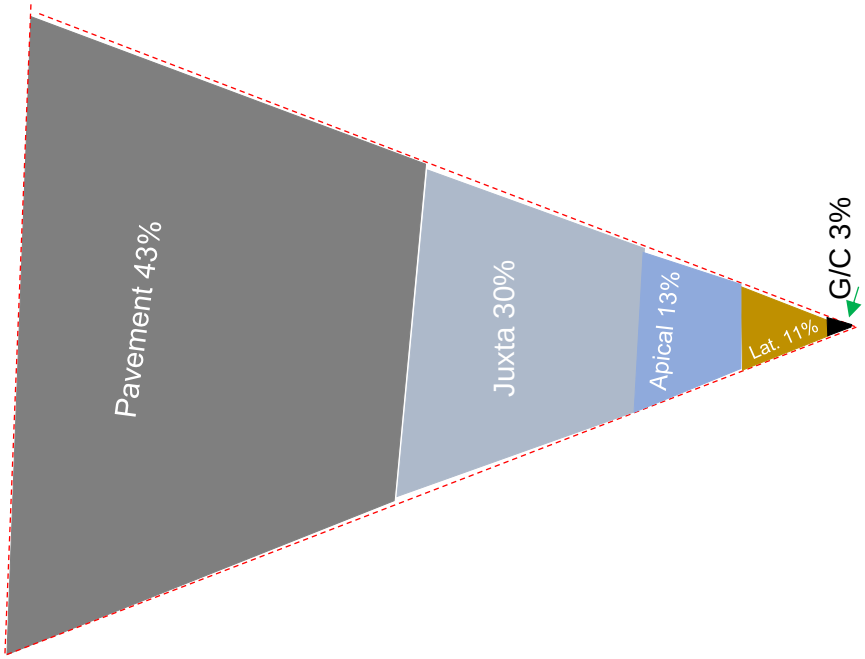

Figure 6.1 Relative cell sizes of cell types on the abaxial epidermis of *T. virginiana* mature leaf drawn to scale.
This figure shows diagrammatic representation of sizes (as surface areas) of cell types, pavement, juxta apical, apical and lateral subsidiary as well as the guard cells on the abaxial leaf epidermis of mature leaf of *T. virginiana*. Cell sizes were scaled within an equilateral triangle using the area of the triangle in relation to the sizes of the cells. Shown cell height as well as distance from next cell to the right (or apex of triangle for guard cell (G/C)) represent the size of the cell. The overall structure resembles a pressure device, broad at the base and tapering to the tip. This agrees with the description of the epidermis as a hydraulic machine (hydraulic press or anvil) that allows small work at the base (pavement) to be translated into enormous force at the tip (G/C).

Such arrangements enable slight or sometimes unnoticeable changes in the large pavement cells to cause significant changes in the guard cells. This may also explain why plants with smaller guard cells respond faster than plants with larger guard cells (Willmer and Fricker, 1996). Results in this study, however, indicate that such direct transmission of force as implied in fig. 6.1 is not always the case. Some changes in the pavement cells may sometimes detour to other cell types before arriving at the guard cells or altogether ending in such other cells. Additionally, pavement cells have not been implicated in sensing stimuli involved in photoactive stomatal opening although it has been argued that environmental cues may be sensed by the leaf cuticle. Such cues as humidity and presence of pathogens may be sensed by the leaf cuticle, and transcuticular transpiration depends mainly on the water status of the pavement cells (Boyer *et al*., 1997; Melotto *et al*., 2006). As demonstrated in experiments on epidermal strips placed in distilled water, the pavement cells supply the solutes required for effecting stomatal moments and also moderate guard cell

size during stomatal movements. These, in addition to mechanical support, appear to be the only function of the pavement and other cells of the epidermis with regards to stomatal function since stomata in detached guard cell has been shown to function normally.

Despite this, results in this and other studies (Penny and Bowling, 1974; Edwards and Bowling, 1984) have shown that solute concentration and osmotic changes occur simultaneously in all cells of the epidermis during stomatal movements. Concomitant changes in pH have also been shown (Bowling and Edwards, 1984). These changes in pH, solute concentrations and π have been concluded as resulting in the stomatal movements. Therefore, feedback systems must invariably connect the intact guard cell to the rest of the epidermal cells (Hedrich and Marten, 1993; Hedrich *et al*., 1994). Thus all cells of the epidermis may participate through this signalling system to control stomatal movement.

6.8 Limitations of the research

Certain constraints apply to the interpretation of the result of this study. In the first instance, all the plants used for this study are clones from the same vegetative parent. Fricke *et al.*, (1994a) observed that plants propagated from the same parent show insignificant plant-plant variation in both bulk leaf and epidermal strip solute composition. The cellular heterogeneity observed in this study is, however, made more reliable by this constraint, thus eliminating the possibility of plant-plant variation being the major source of the observed heterogeneity at single cell resolution. Nevertheless, this constraint may hamper the generalization of the observations to all *T. virginiana* plants. An extension of this study to a sample of this plant population would confirm generalization of these observations.

The stomatal conditions studied in this project, open and closed conditions, were at steady states (Edwards and Bowling, 1984)). Solute concentrations at these steady states may not reveal the events at any other stage(s) of stomatal opening. For example, the solute concentrations at the *sphannungsphase* before water influx due to the solute concentration changes (section 1.9) may differ from concentration when steady state has been reached. From the end of this stage when stomata are

still closed, and through all the degrees of opening, to the attainment of the maximum aperture (see section 2.5) the changes in solute concentration and osmolality which result as a consequence were not considered. The study of the changes at these stages would add a lot of details to the knowledge provided by the study.

6.9 Conclusions and future work

In the present era of efforts variously pursued towards curtailing climate change and its impacts, detailed knowledge of stomatal control mechanisms is needed to develop plants that can perform efficiently in these shifting climatic conditions. The overall aim is to complement efficient irrigation systems with plants that have optimum water use efficiency, which can be achieved through genetic engineering or other breeding programmes.

The study presented in this thesis focused on vacuolar solutes involved in the control of stomatal function. This was studied in *T. virginiana* a commonly-used plant in this field because of its simple and elaborate arrangement of its epidermal cells including the guard cells. Having known the baseline concentrations of these solutes from this study, it would be interesting to understand the variations in these concentrations as stomatal opening progresses. This would give a good comparison to the (final) steady state concentrations at fully open stomata, shown in this study. Such comparison may throw more light on molecular events of stomatal opening, and show for example, if solutes gradients are variously formed and broken or solute movements are substantially different before the steady state at full stomatal aperture is achieved.

Additionally, as much as it appears obvious that solute movements and osmotic changes in different epidermal cell types orchestrate stomatal movement, direct experimental evidence by microsurgery techniques may be helpful. For example, studies using lesions that disconnect the pavement cell symplast and apoplast from the rest of the cells in an intact leaf tissue may provide valuable information on the specific role of the pavement cells in stomatal movement. Mutant studies (nil pavement cell mutants) may also be invaluable in this respect.

The hypothesis was that solute concentration gradients exist across cells of the leaf epidermis and that changes in the direction of these gradients result in stomatal opening and closing. The results presented in this thesis indicate that these solute concentration gradients exist for all osmotically-active solutes, though not as a continuous gradient from pavement cells through the juxta apical, apical and lateral subsidiary to the guard cells. Different groups of solutes show different gradients, some extending through all the cell types, some within the stomatal complex only, some to varying extents and some others even in opposing direction to stomatal movement. In all, changes in these gradients appear to lead to opening and closing of the stomata.

These findings will help in the targeting of specific epidermal developmental traits in plant breeding for productivity. It has strengthened the view that the mesophyll plays no part in photoactive stomatal control (Azoulay-Shemer *et al*., 2016) since normal photoactive stomatal responses occur in epidermal strips placed in distilled water. Genetic manipulations aimed at producing plants with minimal vacuolar pH changes during stomatal movements, though of remote possibility, may produce plants that use mainly Cl^- as the major osmoticum. Crop plants with such adaptation may increase yield due to energy saved from avoiding the process of generating malate during stomatal movement. However, the salutary task of mapping out guard cell pH changes during stomatal movements in the wild or even cultivated plants must precede such genetic manipulation(s).

Other stimuli may control stomatal movements in spite of the presence of optimum light conditions. For example, in moderate to severe drought (water deficiency) stomata remain closed despite a range of otherwise optimum light conditions. Similarly, high humidity may override optimum lighting conditions and prevent stomatal opening. However, in any range approximate to optimum conditions, photoactive responses predominate. In addition, for any food or crop production process using plants, light becomes a *sine qua non*. Thus, the ranges of optimum light conditions are the common and desired practices in most crop production schemes. Nevertheless, often in practice and commonly in the wild, plants survive and often flourish by processing many of the external and internal stimuli concurrently. The control of stomatal response to light by the behaviour of solutes in forming and changing gradients to open and close the stomata may therefore, provide great improvements in crop productivity.

While studying processes at single cell resolution it is important to keep in view, the wider consequences and implications of the different processes on the plant. Studying the stomata at single cell level makes such generalization easier as whole plant application of single stomatal processes is only a multiplication of the single cell process.

This work has shown that various concentration gradient of osmotically-active solutes are created within the leaf epidermal trough during stomatal opening and closing to drive these (opening and closing) processes. All the osmotically-active solutes involved in stomatal movements are charged solutes, and the pattern of osmotic pressure changes followed those of the concentration changes in these charged solutes. Cl^- was the major counterion to K^+, which formed the major osmoticum. Importantly, the lateral subsidiary cell appears to control solute availability to guard cell apoplast, while the juxta apical cells serve as solute reservoirs for stomatal movements. Attention should now be aimed at modulating solute availability to the guard cells by focussing on engineering the mechanical (cell wall) and transport properties of the lateral subsidiary cells.

References

Ache, P., Becker, D., Ivashikina, N., Dietrich, P., Roelfsema, M. R. G. and Hedrich, R. (2000). GORK, A Delayed Outward Rectifier Expressed in Guard Cells of *Arabidopsis thaliana*, is a K^+-Selective, K^+-Sensing Ion Channel. *FEBS Letters*, **486**, 93–98.

Ackerly, D. (1992). Light, Leaf Age, and Leaf Nitrogen Concentration in a Tropical Vine. *Oecologia*, **89**, 596–600.

Adams, M. J. (1975). Potato Tuber Lenticels: Susceptibility to Infection by *Erwinia carotovora* var. *atroseptica* and *Phytophthora infestans. Annals of Applied Biology*, **79**, 275–282.

Allaway, W. G. (1973). Accumulation of Malate in Guard Cells of *Vicia faba* during Stomatal Opening. *Planta*, **110**, 63–70.

Allaway, W. G. and Milthorpe, F. L. (2012). Structure and Functioning of Stomata. *Soil Water Measurement, Plant Responses, and Breeding for Drought Resistance*, **4**, 57.

Allaway, W. G. and Setterfield, G. (1972). Ultrastructural Observations on Guard Cells of *Vicia faba* and *Allium porrum. Canadian Journal of Botany*. *NRC Research Press Ottawa, Canada*, **50**, 1405–1413.

Allaway, W. and Hsiao, T. (1973). Preparation of Rolled Epidermis of *Vicia faba* L. so that Stomata are the Only Viable Cells: Analysis of Guard Cell Potassium by Flame Photometry. *Australian Journal of Biological Sciences*, **26**, 309-318.

Allen, G. J., Amtmann, A. and Sanders, D. (1998). Calcium-Dependent and Calcium-Independent K^+ Mobilization Channels in *Vicia faba* Guard Cell Vacuoles. *Journal of Experimental Botany*, **49**, 305–318.

Allen, R. D. (1969). Mechanism of the Seismonastic Reaction in *Mimosa pudica*. *Plant Physiol*, **44**, 1101–1107.

Alnusaire, T. S. (2016). The potential for wheat roots in phytoremediation of phenolic compounds. PhD. Thesis: Prifysgol Bangor University, UK.

Alvim, P. de T. (1949). Studies on the Mechanism of Stomatal Behavior. *American Journal of Botany*, **36**, 781.

Amalou, Z., Gibrat, R., Brugidou, C., Trouslot, P. and d'Auzac, J. (1992). Evidence for an Amiloride-Inhibited $Mg^{2+}/2H^+$ Antiporter in Lutoid (Vacuolar) Vesicles from Latex of *Hevea brasiliensis. Plant Physiology*, **100**, 255–260.

Amalou, Z., Gibrat, R., Trouslot, P. and d'Auzac, J. (1994). Solubilization and Reconstitution of the $Mg^{2+}/2H^+$ Antiporter of the Lutoid Tonoplast from *Hevea brasiliensis* Latex. *Plant Physiology*, **106**, 79–85.

Andrés, Z., Pérez-Hormaeche, J., Leidi, E. O., Schlücking, K., Steinhorst, L., McLachlan, D. H., Schumacher, K., Hetherington, A. M., Kudla, J., Cubero, B. and Pardo, J. M. (2014). Control of Vacuolar Dynamics and Regulation of Stomatal Aperture by Tonoplast Potassium Uptake. *Proceedings of the National Academy of Sciences of the United States of America*, **111**, 1806-1814.

De Angeli, A., Monachello, D. and Ephritikhine, G. (2006). The Nitrate / Proton Antiporter AtCLCa Mediates Nitrate Accumulation in Plant Vacuoles. *Nature*, **442**, 939–942.

Antunes, W. C., Provart, N. J., Williams, T. C. R. and Loureiro, M. E. (2012). Changes in

Stomatal Function and Water Use Efficiency in Potato Plants with Altered Sucrolytic Activity. *Plant, Cell and Environment*, **35**, 747–759

Apple, M. E., Olszyk, D. M., Ormrod, D. P., Lewis, J., Southworth, D. and Tingey, D. T. (2000). Morphology and Stomatal Function of Douglas Fir Needles Exposed to Climate Change: Elevated CO_2 and Temperature, *International journal of plant sciences*, **161**, 127–132.

Armbrecht, L. and Dittrich, P. S. (2016). Recent Advances in the Analysis of Single Cells, *Analytical Chemistry,* **89**, 2–21.

Armitage, A. M. (2008). Herbaceous perennial plants: A treatise on their identification, culture, and garden attributes. 3rd edn., Champaign IL USA: *Stipes Pub LLC.*

Assmann, S. M. (1988). Enhancement of the Stomatal Response to Blue Light by Red Light, Reduced Intercellular Concentrations of CO_2, and Low Vapor Pressure Differences. *Plant Physiol*, **87**, 226–231.

Assmann, S., Simoncini, L. and Schroeder, J. (1985). Blue Light Activates Electrogenic Ion Pumping in Guard Cell Protoplasts of *Vicia faba. Nature*, **318**, 285–287.

Atkin, R. K., Barton, G. E. and Robinson, D. K. (1973). Effect of Root-Growing Temperature on Growth Substances in Xylem Exudate of *Zea mays. Journal of experimental botany*, **24**, 475–487.

Author, R., Moshelion, M., Becker, D., Biela, A., Uehlein, N., Hedrich, R., Otto, B., Levi, H., Moran, N. and Kaldenhoff, R. (2002). Plasma Membrane Aquaporins in the Motor Cells of *Samanea saman*: Diurnal and Circadian. *The Plant Cell*, **14**, 727–739.

Aylor, D. E., Parlange, J.Y. and Krikorian, A. D. (1973). Stomatal Mechanics. *American Journal of Botany*, **60**, 163–171.

Azoulay-Shemer, T., Bagheri, A. and Wang, C. (2016). Starch Biosynthesis in Guard Cells But Not in Mesophyll Cells is Involved in CO_2-Induced Stomatal Closing. *Plant Physiology*, **171**, 788–798.

Azoulay-Shemer, T., Palomares, A., Bagheri, A., Israelsson-Nordstrom, M., Engineer, C. B., Bargmann, B. O. R., Stephan, A. B. and Schroeder, J. I. (2015). Guard Cell Photosynthesis is Critical for Stomatal Turgor Production, yet Does Not Directly Mediate CO_2 - and ABA-Induced Stomatal Closing. *The Plant Journal*, **83**, 567–581.

Bange, G. (1959). Interactions in the Potassium and Sodium Absorption by Intact Maize Seedlings. *Plant and Soil*, **11**, 17–29.

Bange, G. and Overstreet, R. (1960). Some Observations on Absorption of Caesium by Excised Barley Roots. *Plant Physiology*, **35**, 605–608.

Bar, M. and Ori, N. (2014). Leaf Development and Morphogenesis. *Development*, **141**, 4219–4230.

Barkla, B. J., Zingarelli, L., Blumwald, E. and Smith, J. (1995). Tonoplast Na^+/H^+ Antiport Activity and its Energization by the Vacuolar H^+-ATPase in the Halophytic Plant *Mesembryanthemum crystallinum* L. *Plant Physiology*, **109**, 549–556.

Barragán, V., Leidi, E. O., Andrés, Z., Rubio, L., De Luca, A., Fernández, J. A., Cubero, B. and Pardo, J. M. (2012). Ion Exchangers NHX1 and NHX2 Mediate Active Potassium Uptake into Vacuoles to Regulate Cell Turgor and Stomatal Function in *Arabidopsis. The Plant Cell*, **24**, 1127–1142.

Bauer, H., Ache, P., Lautner, S., Fromm, J. and Hartung, W. (2013a). The Stomatal Response to Reduced Relative Humidity Requires Guard Cell-Autonomous ABA Synthesis. *Current Biology*, **23**, 53–57.

Bauer, H., Ache, P., Wohlfart, F., Al-Rasheid, K. A. S., Sonnewald, S., Sonnewald, U., Kneitz, S., Hetherington, A. M. and Hedrich, R. (2013b). How Do Stomata Sense Reductions in Atmospheric Relative Humidity? *Molecular plant*, **6**, 1703–6.

Bazzanella, A., Lochmann, H., Tomos, A. D. and Bächmann, K. (1998). Determination of Inorganic Cations and Anions in Single Plant Cells by Capillary Zone Electrophoresis. *Journal of Chromatography*, **809**, 231–239.

Bearce, B. C. and Kohl Jr, H. C. (1970). Measuring Osmotic Pressure of Sap within Live Cells by Means of a Visual Melting Point Apparatus. *Plant Physiology*, **46**, 515–519.

Beckers, J. L. and Boček, P. (2004). Calibrationless Quantitative Analysis by Indirect UV Absorbance Detection in Capillary Zone Electrophoresis: The Concept of the Conversion Factor. *Electrophoresis*, **25**, 338–343.

Beerling, D. J., Chaloner, W. G., Huntley, B., Pearson, J. A., Tooley, M. J. and Woodward, F. I. (1992). Variations in the Stomatal Density of *Salix herbacea* L. under the Changing Atmospheric CO_2 Concentrations of Late-and Post-Glacial Time. *Philosophical Transactions of the Royal Society of London B: Biological Sciences*, **336**, 215–224.

Beerling, D. J. and Franks, P. J. (2009). Evolution of Stomatal Function in 'Lower' Land Plants. *New Phytologist*, **183**, 921–925.

Bell, C., Fordham, M., Richardson, P., Cram, J. and Tomos, D. (1995). Cellular and Subcellular Compartmentation of Sulphate in Leaves in Relation to Low Sulphur Mobility. *Zeitschrift für Pflanzenernährung und Bodenkunde*. *Wiley-Vch Verlag*, **158**, 63–65.

Berger, D. and Altmann, T. (2000). A Subtilisin-like Serine Protease Involved in the Regulation of Stomatal Density and Distribution in *Arabidopsis thaliana*. *Genes and development*, **14**, 1119–1131.

Berger, F., Linstead, P., Dolan, L. and Haseloff, J. (1998). Stomata Patterning on the Hypocotyl of *Arabidopsis thaliana* is Controlled by Genes Involved in the Control of Root Epidermis Patterning. *Developmental Biology*, **194**, 226–234.

Berry, J. and Bjorkman, O. (1980). Photosynthetic Response and Adaptation to Temperature in Higher Plants. *Annual Review of Plant Physiology*, **31**, 491–543.

Bethke, P. C. and Jones, R. L. (1994). Ca^{2+}-Calmodulin Modulates Ion Channel Activity in Protein Vacuoles of Barley Aleurone Cells. *The Plant Cell*, **6**, 277–285.

Bidhendi, A. J. and Geitmann, A. (2016). Relating the Mechanics of the Primary Plant Cell Wall to Morphogenesis. *Journal of Experimental Botany*, **67**, 449–461.

Binzel, M. L., Hess, F. D., Bressan, R. A. and Hasegawa, P. M. (1988). Intracellular Compartmentation of Ions in Salt Adapted Tobacco Cells. *Plant Physiol*, **86**, 607–614.

Björkman, O. (1981). Responses to Different Quantum Flux Densities. In *Physiological Plant Ecology I*. Berlin, Heidelberg: *Springer Berlin Heidelberg*, 57–107.

Blanke, M. M. and Lenz, F. (1989). Fruit Photosynthesis. *Plant, Cell and Environment*, **12**, 31–46.

Blackman, L. M. and Overall, R. L. (2001). Structure and Function of Plasmodesmata.

Functional Plant Biology, **28**, 709–727.

Blatt, M. R. (1988). Potassium-Dependent, Bipolar Gating of K^+ Channels in Guard Cells. *J. Membrane Biol*, **102**, 235–246.

Blatt, M. R. (1990). Potassium Channel Currents in Intact Stomatal Guard Cells: Rapid Enhancement by Abscisic Acid. *Planta*, **180**, 445–455.

Blatt, M. R. (1992). K^+ Channels of Stomatal Guard Cells. Characteristics of the Inward Rectifier and its Control by pH. *The Journal of General Physiology*, **99**, 615–644.

Blatt, M. R. (2016). Plant Physiology: Redefining the Enigma of Metabolism in Stomatal Movement. *Current Biology*, **26**, 107–109.

Blumwald, E. (2000). Sodium Transport and Salt Tolerance in Plants. *Current Opinion in Cell Biology*, **12**, 431–434.

Blumwald, E., Aharon, G. S. and Apse, M. P. (2000). Sodium Transport in Plant Cells. *Biochimica et Biophysica Acta (BBA) - Biomembranes*, **1465**, 140–151.

Blumwald, E. and Poole, R. J. (1985). Na^+/H^+ Antiport in Isolated Tonoplast Vesicles from Storage Tissue of *Beta vulgaris. Plant Physiology*, **78**, 163–167.

Blumwald, E. and Poole, R. J. (1986). Kinetics of Ca^{2+}/H^+ Antiport in Isolated Tonoplast Vesicles from Storage Tissue of *Beta vulgaris* L. *Plant Physiology*, **80**, 727–731.

Blumwald, E. and Poole, R. J. (1987). Salt Tolerance in Suspension Cultures of Sugar Beet : Induction of Na^+/H^+ Antiport Activity at the Tonoplast by Growth in Salt. *Plant Physiology*, **83**, 884–887.

Boetsch, J., Chin, J. and Croxdale, J. (1995). Arrest of Stomatal Initials in *Tradescantia* is Linked to the Proximity of Neighboring Stomata and Results in the Arrested Initials Acquiring Properties of Epidermal Cells. *Developmental biology*, **168**, 28–38.

Bondoux, G., Jandik, P. and Jones, W. R (1992). New Approach to the Analysis of Low Levels of Anions in Water. *Journal of chromatography*, **602**, 79–88

Boraas, M. E., Seale, D. B. and Boxhorn, J. E. (1998). Phagotrophy by a Flagellate Selects for Colonial Prey: A Possible Origin of Multicellularity. *Evolutionary Ecology*, **12**, 152–164.

Bosabalidis, A. M. and Kofidis, G. (2002). Comparative Effects of Drought Stress on Leaf Anatomy of Two Olive Cultivars. *Plant Science*, **163**, 375–379.

Boursier, P. and Läuchli, A. (1989). Mechanisms of Chloride Partitioning in the Leaves of Salt-stressed *Sorghum bicolor* L. *Physiologia Plantarum*, **77**, 537–544.

Bowling, D. J. F. (2016). Ionic Gradients in Higher Plant Tissues. In *Botany: Republished Bowling, D. J. F. (1976): Proceedings of the Fiftieth Anniversary Meeting of the Society for Experimental Biology*, 391–400.

Bowling, D. J. F. and Edwards, A. (1984). pH Gradients in the Stomatal Complex of *Tradescantia virginiana. Journal of experimental botany*, **35**, 1641–1645.

Boyer, J. S., Wong, S. C. and Farquhar, G. D. (1997). CO_2 and Water Vapor Exchange across Leaf Cuticle (Epidermis) at Various Water Potentials. *Plant Physiology*, **114**, 185–191.

Bradfield, E. (1976). Calcium Complexes in the Xylem Sap of Apple Shoots. *Plant and Soil*, **44**, 495–499.

Brandt, B., Munemasa, S., Wang, C., Nguyen, D., Yong, T., Yang, P. G., Poretsky, E., Belknap, T. F., Waadt, R., Alemán, F. and Schroeder, J. I. (2015). Calcium Specificity Signalling Mechanisms in Abscisic Acid Signal Transduction in *Arabidopsis* Guard Cells. *eLife Sciences Publications, Ltd*, **4,** 1-25.

Braybrook, S. and Kuhlemeier, C. (2010). How a Plant Builds Leaves. *The Plant Cell*, **22**, 1006–1018.

Brodribb, T. J. and McAdam, S. A. (2011). Passive Origins of Stomatal Control in Vascular Plants. *Science*, **331**, 582–585.

Bunce, J. (1997). Does Transpiration Control Stomatal Responses to Water Vapour Pressure Deficit? *Plant, Cell and Environment*, **20**, 131–135.

Bunce, J. A. (1985). Effect of Boundary Layer Conductance on the Response of Stomata to Humidity. *Plant, Cell and Environment*, **8**, 55–57.

Byrne, M., Barley, R., Curtis, M. and Arroyo, J. (2000). Asymmetric Leaves1 Mediates Leaf Patterning and Stem Cell Function in *Arabidopsis. Nature*, **408**, 967–971.

Byrne, M., Simorowski, J. and Martienssen, R. (2002). Asymmetric Leaves1 Reveals Knox Gene Redundancy in *Arabidopsis. Development*, **129**, 1957–1965.

Caffalla, K. H. and Mohnen, D. (2009). The Structure, Function, and Biosynthesis of Plant Cell Wall Pectic Polysaccharides. *Carbohydrate Research*, **344**, 1879–1900.

Campbell, D. H. (1881). On the Development of the Stomata of *Tradescantia* and Indian Corn. *The American Naturalist*, **15**, 761–766.

Canny, M. J. (1990). What Becomes of the Transpiration Stream? *New Phytologist*, **114**, 341–368.

Carpita, N., Sabularse, D., Montezinos, D. and Delmer, D. P. (1979). Determination of the Pore Size of Cell Walls of Living Plant Cells. *Science*, **205**, 1144–1147.

Carr, D. J. (1976). Historical Perspectives on Plasmodesmata, In Gunning B.E.S., R. A. W. eds. *Intercellular Communication in Plants: Studies on Plasmodesmata*. *Springer Berlin Heidelberg*, 291–295.

Cavalier-Smith, T. (2017). Origin of Animal Multicellularity: Precursors, Causes, Consequences—the Choanoflagellate/sponge Transition, Neurogenesis and the Cambrian Explosion. *Philosophical Transactions of the Royal Society B: Biological Sciences*, **372**, 1–16.

Ceoper, J. B., Chen, J. A., Van Hoist, G.J. and Vamer, J. E. (1987). Hydroxyproline-Rich Glycoproteins of Plant Cell Walls. *Trends in Biochemical Sciences*, **12**, 24–27.

Cerioli, S., Marocco, A., Maddaloni, M., Motto, M. and Salamini, F. (1994). Early Event in Maize Leaf Epidermis Formation as Revealed by Cell Lineage Studies. *Development*, **120**, 2113–2120.

Chabot, B. F. and Chabot, J. F. (1977). Effects of Light and Temperature on Leaf Anatomy and Photosynthesis in *Fragaria vesca*. *Oecologia*, **26**, 363–377.

Chalfie, M., Tu, Y., Euskirchen, G., Ward, W. W. and Prasher, D. C. (1994). Green Fluorescent Protein as a Marker for Gene Expression. *Science*, **263,** 802–805.

Chardonnens, A. N., ten Bookum, W. M., Kuijper, L. D. J., Verkleij, J. A. C. and Ernst, W. H.

O. (1998). Distribution of Cadmium in Leaves of Cadmium Tolerant and Sensitive Ecotypes of *Silene vulgaris*. *Physiologia Plantarum*, **104**, 75–80.

Charlton, W. A. (1988). Stomatal Pattern in Four Species of Monocotyledons. *Annals of botany*, **61**, 611–621.

Charlton, W. A. (1990). Differentiation in Leaf Epidermis of *Chlorophytum comosum* Baker. *Annals of Botany*, **66**, 567–578.

Chater, C., Kamisugi, Y., Movahedi, M., Fleming, A., Cuming, A. C., Gray, J. E. and Beerling, D. J. (2011). Regulatory Mechanism Controlling Stomatal Behavior Conserved Across 400 Million Years of Land Plant Evolution. *Current Biology*, **21**, 1025–1029.

Chater, C., Peng, K., Movahedi, M., Dunn, J. A., Walker, H. J., Liang, Y.K., McLachlan, D. H., Casson, S., Isner, J. C., Wilson, I., Neill, S. J., Hedrich, R., *et al.* (2015). Elevated CO_2-Induced Responses in Stomata Require ABA and ABA Signaling. *Current Biology*, **25**, 2709–2716.

Cheeseman, J. (1982). Pump-Leak Sodium Fluxes in Low Salt Corn Roots. *Journal of Membrane Biology*, **70**, 157–164.

Cheeseman, J. M. (1988). Mechanisms of Salinity Tolerance in Plants. *Plant Physiology*, **87**, 547–550.

Cheung, Y. N. S., Tyree, M. T. and Dainty, J. (1975) Water Relations Parameters on Single Leaves Obtained in a Pressure Bomb and Some Ecological Interpretations. *Canadian Journal of Botany*, **53**, 1342–1346.

Chitwood, D., Nogueira, F. and Howell, M. (2009). Pattern Formation via Small RNA Mobility. *Genes and development*, **23**, 549–554.

Chrispeels, M. J., Morillon, R., Maurel, C., Gerbeau, P., Kjellbom, P. and Johansso, I. (2001). Aquaporins of Plants: Structure, Function, Regulation, and Role in Plant Water Relations. *Aquaporins*, **51**, 277–334.

Christodoulakis, N. S., Menti, J. and Galatis, B. (2002). Structure and Development of Stomata on the Primary Root of *Ceratonia siliqua* L. *Annals of botany*, **89**, 23–29.

Clarkson, D. T. (1993). Roots and the Delivery of Solutes to the Xylem. *Philosophical transactions*, **341**, 5–17.

Clipson, N. J. W., Tomos, A. D., Flowers, T. J. and Jones, R. G. W. (1985). Salt Tolerance in the Halophyte *Suaeda maritima* L. Dum.:The Maintenance of Turgor Pressure and Water-Potential Gradients in Plants Growing at Different Salinities. *Planta*, **165**, 392–396.

Condon, A. G., Richards, R. A., Rebetzke, G. J. and Farquhar, G. D. (2004). Breeding for High Water-Use Efficiency. *Journal of Experimental Botany*, **55**, 2447–2460.

Condon, A. G., Richards, R. A., Rebetzke, G. L. and Farquhar, G. (2002). Improving Intrinsic Water-Use Efficiency and Crop Yield. *Crop Science*, **42**, 122-131.

Conn, S., Conn, V., Tyerman, S. and Kaiser, B. (2011). Magnesium Transporters, MGT2/MRS2-1 and MGT3/MRS2-5, are Important for Magnesium Partitioning within *Arabidopsis thaliana* Mesophyll Vacuoles. *New*, **190**, 583–594.

Conn, S. and Gilliham, M. (2010). Comparative Physiology of Elemental Distributions in Plants. *Annals of botany*, **105**, 1081–1102.

Conn, S., Gilliham, M., Athman, A. and Schreiber, A. (2011). Cell-Specific Vacuolar Calcium

Storage Mediated by CAX1 Regulates Apoplastic Calcium Concentration, Gas Exchange, and Plant Productivity in *Arabidopsis. The Plant*, **23**, 240–257.

Cooke, J. and Baerdemaeker, J. De (1976). A Finite Element Shell Analysis of Guard Cell Deformations. *Transactions of the American Society of Agricultural Engineers*, **19**, 1107–1121.

Cornish, K. and Zeevaart, J. (1986). Abscisic Acid Accumulation by *In Situ* and Isolated Guard Cells of *Pisum sativum* L. and *Vicia faba* L. in Relation to Water Stress. *Plant Physiology* , **81**, 1017–1021.

Cosgrove, D. J. (2000). Loosening of Plant Cell Walls by Expansins. *Nature*, **407**, 321–326.

Cram, W. J. (1988). Transport of Nutrient Ions across Cell Membranes *In Vivo*. *Advances in plant nutrition (USA)*, **3**, 1–53.

Crawford, K. M. and Zambryski, P. C. (2001). Non-Targeted and Targeted Protein Movement through Plasmodesmata in Leaves in Different Developmental and Physiological States. *Plant Physiology*, **125**, 1802–1812.

Croxdale, J. (1998). Stomatal Patterning in Monocotyledons: *Tradescantia* as a Model System. *Journal of Experimental Botany*, **49**, 279–292.

Croxdale, J., Smith, J., Yandell, B. and Johnson, J. B. (1992). Stomatal Patterning in *Tradescantia*: An Evaluation of the Cell Lineage Theory. *Developmental biology*, **149**, 158–167.

Dai, S. and Chen, S. (2012). Single-Cell-Type Proteomics: Toward a Holistic Understanding of Plant Function. *Molecular and cellular proteomics*, **11**, 1622–1630.

Dale, J. E. (1982). The growth of leaves. Edited by The Institute of Biology's Studies in Biology No. 137. London, Uk, *Edward Arnold Ltd.*

Daloso, D. M., Dos Anjos, L. and Fernie, A. R. (2016). Roles of Sucrose in Guard Cell Regulation. *New Phytologist*, **211**, 809–818.

Daloso, D. M., Williams, T. C. R., Antunes, W. C., Pinheiro, D. P., Müller, C., Loureiro, M. E. and Fernie, A. R. (2015). Guard Cell-specific Upregulation of Sucrose Synthase3 Reveals that the Role of Sucrose in Stomatal Function is Primarily Energetic. *New Phytologist*, **209**, 1470–1483.

Darwin, F. (1898). Observations on Stomata. *Philosophical Transactions of the Royal Society of London. Series B, Containing Papers of a Biological Character*. *Royal Society*, **190**, 531–621.

Davidson, R. L. (1969). Effect of Root/Leaf Temperature Differentials on Root/Shoot Ratios in Some Pasture Grasses and Clover. *Annals of Botany*, **33**, 561–569.

Dawson, R. M. C., Elliott, D. C., Elliott, W. H. and Jones, K. M. (1986). Data for Biochemical Research. 3rd edn. United states: *Oxford science publications, Oxford press, New york.*

Deeken, R., Geiger, D., Fromm, J., Koroleva, O., Ache, P., Langenfeld-Heyser, R., Sauer, N., May, S. T. and Hedrich, R. (2002). Loss of the AKT2/3 Potassium Channel Affects Sugar Loading into the Phloem of *Arabidopsis. Planta*, **216**, 334–344.

DeMichele, D. W. and Sharpe, P. J. H. (1973). An Analysis of the Mechanics of Guard Cell Motion. *Journal of theoretical biology*, **41**, 77–96.

Demidchik, V., Davenport, R. J. and Tester, M. (2002). Nonselective Cation Channels in

Plants. *Annual Review of Plant Biology*, **53**, 67–107.

Dengler, N. G. (1984). Comparison of Leaf Development in Normal ($^{+}/^{+}$), Entire (e/e), and Lanceolate (La/$^{+}$) Plants of Tomato, *Lycopersicon esculentum* 'Ailsa Craig'. *Botanical Gazette*, **145**, 66–77.

Dick-Perez, M., Wang, T., Salazar, A., Zabotina, O. A. and Hong, M. (2012). Multidimensional Solid-State NMR Studies of the Structure and Dynamics of Pectic Polysaccharides in Uniformly 13 C-Labeled Arabidopsis Primary Cell Walls. *Magnetic resonance in chemistry*, **50**, 539–550.

Dietz, K.J., Hollenbach, B., Kirch, J. and Veit, M. (1994). Cell Type and Organelle-Specific Accumulation and Trans-Tonoplast Transport of Flavonoids in Barley Leaves. *Acta Horticulturae*, **8**, 109–112.

Dietz, K.J., Schramm, M., Lang, B., Lanzl-Schramm, A., Dürr, C. and Martinoia, E. (1992b). Characterization of the Epidermis from Barley Primary Leaves. *Planta*, **187**, 431–437.

Dietz, K. J., Schramm, M., Betz, M., Busch, H., Dürr, C. and Martinoia, E. (1992a). Characterization of the Epidermis from Barley Primary Leaves: I. Isolation of Epidermal Protoplasts. *Planta*, **187**, 425–430.

Dietz, K. J., Schramm, M., Lang, B., Lanzl-Schramm, A., Dürr, C. and Martinoia, E. (1992). Characterization of the Epidermis from Barley Primary Leaves: II. The Role of the Epidermis in Ion Compartmentation. *Planta*, **187**, 431–437.

Ding, B., Turgeon, R. and Parthasarathy, M. V. (1992). Substructure of Freeze-Substituted Plasmodesmata. *Protoplasma*, **169**, 28–41.

Dlugokencky, E. d and Tans, P. (2017). Trends in Atmospheric Carbon Dioxide: National Oceanic and Atmospheric Administration. *Earth System Research Laboratory (NOAA/ESRL); available at: http:// www.esrl.noaa.gov/gmd/ccgg/t*. *Nature Research.*

Dodd, A. N., Kudla, O. and Sanders, D. (2010). The Language of Calcium Signaling. *Annu. Rev. Plant Biol*, **61**, 593–620.

Drake, P., Froend, R. and Franks, P. (2013). Smaller, Faster Stomata: Scaling of Stomatal aperture, Rate of Response, and Stomatal Conductance. *Journal of Experimental* , **64**, 495–505.

Dunn, D. B., Sharma, G. K. and Campbell, C. C. (1965). Stomatal Patterns of Dicotyledons and Monocotyledons. *American Midland Naturalist*, **74**, 185–195.

Edwards, A. and Bowling, D. J. F. (1984). An Electrophysiological Study of the Stomatal Complex of *Tradescantia virginiana. Journal of Experimental Botany*, **35**, 562–567.

Edwards, D., Edwards, D. S. and Rayner, R. (1982). The Cuticle of Early Vascular Plants and its Evolutionary Significance. In *The Plant Cuticle*. Cutler DF eds, *Academic Press*, 341–361.

Edwards, D., Kerp, H. and Hass, H. (1998). Stomata in Early Land Plants: An Anatomical and Ecophysiological Approach. *Journal of experimental botany*, **49**, 255–278.

Edwards, M. and Meidner, H. (1977). Direct Measurements of Turgor Pressure Potentials: III. (A) Injections of Solutions into Stomatal Cells, and (B) Comparisons of Pressure Potentials in Stomatal Cells of Pressure Potentials in Stomatal Cells of Different Species. *Journal of Experimental Botany* , **28**, 669–677.

Edwards, M. and Meidner, H. (1978). Stomatal Responses to Humidity and the Water

Potentials of Epidermal and Mesophyll Tissue. *Journal of Experimental Botany*, **29**, 771–780.

Edwards, M. and Meidner, H. (1979). Direct Measurements of Turgor Pressure Potentials: IV. Naturally Occurring Pressures in Guard Cells and their Relation to Solute and Matric Potentials in the Epidermis. *Journal of Experimental Botany*, **30**, 829–837.

Edwards, M., Meidner, H. and Sheriff, D. W. (1976). Direct Measurements of Turgor Pressure Potentials of Guard Cells II. The Mechanical Advantage of Subsidiary Cells, the Spannunqsphase, and the Optimum Leaf Water Deficit. *Journal of experimental botany*, **27**, 163–171.

Ehlers, K. and Kollmann, R. (1996). Formation of Branched Plasmodesmata in Regenerating *Solanum nigrum*-Protoplasts. *Planta*, **199**, 126–128.

Ehlers, K. and Kollmann, R. (2001). Primary and Secondary Plasmodesmata: Structure, Origin, and Functioning. *Protoplasma*, **216**, 1–30.

Eichert, T. and Burkhardt, J. (2001). Quantification of Stomatal Uptake of Ionic Solutes Using a New Model System. *Journal of Experimental Botany*, **52**, 771–781.

Eichert, T., Goldbach, H. E. and Burkhardt, J. (1998). Evidence for the Uptake of Large Anions through Stomatal Pores. *Botanica Acta*, **111**, 461–466.

Eisenach, C. and De Angeli, A. (2017). Ion Transport at the Vacuole during Stomatal Movements. *Plant Physiology*, **174**, 520–530.

Eltayef, K. M. (2014). Water and Solute Relations of Salt stressed Wheat and Annual *Suaeda maritima.* PhD. Thesis, Prifysgol Bangor University, UK.

Emery, J., Floyd, S., Alvarez, J., Eshed, Y. and Hawker, N. (2003). Radial Patterning of *Arabidopsis* Shoots by Class III HD-ZIP and KANADI Genes. *Current Biology*, **13**, 1768–1774.

Emmerlich, V., Linka, N., Reinhold, T., Hurth, M. A., Traub, M., Martinoia, E. and Neuhaus, H. E. (2003). The Plant Homolog to the Human Sodium/dicarboxylic Cotransporter is the Vacuolar Malate Carrier. *Proceedings of the National Academy of Sciences of the United States of America*, **100**, 11122–11126.

Epimashko, S., Meckel, T., Fischer-Schliebs, E., Lüttge, U. and Thiel, G. (2004). Two Functionally Different Vacuoles for Static and Dynamic Purposes in One Plant Mesophyll Leaf Cell. *The Plant Journal*, **37**, 294–300.

Epstein, E. (1966). Dual Pattern of Ion Absorption by Plant Cells and by Plants. *Nature*, **212**, 1324–1327.

Epstein, E. (1972). Mineral Nutrition of Plants: Principles and Perspectives. New York: *Wiley.*

Ernest, E. C. M. (1935). Factors Rendering the Plasmolytic Method Inapplicable in the Estimation of Osmotic Values of Plant Cells. *Plant Physiology*, **10**, 553–558.

Erwee, M. G. and Goodwin, P. B. (1985). Symplast Domains in Extrastelar Tissues of *Egeria densa* Planch. *Planta*, **163**, 9–19.

Erwee, M., Goodwin, P. and Bel, A. (1985). Cell-Cell Communication in the Leaves of *Commelina cyanea* and Other Plants. *Plant, Cell and Environment*, **8**, 173–178.

Esau, K. (1977). Anatomy of Seed Plants. 2nd edn. New York: *John Wiley and Sons, Ltd.*

Fairley-Grenot, K. A. and Assmann, S. M. (1993). Comparison of K^+-Channel Activation and Deactivation in Guard Cells from a Dicotyledon (*Vicia faba* L.) and a Graminaceous Monocotyledon (*Zea mays*). *Planta*, **189**, 410–419.

Fan, L.M., Zhao, Z. and Assmann, S. M. (2004). Guard Cells: A Dynamic Signaling Model. *Current opinion in plant biology*, **7**, 537–546.

Fanourakis, D., Carvalho, S. M. P., Almeida, D. P. F. and Heuvelink, E. (2011). Avoiding High Relative Air Humidity during Critical Stages of Leaf Ontogeny is Decisive for Stomatal Functioning. *Physiologia Plantarum*, **142**, 274–286.

Faraday, D. C. (1982). Comparative Ultrastructure of Guard Cells of C3, C4, and CAM Plants. In Ting, I.P and Gibbs, M. edn *Crassulacean Acid Metabolism*. maryland, USA, *American Society of Plant Physiologists*, 18–30.

Farquhar, G. D. and Sharkey, T. D. (1982). Stomatal Conductance and Photosynthesis., *Annual review of plant physiology*, **33**, 317–345.

Felle, H. H. (1993). Ion-Selective Microelectrodes: Their Use and Importance in Modern Plant Cell Biology. *Botanica Acta*, **106**, 5–12.

Felle, H. H., Hanstein, S., Steinmeyer, R. and Hedrich, R. (2000). Dynamics of Ionic Activities in the Apoplast of the Sub-Stomatal Cavity of Intact *Vicia faba* Leaves during Stomatal Closure Evoked by ABA and Darkness. *The Plant Journal*, **24**, 297–304.

Ferguson, C. and Simon, E. (1973). Membrane Lipids in Senescing Green Tissues. *Journal of Experimental Botany*, **24**, 307–316.

Ferrer, J.L., Austin, M. B., Stewart, C. and Noel, J. P. (2008). Structure and Function of Enzymes Involved in the Biosynthesis of Phenylpropanoids. *Plant Physiology and Biochemistry*, **46**, 356–370.

Finkelstein, R. (2013). Abscisic Acid Synthesis and Response. *The Arabidopsis Book*. *American Society of Plant Biologists* , **11**, e0166.

Finley, D. S. (1999). Patterns of Calcium Oxalate Crystals in Young Tropical Leaves: A Possible Role as an Anti-Herbivory Defence. *Revista de Biología Tropical*. *Universidad de Costa Rica*, **47**, 27–31.

Fischer, R. A. (1968a). Stomatal Opening: Role of Potassium Uptake by Guard Cells. *Science*, **160**, 784–785.

Fischer, R. A. (1968b). Stomatal Opening in Isolated Epidermal Strips of *Vicia faba*. I. Response to Light and to CO_2-Free Air. *Plant Physiol*, **43**, 1947–1952.

Fischer, R. A. (1973). The Relationship of Stomatal Aperture and Guard Cell Turgor Pressure in *Vicia faba*. *Journal of experimental botany*, **24**, 387–399.

Fischer, R. A. and Hsiao, T. C. (1968). Stomatal Opening in Isolated Epidermal Strips of *Vicia faba*. II. Responses to KCl Concentration and the Role of Potassium Absorption. *Plant Physiol*, **43**, 1953–1958.

Fischer, R. A. (1971). Role of Potassium in Stomatal Opening in the Leaf of *Vicia faba. Plant Physiol*, **47**, 555–558.

Fitzsimons, P. and Weyers, J. (1986). Volume Changes of *Commelina communis* Guard Cell Protoplasts in Response to K^+, Light and CO_2.. *Physiologia plantarum*, **66**, 463–468.

Fleischer, A., O'Neill, M. A. and Ehwald, R. (1999). The Pore Size of Non-

Graminaceous Plant Cell Walls is Rapidly Decreased by Borate Ester Cross-Linking of the Pectic Polysaccharide Rhamnogalacturonan II. *Plant physiology*, **121**, 829–838.

Fleurat-Lessard, P., Frangne, N., Maeshima, M., Ratajczak, R., Bonnemain, J. L. and Martinoia, E. (1997). Increased Expression of Vacuolar Aquaporin and H^+-ATPase Related to Motor Cell Function in *Mimosa pudica* L. *Plant Physiology*, **114**, 827–834.

Fowler, J. E. and Freeling, M. (1996). Genetic Analysis of Mutations that Alter Cell Fates in Maize Leaves: Dominant Liguleless Mutations. *Developmental genetics*, **18**, 198–222.

Francesca, B. and Malone, M. (1993). Wound-Induced Hydraulic Signals: Survey of Occurrence in a Range of Species. *Journal of experimental Biology*, **261**, 741–746.

Franks, P. J. and Beerling, D. J. (2009). Maximum Leaf Conductance Driven by CO_2 Effects on Stomatal aperture and Density Over Geologic Time. *Proceedings of the National Academy of Sciences of the United States of America*, **106**, 10343–10347.

Franks, P. J., Cowan, I. R. and Farquhar, G. D. (1998). A Study of Stomatal Mechanics Using the Cell Pressure Probe. *Plant, Cell and Environment*, **21**, 94–100.

Franks, P. J., Cowan, I. R., Tyerman, S. D., Cleary, A. L., Lloyd, J. and Farquhar, G. D. (1995). Guard Cell Pressure/Aperture Characteristics Measured with the Pressure Probe, *Plant, Cell and Environment*, **18**, 795–800.

Frechilla, S., Talbott, L. D., Bogomolni, R. A. and Zeiger, E. (2000). Reversal of Blue Light-Stimulated Stomatal Opening by Green Light. *Plant CellPhysiol*, **41**, 171–176.

Frechilla, S., Zhu, J., Talbott, L. D. and Zeiger, E. (1999). Stomata from Npql, a Zeaxanthin-Less *Arabidopsis* Mutant, Lack a Specific Response to Blue Light. *Plant Cell Physiol*, **40**, 949–954.

Freeling, M. (1992). A Conceptual Framework for Maize Leaf Development. *Developmental biology*, **153**, 44–58.

Frey, B., Keller, C. and Zierold, K. (2000). Distribution of Zn^{2+} in Functionally Different Leaf Epidermal Cells of the Hyperaccumulator *Thlaspi caerulescens. Plant, Cell and Environment*, **23**, 675–687.

Fricke, W. (2004). Solute Sorting in Grass Leaves: The Transpiration Stream. *Planta*, **219**, 507–514.

Fricke, W., Hinde, P. S., Leigh, R. A. and Tomos, A. D. (1995). Vacuolar Solutes in the Upper Epidermis of Barley Leaves: Intercellular Differences Follow Patterns. *Planta*, **196**, 40–49.

Fricke, W., Leigh, R. A. and Tomos, A. D. (1994a). Concentrations of Inorganic and Organic Solutes in Extracts from Individual Epidermal, Mesophyll and Bundle-Sheath Cells of Barley Leaves. *Planta*, **192**, 310–316.

Fricke, W., Leigh, R. A. and Tomos, A. D. (1994b). Epidermal Solute Concentrations and Osmolality in Barley Leaves Studied at the Single-Cell Level. *Planta*, **192**, 317–323.

Fricke, W., Leigh, R. A. and Tomos, A. D. (1996). The Intercellular Distribution of Vacuolar Solutes in the Epidermis and Mesophyll of Barley Leaves Changes in Response to NaCl. *Journal of Experimental Botany*, **47**, 1413–1426.

Fricke, W., Pritchard, J., Leigh, R. A. and Tomos, A. D. (1994c). Cells of the Upper and

Lower Epidermis of Barley (*Hordeum Vulgare* L.) Leaves Exhibit Distinct Patterns of Vacuolar Solutes. *Plant Physiol*, **104**, 1201–1208.

Fried, M., Hagen, C., Rio, J. Del and Leggett, J. (1957). Kinetics of Phosphate Uptake in the Soil-Plant System. *Soil Science*, **84**, 427–438.

Fujino, M. (1959). Stomatal Movement and Active Migration of Potassium. *Kagaku*, **29**, 660–661.

Fujino, M. (1967). Role of Adenosinetriphosphate and Adenosinetriphosphatase in Stomatal Movement. *Sci. Bull. Pac. Educ, Nagasaki Univ.*, **18**, 1–47.

Galatis, B. (1980). Microtubules and Guard-Cell Morphogenesis in Zea Mays L. *Journal of Cell Science*, **45**, 211–244.

Galinat, W. C. (1959). The Phytomer in Relation to Floral Homologies in the American *Maydeae. Botanical Museum Leaflets, Harvard University*, **19**, 1–32.

Gao, Y.Q., Wu, W.H. and Wang, Y. (2017). The K^+ Channel KZM2 is Involved in Stomatal Movement by Modulating Inward K^+ Currents in Maize Guard Cells. *The Plant Journal*, **92**, 662–675.

Garnier, E. and Laurent, G. (1994). Leaf Anatomy, Specific Mass and Water Content in Congeneric Annual and Perennial Grass Species. *New Phytologist*. **128**, 725–736.

Gassmann, W., Rubio, F. and Schroeder, J. I. (1996). Alkali Cation Selectivity of the Wheat Root High-Affinity Potassium Transporter HKT1. *The Plant Journal*, **10**, 869–882.

Gaxiola, R. A., Rao, R., Sherman, A., Grisafi, P., Alper, S. L. and Fink, G. R. (1999). The *Arabidopsis thaliana* Proton Transporters, AtNhx1 and Avp1, can Function in Cation Detoxification in Yeast. *Proceedings of the National Academy of Sciences of the United States of America*, **96**, 1480–5.

Gay, A. P. and Hurd, R. G. (1975). The Influence of Light on Stomatal Density in the Tomato. *New Phytologist*, **75**, 37–46.

Geiger, D., Maierhofer, T., AL-Rasheid, K. A. S., Scherzer, S., Mumm, P., Liese, A., Ache, P., Wellmann, C., Marten, I., Grill, E., Romeis, T. and Hedrich, R. (2011). Stomatal Closure by Fast Abscisic Acid Signaling is Mediated by the Guard Cell Anion Channel SLAH3 and the Receptor RCAR1. *Science Signaling*, **4,** 32-45.

Geisler, M., Nadeau, J. and Sack, F. D. (2000). Oriented Asymmetric Divisions that Generate the Stomatal Spacing Pattern in *Arabidopsis* are Disrupted by the Too Many Mouths Mutation. *The Plant Cell*, **12**, 2075–2086.

Gepstein, S., Jacobs, M. and Taiz, L. (1982). Inhibition of Stomatal Opening in *Vicia faba* Epidermal Tissue by Vanadate and Abscisic Acid. *Plant Science Letters*, **28**, 63–72.

Gilroy, S., Hughes, W. A. and Trewavas, A. J. (1989). A Comparison between Quin-2 and Aequorin as Indicators of Cytoplasmic Calcium Levels in Higher Plant Cell Protoplasts. *Plant Physiol*, **90**, 482–491.

Gindel, I. (1969). Stomata Constellation in the Leaves of Cotton, Maize and Wheat Plants as a Function of Soil Moisture and Environment. *Physiologia Plantarum*, **22**, 1143–1151.

Glinka, Z. (1971). The Effect of Epidermal Cell Water Potential on Stomatal Response to Illumination of Leaf Discs of *Vicia faba. Physiologia Plantarum*, **24**, 476–479.

Glover, B. J. (2000). Differentiation in Plant Epidermal Cells. *Journal of experimental botany*,

51, 497–505.

Glover, B. J., Perez-Rodriguez, M. and Martin, C. (1998). Development of Several Epidermal Cell Types can be Specified by the Same MYB-Related Plant Transcription Factor. *Development*, **125**, 3497–3508.

Gobert, A., Isayenkov, S., Voelker, C., Czempinski, K. and Maathuis, F. J. M. (2007) .The Two-Pore Channel TPK1 Gene Encodes the Vacuolar K^+ Conductance and Plays a Role in K^+ Homeostasis. *Proceedings of the National Academy of Sciences of the United States of America*, **104**, 10726–10731.

Gonzalez, E., Arrese-Igor, C. and Aparicio-Tejo, P. (2002). Solute Heterogeneity and Osmotic Adjustment in Different Leaf Structures of Semi-Leafless Pea (*Pisum sativum* L.) Subjected to Water Stress. *Plant*, **4**, 558–566.

Gonzalez, R. and Markham, K. (1994). Sediment-Based Carbon Nutrition in Tropical Alpine *Isoetes* , In *Tropical alpine environments: plant form and function,* Rundel PW, *Cambridge University Press*, 167–194.

Goodwin, P. B. (1983). Molecular Size Limit for Movement in the Symplast of the *Elodea* Leaf. *Planta*, **157**, 124–130.

Goodwin, P. and Erwee, M. (1990). Compartmentation of Fluorescent Tracers Injected into the Epidermal Cells of *Egeria densa* Leaves. *Planta*, **181**, 129–136.

Gray, J., Holroyd, G., Lee, F. Van Der and Bahrami, A. (2000). The HIC Signalling Pathway Links CO_2 Perception to Stomatal Development. *Nature*, **408**, 713–716.

Green, P. and Stanton, F. (1967). Turgor Pressure: Direct Manometric Measurement in Single Cells of *Nitella*. *Science*, **155**, 1675–1676.

Guo, F.Q., Young, J. and Crawford, N. M. (2003). The Nitrate Transporter AtNRT1.1 (CHL1) Functions in Stomatal Opening and Contributes to Drought Susceptibility in *Arabidopsis. The Plant Cell*, **15**, 107–117.

Gupta, B. (1961). Correlation of Tissues in Leaves: 2. Absolute Stomatal Numbers. *Annals of Botany*, **25**, 71–77.

Ha, C. M., Kim, G. T., Kim, B. C., Jun, J. H., Soh, M. S., Ueno, Y., Machida, Y., Tsukaya, H. and Nam, H. G. (2003). The Blade-On-Petiole 1 Gene Controls Leaf Pattern Formation through the Modulation of Meristematic Activity in *Arabidopsis. Development*, **130**, 161–172.

Hake, S. and Freeling, M. (1986). Analysis of Genetic Mosaics Shows that the Extra Epidermal Cell Divisions in Knotted Mutant Maize Plants are Induced by Adjacent Mesophyll Cells. *Nature*, **320**, 621–623.

Hake, S., Vollbrecht, E. and Freeling, M. (1989). Cloning Knotted, the Dominant Morphological Mutant in Maize Using Ds2 as a Transposon Tag, *The EMBO journal*, **8**, 15–22.

Hall, J. L. and Flowers, T. J. (1973). The Effect of Salt on Protein Synthesis in the Halophyte *Suaeda maritima. Planta*, **110**, 361–368.

Hamilton, D. W., Hills, A., Kohler, B. and Blatt, M. R. (2000). Ca^{2+} Channels at the Plasma Membrane of Stomatal Guard Cells are Activated by Hyperpolarization and Abscisic Acid. *Proceedings of the National Academy of Sciences of the United States of America*, **97**, 4967–4972.

Han, S., Tang, R., Anderson, L. K., Woerner, T. E. and Pei, Z.M. (2003). A Cell Surface

Receptor Mediates Extracellular Ca^{2+} Sensing in Guard Cells. *Nature*, **425**, 196–200.

Hanes, C. S. (1940). The Reversible Formation of Starch from Glucose-1-Phosphate Catalysed by Potato Phosphorylase. *Proceedings of the Royal Society of London B: Biological Sciences*, **129**, 174–208.

Harberd, N. P. and Freeling, M. (1989). Genetics of Dominant Gibberellin-Insensitive Dwarfism in Maize. *Genetics*, **121**, 827–838.

Hareven, D., Gutfinger, T., Parnis, A., Eshed, Y. and Lifschitz, E. (1996). The Making of a Compound Leaf: Genetic Manipulation of Leaf Architecture in Tomato. *Cell*, **84**, 735–744.

Hasegawa, P. M. (2013). Sodium (Na^+). Homeostasis and Salt Tolerance of Plants. *Environmental and Experimental Botany*, **92**, 19–31.

Haseloff, J. and Siemering, K. R. (2006). The Uses of Green Fluorescent Protein in Plants. *Methods Biochem. Anal*, **47**, 259–284.

Haseloff, J., Siemering, K. R., Prasher, D. C. and Hodge, S. (1997). Removal of a Cryptic Intron and Subcellular Localization of Green Fluorescent Protein are Required to Mark Transgenic *Arabidopsis* Plants Brightly. *Applied Biological Sciences*, **94**, 2122–2127.

Hashimoto, M., Negi, J., Young, J. and Israelsson, M. (2006). *Arabidopsis* HT1 Kinase Controls Stomatal Movements in Response to CO_2. *Nature cell*, **8**, 391–397.

Hasselbalch, K. A. (1916). The Calculation of Blood pH via the Partition of Carbon Dioxide in Plasma and Oxygen Binding of the Blood as a Function of Plasma pH. *Biochem Z*, **78**, 112–144.

He, Z. H., Fujiki, M. and Kohorn, B. D. (1996). A Cell Wall-Associated, Receptor-like Protein Kinase. *The Journal of biological chemistry*, **271**, 19789–19793.

Heath, O. V. S. (1938). An Experimental Investigation of the Mechanism of Stomatal Movement, with Some Preliminary Observations upon the Response of the Guard Cells to “Shock”. *New Phytologist*, **37**, 385–395.

Heath, O. V. S. (1975). Stomata. 1st edn. Edited by J. Head. London, *Oxford University Press London,* UK.

Hedrich, R., Busch, H., Becker, D., Gambale, F., Dreyer, I., Kiich, A., Neuwinger, K. and Palme, K. (1995). Inward Rectifier Potassium Channels in Plants Differ from their Animal Counterparts in Response to Voltage and Channel Modulators. *European Biophysics Journal*, **24**, 107–115.

Hedrich, R., Busch, H. and Raschke, K. (1990). Ca^{2+} and Nucleotide Dependent Regulation of Voltage Dependent Anion Channels in the Plasma Membrane of Guard Cells. *The EMBO Journal*, **9**, 3889–3892.

Hedrich, R. and Marten, I. (1993). Malate-Induced Feedback Regulation of Plasma Membrane Anion Channels Could Provide a CO_2 Sensor to Guard Cells. *The EMBO Journal*, **12**, 897–901.

Hedrich, R., Marten, I., Lohse, G., Dietrich, P., Winter, H., Lohaus, G. and Heldt, H. H.-W. (1994). Malate-sensitive Anion Channels Enable Guard Cells to Sense Changes in the Ambient CO_2 Concentration. *The Plant Journal*, **6**, 741–748.

Heisler, M., Ohno, C., Das, P., Sieber, P. and Reddy, G. (2005). Patterns of Auxin Transport and Gene Expression during Primordium Development Revealed by Live Imaging of the

Arabidopsis Inflorescence Meristem. *Current biology*, **15**, 1899–1911.

Hepler, P. (1982). Endoplasmic Reticulum in the Formation of the Cell Plate and Plasmodesmata. *Protoplasma*, **111**, 121–133.

Hernandez, M., Passas, H. and Smith, L. (1999). Clonal Analysis of Epidermal Patterning during Maize Leaf Development. *Developmental biology*, **216**, 646–658.

Hetherington, A. M. and Woodward, I. F. (2003). The Role of Stomata in Sensing and Driving Environmental Change. *Nature*, **424**, 901–908.

Hew, C. S., Lee, G. L. and Wong, S. C. (1980). Occurrence of Non-Functional Stomata in the Flowers of Tropical Orchids. *Ann Bot.*, **46**, 195–201.

Hill, B. and Findlay, G. (1981). The Power of Movement in Plants: The Role of Osmotic Machines. *Quarterly reviews of biophysics*, **14**, 173–222.

Hinde, P. (1994). The Role of Potassium as an Osmoticum in Barley Leaf Cells. *PhD.Thesis,* Prifysgol Bangor University, UK.

Hirsch, R. E., Lewis, B. D., Spalding, E. P. and Sussman, M. R. (1998). A Role for the AKT1 Potassium Channel in Plant Nutrition. *Science*, **280**, 918–921.

Hirschi, K. D., Zhent, R.-G., Cunningham, K. W., Reat, P. A. and Fink, G. R. (1996). CAX1, an H^+/Ca^{2+} Antiporter from *Arabidopsis. Plant Biology*, **93**, 8782–8786.

Hjerten, S., Ferenc Kilar, K. E., Liao, J.L., Chen, A. J. C., Siebert, C. J. and Zhu, M.D. (1987). Carrier-Free Zone Electrophoresis, Displacement Electrophoresis and Isoelectric Focusing in a High-Performance Electrophoresis Apparatus. *Journal of Chromatography*, **403**, 47–61.

Horner, H. T., Healy, R. A., Cervantes-Martinez, T. and Palmer, R. G. (2003). Floral Nectary Fine Structure and Development in *Glycine max* L.(Fabaceae). *International journal of plant sciences*, **164**, 675–690.

Hosy, E., Vavasseur, A. and Mouline, K. (2003). The *Arabidopsis* Outward K^+ Channel, GORK, is Involved in Regulation of Stomatal Movements and Plant Transpiration. *Proceedings of the National Academy of Sciences of the United States of America*, **100**, 5549–5554.

Hsiao, T. C., Allaway, W. G. and Evans, L. T. (1973). Action Spectra for Guard Cell Rb^+ Uptake and Stomatal Opening in *Vicia faba. Plant Physiol*, **51**, 82–88.

http 1 (2006). University of Rhode Island CHM 112 Home Page. *Chemistry 112.*

Hu, H., Boisson-Dernier, A. and Israelsson-Nordström, M. (2010). Carbonic Anhydrases are Upstream Regulators of CO_2-Controlled Stomatal Movements in Guard Cells. *Nature Cell*, **12**, 87–93.

Huffaker, R. and Wallace, A. (1959). Sodium Absorption by Different Plant Species at Different Potassium Levels. *Soil Science*, **87**, 130–134.

Humble, G. D. and Hsiao, T. C. (1969). Specific Requirement of Potassium for Light-Activated Opening of Stomata in Epidermal Strips. *Plant Physiol*, **44**, 230–234.

Humble, G. D. and Raschke, K. (1971). Stomatal Opening Quantitatively Related to Potassium Transport: Evidence from Electron Probe Analysis. *Plant Physiology*, **48**, 447–453.

Hüsken, D., Steudle, E., Zimmermann, U., Husken, D., Steudle, E. and Zimmermann, U. (1978). Pressure Probe Technique for Measuring Water Relations of Cells in Higher Plants. *Plant Physiology*, **61**, 158–163.

Iino, M., Long, C. and Wang, X. (2001). Auxin-and Abscisic Acid-Dependent Osmoregulation in Protoplasts of *Phaseolus vulgaris* Pulvini. *Plant Cell Physiol*, **42**, 1219–1227.

Ilan, N., Moran, N. and Schwartz, A. (1995). The Role of Potassium Channels in the Temperature Control of Stomatal Aperture. *Plant physiology*, **108**, 1161–1170.

Irving, H. R., Gehring, C. A. and Parish, R. W. (1992). Changes in Cytosolic pH and Calcium of Guard Cells Precede Stomatal Movements. *Proceedings of the National Academy of Sciences of the United States of America*, **89**, 1790–1794.

Irving, M. S. (1996). Reversible Plant Movement Studied at Single Cell Resolution. PhD. Thesis, Prifysgol Bangor University, UK.

Irving, M. S., Ritter, S., Tomos, A. D. and Koller, D. (1997). Phototropic Response of the Bean Pulvinus: Movement of Water and Ions. *Botanica Acta*, **110**, 118–126.

Ishikawa, H., Aizawa, H., Kishira, H., Ogawa, T. and Sakata, M. (1983). Light-Induced Changes of Membrane Potential in Guard Cells of *Vicia faba. Plant and Cell Physiol*, **24**, 769–772.

Itai, C., Roth-Bejerano, N. and Zvilich, M. (1982). Involvement of Epidermal Cells in Stomatal Movement: The Effect of ABA. *Physiologia Plantarum*, **55**, 35–38.

Ivashikina, N. and Hedrich, R. (2005). K^+ Currents through SV-Type Vacuolar Channels are Sensitive to Elevated Luminal Sodium Levels. *The Plant Journal*, **41**, 606–614.

Jackson, D. (1996). Plant Morphogenesis: Designing Leaves. *Current Biology*, **6**, 917–919.

Jackson, D., Veit, B. and Hake, S. (1994). Expression of Maize Knotted1 Related Homeobox Genes in the Shoot Apical Meristem Predicts Patterns of Morphogenesis in the Vegetative Shoot. *Development*, **120**, 405–413.

Jacoby, B. and Dagan, J. (1969). Effects of Age on Sodium Fluxes in Primary Bean Leaves. *Physiologia Plantarum*, **22**, 29–36.

James, J. J., Alder, N. N., Mühling, K. H., Läuchli, A. E., Shackel, K. A., Donovan, L. A. and Richards, J. H. (2006). High Apoplastic Solute Concentrations in Leaves Alter Water Relations of the Halophytic Shrub. *Sarcobatus vermiculatus*, *Journal of Experimental Botany*, **57**, 139–147.

Jarvis, P. G. and Morison, J. I. L. (1981). The Control of Transpiration and Photosynthesis by the Stomata. In PG *et al*. edn *Stomatal physiology*. SEB Semina. *Cambridge University Press, Cambridge UK*, 247–279.

Jasinski, S., Piazza, P., Craft, J., Hay, A., Woolley, L. and Rieu, I. (2005). KNOX Action in *Arabidopsis* is Mediated by Coordinate Regulation of Cytokinin and Gibberellin Activities, *Current Biology*, **15**, 1560–1565.

Jauh, G. Y., Phillips, T. E. and Rogers, J. C. (1999). Tonoplast Intrinsic Protein Isoforms as Markers for Vacuolar Functions. *The Plant Cell*, **11**, 1867–1882.

Javelle, M., Vernoud, V., Rogowsky, P. M. and Ingram, G. C. (2011). Epidermis: The Formation and Functions of a Fundamental Plant Tissue. *New Phytologist*, **189**, 17–39.

Jellings, A. J. and Leech, R. M. (1984). Anatomical Variation in First Leaves of Nine

Tritucum Genotypes, and its Relationship to Photosynthetic Capacity. *New Phytologist*, **96**, 371–382.

Jenkins, G. I. (1998). Signal Transduction Networks and the Integration of Responses of Environmental Stimuli. *Advances in Botanical Research*, **29**, 53–73.

Jinno, N. and Kuraishi, S. (1982). Acid-Induced Stomatal Opening in *Commelina communis* and *Vicia faba*. *Plant Cell Physiol.*, **23**, 1169–1174.

Johansson, F., Sommarin, M. and Larsson, C. (1993). Fusicoccin Activates the Plasma Membrane H^+-ATPase by a Mechanism Involving the C-Terminal Inhibitory Domain. *The Plant Cell*, **5**, 321–327.

Johansson, G., Isaksson, R. and Harang, V. (2003). Migration Time and Peak Area Artifacts Caused by Systemic Effects in Voltage Controlled Capillary Electrophoresis. *Journal of Chromatography A*, **1004**, 91–98.

Jones, L., Milne, J., Ashford, D. and McQueen-Mason, S. (2003). Cell Wall Arabinan is Essential for Guard Cell Function. *Proceedings of the National Academy of Sciences of the United States of America*, **100**, 11783–11788.

Jorgenson, J. W. and Lukács, K. D. (1981). Zone Electrophoresis in Open-Tubular Glass Capillaries. *Anal. Chem*, **53**, 1298–1302.

Jossier, M., Kroniewicz, L., Dalmas, F., Le Thiec, D., Ephritikhine, G., Thomine, S., Barbier-Brygoo, H., Vavasseur, A., Filleur, S. and Leonhardt, N. (2010). The *Arabidopsis* Vacuolar Anion Transporter, AtCLCc, is Involved in the Regulation of Stomatal Movements and Contributes to Salt Tolerance. *The Plant Journal*, **64**, 563–576.

Jungk, A. (2001). Root Hairs and the Acquisition of Plant Nutrients from Soil. *Journal of Plant Nutrition and Soil Science*. *Wiley-vch Verlag GmbH*, **164**, 121–129.

Kahn, J. and Hanson, J. (1957). The Effect of Calcium on Potassium Accumulation in Corn and Soybean Roots. *Plant physiology*, **32**, 312–316.

Kalisky, T. and Quake, S. R. (2011). Single-Cell Genomics. *Nature methods*, **8**, 311–314.

Kalve, S., Vos, D. De and Beemster, G. T. S. (2014). Leaf Development: A Cellular Perspective. *Frontiers in plant science*, **5**, 1-25.

Kang, J., Hwang, J., Lee, M. and Kim, Y. (2010). PDR-Type ABC Transporter Mediates Cellular Uptake of the Phytohormone Abscisic Acid. *Proceedeings of the National Academy of Sciences of the United States of America*, **107**, 2355–2360.

Karley, A. J., Leigh, R. A. and Sanders, D. (2000a). Where Do All The Ions Go? The Cellular Basis of Differential Ion Accumulation in Leaf Cells. *Trends in Plant Science*, **5**, 465–470.

Karley, A., Leigh, R. and Sanders, D. (2000b). Differential Ion Accumulation and Ion Fluxes in the Mesophyll and Epidermis of Barley, *Plant Physiology*, **122**, 835–844.

Keeley, J. E., Osmond, C. B. and Raven, J. A. (1984). Stylites, a Vascular Land Plant without Stomata Absorbs CO_2 via its Roots. *Nature*, **310**, 694–695.

Keller, B. U., Hedrich, R. and Raschke, K. (1989). Voltage-Dependent Anion Channels in the Plasma Membrane of Guard Cells. *Nature*, **341**, 450–453.

Kenrick, P. and Crane, P. (1997). The Origin and Early Evolution of Plants on Land. *Nature*, **389**, 33–39.

Kerstetter, R., Bollman, K., Taylor, R. and Bomblies, K. (2001). KANADI Regulates Organ Polarity in *Arabidopsis. Nature*, **411**, 706–709.

Kim, T.-H., Böhmer, M., Hu, H., Nishimura, N. and Schroeder, J. I. (2010). Guard Cell Signal Transduction Network: Advances in Understanding Abscisic Acid, CO_2, and Ca^{2+} Signaling. *Annual review of plant biology*, **61**, 561–91.

King, L. S., Kozono, D. and Agre, P. (2004). From Structure to Disease: The Evolving Tale of Aquaporin Biology. *Nature*, **5**, 687–698.

Kinoshita, T. and Shimazaki, K. (1999). Blue Light Activates the Plasma Membrane H^+-ATPase by Phosphorylation of the C-Terminus in Stomatal Guard Cells. *The EMBO Journal*, **18**, 5548–5558.

Van Kirk, C. A. and Raschke, K. (1978a). Presence of Chloride Reduces Malate Production in Epidermis during Stomatal Opening. *Plant Physiol*, **61**, 361–364.

Van Kirk, C. A. and Raschke, K. (1978b). Release of Malate from Epidermal Strips during Stomatal Closure. *Plant Physiol*, **61**, 474–475.

Kirschbaum, M. U. F., Gross, L. J. and Pearcy, R. W. (1988). Observed and Modelled Stomatal Responses to Dynamic Light Environments in the Shade Plant Alocasia Macrorrhiza. *Plant, cell & environment*, **11**, 111–121.

Klein, M., Cheng, G., Chung, M. and Tallman, G. (1996). Effects of Turgor Potentials of Epidermal Cells Neighbouring Guard Cells on Stomatal Opening in Detached Leaf Epidermis and Intact Leaflets of *Vicia faba* L. (Faba Bean). *Plant, Cell and Environment*, **19**, 1399–1407.

Knox, J. P. (1997). The Use of Antibodies to Study the Architecture and Developmental Regulation of Plant Cell Walls. *Academic Press*, **171**, 79–120.

Kolb, H.-A., Marten, I. and Hedrich, R. (1995). Hodgkin-Huxley Analysis of a GCAC1 Anion Channel in the Plasma Membrane of Guard Cells. *J. Membrane Biol*, **146**, 273–282.

Koller, D., Ritter, S. and Heller, E. (2001). Light-Driven Movements of the Primary Leaves of Bean (*Phaseolus vulgaris* L.): A Kinetic Analysis. *Israel Journal of Plant Sciences*, **49**, 2–7.

Kollist, H., Nuhkat, M. and Roelfsema, M. R. G. (2014). Closing Gaps: Linking Elements that Control Stomatal Movement. *New Phytologist*, **203**, 44–62.

Kondo, N. and Maruta, I. (1987). Abscisic Acid-Induced Stomatal Closure in *Vicia faba* Epidermal Strips. Excretion of Solutes from Guard Cells and Increase in Elastic Modulus of Guard Cell Wall. *Plant Cell Physiology*, **28**, 355–364.

Korn, R. W. (1972). Arrangement of Stomata on the Leaves of *Pelargonium zonale* and *Sedum stahlii. Annals of Botany*, **36**, 325–333.

Koroleva, O. A., Farrar, J. F., Deri Tomos, A. and Pollock, C. J. (1998). Carbohydrates in Individual Cells of Epidermis, Mesophyll, and Bundle Sheath in Barley Leaves with Changed Export or Photosynthetic Rate. *Plant Physiology*, **118**, 1525–1532.

Koroleva, O. A., Tomos, A. D., Farrar, J., Roberts, P. and Pollock, C. J. (2000). Tissue Distribution of Primary Metabolism between Epidermal, Mesophyll and Parenchymatous Bundle Sheath Cells in Barley Leaves. *Functional Plant Biology*, **27**, 747–755.

Koroleva, O., Farrar, J. and Tomos, A. (1997). Patterns of Solute in Individual Mesophyll,

Bundle Sheath and Epidermal Cells of Barley Leaves Induced to Accumulate Carbohydrate. *The New Phytologist*, **136**, 97–104.

Kuiper, P. (1964). Dependence upon Wavelength of Stomatal Movement in Epidermal Tissue of *Senecio odoris. Plant Physiology*, **39**, 952–955.

Küpper, H., Jie Zhao, F. and McGrath, S. P. (1999). Cellular Compartmentation of Zinc in Leaves of the Hyperaccumulator *Thlaspi caerulescens. Plant Physiology*, **119**, 305–311**.**

Kurkdjian, A. and Guern, J. (1989). Intracellular pH: Measurement and Importance in Cell Activity. *Annu. Rev. Plant Physiol*, **40**, 271–303.

Kutik, J. (1973). The Relationships between Quantitative Characteristics of Stomata and Epidermal Cells of Leaf Epidermis, *Biologia Plantarum*, **15**, 324–328.

Kwak, J. M., Murata, Y., Baizabal-Aguirre, V. M., Merrill, J., Wang, M., Kemper, A., Hawke, S. D., Tallman, G. and Schroeder, J. I. (2001). Dominant Negative Guard Cell K^+ Channel Mutants Reduce Inward-Rectifying K^+ Currents and Light-Induced Stomatal Opening in *Arabidopsis. Plant Physiology*, **127**, 473–485.

Laisk, A. G. U., Oja, V. and Kull, K. (1980). Statistical Distribution of Stomatal Apertures of *Vicia faba* and *Hordeum vulgare* and the Spannungsphase of Stomatal Opening. *Journal of experimental botany*, **31**, 49–58.

Lake, J. A. and Woodward, F. I. (2008). Response of Stomatal Numbers to CO_2 and Humidity: Control by Transpiration Rate and Abscisic Acid. *New Phytologist*, **179**, 397–404.

Lange, O. L., Lösch, R., Schulze, E.D. and Kappen, L. (1971). Responses of Stomata to Changes in Humidity. *Planta*, **100**, 76–86.

Lang-Pauluzzi, I. (2000). The Behaviour of the Plasma Membrane during Plasmolysis: A Study by UV Microscopy. *Journal of Microscopy*, **198**, 188–198.

Larkin, J. C., Marks, M. D., Nadeau, J. and Sack, F. (1997). Epidermal Cell Fate and Patterning in Leaves. *The Plant Cell*, **9**, 1109–1120.

Lawson, T. (2009). Guard Cell Photosynthesis and Stomatal Function. *New Phytologist*, **181**, 13–34.

Lefebvre, D. D. (1985). Stomata on the Primary Root of *Pisum sativum* L. *Annals of Botany*, **55**, 337–341.

Leigh, R. A. (1997). Solute Composition of Vacuoles. *Advances in Botanical Research*, **25**, 171–194.

Leigh, R. A. and Storey, R. (1993). Intercellular Compartmentation of Ions in Barley Leaves in Relation to Potassium Nutrition and Salinity. *Journal of experimental botany*, **44**, 755–762.

Leigh, R. A. and Tomos, A. D. (1993). Ion Distribution in Cereal Leaves: Pathways and Mechanisms. *Philosophical Transactions: Biological Sciences, Royal Society*, **341**, 75–86.

Leigh, R. A., Walker, D. J. and Miller, A. J. (1996). Potassium Homeostasis in Vacuolate Plant Cells. *Proceedings of the National Academy of Sciences of the United States of America*, **93**, 10510–10514.

Leigh, R. A. and Wyn Jones, R. G. (1984.) A Hypothesis Relating Critical Potassium Concentrations for Growth to the Distribution and Functions of this Ion in the Plant Cell. *New Phytologist*, **97**, 1–13.

Leigh, R., Chater, M. and Storey, R. (1986). Accumulation and Subcellular Distribution of Cations in Relation to the Growth of Potassium-Deficient Barley. *Plant, Cell and Development*, **9**, 595–604.

Levchenko, V., Konrad, K. R., Dietrich, P., Roelfsema, M. R. G. and Hedrich, R. (2005). Cytosolic Abscisic Acid Activates Guard Cell Anion Channels Without Preceding Ca^{2+} Signals. *Proceedings of the National Academy of Sciences of the United States of America*, **102**, 4203–4208.

Levitt, J. (1967). The Mechanism of Stomatal Action. *Planta*, **74**, 101–118.

Levitt, J. (1974). The Mechanism of Stomatal Movement--Once More, *Protoplasma*, **82**, 1–17.

Leymarie, J., Vavasseur, A. and Lascève, G. (1998). CO_2 Sensing in Stomata of Abi1-1 and Abi2-1 Mutants of *Arabidopsis thaliana. Plant Physiology and Biochemistry*, **36**, 539–543.

Lin, Y., Trouillon, R., Safina, G. and Ewing, A. G. (2011). Chemical Analysis of Single Cells, *Analytical Chemistry*, **83**, 4369–4392.

Lincoln, C., Long, J., Yamaguchi, J., Serikawa, K. and Hake, S. (1994). A knotted1-like Homeobox Gene in *Arabidopsis* is Expressed in the Vegetative Meristem and Dramatically Alters Leaf Morphology When Overexpressed in Transgenic Plants. *The Plant Cell*, **6**, 1859–1876.

Linder, B. and Raschke, K. (1992). A Slow Anion Channel in Guard Cells, Activating at Large Hyperpolarization, may be Principal for Stomatal Closing. *FEBS Letters*, **313**, 27–30.

Liqun, D., Gul, S. A., Kayla, A. S., Jingguo, H., Tianbao, Yang, A. S. N. R. and Poovaiah, B. W. (2009). Ca^{2+}/calmodulin Regulates Salicylic-Acid-Mediated Plant Immunity. *Nature*, **457**, 1154–1158.

Liu, J. and Zhu, J. K. (1997). An *Arabidopsis* Mutant that Requires Increased Calcium for Potassium Nutrition and Salt Tolerance. *Proceedings of the National Academy of Sciences of the United States of America*, **94**, 14960–14964.

Liu, J. and Zhu, J. K. (1998). A Calcium Sensor Homolog Required for Plant Salt Tolerance. *Science*, **280**, 1943–1945.

Liu, K., Fu, H., Bei, Q. and Luan, S. (2000). Inward Potassium Channel in Guard Cells as a Target for Polyamine Regulation of Stomatal Movements. *Plant Physiology*, **124**, 1315–1325.

Liu, T.Y., Huang, T. K., Yang, S.Y., Hong, Y.T., Huang, S.M., Wang, F.N., Chiang, S.F., Tsai, S.Y., Lu, W.C. and Chiou, T.J. (2016). Identification of Plant Vacuolar Transporters Mediating Phosphate Storage. *Nature communications*, **7**, 11095–11106

Liu, T., Ohashi-Ito, K. and Bergmann, D. (2009). Orthologs of *Arabidopsis thaliana* Stomatal bHLH Genes and Regulation of Stomatal Development in Grasses. *Development*, **136**, 2265–2276.

Lochmann, H., Bazzanella, A. and Bächmann, K. (1998). Analysis of Solutes and Metabolites in Single Plant Cell Vacuoles by Capillary Electrophoresis. *Journal of Chromatography A*, **817**, 337–343.

Lochmann, H., Bazzanella, A., Kropsch, S. and Bachmann, K. (2001). Determination of Tobacco Alkaloids in Single Plant Cells by Capillary Electrophoresis. *Journal of Chromatography A*, **917**, 311–317.

Lorenzen, I., Aberle, T. and Plieth, C. (2004). Salt Stress-Induced Chloride Flux: A Study Using Transgenic *Arabidopsis* Expressing a Fluorescent Anion Probe. *The Plant Journal*, **38**, 539–544.

Louguet, P., Coudret, A., Couot-Gastelier, J. and Lasceve, G. (1990). Structure and Ultrastructure of Stomata. *Biochemie und Physiologie der Pflanzen*, **186**, 273–287.

Lowry, O. (2012). A flexible System of Enzymatic Analysis. Edited by U. Eds. London: *Academic Press.*

Lu, Z., Quinones, M. A. and Zeiger, E. (1993). Abaxial and Adaxial Stomata from Pima Cotton (*Gossypium barbadense* L.) Differ in their Pigment Content and Sensitivity to Light Quality. *Plant, Cell and Environment*, **16**, 851–858.

Luan, M., Tang, R.J., Tang, Y., Tian, W., Hou, C., Zhao, F., Lan, W. and Luan, S. (2017). Transport and Homeostasis of Potassium and Phosphate: Limiting Factors for Sustainable Crop Production. *Journal of Experimental Botany*, **68**, 3091–3105.

Lucas, W. J. and Wolf, S. (1993). Plasmodesmata: The Intercellular Organelles of Green Plants. *Trends in Cell Biology*, **3**, 308–315.

Ludewig, U., Neuhäuser, B. and Dynowski, M. (2007). Molecular Mechanisms of Ammonium Transport and Accumulation in Plants. *FEBS letters*, **581**, 2301–2308.

Luttge, U. (2002). CO_2-Concentrating: Consequences in Crassulacean Acid Metabolism. *Journal of experimental botany*, **53**, 2131–2142.

Ma, Y., Szostkiewicz, I., Korte, A., Moes, D., Yang, Y., Christmann, A. and Grill, E. (2009). Regulators of PP2C Phosphatase Activity Function as Abscisic Acid Sensors. *Science*, **324**, 1064–1068.

MacAlister, C. A., Ohashi-Ito, K. and Bergmann, D. C. (2007). Transcription Factor Control of Asymmetric Cell Divisions that Establish the Stomatal Lineage. *Nature*, **445**, 537–540.

Macallum, A. B. (1905). On the Distribution of Potassium in Animal and Vegetable Cells. *The Journal of Physiology*, **32**, 95–198.

MacRrobbie, E. A. (2006). Osmotic Effects on Vacuolar Ion Release in Guard Cells. *Proceedings of the National Academy of Sciences of the United States of America*, **103**, 1135–1140.

MacRrobbie, E. A. C. (1998). Signal Transduction and Ion Channels in Guard Cells. *Phil. Trans. R. Soc. Lond. B*, **353**, 1475–1488.

MacRrobbie, E. A. C. (1980). Osmotic Measurements on Stomatal Cells of *Commelina communis* L. *Journal of Membrane Biology*, **53**, 189–198.

MacRrobbie, E. A. C. (1981). Effects of ABA in 'isolated'Guard Cells of *Commelina communis* L. *Journal of experimental botany*, **32**, 563–572.

MacRrobbie, E. A. C. (2006). Control of Volume and Turgor in Stomatal Guard Cells. *The Journal of Membrane Biology*, **210**, 131–142.

MacRrobbie, E. A. C. and Lettau, J. (1980a). Ion Content and Aperture in "isolated" Guard Cells of *Commelina communis* L. *Journal of Membrane Biology*, **53**, 199–205.

MacRrobbie, E. A. C. and Lettau, J. (1980 b). Potassium Content and Aperture in "intact" Stomatal and Epidermal Cells of *Commelina communis* L. *The Journal of membrane biology*, **56**, 249–256.

Maier-Maercker, U. (1979). Peristomatal Transpiration and Stomatal Movement: A Controversial View III. Visible Effects of Peristomatal Transpiration on the Epidermis. *Zeitschrift für Pflanzenphysiologie*. *Urban and Fischer*, **91**, 225–238.

Majore, I., Wilhelm, B. and Marten, I. (2002). Identification of K^+ Channels in the Plasma Membrane of Maize Subsidiary Cells. *Plant and Cell Physiology*, **43**, 844–852.

Malone, M. (1992). Kinetics of Wound-Induced Hydraulic Signals and Variation Potentials in Wheat Seedlings. *Planta*, **187**, 505–510.

Malone, M., Leigh, R. A. and Tomos, A. D. (1989). Extraction and Analysis of Sap from Individual Wheat Leaf Cells: The Effect of Sampling Speed on the Osmotic Pressure of Extracted Sap. *Plant, Cell and Environment*, **12**, 919–926.

Malone, M., Leigh, R. A. and Tomos, A. D. (1991). Concentrations of Vacuolar Inorganic Ions in Individual Cells of Intact Wheat Leaf Epidermis. *Journal of Experimental Botany*, **42**, 305–309.

Mansfield, T. A. and Meidner, H. (1966). Stomatal Opening in Light of Different Wavelengths: Effects of Blue Light Independent of Carbon Dioxide Concentration. *Journal of Experimental Botany*. *Oxford University Press*, **17**, 510–521.

Marschner, H. (2011). Marschner's Mineral Nutrition of Higher Plants. 3rd edn. Edited by P. Marschner. London: *Academic Press.*

Martin, E. S., Donkin, M. E. and Stevens, R. A. (1983). Stomata. *Studies in Biology, No. 155*. 1st eds. london, Uk: *Edward Arnold.*

Martin, E. S. and Meidner, H. (1971). Endogenous Stomatal Movements in *Tradescantia virginiana. New Phytologist*, **70**, 923–928.

Martin, E. S. and Meidner, H. (1972). The Phase-Response of the Dark Stomatal Rhythm in *Tradescantia Virginiana* to Light and Dark Treatments. *New Phytologist*, **71**, 1045–1054.

Martinoia, E., Maeshima, M. and Neuhaus, H. E. (2006). Vacuolar Transporters and their Essential Role in Plant Metabolism. *Journal of Experimental Botany*, **58**, 83–102.

Massonneau, A., Martinoia, E., Dietz, K.-J. and Mimura, T. (2000). Phosphate Uptake across the Tonoplast of Intact Vacuoles Isolated from Suspension-Cultured Cells of *Catharanthus roseus* (L.) G. Don. *Planta*, **211**, 390–395.

Mathur, J. (2007). The Illuminated Plant Cell. *Trends in Plant Science*, **12**, 506–513.

Matrosova, A., Bogireddi, H. and Mateo-Peñas, A. (2015). The HT1 Protein Kinase is Essential for Red Light-Induced Stomatal Opening and Genetically Interacts with OST1 in Red Light and CO_2-Induced Stomatal. *The New Phytologist,* **208**, 1126–1137.

Matthew, W. B., Martin, K., Jeffrey, D. S. and Andrew, J. R. (2012). Aggregative Multicellularity Evolved Independently in the Eukaryotic Supergroup Rhizaria. *Current Biology*, **22**, 1123–1127.

McAdam, S. and Brodribb, T. (2015) The Evolution of Mechanisms Driving the Stomatal Response to Vapour Pressure Deficit. *Plant Physiology*, **167**, 833–843.

McAdam, S. and Sussmilch, F. (2016). Stomatal Responses to Vapour Pressure Deficit are Regulated by High Speed Gene Expression in Angiosperms. *Plant, cell and development*, **39**, 485–491.

Mcainsh, M. R., Webb, A. A. R., Taylor, J. E. and Hetherington, A. M. (1995). Stimulus-

Induced Oscillations in Guard Cell Cytosolic Free Calcium. *The Plant Cell*, **7**, 1207–1219.

Mcqueen-Mason, S., Durachko, D. M. and Cosgrove, D. J. (1992). Two Endogenous Pmteins That Lnduce Cell Wall Extension in Plants. *The Plant Cell*, **4**, 1425–1433.

McQueen-Mason, S. J. and Cosgrove, D. J. (1995). Expansin Mode of Action on Cell Walls (Analysis of Wall Hydrolysis, Stress Relaxation, and Binding). *Plant Physiology*, **107**, 87–100.

Meidner, H. (1975). Water Supply, Evaporation, and Vapour Diffusion in Leaves. *Journal of Experimental Botany*, **26**, 666–672.

Meidner, H. (1982). Guard Cell Pressures and Wall Properties during Stomatal Opening. *Journal of Experimental Botany*, **33**, 355–359.

Meidner, H. (1987). Three Hundred Years of Research into Stomata. In E Zeiger, G. D. F. and I. R. C. edn *Stomatal Function*. 1st eds. Stanford, CA.: *Stanford University Press*, 7–29.

Meidner, H. and Bannister, P. (1979). Pressure and Solute Potentials in Stomatal Cells of *Tradescantia virginiana. Journal of Experimental Botany*, **30**, 255–265.

Meidner, H. and Edwards, M. (1975). Direct Measurements of Turgor Pressure Potentials of Guard Cells, I. *Journal of Experimental Botany*, **26**, 319–330.

Meidner, H. and Mansfield, T. A. (1968). Physiology of Stomata. 1st edn. Edited by M. Wilkins. London, Uk: *McGraw-Hill, London.*

Meijer, M. and Murray, J. A. H. (2001). Cell Cycle Controls and the Development of Plant Form. *Current Opinion in Plant Biology*, **4**, 44–49.

Melotto, M., Underwood, W., Koczan, J., Nomura, K. and He, S. Y. (2006). Plant Stomata Function in Innate Immunity against Bacterial Invasion. *Cell*, **126**, 969–980.

Mengel, K. and Kirkby, E. A. (1978). Principles of Plant Nutrition. *International Potash Institute,* Baumgartlistrasse, Switzerland.

Merilo, E., Laanemets, K., Hu, H. and Xue, S. (2013). PYR/RCAR Receptors coPYR/RCAR Receptors Contribute to Ozone-, Reduced Air Humidity-, Darkness-, and CO_2-Induced Stomatal Regulation contribute to Ozone-, Reduced Air Humidity-, Darkness-, and CO_2-Induced Stomatal Regulation. *Plant*, **162**, 1652–1668.

Meyer, A. J., May, M. J. and Fricker, M. (2001). Quantitative *In Vivo* Measurement of Glutathione in *Arabidopsis* Cells. *The Plant Journal*, **27**, 67–78.

Meyer, S. and Angeli, D. (2010). Intra-and Extra-Cellular Excretion of Carboxylates. *Trends in Plant Science*, **15**, 40–47.

Miedema, H. and Assmann, S. M. (1998). The Calculation of Intracellular Ion Concentrations and Membrane Potential from Cell-Attached and Excised Patch Measurements. Cytosolic K + Concentration and Membrane Potential in *Vicia Faba* Guard Cells. *J. Membrane Biol.*, **166**, 101–110.

Miedema, H., Bothwell, J. H. F., Brownlee, C. and Davies, J. M. (2001). Calcium Uptake by Plant Cells – Channels and Pumps Acting in Concert. *Trends in Plant Science*, **6**, 514–519.

Milanowska, J. and Gruszecki, W. I. (2005). Heat-Induced and Light-Induced Isomerization of the Xanthophyll Pigment Zeaxanthin. *Journal of Photochemistry and Photobiology B: Biology*, **80**, 178–186.

Miller, A. J. and Wells, D. M. (2006). Electrochemical Methods and Measuring Transmembrane Ion Gradients. In *Plant Electrophysiology – Theory and Methods*. Volkov AJ,. *Berlin: Springer-Verlag*, 15–34.

Mimura, T., Dietz, K.J., Kaiser, W., Schramm, M. J., Kaiser, G. and Heber, U. (1990). Phosphate Transport Across Biomembranes and Cytosolic Phosphate Homeostasis in Barley Leaves. *Planta*, **180**, 139–146.

Mishkind, M. and Palevitz, B. (1981). Cell Wall Architecture: Normal Development and Environmental Modification of Guard Cells of the *Cyperaceae* and Related Species. *Plant, Cell and Environment*, **4**, 319–328.

Misson, J., Thibaud, M.-C., Bechtold, N., Raghothama, K. and Nussaume, L. (2004). Transcriptional Regulation and Functional Properties of *Arabidopsis* Pht1;4, a High Affinity Transporter Contributing Greatly to Phosphate Uptake in Phosphate Deprived Plants. *Plant Molecular Biology*, **55**, 727–741.

Mittelheuser, C. and Van Steveninck, R. (1969). Stomatal Closure and Inhibition of Transpiration Induced by (RS)-Abscisic Acid. *Nature*, **221**, 281–282.

Miyawaki, A., Llopis, J., Heim, R., Mccaffery, J. M., Adams, J. A., Ikurak, M. and Tsien, R. Y. (1997). Fluorescent Indicators for Ca^{2+} Based on Green Fluorescent Proteins and Calmodulin. *Nature*, **388**, 882–887.

von Mohl, H. (1856). Welche Ursachen Bewirken Die Erweiterung Und Verengung Der Spaltöffnungen. *Bot.Ztg*, **14**, 697–704.

Mohnen, D. (2008). Pectin Structure and Biosynthesis. *Current Opinion in Plant Biology*, **11**, 266–277.

Monro, J. A., Penny, D. and Bailey, R. W. (1976). The Organization and Growth of Primary Cell Walls of Lupin Hypocotyl. *Phytochemistry*, **15**, 1193–1198.

Mott, K. (1988). Do Stomata Respond to CO_2 Concentrations Other than Intercellular? *Plant Physiology*, **86**, 200–203.

Mott, K. A. and Franks, P. J. (2001). The Role of Epidermal Turgor in Stomatal Interactions Following a Local Perturbation in Humidity. *Plant, Cell and Environment*, **24**, 657–662.

Muelleri, Z., Garrill, A., Tyerman, S. D. and Findlay, G. P. (1994). Ion Channels in the Plasma Membrane of Protoplasts from the Halophytic Angiosperm. *J. Membrane Biol*, **142**, 381–393.

Murguia, R. J., Belles, M. J. and Serrano, R. (1995). A Salt-Sensitive 3'(2'),5'-bisphosphate Nucleotidase Involved in Sulfate Activation. *Science*, **267**, 232–234.

Mustilli, A., Merlot, S., Vavasseur, A. and Fenzi, F. (2002). *Arabidopsis* OST1 Protein Kinase Mediates the Regulation of Stomatal Aperture by Abscisic Acid and Acts Upstream of Reactive Oxygen Species Production. *The Plant Cell*, **14**, 3089–3099.

Nadeau, J. A. and Sack, F. D. (2002). Control of Stomatal Distribution on the *Arabidopsis* Leaf Surface. *Science*, **296**, 1697–1700.

Nagai, M., Ohnishi, M., Uehara, T., Yamagami, M., Miura, E., Kamakura, M., Kitamura, A., Sakaguchi, S. S.I., Sakamoto, W., Shimmen, T., Fukaki, H., Reid, R. J., *et al.* (2013). Ion Gradients in Xylem Exudate and Guttation Fluid Related to Tissue Ion Levels along Primary Leaves of Barley. *Plant, Cell and Environment*, **36**, 1826–1837.

Nambara, E. and Marion-Poll, A. (2005). Abscisic Acid Biosynthesis and Catabolism. *Annual Review of Plant Biology*, **56**, 165–185.

Negi, J., Matsuda, O., Nagasawa, T., Oba, Y., Takahashi, H., Kawai-Yamada, M., Uchimiya, H., Hashimoto, M. and Iba, K. (2008). CO_2 Regulator SLAC1 and its Homologues are Essential for Anion Homeostasis in Plant Cells. *Nature*, **452**, 483–486.

Nejad, A. R., Harbinson, J. and van Meeteren, U. (2006). Dynamics of Spatial Heterogeneity of Stomatal Closure in *Tradescantia virginiana* Altered by Growth at High Relative Air Humidity. *Journal of experimental botany*, **57**, 3669–3678.

Nejad, A. R. and van Meeteren, U. (2007). The Role of Abscisic Acid in Disturbed Stomatal Response Characteristics of *Tradescantia virginiana* during Growth at High Relative Air Humidity. *Journal of experimental botany*, **58**, 627–636.

Nejad, A. R. and van Meeteren, U. (2008). Dynamics of Adaptation of Stomatal Behaviour to Moderate or High Relative Air Humidity in *Tradescantia virginiana. Journal of experimental botany*, **59**, 289–301.

Nejad, A. R. and Meeteren, U. Van (2005). Stomatal Response Characteristics of *Tradescantia virginiana* Grown at High Relative Air Humidity. *Physiologia Plantarum*, **125**, 324–332.

Nelson, S. and Mayo, J. (1975). The Occurrence of Functional Non-Chlorophyllous Guard Cells in *Paphiopedilum* Spp. *Canadian Journal of Botany*, **53**, 1–7.

Nobel, P. S. (2009). Physicochemical and Environmental Plant Physiology. 4th eds. Edited by P. S. Nobel. *Academic Press* New York, USA.

Nonami, H. and Schulze, E.D. (1989). Cell Water Potential, Osmotic Potential, and Turgor in the Epidermis and Mesophyll of Transpiring Leaves: Combined Measurements with the Cell Pressure Probe and Nanoliter Osmometer. *Planta*, **177**, 35–46.

Nonami, H., Schulze, E.D. and Ziegler, H. (1990). Mechanisms of Stomatal Movement in Response to Air Humidity, Irradiance and Xylem Water Potential. *Planta*, **183**, 57–64.

Ohashi-Ito, K. and Bergmann, D. (2006). *Arabidopsis* FAMA Controls the Final Proliferation/Differentiation Switch during Stomatal Development. *The Plant Cell*, **18**, 2493–2505.

Okorokov, L. A., Lichko, L. P. and Kulaev, I. S. (1980). Vacuoles: Main Compartments of Potassium, Magnesium, and Phosphate Ions in *Saccharomyces carlsbergensis* Cells. *Journal of Bacteriology*, **144**, 661–665.

Olesen, P. (1979). The Neck Constriction in Plasmodesmata. *Planta*, **144**, 349–358.

Olias, R., Eljakaoui, Z., Li, J., De Morales, P. A., Marín-Manzano, M. C., Pardo, J. M. and Belver, A. (2009). The Plasma Membrane Na^+/H^+ Antiporter SOS1 is Essential for Salt Tolerance in Tomato and Affects the Partitioning of Na^+ between Plant Organs. *Plant, Cell and Environment*, **32**, 904–916.

O'Neill, M. A., Eberhard, S., Albersheim, P. and Darvill, A. G. (2001). Requirement of Borate Cross-Linking of Cell Wall Rhamnogalacturonan II for Arabidopsis Growth. *Science*, **294**, 846–849.

O'Neill, M. A. and York, W. S. (2003). The Composition and Structure of Plant Primary Cell Walls, In Rose Jocelyn K. eds. *The plant cell wall* . 1st edn. Florida, USA.: *CRC Press*, 1–54.

Oparka, K. J. and Hawes, C. (1992). Vacuolar Sequestration of Fluorescent Probes in Plant Cells: A Review. *Journal of Microscopy*, **166**, 15–27.

Oparka, K. J., Roberts, A. G., Boevink, P., Cruz, S. S., Roberts, I., Pradel, K. S., Imlau, A., Kotlizky, G., Sauer, N. and Epel, B. (1999). Simple, but Not Branched, Plasmodesmata Allow the Nonspecific Trafficking of Proteins in Developing Tobacco Leaves. *Cell*. *Cell Press*, **97**, 743–754.

Outlaw, W. H. (Jr.) (1983). Current Concepts on the Role of Potassium in Stomatal Movements. *Physiologia Plantarum*, **59**, 302–311.

Outlaw, W. H. (Jr.) (1987). An Introduction to Carbon Metabolism in Guard Cells, In E. Zieger, G. D. Farguhar, and I. R. C. P. A. edn. *Stomatal Function*. Califonia, USA: *Stanford University Press*, 115–123.

Outlaw, W. H. (Jr.) and Lowry, O. H. (1977). Organic Acid and Potassium Accumulation in Guard Cells during Stomatal Opening. *Proceedings of the National Academy of Sciences of the United States of America*, **74**, 4434–4438.

Outlaw, W. H. (Jr.) and Manchester, J. (1979). Guard Cell Starch Concentration Quantitatively Related to Stomatal Aperture. *Plant Physiology*, **64**, 79–82.

Overall, R. L. (1999). Substructure of Plasmodesmata, In van Bel, A. and van Kesteren, W. eds. *Plasmodesmata: structure, function, role in cell communication*. *Springer Berlin Heidelberg*, 129–148.

Overall, R. L. and Blackman, L. M. (1996). A Model of the Macromolecular Structure of Plasmodesmata. *Trends in Plant Science*, **1**, 307–311.

Paciorek, T. and Friml, J. (2006). Auxin Signaling. *J Cell Sci*, **119**, 1199–1202.

Palevitz, B. and Hepler, P. (1985). Changes in Dye Coupling Of Stomatal Cells of *Allium* and *Commelina* Demonstrated by Microinjection of Lucifer Yellow. *Planta*, **164**, 473–479.

Palin, R. and Geitmann, A. (2012). The Role of Pectin in Plant Morphogenesis. *BioSystems*, **109**, 397–402.

Pallaghy, C. K. (1971). Stomatal Movement and Potassium Transport in Epidermal Strips of *Zea mays*; The Effect of CO_2. *Planta*, **101**, 287–295.

Pallaghy, C. K. and Fischer, R. A. (1974). Metabolic Aspects of Stomatal Opening and Ion Accumulation by Guard Cells in *Vicia faba. Zeitschrift für Pflanzenphysiologie*, **71**, 332–344.

Pallas, J. and Wright, B. (1973). Organic Acid Changes in the Epidermis of *Vicia faba* and their Implication in Stomatal Movement. *Plant physiology*, **51**, 588–590.

Paris, N., Stanley, C. M., Jones, R. L. and Rogers, J. C. (1996). Plant Cells Contain Two Functionally Distinct Vacuolar Compartments. *Cell*, **85**, 563–572.

Park, S.Y., Fung, P., Nishimura, N., Jensen, D. R., Fujii, H., Zhao, Y., Lumba, S., Santiago, J., Rodrigues, A., Chow, T.F. F., Alfred, S. E., Bonetta, D., *et al.* (2009). Abscisic Acid Inhibits Type 2C Protein Phosphatases via the PYR/PYL Family of START Proteins. *Science*, **324**, 1068–71.

Passioura, J. B. (1963). A Mathematical Model for the Uptake of Ions from the Soil Solution.

Plant and Soil, **18**, 225–238.

Patakas, A. and Noitsakis, B. (2001). Leaf Age Effects on Solute Accumulation in Water-Stressed Grapevines. *Journal of plant physiology*, **158**, 63–69.

Peaucelle, A., Braybrook, S. A., Le Guillou, L., Bron, E., Kuhlemeier, C. and Höfte, H. (2011). Pectin-Induced Changes in Cell Wall Mechanics Underlie Organ Initiation in Arabidopsis. *Current Biology*, **21**, 1720–1726.

Pei, Z. M., Ward, J. M., Harper, J. F. and Schroeder, J. I. (1996). A Novel Chloride Channel in *Vicia faba* Guard Cell Vacuoles Activated by the Serine/threonine Kinase, CDPK. *The EMBO journal*., **15**, 6564–74.

Penny, M. G. and Bowling, D. J. F. (1974). A Study of Potassium Gradients in the Epidermis of Intact Leaves of *Commelina communis* L. in Relation to Stomatal Opening. *Planta*, **119**, 17–25.

Penny, M. G. and Bowling, D. J. F. (1975). Direct Determination of pH in the Stomatal Complex of *Commelina communis. Planta*, **122**, 209–212.

Penny, M. G., Kelday, L. S. and Bowling, D. J. F. (1976). Active Chloride Transport in the Leaf Epidermis of *Commelina communis* in Relation to Stomatal Activity. *Planta*, **130**, 291–294.

Pfeiffer, W. and Hager, A. (1993). A Ca^{2+}-ATPase and a Mg^{2+}/H^{+}-Antiporter are Present on Tonoplast Membranes from Roots of *Zea mays* L. *Planta*, **191**, 377–385.

Pfluger, J. and Zambryski, P. C. (2001). Cell Growth: The Power of Symplastic Isolation. *Current Biology*, **11**, R436–R439.

Philip, J. R. (1958). Osmiosis and Diffusion in Tissue: Half-Times and Internal Gradients. *Plant Physiology*, **33**, 275–278.

Pillitteri, L. and Bogenschutz, N. (2008). The bHLH Protein, MUTE, Controls Differentiation of Stomata and the Hydathode Pore in *Arabidopsis*. *Plant and cell physiology*, **49**, 934–943.

Pillitteri, L. J. and Dong, J. (2013). Stomatal Development in *Arabidopsis. The Arabidopsis book,* **11**, e0126

Pillitteri, L., Sloan, D., Bogenschutz, N. and Torii, K. (2007). Termination of Asymmetric Cell Division and Differentiation of Stomata. *Nature*, **445**, 501–505.

Pitman, M. (1963). The Determination of the Salt Relations of the Cytoplasmic Phase in Cells of Beetroot Tissue. *Australian Journal of Biological Sciences*, **16**, 647–668.

Poethig, R. S. and Szymkowiak, E. J. (1995). Clonal Analysis of Leaf Development in Maize. *Maydica (Italy)*, **40**, 67–76.

Poethig, S. (1984). Cellular Parameters of Leaf Morphogenesis in Maize and Tobacco. In *White, R, A,, Dickison, W, C edn. Contemporary problems in plant anatomy.Academic Press: Orlando USA,* 235–259.

Pospíšilov, J. (1996). Effect of Air Humidity on the Development of Functional Stomatal Apparatus. *Biologia Plantarum*, **38**, 197–204.

Postel, S. (1993). Last Oasis: Facing Water Scarcity. *American Journal of Alternative Agriculture*, **8**, 94–96.

Postel, S. L., Daily, G. C. and Ehrlich, P. R. (1996). Human Appropriation of Renewable

Fresh Water. *American Association for the Advancement of Science*, **271**, 785–788.

Powles, J. E., Buckley, T. N., Nicotra, A. B. and Farquhar, G. D. (2006). Dynamics of Stomatal Water Relations Following Leaf Excision. *Plant, Cell and Environment*, **29**, 981–992.

Pratt, J., Boisson, A.-M., Gout, E., Bligny, R., Douce, R. and Aubert, S. (2009). Phosphate (Pi) Starvation Effect on the Cytosolic Pi Concentration and Pi Exchanges across the Tonoplast in Plant Cells: An in Vivo ^{31}P-Nuclear Magnetic Resonance Study Using Methylphosphonate as a Pi Analog. *Plant Physiology*, **151**, 1646–1657.

Pressel, S., Goral, T. and Duckett, J. G. (2014). Stomatal Differentiation and Abnormal Stomata in Hornworts. *Journal of Bryology*, **36**, 87–103.

Preuss, C. P., Huang, C. Y., Gilliham, M. and Tyerman, S. D. (2010). Channel-Like Characteristics of the Low-Affinity Barley Phosphate Transporter PHT1;6 When Expressed in *Xenopus* Oocytes. *Plant Physiology*, **152**, 1431–1441.

Qu, X., Peterson, K. M. and Torii, K. U. (2017). Stomatal Development in Time: The Past and the Future. *Current Opinion in Genetics and Development*, **45**, 1–9.

Rains, D. W. and Epstein, E. (1967). Sodium Absorption by Barley Roots: Role of the Dual Mechanisms of Alkali Cation Transport. *Planit Physiol*, **42**, 314–318.

Ranathunge, K., Steudle, E. and Lafitte, R. (2005). Blockage of Apoplastic Bypass-Flow of Water in Rice Roots by Insoluble Salt Precipitates Analogous to a Pfeffer Cell. *Plant, Cell and Environment*, **28**, 121–133.

Raschke, K. (1975). Stomatal Action. *Annual Review of Plant Physiology*, **26**, 309–340.

Raschke, K. (1979). Movements of Stomata. *Encyclopedia of Plant Physiology*, **7**, 383–441.

Raschke, K. and Fellows, M. P. (1971). Stomatal Movement in *Zea mays*: Shuttle of Potassium and Chloride between Guard Cells and Subsidiary Cells. *Planta*, **101**, 296–316.

Raschke, K. and Humble, G. D. (1973). No Uptake of Anions Required by Opening Stomata of *Vicia faba*: Guard Cells Release Hydrogen Ions. *Planta*, **115**, 47–57.

Raschke, K., Patzke, J., Daley, P. and Berry, J. (1990). Spatial and Temporal Heterogeneities of Photosynthesis Detected through Analysis of Chlorophyll-Fluorescence Images of Leaves. *Current research in Photosynthesis*, **19**, 3367–3372.

Raschke, K. and Schnabl, H. (1978). Availability of Chloride Affects the Balance between Potassium Chloride and Potassium Malate in Guard Cells of *Vicia faba* L. *Plant Physiology*, **62**, 84–87.

Rasehke, K. (1975). Simultaneous Requirement of Carbon Dioxide and Abscisic Acid for Stomatal Closing in *Xanthium strumarium* L. *Planta*, **125**, 243–259.

Rausch, C. and Bucher, M. (2002). Molecular Mechanisms of Phosphate Transport in Plants. *Planta*, **216**, 23–37.

Raven, J. A. (1977). The Evolution of Vascular Land Plants in Relation to Supracellular Transport Processes. *Advances in botanical research*, **5**, 153–219.

Reed, H. S. and Hirano, E. (1931). The Density of Stomata in Citrus Leaves. *Journal of Agricultural Research*, **43**, 209-222.

Richardson, P. (1993). Intercellular Distribution of Nitrate in Wheat Leaves. Ph.D. Thesis,

Prifysgol Bangor University, UK.

Ritte, G., Rosenfeld, J., Rohrig, K. and Raschke, K. (1999). Rates of Sugar Uptake by Guard Cell Protoplasts of *Pisum sativum* L. Related to the Solute Requirement for Stomatal Opening. *Plant Physiology*, **121**, 647–656.

Robards, A. W. (1976). Plasmodesmata in Higher Plants. In *Intercellular Communication in Plants: Studies on Plasmodesmata*. Berlin, Heidelberg, Heidelberg: *Springer Berlin Heidelberg*, 15–57.

Roberts, I. M., Boevink, P., Roberts I, A. G., Sauer, N., Reichel, C. and Oparka, K. J. (2001). Dynamic Changes in the Frequency and Architecture of Plasmodesmata during the Sink-Source Transition in Tobacco Leaves. *Protoplasma*, **218**, 31–44.

Robinson-Beers, K. and Evert, R. F. (1991). Fine Structure of Plasmodesmata in Mature Leaves of Sugarcane. *Planta*, **184**, 307–318.

Robinson, R. A. and Stokes, R. H. (2002). Electrolyte solutions. 2nd Revision. Edited by R. H. Stokes and Armidale. Mineola, New York U.S: *Dover publication.*

Roelfsema, G., Rob, M., Hedrich, R. and Geiger, D. (2012). Anion Channels: Master Switches of Stress Responses. *Trends in Plant Science*, **17**, 221–229.

Roelfsema, M. R. G., Konrad, K. R., Marten, H., Psaras, G. K., Hartung, W. and Hedrich, R. (2006). Guard Cells in Albino Leaf Patches do not Respond to Photosynthetically Active Radiation, but are Sensitive to Blue Light, CO_2 and Abscisic Acid. *Plant, Cell and Environment*, **29**, 1595–1605.

Roelfsema, M. R. G. and Prins, H. B. A. (1997). Ion Channels in Guard Cells of *Arabidopsis thaliana* (L.). *Planta*, **202**, 18–27.

Roelfsema, M. R. G., Steinmeyer, R., Staal, M. and Hedrich, R. (2001). Single Guard Cell Recordings in Intact Plants: Light-Induced Hyperpolarization. *The Plant Journal*, **26**, 1–13.

Rogers, C. A., Powell, R. D. and Sharpe, P. J. H. (1979). Relationship of Temperature to Stomatal Aperture and Potassium Accumulation in Guard Cells of *Vicia faba. Plant Physiol*, **63**, 388–391.

Rogers, J. C. (1998). Compartmentation of Plant Cell Proteins in Separate Lytic and Protein Storage Vacuoles. *Journal of Plant Physiology*, **152**, 653–658.

Royer, D. L. (2001). Stomatal Density and Stomatal Index as Indicators of Paleoatmospheric CO_2 Concentration. *Review of Palaeobotany and Palynology*, **114**, 1–28.

Ruan, Y.L., Llewellyn, D. J. and Furbank, R. T. (2001). The Control of Single-Celled Cotton Fiber Elongation by Developmentally Reversible Gating of Plasmodesmata and Coordinated Expression of Sucrose and K^+ Transporters and Expansin. *The Plant Cell*, **13**, 47–60.

Rubio, F., Gassmann, W. ; and Schroeder, J. I. (1995). Sodium-Driven Potassium Uptake by the Plant Potassium Transporter. *Science*, **270**, 1660–1663.

Ruiz, L. and Mansfield, T. (1994). A Postulated Role for Calcium Oxalate in the Regulation of Calcium Ions in the Vicinity of Stomatal Guard Cells. *New Phytologist*, **127**, 473–481.

Russin, W. A. and Evert, R. F. (1985). Studies on the Leaf of *Populus deltoides* (Salicaceae): Ultrastructure, Plasmodesmatal Frequency, and Solute Concentrations. *American Journal of Botany*, **72**, 1232–1247.

Sack, F. (1994). Structure of the Stomatal Complex of the Monocot *Flagellaria indica.*

American journal of botany, **81**, 339–344.

Sack, F. D. (1987). The Development and Structure of Stomata, In Zeiger, E., Farquhar, G. D., and Cowan, I. R. eds. *Stomatal function*. *Stanford University Press Stanford.* 59–89.

Sack, L. and Buckley, T. N. (2016). The Developmental Basis of Stomatal Density and Flux. *Plant Physiology*, **171**, 2358–2363.

Saito, M., Homma, T., Nemoto, Y. and Matsuoka, H. (1993) Intracellular Potential Change of *Tradescantia virginiana* L. Leaf in Response to CO_2 Stress. *Bioelectrochemistry and bioenergetics*, **32**, 133–143.

Sakamoto, T., Kamiya, N. and Ueguchi-Tanaka, M. (2001). KNOX Homeodomain Protein Directly Suppresses the Expression of a Gibberellin Biosynthetic Gene in the Tobacco Shoot Apical Meristem. *Genes and development*, **15**, 581–590.

Salisbury, E. J. (1928). On the Causes and Ecological Significance of Stomatal Frequency, with Special Reference to the Woodland Flora. *Philosophical Transactions of the Royal Society, London. Series B, Containing Papers of a Biological Character*, **216**, 1–65.

Sanders, D., Brownlee, C. and Harper, J. F. (1999). Communicating with Calcium. *The Plant Cell*, **11**, 691–706.

Sanders, D., Pelloux, J., Brownlee, C. and Harper, J. F. (2002). Calcium at the Crossroads of Signaling. *The Plant cell*, **14 Suppl**, S401-417.

Santelia, D. and Lawson, T. (2016). Rethinking Guard Cell Metabolism. *Plant Physiology*, **172**, 1371–1392.

Satina, S., Blakeslee, A. and Avery, A. (1940,) Demonstration of the Three Germ Layers in the Shoot Apex of *Datura* by Means of Induced Polyploidy in Periclinal Chimeras. *American Journal of Botany*, **27**, 895–905.

Satina, S. and Blakeslee, A. F. (1941). Periclinal Chimeras in *Datura stramonium* in Relation to Development of Leaf and Flower. *American Journal of Botany*, **28**, 862–871.

Sawhney, B. L. and Zelitch, I. (1969). Direct Determination of Potassium Ion Accumulation in Guard Cells in Relation to Stomatal Opening in Light. *Plant Physiol*, **44**, 1350–1354.

Sayre, J. D. (1926). Physiology of Stomata of *Rumex patientia*. *The Ohio Journal of Science*, **26**, 5–233

Scanlon, M. (2003). The Polar Auxin Transport Inhibitor N-1-Naphthylphthalamic Acid Disrupts Leaf Initiation, KNOX Protein Regulation, and Formation of Leaf Margins in Maize. *Plant Physiology*, **133**, 597–605.

Scarth, G. (1932). Mechanism of the Action of Light and Other Factors on Stomatal Movement. *Plant Physiology*, **7**, 481–504.

Schmidt, C. and Schroeder, J. I. (1994). Anion Selectivity of Slow Anion Channels in the Plasma Membrane of Guard Cells (Large Nitrate Permeability). *Plant Physiology*, **106**, 383–391.

Schnabl, H. and Kottmeier, C. (1984). Determination of Malate Levels during the Swelling of Vacuoles Isolated from Guard-Cell Protoplasts. *Planta*, **161**, 27–31.

Schnabl, H. and Raschke, K. (1980). Potassium Chloride as Stomatal Osmoticum in *Allium cepa* L., a Species Devoid of Starch in Guard Cells. *Plant Physiol*, **65**, 88–93.

Schnabl, H. and Ziegler, H. (1977). The Mechanism of Stomatal Movement in *Allium Cepa* L. *Planta*, **136**, 37–43.

Schneeberger, R., Tsiantis, M. and Freeling, M. (1998). The Rough Sheath2 Gene Negatively Regulates Homeobox Gene Expression during Maize Leaf Development. *Development*, **125**, 2857–2865.

Schnepf, E. and Sych, A. (1983). Distribution of Plasmodesmata in Developing Sphagnum Leaflets. *Protoplasma*, **116**, 51–56.

Schönherr, J. (1982). Resistance of Plant Surfaces to Water Loss: Transport Properties of Cutin, Suberin and Associated Lipids. In *Physiological plant ecology II. Encyclopedia of Plant Physiology (New Series)*. *B. Springer, Berlin, Heidelberg.*

Schroeder, J. and Hagiwara, S. (1989). Cytosolic Calcium Regulates Ion Channels in the Plasma Membrane of *Vicia faba* Guard Cells. *Nature*, **338**, 427–430.

Schroeder, J. I. (1988). K^+ Transport Properties of K^+ Channels in the Plasma Membrane of *Vicia faba* Guard Cells. *The Journal of General Physiology*, **92**, 667–683.

Schroeder, J. I. and Hagiwarat, S. (1990). Repetitive Increases in Cytosolic Ca^{2+} of Guard Cells by Abscisic Acid Activation of Nonselective Ca^{2+} Permeable Channels., *Botany*, **87**, 9305–9309.

Schroeder, J. I. and Nambara, E. (2006). A Quick Release Mechanism for Abscisic Acid. *Cell*, **126**, 1023–1025.

Schroeder, J. I., Raschket, K. and Neher, E. (1987). Voltage Dependence of K^+ Channels in Guard-Cell Protoplasts. *Biophysics*, **84**, 4108–4112.

Schroeder, J. and Keller, B. (1992). Two Types of Anion Channel Currents in Guard Cells with Distinct Voltage Regulation. *Proceedings of the National Academy of Sciences of the United States of America*, **89**, 5025–5029.

Schulz-Lessdorf, B. and Hedrich, R. (1995) Protons and Calcium Modulate SV-Type Channels in the Vacuolar-Lysosomal Compartment-Channel Interaction with Calmodulin Inhibitors. *Planta*, **197**, 655–671.

Schwartz, A. (1985). Role of Ca^{2+} and EGTA on Stomatal Movements in *Commelina communis* L. *Plant Physiology*, **79**, 1003–1005.

Scripps (2017). The Keeling Curve: A Daily Record of Atmospheric Carbon Dioxide. *Scripps Institution of Oceanography, UC San Diego; available at: http://keelingcurve.ucsd. edu.*

Seagull, R. (1983). Differences in the Frequency and Disposition of Plasmodesmata Resulting from Root Cell Elongation. *Planta*, 497–504.

Serrano, E. and Zeiger, E. (1988). Red Light Stimulates an Electrogenic Proton Pump in *Vicia faba* Guard Cell Protoplasts. *Proceedings of the National Academy of Sciences of the United States of America*, **85**, 436–440.

Shabala, S. and Newman, I. (1999). Light-Induced Changes in Hydrogen, Calcium, Potassium, and Chloride Ion Fluxes and Concentrations from the Mesophyll and Epidermal Tissues of Bean Leaves. Understanding the Ionic Basis of Light-Induced Bioelectrogenesis. *Plant Physiology*, **119**, 1115–1124.

Shackel, K. A. (1987). Direct Measurement of Turgor and Osmotic Potential in Individual Epidermal Cells: Independent Confirmation of Leaf Water Potential as Determined by *In Situ* Psychrometry. *Plant Physiol*, **83**, 719–722.

Shackel, K. A. and Brinckmann, E. (1985). In Situ Measurement of Epidermal Cell Turgor, Leaf Water Potential, and Gas Exchange in *Tradescantia virginiana* L. *Plant Physiology*, **78**, 66–70.

Shapira, O., Khadka, S., Israeli, Y., Shani, U. and Schwartz, A. (2009). Functional Anatomy Controls Ion Distribution in Banana Leaves: Significance of Na^+ Seclusion at the Leaf Margins. *Plant, Cell and Environment*, **32**, 476–485.

Sharkey, T. D. and Raschke, K. (1981). Effect of Light Quality on Stomatal Opening in Leaves of *Xanthium strumarium* L. *Plant Physiol*, **68**, 1170–1174.

Sharpe, P. J. H. and Wu, H. (1978). Stomatal Mechanics: Volume Changes during Opening. *Plant, Cell and Environment*, **1**, 259–268.

Shaul, O., Hilgemann, D. W., De-Almeida-Engler, J., Montagu, M. Van, Inzé, D. and Galili, G. (1999). Cloning and Characterization of a Novel Mg^{2+}/H^+ Exchanger. *The EMBO Journal*, **18**, 3973–3980.

Shaw, M. (1954). Chloroplasts in the Stomata of *Allium cepa* L. *New Phytologist*, **53**, 344–347.

Sheriff, D. and Meidner, H. (1974). Water Pathways in Leaves of *Hedera helix* L. and *Tradescantia virginiana* L. *Journal of Experimental Botany*, **25**, 1147–1156.

Sheriff, D. W. (1977). Where Is Humidity Sensed When Stomata Respond to it Directly? *Ann. Bot*, **41**, 1083–1084.

Shihabi, Z. K., Kute, T., Garcia, L. L. and Hinsdale, M. (1994). Analysis of Isoflavones by Capillary Electrophoresis. *Journal of Chromatography A*, **680**, 181–185.

Shimazaki, K., Iino, M. and Zeiger, E. (1986) Blue Light-Dependent Proton Extrusion by Guard-Cell Protoplasts of *Vicia faba. Nature*, **319**, 324–326.

Shin, H.-S. H., Shin, H.-S. H., Dewbre, G. R. and Harrison, M. J. (2004). Phosphate Transport in *Arabidopsis* : Pht1;1 and Pht1;4 Play a Major Role in Phosphate Acquisition from Both Low- and High-Phosphate Environments. *The Plant Journal*, **39**, 629–642.

Siegel, R. S., Xue, S., Murata, Y., Yang, Y., Nishimura, N., Wang, A. and Schroeder, J. I. (2009). Calcium Elevation-Dependent and Attenuated Resting Calcium-Dependent Abscisic Acid Induction of Stomatal Closure and Abscisic Acid-Induced Enhancement of Calcium Sensitivities of S-Type Anion and Inward-Rectifying K^+ Channels in *Arabidopsis* Guard Cells. *The Plant Journal*, **59**, 207–220.

Singh, A. P. and Srivastava, L. M. (1973). The Fine Structure of Pea Stomata. *Protoplasma*, **76**, 61–82.

Sinha, N. and Hake, S. (1990). Mutant Characters of Knotted Maize Leaves are Determined in the Innermost Tissue Layers. *Developmental Biology*, **141**, 203–210.

Slavík, B. (1963). The Distribution Pattern of Transpiration Rate, Water Saturation Deficit, Stomata Number and Size, Photosynthetic and Respiration Rate in the Area of the Tobacco Leaf Blade. *Biologia Plantarum*, **5**, 143–153.

Small, H. and Miller Jr, T. E. (1982). Indirect Photometric Chromatography. *Analytical chemistry*, **54**, 462–469.

Smith, F. W. (2001). Sulphur and Phosphorus Transport Systems in Plants. *Plant and Soil*, **232**, 109–118.

Smith, L. G., Greene, B., Veit, B. and Hake, S. (1992). A Dominant Mutation in the Maize Homeobox Gene, Knotted-1, Causes its Ectopic Expression in Leaf Cells with Altered Fates. *Development*, **116**, 21–30.

Smith, S., Weyers, J. D. B. and Berry, W. G. (1989). Variation in Stomatal Characteristics over the Lower Surface of *Commelina communis* Leaves. *Plant, Cell and Environment*, **12**, 653–659.

Soga, T. and Ross, G. A. (1999). Simultaneous Determination of Inorganic Anions, Organic Acids, Amino Acids and Carbohydrates by Capillary Electrophoresis. *Journal of Chromatography A*, **837**, 231–239.

Søndergaard, R. V, Henriksen, J. R. and Andresen, T. L. (2014). Design, Calibration and Application of Broad-Range Optical Nanosensors for Determining Intracellular pH. *Nature Protocols*, **9**, 2841–2858.

Sottocornola, B., Visconti, S., Orsi, S., Gazzarrini, S., Giacometti, S., Olivari, C., Camoni, L., Aducci, P., Marra, M., Abenavoli, A., Thiel, G. and Moroni, A. (2006). The Potassium Channel KAT1 is Activated by Plant and Animal 14-3-3 Proteins. *The Journal of biological chemistry*, **281**, 35735–35741.

Spence, R. D., Sharpe, P. J. H. and Powell, R. D. (1984). Response of Guard Cells to Temperature at Different Concentrations of Carbon Dioxide in *Vicia faba* L. *New Phytologist*, **97**, 129–144.

Staehelin, L. and Hepler, P. (1996). Cytokinesis in Higher Plants. *Cell*, **84**, 821–824.

Stebbins, G. and Jain, S. (1960). Developmental Studies of Cell Differentiation in the Epidermis of Monocotyledons: I. *Allium, Rhoeo, and Commelina. Developmental Biology*, **2**, 409–426.

Stebbins, G. L. and Shah, S. S. (1960). Developmental Studies of Cell Differentiation in the Epidermis of Monocotyledons: II. Cytological Features of Stomatal Development in the Gramineae. *Developmental biology*, **2**, 477–500.

Steeves, T. A. and Sussex, I. M. (1989). Patterns in plant development. 2nd eds. Cambridge, UK: *Cambridge University Press.*

Steudle, E. and Zimmermann, U. (1977). Effect of Turgor Pressure and Cell Size on the Wall Elasticity of Plant Cells. *Plant Physiol*, **59**, 285–289.

Sturaro, M., Hartings, H., Schmelzer, E., Velasco, R., Salamini, F. and Motto, M. (2005). Cloning and Characterization of GLOSSY1, a Maize Gene Involved in Cuticle Membrane and Wax Production. *Plant Physiology*, **138**, 478–489.

Svatoš, A. (2011). Single-Cell Metabolomics Comes of Age: New Developments in Mass Spectrometry Profiling and Imaging. *Analytical Chemistry*, **83**, 5037–5044.

Sylvester, A. W., Smith, L. and Freeling, M. (1996). Acquisition of Identity in the Developing Leaf. *Annual Review of Cell and Developmental Biology*, **12**, 257–304.

Sze, H. (1985). H^+-Translocating ATPases: Advances Using Membrane Vesicles. *Annual Review of Plant Physiology*, **36**, 175–208.

Szymkowiak, E. J. (1990). Interactions between Cells Derived from the Three Shoot Apical Meristem Layers of Tomato and Related Species in Graft Generated Chimeras. *PhD.Thesis,* Yale University, New Haven, USA.

Szyroki, A., Ivashikina, N., Dietrich, P., Roelfsema, M. R., Ache, P., Reintanz, B., Deeken,

R., Godde, M., Felle, H., Steinmeyer, R., Palme, K. and Hedrich, R. (2001). KAT1 is not Essential for Stomatal Opening. *Proceedings of the National Academy of Sciences of the United States of America*, **98**, 2917–2921.

Taiz, L. (1984). Plant Cell Expansion: Regulation of Cell Wall Mechanical Properties. *Annual Review of Plant Physiology*, **35**, 587–657.

Taiz, L., Zeiger, E., Møller, I. M. and Murphy, A. (2015). Plant physiology and development. 6th eds. Edited by A. D. Sinauer. Massachusetts, USA: *Sinauer Associates, Incorporated.*

Takashi, F., Shuichi, M., Mónica Lorenzo, T., Tsuyoshi, E., Iwao, S., Hajime, M., Tsuyama, N. and Masujima, T. (2015). Direct Metabolomics for Plant Cells by Live Single-Cell Mass Spectrometry. *Nature protocols*, **10**, 1445–1456.

Tal, M. and Imber, D. (1971). Abnormal Stomatal Behavior and Hormonal Imbalance in Flacca, a Wilty Mutant of Tomato III. Hormonal Effects on the Water Status in the Plant. *Plant Physiol*, **47**, 849–850.

Talbott, L. D. and Zeiger, E. (1996) Central Roles for Potassium and Sucrose in Guard-Cell Osmoregulation. *Plant Physiology*, **111**, 1051–1057.

Talbott, L. D. and Zeiger, E. (1998). The Role of Sucrose in Guard Cell Osmoregulation. *Journal of Experimental Botany*, **49**, 329–337.

Talbott, L., Rahveh, E. and Zeiger, E. (2003). Relative Humidity is a Key Factor in the Acclimation of the Stomatal Response to CO_2. *Journal of Experimental Botany*, **54**, 2141–2147.

Talbott, L., Srivastava, A. and Zeiger, E. (1996). Stomata from Growth-Chamber-Grown *Vicia faba* Have an Enhanced Sensitivity to CO_2. *Plant, cell and environment0*, **19**, 1188–1194.

Tanaka, Y., Kutsuna, N., Kanazawa, Y., Kondo, N., Hasezawa, S. and Sano, T. (2007). Intra-Vacuolar Reserves of Membranes During Stomatal Closure: The Possible Role of Guard Cell Vacuoles Estimated by 3-D Reconstruction. *Plant Cell Physiol.*, **48**, 1159–1169.

Tanaka, Y., Nose, T., Jikumaru, Y. and Kamiya, Y. (2013). ABA Inhibits Entry into Stomatal-lineage Development in *Arabidopsis* Leaves. *The Plant Journal*, **74**, 448–457.

Tandy, S., Brittain, S. R., Grail, B. M., Mcleod, C. W., Paterson, E., Tomos, A. D., Tandy, S., Grail, B. M., Tomos, A. D., Brittain, S. R., Mcleod, : C W, Mcleod, C. W., *et al.* (2013). Fine Scale Measurement and Mapping of Uranium in Soil Solution in Soil and Plant-Soil Microcosms, with Special Reference to Depleted Uranium. *Plant soli*, **368**, 471–482.

Tang, F., Lao, K. and Surani, M. A. (2011). Development and Applications of Single-Cell Transcriptome Analysis. *Nature methods*, **8**, s6–s11.

Terashima, I. (1992). Anatomy of Non-Uniform Leaf Photosynthesis. *Photosynthesis research*, **31**, 195–212.

Terena, L., Walker, N. A., Hepler, P. K. and Overall, R. L. (2000). Physiological Elevations in Cytoplasmic Free Calcium by Cold or Ion Injection Result in Transient Closure of Higher Plant Plasmodesmata. *Planta*, **210**, 329–335.

Tester, M. and Leigh, R. A. (2001). Partitioning of Nutrient Transport Processes in Roots. *Journal of Experimental Botany*, **52**, 445–457.

Thomas, D. A. (1970). The Regulation of Stomatal Aperture in Tobacco Leaf Epidermal

Strips I. The Effect of Ions. *Australian Journal of Biological Sciences*, **23**, 961–979.

Thomas, J. F. and Harvey, C. N. (1983). Leaf Anatomy of Four Species Grown under Continuous CO_2 Enrichment. *Botanical Gazette*, **144**, 303–309.

Tian, W., Hou, C., Ren, Z., Pan, Y., Jia, J. and Zhang, H. (2015). A Molecular Pathway for CO_2 Response in *Arabidopsis* Guard Cells. *Nature*, **6**, 6057–6067.

Timmerman, H. A. (1927) Stomatal Numbers: Their Value for Distinguishing Species. *Pharm.J*, **118**, 241–243.

Tomos, A. D. (1988). Cellular Water Relations of Plants. *Water Sci.Rev*, **3**, 186–277.

Tomos, A. D. (2016). Use of CE to Analyze Solutes in Pico-and Nano-Liter Samples from Plant Cells and Rhizosphere. In S.K. P. edn, *Capillary Electrophoresis. Methods in Molecular Biology, vol 1483*. Schmitt-Ko. *Humana Press, New York, USA*, 181–194.

Tomos, A. D., Leigh, R. A., Palta, J. A. and Williams, J. H. (1992). Sucrose and Cell Water Relations. In Pollock, *et al.,* edn, *Carbon partitioning within and between organisms*. *Oxford Bios Scientific Publishers Limited, UK*, 71–89.

Tomos, A. D., Hinde, P., Richardson, P., Pritchard, J. and Fricke, W. (1994). Microsampling and Measurements of Solutes in Single Cells. In Harris, KJ Oparka, E. edn, Plant cell biology: *A Practical Approach*. *IRC Press, Oxford, UK*, 297–314.

Tomos, D. A. and Leigh, R. A. (1999). The Pressure Probe: A Versatile Tool in Plant Cell Physiology. *Annual review of plant biology*, **50**, 447–472.

Tomos, A. D., Leigh, R. A. and Koroleva, O. A. (2000). Spatial and Temporal Variation in Vacuolar Contents. *Annual plant reviews*, **5**, 174–198.

Tomos, A. D. and Sharrock, R. A. (2001). Cell Sampling and Analysis (SiCSA): Metabolites Measured at Single Cell Resolution. *Journal of Experimental Botany*, **52**, 623–630.

Tomos, D. (2000). The Plant Cell Pressure Probe. *Biotechnology Letters*, **22**, 437–442.

Tomos, D. A., Steudle, E., Zimmermann, U. and Schulze, E.D. (1981). Water Relations of Leaf Epidermal Cells of *Tradescantia virginiana. Plant Physiol.*, **68**, 1135–1143.

Tomos, D. and Zimmermann, U. (1983). Water Relations of the Stomatal Complex of *Rhoeo discolor* and *Tradescantia virginiana* Measured with a Micro Pressure-Probe. *International Symposium of the Phytochemical Society Europe, Toulouse.*

Toriyama, H. and Sato, S. (1968). On the Membrane of the Tannin Vacuole in the *Mimosa* Motor Cell. *Proceedings of the Japan Academy*, **44**, 528–531.

Trejo, C. L., Clephan, A. L. and Davies, W. J. (1995). How Do Stomata Read Abscisic Acid Signals? *Plant Physiology*, **109**, 803–811.

Trewavas, A. J. and Malhó, R. (1998). Ca^{2+} Signalling in Plant Cells: The Big Network. *Current Opinion in Plant Biology*, **1**, 428–433.

Tsukaya, H. (2013). Leaf Development. *The Arabidopsis book*, **11**, e0163.

Tsunekawa, K., Shijuku, T., Hayashimoto, M., Kojima, Y., Onai, K., Morishita, M., Ishiura, M., Kuroda, T., Nakamura, T., Kobayashi, H., Sato, M., Toyooka, K., *et al.* (2009). Identification and Characterization of the Na^+/H^+ Antiporter Nhas3 from the Thylakoid Membrane of *Synechocystis* Sp. PCC 6803. *The Journal of biological chemistry*, **284**, 16513–21.

Turgeon, R. (1989). The Sink-Source Transition in Leaves. *Plant Biology*, **40**, 119–38

Turner, N. C. (1986). Adaptation to Water Deficits : A Changing Perspective. *Aust . J . Plant Physiol*, **13**, 175–90.

Upchurch Jr, G. (1984). Cuticular Anatomy of Angiosperm Leaves from the Lower Cretaceous Potomac Group. I. Zone 1 Leaves. *American Journal of Botany*, **71**, 192–202.

Vahisalu, T., Kollist, H., Wang, Y.F., Nishimura, N., Chan, W.Y., Valerio, G., Lamminmäki, A., Brosché, M., Moldau, H., Desikan, R., Schroeder, J. I. and Kangasjärvi, J. (2008). SLAC1 is Required for Plant Guard Cell S-Type Anion Channel Function in Stomatal Signalling. *Nature*, **452**, 487–91.

Veit, B. (2004) Determination of Cell Fate in Apical Meristems. *Current Opinion in Plant Biology* , **7**, 57–64.

Veloso, F. A. (2017). On the Developmental Self-Regulatory Dynamics and Evolution of Individuated Multicellular Organisms. *Journal of Theoretical Biology*, **417**, 84–99.

Vincken, J.P., Schols, H. A., Oomen, R. J. F. J., McCann, M. C., Ulvskov, P., Voragen, A. G. J. and Visser, R. G. F. (2003). If Homogalacturonan Were a Side Chain of Rhamnogalacturonan I. Implications for Cell Wall Architecture. *Plant Physiology*, **132**, 1781–1789.

Voitsekhovskaja, O. V., Koroleva, O. A., Batashev, D. R., Knop, C., Tomos, A. D., Gamalei, Y. V., Heldt, H.W. and Lohaus, G. (2006). Phloem Loading in Two *Scrophulariaceae* Species. What Can Drive Symplastic Flow via Plasmodesmata?, *Plant Physiology*, **140**, 383–395.

De Vries, H. (1884). Eine Methode Zur Analyse Der Turgorkraft. *Jahr. wiss. Bot.*, **14**, 427–601.

Waadt, R., Hitomi, K., Nishimura, N., Hitomi, C., Adams, S. R., Getzoff, E. D. and Schroeder, J. I. (2014). FRET-Based Reporters for the Direct Visualization of Abscisic Acid Concentration Changes and Distribution in *Arabidopsis. eLife Sciences Publications,* **3**, 1-28.

Wagner, G. J. (1982). Compartmentation in Plant Cells: The Role of the Vacuole. In *Cellular and Subcellular Localization in Plant Metabolism*. L. L. Crea. New York USA: *Springer*, 1–45.

Wang, C., Huang, W., Ying, Y., Li, S., Secco, D., Tyerman, S., Whelan, J. and Shou, H. (2012). Functional Characterization of the Rice SPX-MFS Family Reveals a Key Role of OsSPX-MFS1 in Controlling Phosphate Homeostasis in Leaves. *New Phytologist*, **196**, 139–148.

Wang, C., Yue, W., Ying, Y., Wang, S., Secco, D., Liu, Y., Whelan, J., Tyerman, S. D. and Shou, H. (2015). Rice SPX-Major Facility Superfamily3, a Vacuolar Phosphate Efflux Transporter, is Involved in Maintaining Phosphate Homeostasis in Rice. *Plant Physiology*, **169**, 2822–2831.

Wang, Z., Wang, F., Hong, Y., Huang, J., Shi, H. and Zhu, J.-K. (2016). Two Chloroplast Proteins Suppress Drought Resistance by Affecting ROS Production in Guard Cells. *Molecular Plant Sciences, Chinese Academy of Sciences* , **172**, 2491–2503.

Wagner, T. A. and Kohorn, B. D. (2001) Wall-Associated Kinases Are Expressed throughout Plant Development and Are Required for Cell Expansion, *The Plant Cell*, **13**, 303–318.

Ward, J. M. and Schroeder, J. I. (1994). Calcium-Activated K^+ Channels and Calcium-

induced Calcium Release by Slow Vacuolar Ion Channels in Guard Cell Vacuoles implicated in the Control of Stomatal Closure. *The Plant Cell*, **6**, 669–683.

Watson, R. T., Rodhe, H., Oeschger, H. and Siegenthaler, U. (1990). Greenhouse Gases and Aerosols. In Houghton, J., Jenkins, G. J., and Ephraums, J. edn *Climate change: the IPCC scientific assessment*. second edn. Melbourne, Sydney, *Cambridge University Press, Cambridge, UK*, 17.

Webb, A. A. R. and Mansfield, T. A. (1992). How Do Stomata Work? *Journal of Biological Education*, **26**, 19–26.

Webb, A. and Hetherington, A. (1997). Convergence of the Abscisic Acid, CO_2, and Extracellular Calcium Signal Transduction Pathways in Stomatal Guard Cells. *Plant Physiology* , **114**, 1557–1560.

Wei, P.C., Zhang, X.Q., Zhao, P. and Wang, X.C. (2011). Regulation of Stomatal Opening by the Guard Cell Expansin *AtEXPA1*. *Plant Signaling & Behavior*, **6**, 740–742.

Weissenbock, G., Schnabl, H., Scharf, H. and Sachs, G. (1987). On the Properties of Fluorescing Compounds in Guard and Epidermal Cells of *Allium Cepa* L. *Planta*, **171**, 88–95.

Wenkert, W. (1980). Measurement of Tissue Osmotic Pressure. *Plant Physiol*, **65**, 614–617.

Weyers, J. D. B. and Meidner, H. (1990). Methods in Stomatal Research. London uk: *Longman Scientific and Technical.*

Weyers, J. D. B. and Lawson, T. (1997). Heterogeneity in Stomatal Characteristics. *Advances in Botanical Research*, **26**, 317–352.

Weyers, J. D. and Travis, A. J. (1981). Selection and Preparation of Leaf Epidermis for Experiments on Stomatal Physiology. *Journal of experimental botany*, **32**, 837–850.

Wildman, B. J., Jackson, P. E., Jones, W. R. and Alden, P. G. (1991). Analysis of Anion Constituents of Urine by Inorganic Capillary Electrophoresis. *Journal of Chromatography A*, **546**, 459–466.

Wilkinson, S., Clephan, A. L. and Davies, W. J. (2001). Rapid Low Temperature-Induced Stomatal Closure Occurs in Cold-Tolerant *Commelina communis* Leaves but not in Cold-Sensitive Tobacco Leaves, via a Mechanism that Involves Apoplastic Calcium but not Abscisic Acid. *Plant Physiology*, **126**, 1566–1578.

Wille, A. C. A. and Lucas, W. J. W. (1984). Ultrastructural and Histochemical Studies on Guard Cells. *Planta*, **160**, 129–142.

Williams, M. L., Thomas, B. J., Farrar, J. F. and Pollock, C. J. (1993). Visualizing the Distribution of Elements within Barley Leaves by Energy Dispersive X-Ray Image Maps (EDX Maps). *New Phytologist*, **125**, 367–372.

Williams, W. T. (1954). A New Theory of the Mechanism of Stomatal Movement. *Journal of Experimental Botany*, **5**, 343–352.

Willis, K. and McElwain, J. (2014). The Evolution of Plants. 2nd edn. London Uk: *Oxford University Press London UK.*

Willmer, C. and Fricker, M. (1996) Stomata. 2nd edn. London, Uk, *Chapman and Hall.*

Willmer, C. M. and Beattie, L. N. (1978). Cellular Osmotic Phenomena During Stomatal Movements of *Commelina communis* I. Limitations of the Incipient Plasmolysis Technique for Determining Osmotic Pressures. *Protoplasma*, **95**, 321–332.

Willmer, C. M. and Mansfield, T. A. (1969). A Critical Examination of the Use of Detached Epidermis in Studies of Stomatal Physiology. *New Phytologist*, **68**, 363–375.

Willmer, C. M. and Pallas, J. E. (1974). Stomatal Movements and Ion Fluxes within Epidermis of *Commelina communis* L. *Nature*, **252**, 126–127.

Willmer, C. M., Pallas Jr, J. E. and Jackson, W. A. (1974). Major Element Composition of Epidermal and Mesophyll Tissues of *Commelina communis* L. and *Vicia faba* L.: Some Further Considerations of the Role of Ions in Stomatal Functioning. *Journal of experimental botany*, **25**, 973–980.

Willmer, C., Ryuzi, K., Pallas, J. E. J. and Black, C. C. J. (1973). Detection of High Levels of Phosphoenolpyruvate Carboxylase in Leaf Epidermal Tissue and its Significance in Stomatal Movements. *Life Sciences*, **12**, 151–155.

Wilson, J. A., Ogunkanmi, A. B. and Mansfield, T. A. (1978). Effects of External Potassium Supply on Stomatal Closure Induced by Abscisic Acid. *Plant, Cell and Environment*, **1**, 199–201.

Windsor, P. J. and Leys, S. P. (2010). Wnt Signaling and Induction in the Sponge Aquiferous System: Evidence for an Ancient Origin of the Organizer. *Evolution and Development*, **12**, 484–493.

Winner, W. E. and Mooney, H. A. (1980). Responses of Hawaiian Plants to Volcanic Sulfur Dioxide: Stomatal Behavior and Foliar Injury. *Science*, **210**, 789–791.

Winter, H., Robinson, D. G. and Heldp, H. W. (1993). Subcellular Volumes and Metabolite Concentrations in Barley Leaves. *Planta*, **191**, 180–190.

Winter, H., Robinson, D. G. and Heldt, H. W. (1994). Subcellular Volumes and Metabolite Concentrations in Spinach Leaves. *Planta*, **193**, 530–535.

Woodward, F. I. (1987). Stomatal Numbers are Sensitive to Increases in CO_2 from Pre-Industrial Levels. *Nature*, **327**, 617–618.

Woodward, F. I. (1998). Do Plants Really Need Stomata? *Journal of experimental botany*, **49**,471–480.

Woodward, F. I. and Kelly, C. K. (1995). The Influence of CO_2 Concentration on Stomatal Density. *New Phytologist*, **131**, 311–327.

Wright, S. and Hiron, R. (1969). (+)-Abscisic Acid, the Growth Inhibitor Induced in Detached Wheat Leaves by a Period of Wilting. *Nature*, **224**, 719–720.

Wright, S. T. C. (1969). An Increase in the "Inhibitor-β" Content of Detached Wheat Leaves Following a Period of Wilting. *Planta*, **86**, 10–20.

Wu, C. H., Lo, Y. S., Lee, Y.H. and Lin, T.I. (1995). Capillary Electrophoretic Determination of Organic Acids with Indirect Detection. *Journal of Chromatography A*, **716**, 291–301.

Wu, H. and Sharpe, P. J. H. (1979). Stomatal Mechanics II: Material Properties of Guard Cell Walls. *Plant, Cell and Environment*, **2**, 235–244.

Xie, X., Wang, Y., Williamson, L., Holroyd, G. H., Tagliavia, C., Murchie, E., Theobald, J., Knight, M. R., Davies, W. J. and Leyser, H. M. (2006). The Identification of Genes Involved in the Stomatal Response to Reduced Atmospheric Relative Humidity. *Current Biology*, **16**, 882–887.

Xue, S., Hu, H., Ries, A., Merilo, E. and Kollist, H. (2011). Central Functions of Bicarbonate

in S-Type Anion Channel Activation and OST1 Protein Kinase in CO_2 Signal Transduction in Guard Cell. *The EMBO*, **30**, 1645–1658.

Yamaguchi, T., Aharon, G. S., Sottosanto, J. B. and Blumwald, E. (2005). Vacuolar Na^+/H^+ Antiporter Cation Selectivity is Regulated by Calmodulin from within the Vacuole in a Ca^{2+}- and pH-Dependent Manner. *Proceedings of the National Academy of Sciences of the United States of America*, **102**, 16107–12.

Yanai, O., Shani, E., Dolezal, K., Tarkowski, P. and Sablowski, R. (2005). *Arabidopsis* KNOX1 Proteins Activate Cytokinin Biosynthesis. *Current Biology*, **15**, 1566–1571.

Yeo, A. and Flowers, T. (2007). The Driving Forces for Water and Solute Movement, In Yeo, A. and Flowers, T. eds. *Plant Solute Transport*. Sussex, UK: *Blackwell Publishing Ltd*. 29–47.

Yeung, E. S. (1989). Indirect Detection Methods: Looking for What Is Not There. *Accounts of Chemical Research*, **22**, 125–130.

Yeung, E. S. (1989). Indirect Detection Methods: Looking for What is Not There. *Accounts of Chemical Research*, **22**, 125–130.

Yoshida, R., Hobo, T., Ichimura, K., Mizoguchi, T., Takahashi, F., Aronso, J., Ecker, J. R. and Shinozaki, K. (2002). ABA-Activated SnRK2 Protein Kinase is Required for Dehydration Stress Signaling in *Arabidopsis. Plant and Cell Physiology*, **43**, 1473–1483.

Yoshida, R., Umezawa, T., Mizoguchi, T., Takahashi, S., Takahashi, F. and Shinozaki, K. (2005). The Regulatory Domain of SRK2E/OST1/SnRK2.6 Interacts with ABI1 and Integrates Abscisic Acid (ABA) and Osmotic Stress Signals Controlling Stomatal Closure in *Arabidopsis. The Journal of biological chemistry*, **281**, 5310–5318.

Zalenskii, V. R. (1904) Data on Quantitative Anatomy of Various Leaves of the Same Plants, *Izv.Kievsk.Politekhn.Inst*, **4**, 1–209.

Zeiger, E. (1983). The Biology of Stomatal Guard Cells. *Annual Review of Plant Physiology*, **34**, 441–474.

Zeiger, E. and Hepler, P. (1977). Light and Stomatal Function: Blue Light Stimulates Swelling of Guard Cell Protoplasts. *Science*, **196**, 887–889.

Zeiger, E., Talbott, L. D., Frechilla, S., Srivastava, A. and Zhu, J. (2002). The Guard Cell Chloroplast: A Perspective for the Twenty-first Century. *New Phytologist*, **153**, 415–424.

Zhang, D., Wadsworth, P. and Hepler, P. K. (1990). Microtubule Dynamics in Living Dividing Plant Cells: Confocal Imaging of Microinjected Fluorescent Brain Tubulin. *Cell Biology*, **87**, 8820–8824.

Zhang, H., Zhu, H., Pan, Y., Yu, Y., Luan, S. and Li, L. (2014). A DTX/MATE-Type Transporter Facilitates Abscisic Acid Efflux and Modulates ABA Sensitivity and Drought Tolerance in *Arabidopsis. Molecular Plant*, **7**, 1522–1532.

Zhang, J. and Davies, W. J. (1987). Increased Synthesis of ABA in Partially Dehydrated Root Tips and ABA Transport from Roots to Leaves. *Journal of Experimental Botany*, **38**, 2015–2023.

Zhang, S. Q. and Outlaw, W. H. (2001). The Guard-Cell Apoplast as a Site of Abscisic Acid Accumulation in *Vicia faba* L. *Plant, Cell and Environment*, **24**, 347–355.

Zhao, F.J., Moore, K. L., Lombi, E. and Zhu, Y. G. (2014a). Imaging Element Distribution

and Speciation in Plant Cells. *Trends in Plant Science*, **19**, 183–192.

Zhao, Z., Crespi, V. H., Kubicki, J. D., Cosgrove, D. J., Zhong, L., Zhao, Z., Kubicki, J. D., Crespi, Á. V. H., Cosgrove, D. J., Zhong, Á. L., Crespi, V. H. and Zhong, L. (2014b). Molecular Dynamics Simulation Study of Xyloglucan Adsorption on Cellulose Surfaces: Effects of Surface Hydrophobicity and Side-Chain Variation. *Cellulose*, **21**, 1025–1039.

Zimmermann, U. (1989). Water Relations of Plant Cells: Pressure Probe Technique. *Methods in enzymology*, **174**, 338–366.

Zimmermann, U., Htisken, D., Schulze, E.D., Husken, D. and Schulze, E.D. (1980). Direct Turgor Pressure Measurements in Individual Leaf Cells of *Tradescantia virginiana. Planta*, **149**, 445–453.

Zocchi, G. and Hanson, J. B. (1982). Calcium Influx into Corn Roots as a Result of Cold Shock. *Plant Physiol*, **70**, 318–319.

Appendix

1. Individual standard curves of all 9 anions

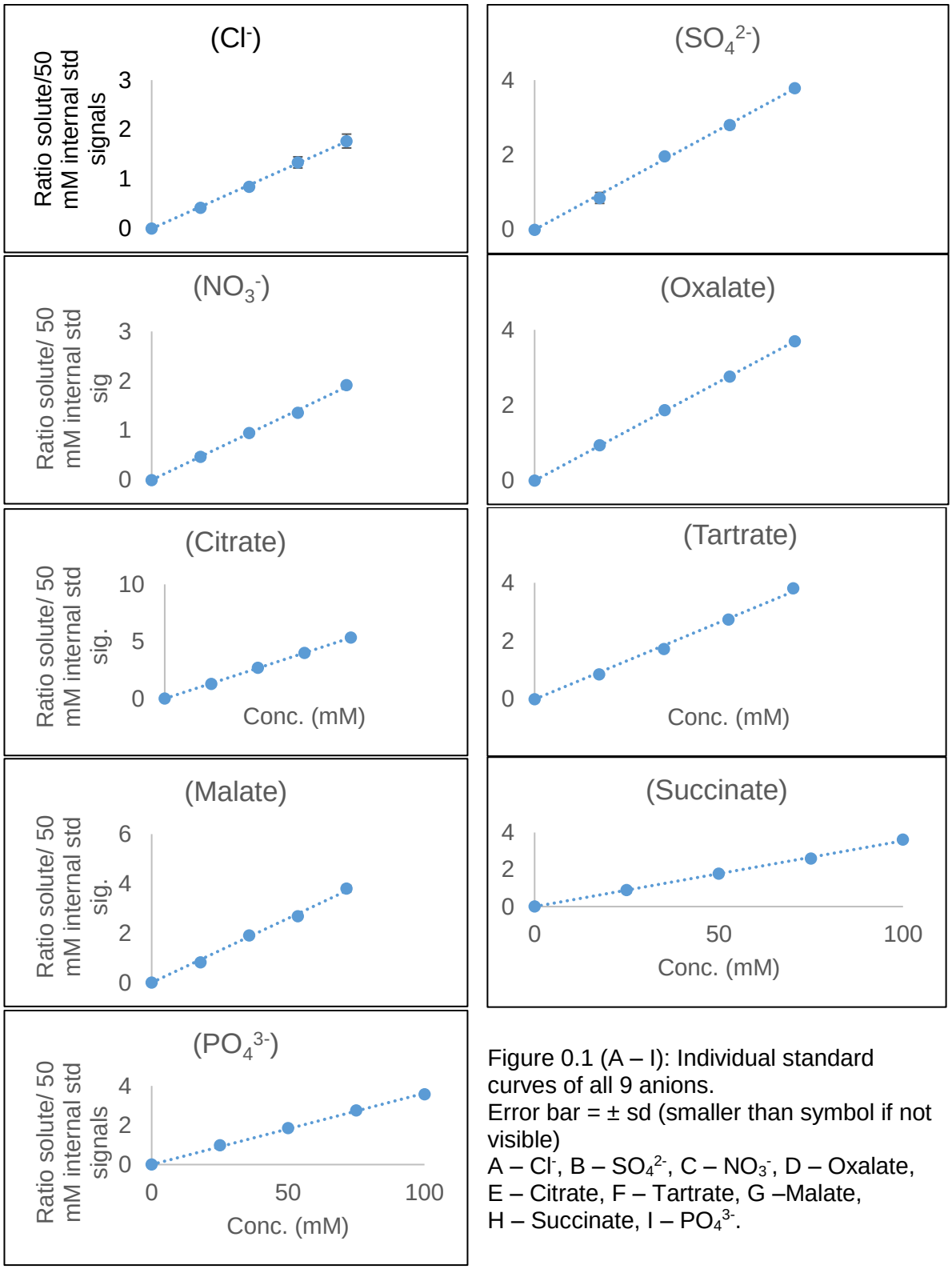

Figure 0.1 (A – I): Individual standard curves of all 9 anions.
Error bar = ± sd (smaller than symbol if not visible)
A – Cl^-, B – SO_4^{2-}, C – NO_3^-, D – Oxalate, E – Citrate, F – Tartrate, G –Malate, H – Succinate, I – PO_4^{3-}.

2. Individual standard curves of all 5 cations

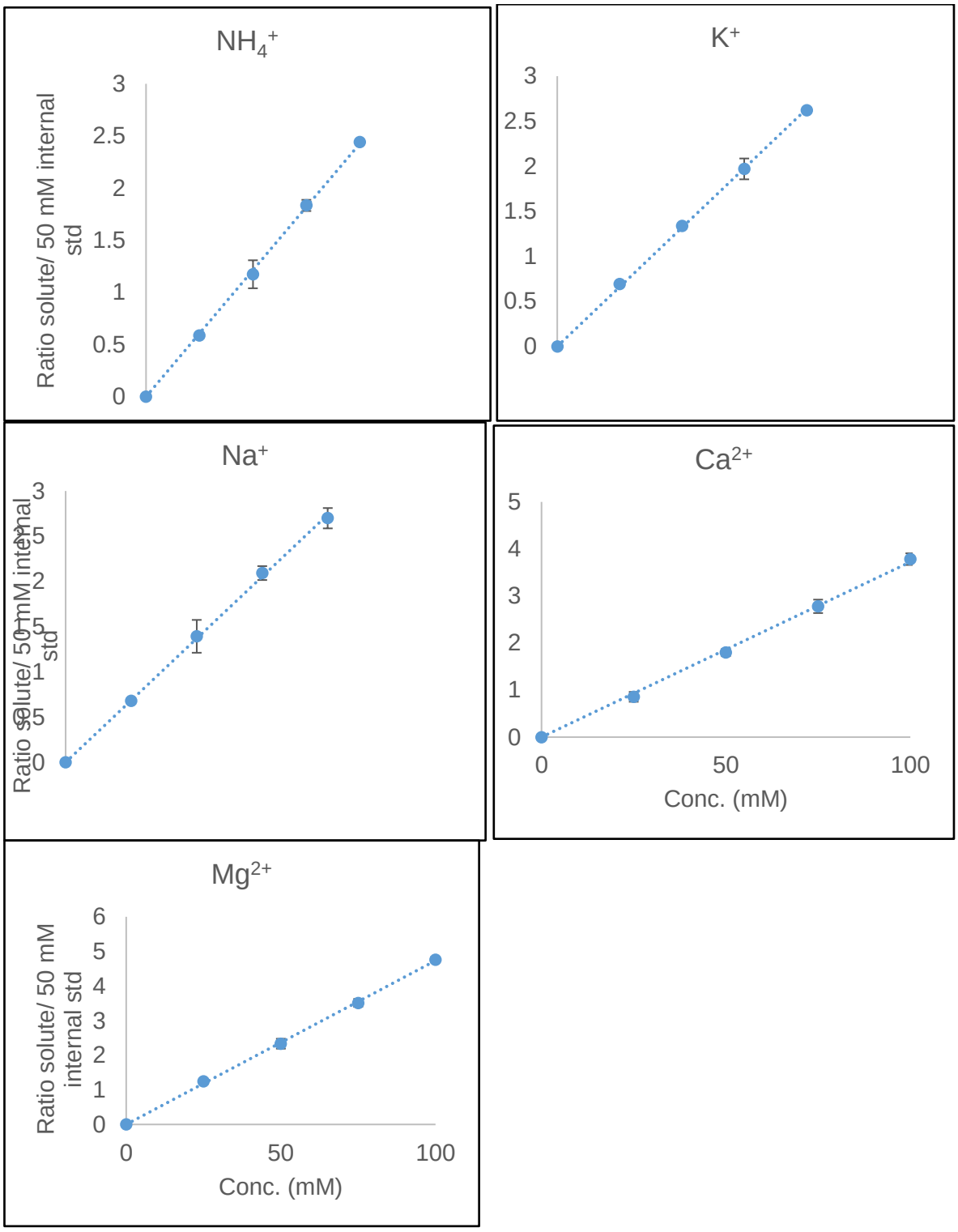

Figure 0.2 (A – E): Individual standard curves of all 5 cations
Error bar = ±sd
A – $NH4^{+}$, B – K^{+}, C – Na^{+}, D – Ca^{2+}, E – Mg^{2+}

3. Standard curves for anions

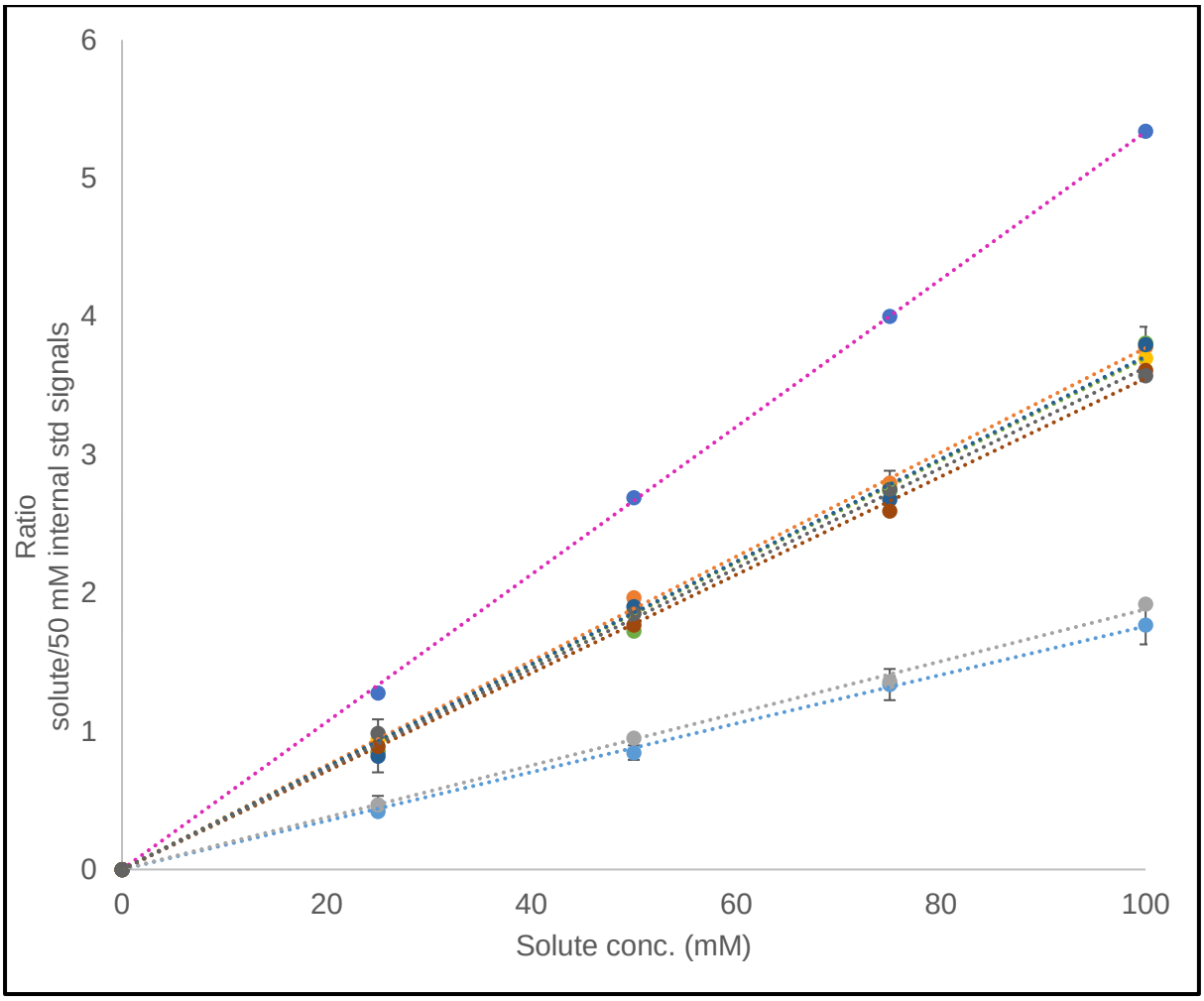

Figure 0.3 Anion standard curves
Error bars represent ± sd. (n= 3) (smaller than symbol if not visible)

Cl^- SO_4^{2-} NO_3^- OXA

C/A TART M/A SUCC PO_4^{3-}

4. Standard curves for cations

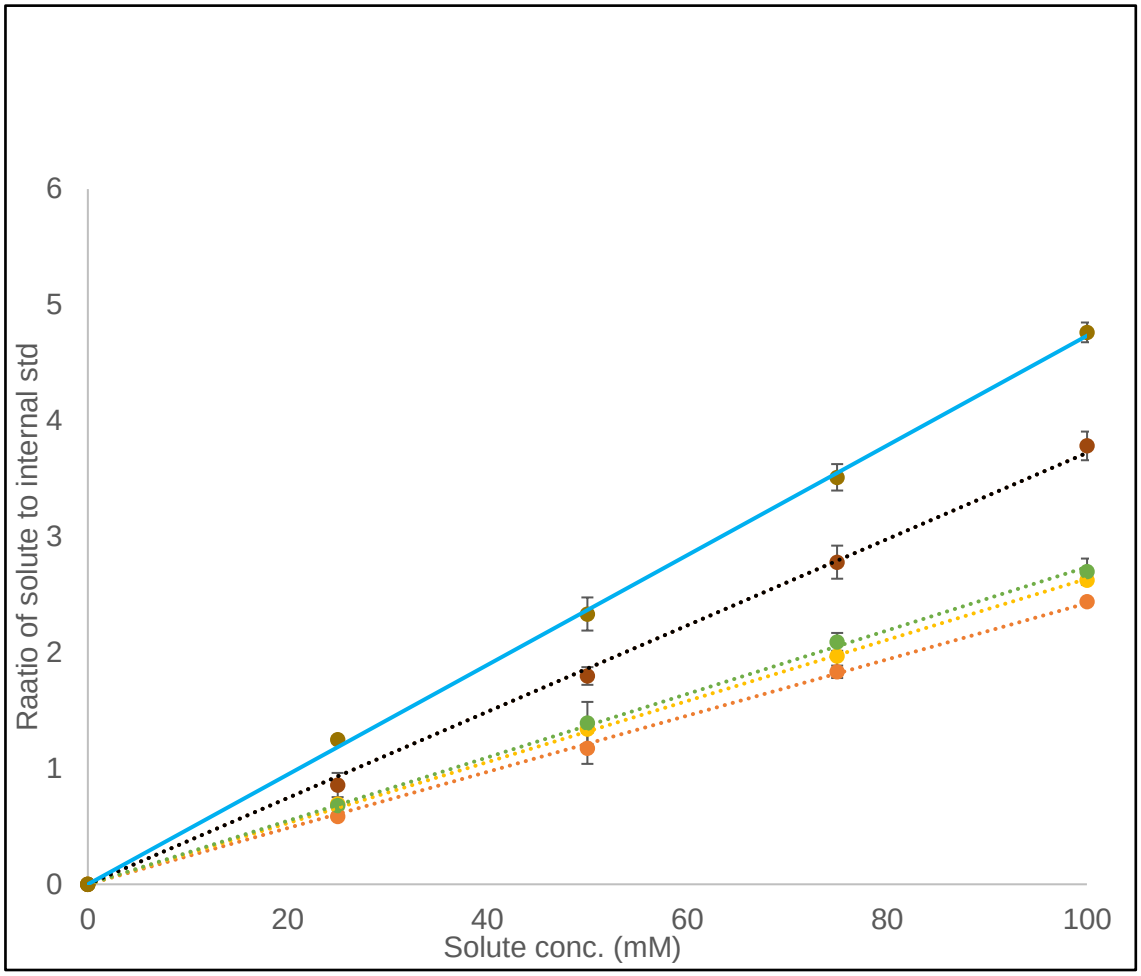

Figure 0.4 Cation standard curve

NH_4^+ K^+ Na^+ Ca^{2+} Mg^{2+}

5. Mean of anions in abaxial epidermal strips

Table 0.1 Mean of anions in abaxial epidermal strips of leaves 4, 5 and 6 of three plants
This table shows the concentrations of anions in abaxial epidermal strip of *T. virginiana* measured by CZE. The 4th, 5th and 6th leaves of three plants were sampled. Each sampled leaf was mature and fully expanded. Results are given as mean ± sd (n = 9). The unidentified anions were not quantified.

Plant 1									
Leaf	Cl^- (mM)	SO_4^{2-} (mM)	NO_3^- (mM)	Oxalate (mM)	Citrate (mM)	Tartrate (mM)	Malate (mM)	Succinate (mM)	PO_4^{3-} (mM)
4	61.61 ± 3.62	16.98 ± 1.51	16.06 ± 0.62	0.72 ± 0.07	20.39 ± 1.31	0.41 ± 0.01	138.83 ± 8.26	0.47 ± 0.02	30.04 ± 1.57
5	52.38 ± 3.37	15.33 ± 3.29	13.81 ± 0.64	0.61 ± 0.06	14.60 ± 0.72	0.37 ± 0.05	131.06 ± 1.40	0.40 ± 0.02	28.30 ± 2.06
6	49.92 ± 2.85	10.86 ± 0.56	11.03 ± 1.16	0.51 ± 0.03	13.69 ± 0.24	0.22 ± 0.02	124.66 ± 1.51	0.31 ± 0.02	26.56 ± 0.63
Plant 2									
Leaf	Cl^- (mM)	SO_4^{2-} (mM)	NO_3^- (mM)	Oxalate (mM)	Citrate (mM)	Tartrate (mM)	Malate (mM)	Succinate (mM)	PO_4^{3-} (mM)
4	62.54 ± 1.73	16.60 ± 0.85	16.57 ± 0.50	0.68 ± 0.03	18.67 ± 0.48	0.41 ± 0.04	141.77 ± 6.05	0.44 ± 0.02	28.88 ± 2.46
5	54.81 ± 1.72	14.70 ± 0.92	13.18 ± 1.35	0.63 ± 0.01	14.46 ± 0.32	0.37 ± 0.01	130.50 ± 3.08	0.40 ± 0.01	27.63 ± 2.23
6	46.68 ± 2.77	11.80 ± 0.32	10.95 ± 0.31	0.47 ± 0.03	11.35 ± 0.53	0.31 ± 0.02	123.42 ± 9.16	0.35 ± 0.00	25.22 ± 2.46
Plant 3									
Leaf	Cl^- (mM)	SO_4^{2-} (mM)	NO_3^- (mM)	Oxalate (mM)	Citrate (mM)	Tartrate (mM)	Malate (mM)	Succinate (mM)	PO_4^{3-} (mM)
4	63.42 ± 5.85	18.12 ± 1.05	16.21 ± 3.21	0.83 ± 0.03	16.80 ± 0.25	0.41 ± 0.01	147.21 ± 5.99	0.48 ± 0.02	29.74 ± 1.28
5	53.19 ± 3.68	14.88 ± 0.81	13.78 ± 1.78	0.65 ± 0.11	14.45 ± 0.79	0.34 ± 0.04	130.58 ± 7.72	0.40 ± 0.04	28.30 ± 3.27
6	47.79 ± 6.16	11.84 ± 0.37	10.67 ± 1.10	0.39 ± 0.12	12.06 ± 0.31	0.26 ± 0.03	123.10 ± 6.15	0.35 ± 0.02	26.50 ± 5.12

6. Mean of cations in abaxial epidermal strips

Table 0.2 Mean of cations in abaxial epidermal strips of leaves 4, 5 and 6 of three plants
This table shows cation concentrations in the abaxial epidermal strip of *T. virginiana* measured by CZE. The 4th, 5th and 6th leaves of three plants were sampled. Each sampled leaf was mature and fully expanded. Results are given as mean ± sd (n = 9).

	Plant 1				
Leaf	NH_4^+ (mM)	K^+(mM)	Na^+ (mM)	Ca^{2+} (mM)	Mg^{2+} (mM)
4	3.29 ± 0.06	284.52 ± 3.58	26.96 ± 0.20	59.35 ± 0.89	23.58 ± 0.56
5	3.03 ± 0.15	269.54 ± 1.02	26.31 ± 0.27	55.05 ± 1.26	21.49 ± 0.28
6	2.31 ± 0.12	262.55 ± 2.97	26.15 ± 0.26	52.89 ± 0.42	20.75 ± 0.19
	Plant 2				
Leaf	NH_4^+ (mM)	K^+(mM)	Na^+ (mM)	Ca^{2+} (mM)	Mg^{2+} (mM)
4	3.25 ± 0.36	286.86 ± 0.26	27.04 ± 0.22	57.63 ± 0.57	24.75 ± 0.57
5	2.95 ± 0.02	271.42 ± 1.19	26.57 ± 0.18	54.56 ± 0.37	21.64 ± 0.36
6	2.42 ± 0.05	263.08 ± 2.48	26.29 ± 0.02	51.46 ± 0.55	20.51 ± 0.23
	Plant 3				
Leaf	NH_4^+ (mM)	K^+(mM)	Na^+ (mM)	Ca^{2+} (mM)	Mg^{2+} (mM)
4	3.28 ± 0.12	297.54 ± 6.09	27.76 ± 0.34	57.53 ± 1.47	23.27 ± 0.45
5	3.03 ± 0.06	275.46 ± 2.39	27.00 ± 0.46	54.59 ± 0.54	22.58 ± 0.53
6	2.60 ± 0.11	268.85 ± 3.66	26.01 ± 0.20	51.56 ± 0.50	21.0 0.77

7. Anion content of cell types at closed stomata

Table 0.3 Anion content of cell types at closed stomata

Cell type	Chloride (mM)	Sulphate (mM)	Nitrate (mM)	Citrate (mM)	Tartrate (mM)	Malate (mM)	Succinate (mM)	Phosphate (mM)
Pavement	132.1 ± 12.4	28.5 ± 4.2	63.5 ± 8.1	3.3 ± 0.5	-	91.5 ± 8.3	-	56.5 ± 5.3
Lateral SS.	147.4 ± 7.1	51.4 ± 2.9	45.0 ± 3.6	73.5 ± 7.3	0.5 ± 0.1	106.7 ± 9.6	18.0 ± 1.7	9.3 ± 1.0
Guard cell	182.1 ± 1.7	33.5 ± 2.5	77.3 ± 6.9	1.5 ± 0.1	0.0 ± 0.0	60.3 ± 4.3	0.3 ± 0.1	18.7 ± 1.9
Apical SS.	120.4 ± 3.2	40.6 ± 2.2	45.9 ± 2.9	20.8 ± 2.0	12.9 ± 1.2	89.3 ± 8.3	12.2 ± 1.1	30.6 ± 2.0
Juxta Apical	108.8 ± 8.0	53.2 ± 3.4	42.5 ± 3.3	19.7 ± 1.6	-	110.0 ± 8.3	-	38.9 ± 2.9

8. Anion content of cell types at open stomata

Table 0.4 Anion content of cell types at open stomata

Cell type	Chloride (mM)	Sulphate (mM)	Nitrate (mM)	Citrate (mM)	Tartrate (mM)	Malate (mM)	Succinate (mM)	Phosphate (mM)
Epidermal	104.81 ± 5.52	60.59 ± 5.18	35.38 ± 3.19	3.10 ± 0.36		79.70 ± 5.56		24.94 ± 2.63
Lateral SS.	146.62 ± 10.02	25.84 ± 3.33	87.02 ± 6.19	64.04 ± 4.20	1.88 ± 0.24	135.68 ± 6.84	13.85 ± 1.79	46.39 ± 6.32
Guard cell	204.44 ± 6.77	54.27 ± 3.29	88.45 ± 6.90	2.78 ± 0.26	10.70 ± 1.31	64.35 ± 2.64	16.79 ± 1.34	53.11 ± 4.86
Apical SS.	115.64 ± 8.42	52.88 ± 3.11	32.41 ± 4.31	33.79 ± 3.21	1.80 ± 0.28	111.52 ± 13.33	1.05 ± 0.14	23.83 ± 2.36
Juxta Apical	102.96 ± 3.10	10.63 ± 1.02	29.41 ± 4.13	16.99 ± 0.55		68.26 ± 4.34		4.06 ± 0.46

9. Cation content of cell types at closed stomata

Table 0.5 Cation content of cell types at closed stomata. (Mean ± standard deviation, n = 9)

Cell type	NH_4^+ (mM)	K^+ (mM)	Na^+(mM)	Ca^{2+} (mM)	Mg^{2+} (mM)
Pavement	10.0 ± 1.1	268.0 ± 8.0	11.1 ± 1.3	60.6 ± 3.9	40.1 ± 3.7
Lateral SS.	14.8 ± 1.2	94.8 ± 5.9	16.7 ± 0.6	148.8 ± 7.4	105.9 ± 2.2
Guard cell	0.6 ± 0.1	305.7 ± 3.6	1.8 ±0.2	36.9 ± 4.3	32.2 ± 2.6
Apical SS.	16.2 ± 3.0	271.3 ± 3.8	16.7 ± 1.6	42.3 ± 1.0	56.4 ± 2.5
Juxta Apical	7.8 ± 0.6	263.1 ± 4.7	12.4 ± 0.9	76.0 ± 5.4	54.8 ± 1.9

10. Cation content of cell types at open stomata

Table 0.6 Cation content of cell types at open stomata. Mean ± sd (n = 27)
For each cell type, three cell were sampled from the same leaf and each cell sample was run in three replicate subsamples. Guard cell samples were pulled from at least ten guard cells and run similar to samples from other cells.

Cell type	NH_4^+ (mM)	K^+ (mM)	Na^+ (mM)	Ca^{2+} (mM)	Mg^{2+} (mM)
Epidermal	12.75 ± 1.64	207.77 ± 16.19	9.79 ± 0.86	61.68 ± 2.94	33.45 ± 3.39
Lateral SS.	15.39 ± 0.69	183.06 ± 0.84	11.53 ± 0.53	152.86 ± 1.51	100.37 ± 1.60
Guard cell	0.50 ± 0.06	420.46 ± 12.73	1.19 ± 0.15	40.16 ± 3.83	69.13 ± 7.33
Apical SS.	16.75 ± 1.49	201.99 ± 2.50	26.36 ± 0.51	89.22 ± 3.95	59.21 ± 3.24
Juxta A.	7.12 ± 0.75	182.65 ± 5.57	5.79 ± 0.49	24.59 ± 3.06	27.03 ± 3.54

11. Differences in solute species concentration at open and closed stomata

This table shows the differences in solute (anion and cation) concentration in each cell between the open and closed stomata states. A two tailed two samples students't-test assuming equal variance was applied to compare the significance of the differences (use of two samples assuming equal variance was because sampling was destructive and could not be obtained from the same cells for both open and closed stomata). Concentrations at closed were subtracted from the equivalent at open stomata condition to get the difference. The % differences is the % increase from the concentrations at closed stomata state. Tartrate was absent in guard cells of closed stomata and hence the zero error in dividing the difference with the (zero) concentration at closed state.

Cell type		**Cl^- (mM)**	**SO_4^{2-} (mM)**	**NO_3^- (mM)**	**Citrate (mM)**	**Tartrate (mM)**	**Malate (mM)**	**Succinate (mM)**	**PO_4^{3-} (mM)**	**Solute sum**
Guard cells	Open	204.4 ± 6.8	54.3 ± 3.3	88.5 ± 6.9	2.8 ± 0.3	10.7 ± 1.3	64.4 ± 2.6	16.8 ± 1.3	53.1 ± 4.9	495.0 ± 11.8
	Closed	182.1 ± 1.7	33.5 ± 2.5	77.3 ± 6.9	1.5 ± 0.1	0.0 ± 0.0	60.3 ± 4.3	0.3 ± 0.1	18.7 ± 1.9	373.7 ± 8.9
	Diff	22.3 ± 5.1	20.8 ± 0.8	11.2 ± 0.0	1.3 ± 1.2	10.7 ± 1.3	4.1 ± 1.7	16.5 ± 1.2	34.4 ± 3.0	
	% diff.	12.3	62.0	14.4	85.3	Zero error	6.7	5496.7	184.0	
	P value	< 0.01	< 0.001	> 0.1	> 0.2	< 0.001	> 0.2	< 0.05	< 0.05	
		NH_4^+ (mM)	**K^+ (mM)**	**Na^+(mM)**	**Ca^{2+} (mM)**	**Mg^{2+} (mM)**				
	Open	0.5 ± 0.1	420.5 ± 12.7	1.2 ± 0.2	40.2 ± 3.8	69.1 ± 7.3				531.5 ± 15.1
	Closed	0.6 ± 0.1	305.7 ± 3.6	1.8 ± 0.2	36.9 ± 4.3	32.2 ± 2.6				377.2 ± 6.2
	Diff	-0.1 ± 0.0	114.8 ± 9.1	-0.6 ± 0.1	3.3 ± 0.5	36.9 ± 4.7				
	% diff.	-16.7	37.5	-33.9	8.8	114.7				
	P value	> 0.2	< 0.001	< 0.05	>0.3	< 0.01				
Pavement cells		**Cl^- (mM)**	**SO_4^{2-} (mM)**	**NO_3^- (mM)**	**Citrate (mM)**	**Tartrate (mM)**	**Malate (mM)**	**Succinate (mM)**	**PO_4^{3-} (mM)**	
	Open	104.81 ± 5.52	60.59 ± 5.18	35.38 ± 3.19	3.10 ± 0.36	-	79.70 ± 5.6	-	24.94 ± 2.63	308.5 ± 10.3
	Closed	132.1 ± 12.4	28.5 ± 4.2	63.5 ± 8.1	3.3 ± 0.5	-	91.5 ± 8.3	-	56.5 ± 5.3	375.4 ± 18.3
	Diff	-27.3 ± 6.9	32.1 ± 1.0	-28.1 ± 4.9	-0.2 ± 0.1	-	-11.8 ± 2.7	-	-31.6 ± 5.9	
	% diff.	-20.7	112.6	-44.3	-6.1	-	-12.9	-	-55.9	
	P value	< 0.05	< 0.01	<0.01	> 0.6	-	> 0.1	-	< 0.001	
		NH_4^+ (mM)	**K^+ (mM)**	**Na^+(mM)**	**Ca^{2+} (mM)**	**Mg^{2+} (mM)**				325.4 ± 16.9
	Open	12.75 ± 1.64	207.77 ± 16.19	9.79 ± 0.86	61.68 ± 2.94	33.45 ± 3.39				389.8 ± 9.8
	Closed	10.0 ± 1.1	268.0 ± 8.0	11.1 ± 1.3	60.6 ± 3.9	40.1 ± 3.7				
	Diff	2.8 ± 0.5	-60.2 ± 8.2	-1.3 ± 0.4	1.1 ± 1.0	-6.7 ± 0.3				
	% diff.	27.5	-22.5	-11.8	1.8	-16.6				
	P value	> 0.07	< 0.01	> 0.2	> 0.7	> 0.08				
Juxta apical		**Cl^- (mM)**	**SO_4^{2-} (mM)**	**NO_3^- (mM)**	**Citrate (mM)**	**Tartrate (mM)**	**Malate (mM)**	**Succinate (mM)**	**PO_4^{3-} (mM)**	

	Open	102.96 ± 3.10	10.63 ± 1.02	29.41 ± 4.13	16.99 ± 0.55		68.26 ± 4.34		4.06 ± 0.46	232.3 ± 6.9
	Closed	108.8 ± 8.0	53.2 ± 3.4	42.5 ± 3.3	19.7 ± 1.6	-	110.0 ± 8.3	-	38.9 ± 2.9	373.1 ± 12.9
	Diff	-5.8 ± 4.9	-42.6 ± 2.4	-13.1 ± 0.8	-2.7 ± 1.1	-	-41.7 ± 0.0	-	-34.8 ± 2.4	
	% diff.	-5.4	-80.0	-30.8	-13.8	-	-37.9	-	-89.6	
	P value	> 0.3	< 0.001	< 0.05	> 0.05	-	< 0.001	-	< 0.001	
		NH_4^+ (mM)	**K^+ (mM)**	**Na^+(mM)**	**Ca^{2+} (mM)**	**Mg^{2+} (mM)**				
	Open	7.12 ± 0.75	182.65 ± 5.57	5.79 ± 0.49	24.59 ± 3.06	27.03 ± 3.54				247.2 ± 7.3
	Closed	7.8 ± 0.6	263.1 ± 4.7	12.4 ± 0.9	76.0 ± 5.4	54.8 ± 1.9				414.1 ± 7.5
	Diff	-0.7 ± 0.2	-80.5 ± 0.9	-6.6 ± 0.4	-51.4 ± 2.3	-27.8 ± 1.6				
	% diff.	-8.7	-30.6	-53.3	-67.6	-50.7				
	P value	> 0.2	< 0.001	< 0.001	< 0.001	< 0.001				
Apical		**Cl^- (mM)**	**SO_4^{2-} (mM)**	**NO_3^- (mM)**	**Citrate (mM)**	**Tartrate (mM)**	**Malate (mM)**	**Succinate (mM)**	**PO_4^{3-} (mM)**	
	Open	115.64 ± 8.42	52.88 ± 3.11	32.41 ± 4.31	33.79 ± 3.21	1.80 ± 0.28	111.52 ± 13.33	1.05 ± 0.14	23.83 ± 2.36	372.9 ± 17.1
	Closed	120.4 ± 3.2	40.6 ± 2.2	45.9 ± 2.9	20.8 ± 2.0	12.9 ± 1.2	89.3 ± 8.3	12.2 ± 1.1	30.6 ± 2.0	372.7 ± 10.2
	Diff	-4.8 ± 5.2	12.3 ± 0.9	-13.5 ± 1.4	13.0 ± 1.2	-11.1 ± 0.9	22.2 ± 5.0	-11.2 ± 1.0	-6.8 ± 0.4	
	% diff.	-4.0	30.2	-29.4	62.5	-86.0	24.9	-91.4	-22.1	
	P value	> 0.4	< 0.01	< 0.05	< 0.01	< 0.001	> 0.07	< 0.001	< 0.05	
		NH_4^+ (mM)	**K^+ (mM)**	**Na^+(mM)**	**Ca^{2+} (mM)**	**Mg^{2+} (mM)**				
	Open	16.75 ± 1.49	201.99 ± 2.50	26.36 ± 0.51	89.22 ± 3.95	59.21 ± 3.24				393.5 ± 5.9
	Closed	16.2 ± 3.0	271.3 ± 3.8	16.7 ± 1.6	42.3 ± 1.0	56.4 ± 2.5				402.9 ± 5.8
	Diff	0.6 ± 1.5	-69.3 ± 1.3	9.7 ± 1.1	46.9 ± 3.0	2.8 ± 0.7				
	% diff.	3.4	-25.5	57.8	110.9	5.0				
	P value	> 0.7	< 0.001	<0.001	< 0.001	0.3				
Lateral		**Cl^- (mM)**	**SO_4^{2-} (mM)**	**NO_3^- (mM)**	**Citrate (mM)**	**Tartrate (mM)**	**Malate (mM)**	**Succinate (mM)**	**PO_4^{3-} (mM)**	
	Open	146.6 ± 10.0	25.8 ± 3.3	87.0 ± 6.2	64.0 ± 4.2	1.9 ± 0.2	135.7 ± 6.8	13.85 ± 1.8	46.4 ± 6.3	521.3 ± 16.0
	Closed	147.4 ± 7.1	51.4 ± 2.9	45.0 ± 3.6	73.5 ± 7.3	0.5 ± 0.1	106.7 ± 9.6	18.0 ± 1.7	9.3 ± 1.0	451.8 ± 14.9
	Diff	-0.8 ± 2.9	-25.6 ± 0.4	42.0 ± 2.6	-9.5 ± 3.1	1.4 ± 0.1	29.0 ± 2.8	-4.2 ± 0.1	37.1 ± 5.3	
	% diff.	-0.5	-49.7	93.4	-12.9	276.0	27.2	-23.1	398.8	
	P value	> 0.9	< 0.001	< 0.001	> 0.1	< 0.05	< 0.05	< 0.05	< 0.001	
		NH_4^+ (mM)	**K^+ (mM)**	**Na^+(mM)**	**Ca^{2+} (mM)**	**Mg^{2+} (mM)**				
	Open	15.4 ± 0.7	183.1 ± 0.8	11.5 ± 0.5	152.9 ± 1.5	100.4 ± 1.6				463.3 ± 2.5
	Closed	14.8 ± 1.2	94.8 ± 5.9	16.7 ± 0.6	148.8 ± 7.4	105.9 ± 2.2				381.0 ± 9.8
	Diff	0.6 ± 0.5	88.3 ± 5.1	-5.2 ± 0.1	4.1 ± 5.9	-5.5 ± 0.6				
	% diff.	4.0	93.1	-31.0	2.7	-5.2				
	P value	> 0.4	< 0.001	< 0.001	> 0.3	< 0.05				

12. Variation in cell size (surface area) along the abaxial epidermis of each of the *T. virginiana* leaves.

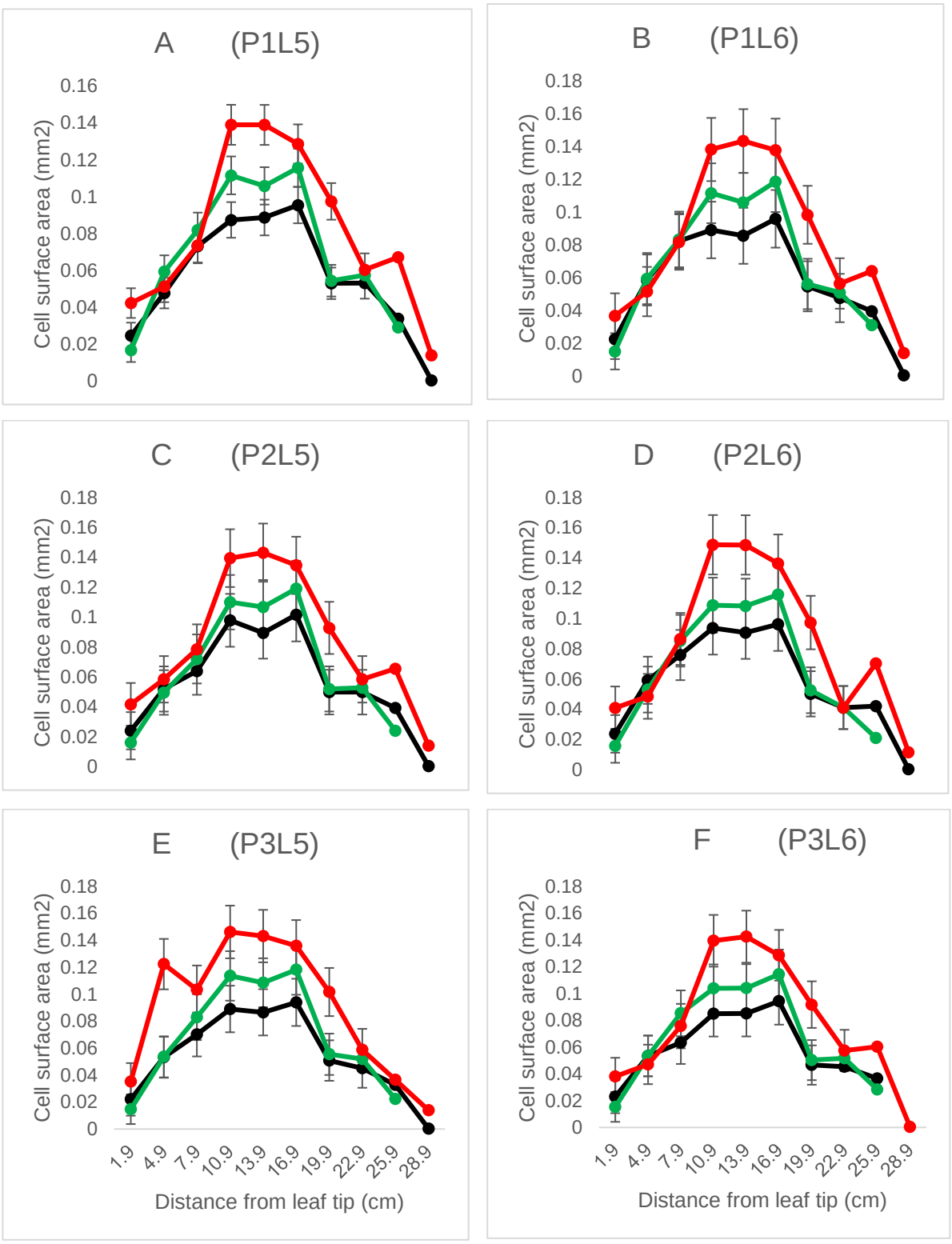

P = Plant; L = Leaf, (e.g. P1L5 stands for plant one leaf five). Juxta apical cells were not found beyond 25.9cm from leaf tip. Error bars – standard deviation.

Pavement cells Juxta apical Stomatal complex

13. Osmotic pressure and sum of solute content in cell types at open and closed stomatal states with associated osmotic coefficient.

Table 0.7 Osmotic pressure and sum of solute content in cell types at open and closed stomatal states with associated osmotic coefficient.

	Closed				Open				Difference	
Cell type	Osmotic pressure (MPa)	Osmolality ($mOsmol.kg^{-1}$)	sum of solute concentration ($mEq.L^{-1}$)	Apparent osmotic coefficient ($Osmol.Mol^{-1}$)	Osmotic pressure (MPa)	Osmolality ($mOsmol.kg^{-1}$)	sum of solute concentration ($mEq.L^{-1}$)	Osmotic coefficient ($Osmol.Mol^{-1}$)	Change in osmotic pressure	Significance (*p* value)
Pavement	1.59 ± 0.07	650.1 ± 28.0	756.3 ± 22.2	0.67	1.38 ± 0.06	563.6 ± 24.7	621.5 ± 16.8	0.67	-0.21	< 0.05
Lateral Subsidiary	1.53 ± 0.04	623.8 ± 17.8	821.8 ± 13.0	0.50	1.68 ± 0.06	683.4 ± 23.5	987.5 ± 27.7	0.50	0.15	< 0.05
Guard cell	1.75 ± 0.06	713.8 ± 24.1	756.8 ± 14.9	0.81	2.26 ± 0.12	922.5 ± 49.7	1022.7 ± 18.1	0.73	0.51	< 0.01
Apical	1.78 ± 0.09	724.3 ± 35.0	776.7 ± 13.8	0.73	1.30 ± 0.06	530.6 ± 25.1	775.3 ± 18.7	0.50	-0.48	< 0.01
Juxta Apical	1.72 ± 0.05	701.5 ± 19.3	800.0 ± 14.2	0.65	1.10 ± 0.07	446.8 ± 26.7	478.6 ± 14.5	0.76	-0.62	< 0.001